

**Molecular and biochemical characterisation of novel
glycosyltransferases in
*Mycobacterium tuberculosis***

By

Helen L. Birch, B.Sc. (Hons)

A thesis submitted to the

**UNIVERSITY OF
BIRMINGHAM**

for the degree of

DOCTOR OF PHILOSOPHY

**School of Biosciences
College of Life and Environmental Sciences
The University of Birmingham**

January 2011

UNIVERSITY OF
BIRMINGHAM

University of Birmingham Research Archive

e-theses repository

This unpublished thesis/dissertation is copyright of the author and/or third parties. The intellectual property rights of the author or third parties in respect of this work are as defined by The Copyright Designs and Patents Act 1988 or as modified by any successor legislation.

Any use made of information contained in this thesis/dissertation must be in accordance with that legislation and must be properly acknowledged. Further distribution or reproduction in any format is prohibited without the permission of the copyright holder.

ABSTRACT

The cell wall mycolyl-arabinogalactan-peptidoglycan complex is essential in mycobacterial species, such as *Mycobacterium tuberculosis* and is the target of several antitubercular drugs. Arabinofuranosyltransferase enzymes, such as EmbA, EmbB, and AftA, play pivotal roles in the biosynthesis of arabinogalactan. The anti-tuberculosis agent ethambutol (EMB) targets arabinogalactan biosynthesis through inhibition of Mt-EmbA and Mt-EmbB and also targets the biosynthesis of the important immunomodulatory molecule lipoarabinomannan (LAM), through inhibition of Mt-EmbC.

A bioinformatics approach identified putative integral membrane proteins in *Mycobacterium smegmatis*, *M. tuberculosis* and the closely related species *Corynebacterium glutamicum*, with features common to the GT-C superfamily of glycosyltransferases. A novel arabinofuranosyltransferase, AftC, was deleted from both *M. smegmatis* and *C. glutamicum* and shown to be an internal branching $\alpha(1\rightarrow3)$ arabinofuranosyltransferase involved in arabinogalactan biosynthesis. Further studies revealed a truncated LAM whereby the arabinan domain was severely reduced and consisted of a simple linear arabinan of approximately 12-15 $\alpha(1\rightarrow5)$ linked Araf residues. This mutant LAM was also shown to be a potent stimulator of TNF- α production using a human macrophage cell line, thus illustrating that masking of the mannan core by arabinan in wild type LAM alters its ability in the production of this cytokine. We also describe a further arabinofuranosyltransferase, AftB. Deletion of its orthologue in *C. glutamicum* resulted in a viable mutant and biochemical analysis revealed the complete absence of terminal $\beta(1\rightarrow2)$ -linked arabinofuranosyl residues. Further analysis confirmed AftB as a terminal $\beta(1\rightarrow2)$ arabinofuranosyltransferase, which was also insensitive to EMB.

The bioinformatic search for cell wall glycosyltransferases led to the identification of a rhamnosyltransferase in *C. glutamicum*, RptA. Deletion resulted in a reduction of terminal-rhamnopyranosyl linked residues and as a result, a corresponding loss of branched 2,5-linked arabinofuranosyl residues. Furthermore, analysis of base-stable extractable lipids from *C. glutamicum* revealed the presence of decaprenyl-monophosphorylrhamnose, a putative substrate for the cognate cell wall transferase. Altogether, these studies have shed further light on the complexities of *Corynebacteriaceae* cell wall biosynthesis, and represent potential new drug targets.

DECLARATION

The work presented in this thesis was carried out in the School of Biosciences at the University of Birmingham, U.K., B15 2TT during the period October 2006 to October 2010. The work in this thesis is original except where acknowledged by references.

No part of the work is being, or has been submitted for a degree, diploma or any other qualification at any other University.

ACKNOWLEDGEMENTS

I would like to take this opportunity to thank all the people who have made this thesis possible. First and foremost, I would like to express my sincere gratitude to my supervisor, Professor Gurdyal S. Besra, for granting me the opportunity to study my MRC funded PhD and whose expertise, understanding, and patience, made this thesis possible.

A special thanks goes out to Dr. Luke Alderwick for his invaluable guidance, motivation and technical support and Dr. Lynn Dover, my undergraduate tutor, for encouraging me to pursue my post-graduate studies. Further thanks go to Dr. Apoorva Bhatt for sharing his expertise so readily and patiently.

I would like to thank Dr. Lothar Eggeling and his lab from the Institute for Biotechnology in Juelich, for performing some of the molecular biology that appears in this thesis and Dr. Ben Appelmek from the University Medical Center in Amsterdam, for his valuable immunological data. Also, a massive thanks to Graham Burns and Peter Ashton for their technical superiority in performing GC and GC/MS.

I would also like to thank all of my colleagues and fellow PhD students for their support: Becci, Justyna, Mimi, Sarah, George, Sid, Albel, Arun, Oona, Hemza, Veemal and Natacha.

Last but not least I would also like to thank my parents, brother and sisters, Robert and Diane and my close friends for all the support they provided me with throughout. Most importantly, I want to acknowledge my partner and best friend, Andy, without his love and encouragement, I would not have finished this thesis.

This thesis is dedicated to Andy

TABLES OF CONTENTS

Abstract	i
Declaration	ii
Acknowledgements	iii
Dedication	iv
Table of Contents	v
List of Figures	ix
List of Tables	xi
List of Abbreviations	xii
Published work associated with this thesis	xviii

1. Introduction.....	1
1.1. Mycobacterial Classification and Phylogenetic Analysis	2
1.1.1. The Genus <i>Mycobacterium</i>	2
1.2. History of tuberculosis.....	4
1.2.1. Discovery of the tubercle bacillus and initial therapies.....	5
1.3. Pathogenesis of tuberculosis.....	6
1.4. Epidemiology of tuberculosis.....	9
1.5. TB drug treatments	11
1.5.1. TB Drug resistance	12
1.6. The mycobacterial cell wall.....	13
1.6.1. The cell wall of <i>M. tuberculosis</i> as a drug target	15
1.6.2. Plasma membrane.....	15
1.6.3. Structure and biosynthesis of peptidoglycan.....	16
1.6.4. Biosynthesis of the linker unit.....	18
1.6.5. Arabinogalactan.....	23
1.6.5.1. Structural features of arabinogalactan	23
1.6.5.2. Synthesis of arabinogalactan biosynthetic precursors	25
1.6.5.2.1. Galactan precursor synthesis	25
1.6.5.2.2. Arabinan precursor synthesis	26
1.6.5.3. Galactan biosynthesis	29
1.6.5.4. Arabinan biosynthesis	31
1.6.5.4.1. Ethambutol inhibition and its use in the identification of the Emb proteins	31
1.6.5.4.2. EMB resistance	34
1.6.5.4.3. Identification of novel arabinofuranosyltransferases and the use of <i>C. glutamicum</i> as a model organism.....	35
1.6.5.4.4. Identification and functional role of AftA.....	37
1.6.6. Mycolic acids.....	38
1.6.6.1. Biosynthesis of mycolic acids	39
1.6.7. Structural features of lipoarabinomannan (LAM) and related biosynthetic precursors (LM and PIMs)	42
1.6.7.1. Phosphatidyl- <i>myo</i> -inositol mannosides (PIMs).....	43
1.6.7.2. Characterisation of LM and LAM.....	43
1.6.7.3. Characterisation of LAM capping	45
1.6.7.4. Biosynthesis of PIMs, LM and LAM.....	47
1.6.7.4.1. Synthesis of precursors.....	47

1.6.7.4.2.	GDP-Man _p biosynthesis	47
1.6.7.4.3.	β-D-mannosyl-1-monophosphoryldecaprenol (PPM) biosynthesis	48
1.6.7.4.4.	Synthesis of PI.....	49
1.6.7.5.	Biosynthesis of PIMs.....	49
1.6.7.6.	Biosynthesis of LM and LAM.....	54
1.6.7.6.1.	The role of MptA, MptB and Rv2181	54
1.6.7.7.	Arabinan biosynthesis in lipoarabinomannan	56
1.6.7.7.1.	The role of EmbC	56
1.6.7.8.	Mannose - capping of LAM	57
1.6.7.9.	Immunomodulatory properties of LAM & LM.....	58
1.6.7.9.1.	Phagosome maturation arrest	58
1.6.7.9.2.	Lipoglycan interaction with the host cell	61
1.6.7.9.3.	LAM and the Mannose receptor.....	61
1.6.7.9.4.	Modulation of DC-SIGN activity.....	62
1.6.7.9.5.	Toll-like receptors	63
1.7.	Project aims	65
2.	Identification and characterisation of AftB and AftC arabinotransferases involved in arabinogalactan biosynthesis	68
2.1.	Introduction	68
2.2.	Results	72
2.2.1.	Genome comparison of the <i>aftB</i> locus.....	72
2.2.2.	Construction of <i>C. glutamicum</i> Δ <i>aftB</i>	74
2.2.3.	In vitro growth analysis of <i>C. glutamicum</i> Δ <i>aftB</i>	75
2.2.4.	Analysis of cell wall associated lipids and bound corynomycolic acid	76
2.2.5.	Cell wall glycosyl compositional and linkage analysis of cell walls	78
2.2.6.	Endogenous <i>in vitro</i> arabinofuranosyltransferase activity of <i>C. glutamicum</i> , <i>C. glutamicum</i> Δ <i>aftB</i> and <i>C. glutamicum</i> Δ <i>aftB</i> complemented with Mt- <i>aftB</i> and product analysis.	81
2.2.7.	ES-MS and GC/MS analysis of product A and B	83
2.2.8.	Genome comparison of the AftC locus	85
2.2.9.	Construction and growth of mutants	86
2.2.10.	Analysis of cell wall bound mycolic acids	89
2.2.11.	Glycosyl compositional analysis of cell walls from <i>M. smegmatis</i> , <i>M.</i> <i>smegmatis</i> Δ <i>aftC</i> and complemented strains	91
2.2.12.	Glycosyl linkage analysis of cell walls	93
2.2.13.	<i>In vitro</i> arabinofuranosyltransferase activity with extracts of <i>M. smegmatis</i> , <i>M. smegmatis</i> Δ <i>aftC</i> and complemented strains.....	95
2.2.14.	Discussion.....	101
3.	Identification and characterisation of a crucial branching α(1→3) arabinofuranosyltransferase involved in LAM bisynthesis.....	109
3.1.	Introduction	109
3.2.	Results	111
3.2.1.	Effects of <i>aftC</i> inactivation on LM/LAM biosynthesis.....	111
3.2.2.	Structural characterisation of AftC-LAM	112
3.2.3.	Effect of ethambutol on AftC-LAM formation	117

3.2.4.	AftC-LAM displays pro-inflammatory properties	118
3.2.5.	Discussion.....	122
4.	Identification of a Rhamnopyransolytransferase (RptA) which utilises a novel decaprenolphosphorhamnose substrate	128
4.1.	Introduction	128
4.2.	Results	129
4.2.1.	Genome comparison of the NCgl0543 (<i>rptA</i>) locus.....	129
4.2.2.	Construction of <i>C. glutamicum</i> Δ <i>rptA</i>	131
4.2.3.	In vitro growth phenotype of <i>C. glutamicum</i> Δ <i>rptA</i>	131
4.2.4.	Glycosyl compositional analysis of cell walls from <i>C. glutamicum</i> , <i>C. glutamicum</i> Δ <i>rptA</i> , <i>C. glutamicum</i> Δ <i>rptA</i> pVWEx-Cg- <i>rptA</i> , and <i>C. glutamicum</i> Δ <i>rptA</i> pVWEx-Rv3779.....	132
4.2.5.	Glycosyl linkage analysis of cell walls from <i>C. glutamicum</i> , <i>C. glutamicum</i> Δ <i>rptA</i> , <i>C. glutamicum</i> Δ <i>rptA</i> pVWEx-Cg- <i>rptA</i> , and <i>C. glutamicum</i> Δ <i>rptA</i> pVWEx-Rv3779.....	134
4.2.6.	Recognition of a rhamnose lipid-linked sugar donor, decaprenyl-P-rhamnose 135	
4.3.	Discussion.....	140
5.	Conclusion and future work.....	144
6.	Materials and Methods	151
6.1.	Chemicals, reagents and growth conditions	151
6.2.	Bacterial growth conditions.....	151
6.2.1.	Construction of <i>C. glutamicum</i> mutants.....	152
6.2.1.1.	Construction of <i>C. glutamicum</i> Δ <i>aftB</i> and complementing strains.....	152
6.2.1.2.	Construction of <i>C. glutamicum</i> Δ <i>aftC</i> and complementing strains.....	154
6.2.1.3.	Construction of <i>C. glutamicum</i> Δ <i>rptA</i> and complementing strains.....	154
6.2.2.	Construction of <i>M. smegmatis</i> mutants	155
6.2.2.1.	Construction of <i>M. smegmatis</i> Δ <i>aftC</i> and complementing strains	155
6.2.3.	mAGP purification procedures.....	157
6.2.3.1.	Acid hydrolysis and alditol acetate derivatisation.....	157
6.2.3.2.	Glycosidic linkage analysis	158
6.2.4.	GC and GC/MS	158
6.3.	Extraction and visualisation of lipids	159
6.3.1.	Cell wall associated lipid extraction.....	159
6.3.2.	Exported (media filtrate) lipid extraction	160
6.3.3.	Cell wall bound lipid extraction	160
6.3.4.	Analysis of AftB muteins	161
6.4.	Extraction and Purifications of lipoglycans.....	162
6.4.1.	NMR spectroscopic analysis of WT-LAM and AftC-LAM.....	163
6.4.2.	SDS PAGE	163

6.5.	Cell free [14C]-labeling assays.....	164
6.5.1.	Preparation of <i>C. glutamicum</i> and <i>M. smegmatis</i> membranes	164
6.5.2.	Preparation of <i>C. glutamicum</i> and <i>M. smegmatis</i> cell wall material	164
6.5.3.	Estimation of protein concentration	165
6.5.4.	Arabinofuranosyltransferase assays	165
6.5.4.1.	Arabinofuranosyltransferase activity with membrane preparations of <i>C. glutamicum</i> , <i>C. glutamicum</i> Δ <i>aftB</i> , and <i>C. glutamicum</i> Δ <i>aftB</i> pMSX-Mt- <i>aftB</i>	165
6.5.4.2.	Analysis of arabinofuranosyltransferase reaction products prepared from <i>C. glutamicum</i> and <i>C. glutamicum</i> Δ <i>aftB</i> membranes.....	167
6.5.4.3.	Arabinofuranosyltransferase activity with membrane preparations of <i>M. smegmatis</i> , <i>M. smegmatis</i> pMV261-Mt- <i>aftC</i> , <i>M. smegmatis</i> Δ <i>aftC</i> and <i>M. smegmatis</i> Δ <i>aftC</i> pMV261-Mt- <i>aftC</i>	167
6.5.4.4.	Characterization of α (1 \rightarrow 3)-arabinofuranosyltransferase activity with membranes prepared from <i>M. smegmatis</i> , <i>M. smegmatis</i> Δ <i>aftC</i> and <i>M. smegmatis</i> Δ <i>aftC</i> pMV261-Mt- <i>aftC</i>	169
6.5.5.	Treatment of <i>M. smegmatis</i> and <i>M. smegmatis</i> Δ <i>aftC</i> with sub-inhibitory concentrations of EMB and subsequent lipoglycan analysis.	173
6.5.6.	Treatment of WT-LAM, AftC-LAM and Pam ₃ CSK ₄ with H ₂ O ₂	173
6.5.7.	Cell culture	174
6.5.8.	Cell stimulation assays	174
6.5.9.	DC-SIGN-Fc ELISA	174
7.	References	177

LIST OF FIGURES

Figure 1.1	The intracellular existence of <i>M. tuberculosis</i>	7
Figure 1.2	Overview of TB infection and host defence.....	8
Figure 1.3	Estimated TB incidence rates in the year 2009 (WHO, 2010).....	10
Figure 1.4	Estimated HIV prevalence in new TB cases in the year 2009 (WHO, 2010).....	10
Figure 1.5	Schematic model of the mycobacterial cellwall.....	14
Figure 1.6	Biosynthesis of peptidoglycan in <i>M. tuberculosis</i>	18
Figure 1.7	The Rha-GlcNAc linker unit. The molecular structure of the LU, the conduit between AG and PG.....	19
Figure 1.8	Formation of linker unit glycolipid-1 (GL-1) and glycolipid-2 (GL2).....	20
Figure 1.9	Biosynthetic pathway of dTDP-rhamnose.....	22
Figure 1.10	Structural features of arabinogalactan.....	24
Figure 1.11	Formation of galactan precursors.....	26
Figure 1.12	Formation of arabinan precursor DPA.....	28
Figure 1.13	Polymerisation of galactan - biosynthesis of GL-4.....	29
Figure 1.14	Polymerisation of galactan.....	30
Figure 1.15	Schematic presentation of arabinogalactan biosynthesis.....	33
Figure 1.16	Early arabinogalactan formation.....	37
Figure 1.17	Structures of representative mycolic acids from <i>M. tuberculosis</i>	39
Figure 1.18	Mycolic acid biosynthesis in <i>M. tuberculosis</i>	41
Figure 1.19	Structure of TDM.....	42
Figure 1.20	Current structural model of mycobacterial LAM.....	44
Figure 1.21	Structural model of mycobacterial ManLAM, PILAM and AraLAM highlighting the different capping motifs found in all mycobacterial LAM.....	46
Figure 1.22	Pathway of mannose biosynthesis in mycobacteria.....	48
Figure 1.23	Pictorial depiction of PIM, LM and LAM biosynthesis.....	50
Figure 1.24	Biogenesis of PIM, LM and LAM.....	52
Figure 1.25	The role of ManLAM and PIMs in phagosome maturation arrest.....	59
Figure 2.1	Comparison of the <i>aftB</i> locus within <i>Corynebacteriaceae</i>	72
Figure 2.2	Construction and characteristics of <i>C. glutamicum</i> Δ <i>aftB</i>	74
Figure 2.3	Quantitative analysis of extractable [¹⁴ C]lipids from <i>C. glutamicum</i> , <i>C. glutamicum</i> Δ <i>aftB</i> and <i>C. glutamicum</i> Δ <i>aftB</i> pMSX-Mt- <i>aftB</i>	76
Figure 2.4	Quantitative analysis [¹⁴ C]CMAMES from <i>C. glutamicum</i> , <i>C. glutamicum</i> Δ <i>aftB</i> and <i>C. glutamicum</i> Δ <i>aftB</i> pMSX-Mt- <i>aftB</i>	77
Figure 2.5	Glycosyl linkage analysis of cell walls of <i>C. glutamicum</i> (A), <i>C. glutamicum</i> Δ <i>aftB</i> (B), <i>C. glutamicum</i> Δ <i>aftB</i> pMSX-Mt- <i>aftB</i>	79
Figure 2.6	Formation of Mt-AftB in <i>C. glutamicum</i>	80
Figure 2.7	Arabinofuranosyltransferase activity in membranes prepared from <i>C. glutamicum</i> , <i>C. glutamicum</i> Δ <i>aftB</i> and <i>C. glutamicum</i> Δ <i>aftB</i> pMSX-Mt- <i>aftB</i>	81
Figure 2.8	ES-MS and GC/MS characterisation of products A and B.....	83
Figure 2.9	Comparison of the <i>aftC</i> locus within the <i>Corynebacteriaceae</i>	84
Figure 2.10	Generation of a <i>MSMEG2785</i> null mutant.....	86
Figure 2.11	Colony morphology of wild-type <i>M. smegmatis</i> and <i>M. smegmatis</i> Δ <i>aftC</i>	87
Figure 2.12	Strategy to delete <i>Cg-aftC</i> using the deletion vector pK19mobsacB Δ <i>aftC</i>	88
Figure 2.13	Analysis of cell wall bound MAMES from <i>M. smegmatis</i> , <i>M. smegmatis</i> Δ <i>aftC</i> , <i>M. smegmatis</i> Δ <i>aftC</i> pMV261-Ms- <i>aftC</i> and <i>M. smegmatis</i> Δ <i>aftC</i> pMV261-Mt- <i>aftC</i>	89
Figure 2.14	Analysis of cell wall bound CMAMES from <i>C. glutamicum</i> and <i>C. glutamicum</i> Δ <i>aftC</i>	90

Figure 2.15	GC analysis of cell walls of <i>M. smegmatis</i> , <i>M. smegmatis</i> Δ <i>aftC</i> , <i>M. smegmatis</i> Δ <i>aftC</i> pMV261- <i>Ms-aftC</i> and <i>M. smegmatis</i> Δ <i>aftC</i> pMV261-Mt- <i>aftC</i>	91
Figure. 2.16	GC/MS analysis of cell walls of <i>M. smegmatis</i> , <i>M. smegmatis</i> Δ <i>aftC</i> , <i>M. smegmatis</i> Δ <i>aftC</i> pMV261- <i>Ms-aftC</i> and <i>M. smegmatis</i> Δ <i>aftC</i> pMV261-Mt- <i>aftC</i>	92
Figure 2.17	GC and GC/MS analysis of cell walls of <i>C. glutamicum</i> and <i>C. glutamicum</i> Δ <i>aftC</i>	93
Figure 2.18	Arabinofuranosyltransferase activity utilising an Ara ₂ acceptor and membranes prepared from <i>M. smegmatis</i> , <i>M. smegmatis</i> Δ <i>aftC</i> and <i>M. smegmatis</i> Δ <i>aftB</i> pMV261-Mt- <i>aftC</i>	95
Figure 2.19	Arabinofuranosyltransferase activity utilising an Ara ₅ acceptor and membranes prepared from <i>M. smegmatis</i> , <i>M. smegmatis</i> Δ <i>aftC</i> and <i>M. smegmatis</i> Δ <i>aftC</i> pMV261-Mt- <i>aftC</i>	97
Figure 2.20	GC/MS characterisation of in vitro synthesised product X from the arabinofuranosyltransferase assays utilising the Ara ₅ acceptor.....	98
Figure 2.21	Proposed mycobacterial arabinan biosynthesis and the role of AftB and AftC.....	103
Figure 3.1	SDS-PAGE analysis of lipoglycans extracted from <i>M. smegmatis</i> and <i>M. smegmatis</i> Δ <i>aftC</i>	110
Figure 3.2	MALDI-TOF-MS analysis of purified WT-LAM (A) and AftC-LAM (B) extracted from <i>M. smegmatis</i> and <i>M. smegmatis</i> Δ <i>aftC</i>	111
Figure 3.3	GC and GC/MS analysis of purified lipoglycans extracted from <i>M. smegmatis</i> (A and B), <i>M. smegmatis</i> Δ <i>aftC</i> (C and D), <i>M. smegmatis</i> Δ <i>aftC</i> pMV261- <i>Ms-aftC</i> (E and F), and <i>M. smegmatis</i> Δ <i>aftC</i> pMV261-Mt- <i>aftC</i> (G and H).112	112
Figure 3.4	Two-dimensional NMR spectra of WT-LAM and AftC-LAM purified from <i>M. smegmatis</i> and <i>M. smegmatis</i> Δ <i>aftC</i>	113
Figure 3.5	Structural representation of WT-LAM and AftC-LAM.....	115
Figure 3.6	SDS-PAGE A) and total sugar analysis B) of [¹⁴ C]-labeled lipoglycans extracted from <i>M. smegmatis</i> and <i>M. smegmatis</i> Δ <i>aftC</i> treated with EMB.....	117
Figure 3.7	TNF- α production by human THP-1 cells and IL-8 production by HEK293 TLR-2 cells in response to WT-LAM and AftC-LAM.....	119
Figure 3.8	Mycobacterial LAM biosynthesis and the role of AftC.....	122
Figure 4.1	Hypothetical spatial organisation and partial sequence of the putative protein <i>NCgl0543</i>	129
Figure 4.3	GC analysis of cell walls of <i>C. glutamicum</i> , <i>C. glutamicum</i> Δ <i>rptA</i> and <i>C. glutamicum</i> Δ <i>rptA</i> pVWEx-Cg- <i>rptA</i>	132
Figure 4.4	GC/MS analysis of cell walls of <i>C. glutamicum</i> , <i>C. glutamicum</i> Δ <i>rptA</i> and <i>C. glutamicum</i> Δ <i>rptA</i> pVWEx-Cg- <i>rptA</i>	134
Figure 4.5	Analysis of [¹⁴ C]GlcNAc, [¹⁴ C]Rha, [¹⁴ C]Gal and [¹⁴ C]Ara labeled glycolipids in <i>C. glutamicum</i>	135
Figure 4.6	Analysis of [¹⁴ C]Rha base stable lipids in <i>C. glutamicum</i> and <i>C. glutamicum</i> Δ <i>rptA</i> and the effect of tunicamycin.....	136
Figure 4.7	Mass spectrometry analysis and identification of decaprenyl-1-monophosphorylrhamnose.....	137

LIST OF TABLES

Table 1.1	<i>Mycobacterium</i> genus with representative slow-growing and fast-growing bacilli.....	4
Table 1.2	Commonly used TB drugs and their targets.....	11
Table 1.3	Genes involved in biosynthesis of LAM and related glycoconjugates.....	54
Table 1.4	Primers used for the generation of knock-out mutants and complemented strains.....	154

LIST OF ABBREVIATIONS

A	adenine
Aa	amino acid
AftA	Arabinofuranosyltransferase A
AftB	Arabinofuranosyltransferase B
AftC	Arabinofuranosyltransferase C
AftD	Arabinofuranosyltransferase D
AftE	Arabinofuranosyltransferase E
AG	arabinogalactan
AIDS	Acquired immuno-deficiency syndrome
Ara	arabinose
<i>Araf</i>	<i>arabinofuranose</i>
AraLAM	un-capped LAM
BCA	bicinchoninic protein assay
BCG	bacillus Calmette-Guérin
BHI	brain heart infusion
BSA	bovine serum albumin
°C	degrees centigrade
C	cytosine
CBB	coomassie brilliant blue
CDP-DAG	cytidine diphosphate-diacylglycerol
CHAPS	3-[(3-cholamidopropyl)dimethylammonio]-1-propanesulfonate
Ci	Curie
CMAME	corynomycolic acid methyl ester
CPM	counts per minute

DAG	diacylglycerol
DAP	diaminopimelic acid
DAT	diacyl trehalose
DC	dendritic cell
DC-SIGN	DC specific intercellular adhesion molecule-3 grabbing non-integrin
DEAE	diethylaminoethyl
DMSO	dimethylsulphoxide
DNA	deoxyribonucleic acid
DPA	decaprenyl-phosphate-D-arabinose
DPG	diphosphatidyl glycerol
DPM	dolichyl-phospho-mannose
DPPR	decaprenylphosphoryl-5- phosphoribose
DPR	decaprenyl-phosphate-D-ribose
DXD	Aspartic acid residue motif present in glycosyltransferases
EDTA	ethylenediaminetetraacetic acid
EMB	ethambutol
<i>f</i>	furanose
FAB	fast atom bombardment
FAS	fatty acid synthase
g	grams
G	guanine
Gal	galactose
<i>Gal^f</i>	galactofuranose
GC/MS	gas chromatography-mass spectrometry
GDP-Man _p	guanosine diphospho-mannose <i>pyranose</i>
GDPMP	GDP-mannose pyrophosphorylase

GL	glycolipid
GlcNAc	N-acetylglucosamine
GMCM	glucose monocorynomycolate
GPI	glycosylphosphatidyl inositol
GPLs	glycopeptidolipids
Gro	glycerol
h	hour
HCl	hydrochloric acid
HIC	hydrophobic interaction chromatography
His-tag	6 histidine residue tag
HIV	human immuno-deficiency virus
Hz	hertz
IL	interleukin
INF- γ	interferon gamma
Ins	inositol
IPTG	isopropylthio- β -D-galactoside
kDa	kilo Dalton
kPa	kilo Pascal
L	litre
LAM	lipoarabinomannan
LB	Luria-Bertani
LM	lipomannan
LOSs	lipooligosaccharides
LPS	lipopolysaccharide
LU	linkage unit
M	molar

MAC	<i>Mycobacterium avium</i> complex
mAGP	mycolyl-arabinogalactan-peptidoglycan complex
MALDI-TOF	matrix assisted laser desorption ionisation-time of flight
ManLAM	LAM with mannosyl caps
Manp	mannopyranose
MBP	mannan binding protein
MDR	multi-drug resistant
mg	milligram
MgtA	α -mannosyl-glucopyranosyluronic acid-transferase A
MHC	major histocompatibility complex
min	minutes
ml	millilitre
mM	millimolar
MOPS	4-morpholine propane sulfonic acid
MPA	molybdophosphoric acid
MPI	mannosyl-phosphatidyl-myo-inositol
MptA	$\alpha(1\rightarrow6)$ mannospyranosyltransferase A
MptB	$\alpha(1\rightarrow6)$ mannospyranosyltransferase B
MptC	$\alpha(1\rightarrow2)$ mannospyranosyltransferase C
MptD	$\alpha(1\rightarrow2)$ mannospyranosyltransferase D
MR	mannose receptor
MS	mass spectrometry
Mur	muramic acid
NAP	naphthol
Nm	nanometres
NMR	nuclear magnetic resonance

NOESY	nuclear overhauser and exchange spectroscopy
OD	optical density
ORF	open reading frame
P	phosphate
p.p.m.	parts per million
PA	phosphatidic acid
PAGE	polyacrylamide gel electrophoresis
PAT	penta-acyl trehalose
PCR	polymerase chain reaction
PDIM	phthiocerol dimycoserolate
PE	phosphatidyl ethanolamine
PG	peptidoglycan
PGls	phenolic glycolipids
PGM	phosphoglucomutase
PI	phosphatidyl-myo-inositol
PILAM	LAM with phosphoinositide caps
PIM	phosphatidyl-myo-inositol mannoside
PMSF	phenylmethylsulfonyl fluoride
Pol-P	polyisoprenoid phosphate
PPM	polyprenyl monophosphate
pRpp	5-phosphoribofuranose pyrophosphate
Rha	rhamnose
ROESY	rotating frame overhauser effect spectroscopy
sec	second
SDS	sodium dodecyl sulfate
SL	sulfolipid

t	terminal
T	thymine
TAE	Tris-acetate EDTA
TAT	tri-acyl trehalose
TB	tuberculosis
TBAH	tetra butylammonium hydroxide
TDM	trehalose dimycolate
TFA	trifluoroacetic acid
TLC	thin-layer chromatography
TLR	toll-like receptor
TMCM	trehalose monocorynomycolate
TMM	trehalose monomycolate
TNF-	tumour necrosis factor
U	uracil
UDP-Glc	uridine diphospho-glucose
UDP-GlcA	UDP-D-glucuronic acid
v/v	volume/volume
w/v	weight per volume
µg	microgram
µl	microlitre
µM	micromolar

PUBLISHED WORK ASSOCIATED WITH THIS THESIS

Birch, H. L., Alderwick, L. J., Bhatt, A. & other authors (2008). Biosynthesis of mycobacterial arabinogalactan: identification of a novel $\alpha(1\rightarrow3)$ arabinofuranosyl transferase. *Mol Microbiol* **69**, 1191-1206.

Birch, H. L., Alderwick, L. J., Rittmann, D., Krumbach, K., Etterich, H., Grzegorzewicz, A., McNeil, M. R., Eggeling, L. & Besra, G. S. (2009). Identification of a terminal rhamnopyranosyltransferase (RptA) involved in *Corynebacterium glutamicum* cell wall biosynthesis. *J Bacteriol* **191**, 4879-4887.

Birch, H. L., Alderwick, L. J., Appelmelk, B. J., Maaskant, J., Bhatt, A., Singh, A., Nigou, J., Eggeling, L., Geurtsen, J. & Besra, G. S. (2010). A truncated lipoglycan from mycobacteria with altered immunological properties. *Proc Natl Acad Sci U S A* **107**, 2634-2639

Seidel, M., Alderwick, L. J., Birch, H. L., Sahm, H., Eggeling, L. & Besra, G. S. (2007). Identification of a Novel Arabinofuranosyltransferase AftB Involved in a Terminal Step of Cell Wall Arabinan Biosynthesis in Corynebacteriaceae, such as *Corynebacterium glutamicum* and *Mycobacterium tuberculosis*. *J Biol Chem* **282**, 14729-14740.

Chapter 1

1.1. Mycobacterial Classification and Phylogenetic Analysis

Tuberculosis (TB) has been a prominent human disease for several thousand years. *Mycobacterium tuberculosis*, the aetiological agent of TB, belongs to the genus *Mycobacterium*, which is presumed to have originated more than 150 million years ago (Daniel, 2006; Hayman, 1984). Phylogenetic analysis of bacilli isolated from patients living in remote East African villages, suggest that these isolates predate the modern *M. tuberculosis* complex (MTBC) members, representing the ancestral species from which these modern members may have evolved (Gutierrez *et al.*, 2005). This has led to the assumption that an ancient predecessor co-existed and co-evolved nearly 3 million years ago with early East African Hominids. The organism which later underwent an “evolutionary bottleneck”, some 20,000 years ago, resulting in the present strains that account for the majority of TB worldwide (Brosch *et al.*, 2002; Daniel, 2006; Kapur *et al.*, 1994; Sreevatsan *et al.*, 1997a).

1.1.1. The Genus *Mycobacterium*

Members of the MTBC include *M. tuberculosis*, *Mycobacterium bovis*, *Mycobacterium bovis* BCG, *Mycobacterium africanum*, *Mycobacterium canettii*, *Mycobacterium leprae* and *Mycobacterium pinnipedii* (Brosch *et al.*, 2002), which belong to the genus *Mycobacterium*. At present over 100 species have been recognised in this genus, the majority of which are saprophytic soil species (Brown-Elliott *et al.*, 2002); however, a minority are pathogenic to humans, such as *M. tuberculosis* and *M. leprae*, causing TB and leprosy, respectively. In addition, *Mycobacterium kansasii*, *Mycobacterium fortuitum* and *Mycobacterium avium* complex (MAC) members cause illness and fatalities in immunocompromised individuals (Kiehn *et al.*, 1985). The *Mycobacterium* genus belongs to the family *Mycobacteriaceae*, positioned in the suborder *Corynebacterineae*, which is included in the suprageneric Acinomycete taxon. *Corynebacterineae* also includes *Corynebacterium*, *Nocardia* and *Rhodococcus*, all of which are classified as Gram-positive, non-motile, aerobic, rod-shaped

bacteria, with characteristically high proportions of guanine and cytosine in their genomes. One of the foremost defining features of this suborder is the existence of mycolic acids (Minnikin & Goodfellow, 1980), unique β -hydroxy- α -alkyl branched long chain fatty acids, which are specific constituents of the cell envelope (Daffé & Draper, 1998; Dover *et al.*, 2004). This distinctive ‘waxy’ cell wall is highly impermeable and is the basis for *M. tuberculosis*’ intrinsic resistance to common antibiotics (Brennan & Nikaido, 1995; Nguyen *et al.*, 2006) and its formidable strength against the bactericidal activities of the macrophage.

Species within the *Mycobacterium* genus exhibit variable growth rates and are classified as either slow or rapid growers (Table 1.1) (Lewin & Sharbati-Tehrani, 2005). A characteristic feature of highly pathogenic species such as *M. tuberculosis* and *M. leprae* is their slow growth rate and fastidious culturing processes. *M. tuberculosis* divides every 15 to 20 hours, taking between 4-6 weeks to obtain visual colonies, which is extremely slow compared to other bacteria, for instance *Escherichia coli* has a doubling time of 20 minutes (Lewin & Sharbati-Tehrani, 2005).

Mycobacterium smegmatis is classified as a fast-growing species, with a doubling time of approximately 3 hours, producing visible colonies in 3-5 days. It is generally considered non-pathogenic in immunocompetent individuals, and thus does not require the Category 3 safety laboratory. There are many similarities between *M. smegmatis* and the much more virulent pathogens, with more than 2000 homologous genes shared with *M. tuberculosis*. These properties make it a very useful model organism for *M. tuberculosis* and other mycobacterial pathogens.

Table 1.1: *Mycobacterium* genus with representative slow-growing and fast-growing bacilli.

Slow Growers		Fast Growers
<i>Mycobacterium africanum</i>	<i>Mycobacterium marinum</i>	<i>Mycobacterium aurum</i>
<i>Mycobacterium avium</i>	<i>Mycobacterium microti</i>	<i>Mycobacterium chelonae</i>
<i>Mycobacterium bovis</i>	<i>Mycobacterium scrofulaceum</i>	<i>Mycobacterium chitae</i>
<i>Mycobacterium intracellulare</i>	<i>Mycobacterium simiae</i>	<i>Mycobacterium fortuitum</i>
<i>Mycobacterium farcinogenes</i>	<i>Mycobacterium szulgai</i>	<i>Mycobacterium phlei</i>
<i>Mycobacterium gastri</i>	<i>Mycobacterium tuberculosis</i>	<i>Mycobacterium porcinum</i>
<i>Mycobacterium kansasii</i>	<i>Mycobacterium ulcerans</i>	<i>Mycobacterium pulveris</i>
<i>Mycobacterium leprae</i>	<i>Mycobacterium xenopi</i>	<i>Mycobacterium smegmatis</i>

1.2. History of tuberculosis

Mycobacterial DNA has been detected in numerous archaeological specimens, proving that TB is an ancient disease, which plagued the prehistoric man. Molecular identification of human TB from 4500 year old Egyptian mummies (Zink *et al.*, 2001) and further palaeomicrobiological evidence (Donoghue *et al.*, 2004) from the United Kingdom (Taylor *et al.*, 2005), South America (Salo *et al.*, 1994), Borneo (Donoghue *et al.*, 2004) and numerous other world-wide locations, illustrate the wide geographical distribution of the disease.

During 460 BC, the first documented account of TB emerged; the term phthisis (to waste away) was introduced into Ancient Greek literature by Hippocrates, who recognised how widespread and prevalent the disease was (Coar, 1982). It wasn't until the writings of Clarissimus Galen (131-201 AD) that Phthisis or 'consumption' was described as ulceration of the lungs, along with wasting away of the body, fever and cough. TB persisted throughout the ages, surging into 17th century Europe, becoming the principal cause of death. Mortality rates reached their pinnacle in the 18th and 19th centuries and TB gained the title the "Great

White Plague”. The name ‘tuberculosis’ was introduced into the medical language after Gaspard Laurent Bayle (1774-1816) proved that tubercles present on the lungs of TB sufferers were the cause of illness.

1.2.1. Discovery of the tubercle bacillus and initial therapies

In 1720, Benjamin Marten, a prominent English Physician, published work proposing that TB was infectious, stating that these ‘minute, living creatures’ enter the body and induce formation of lesions, producing the symptoms of Phthisis (Doetsch, 1978). In 1882, Robert Koch provided unequivocal proof that TB was in fact caused by a bacterium, *M. tuberculosis*, which could be isolated and stained (Koch, 1931). This significant discovery awakened the scientific community to the prospect that this age-old disease could be treated, and research concentrated on producing effective chemotherapeutic agents.

The mid 19th century was accompanied by a decrease in TB mortality rates and a lesser incidence of disease, which may have coincided with the establishment of Hermann Brehmer’s sanatoriums in 1859. These establishments promoted good nutrition, exercise, rest and fresh air (Cox, 1923; Daniel, 2006), providing the first widely practiced anti-tuberculosis treatment. The introduction of active therapy soon followed in the form of pneumothorax and thoracoplasty procedures that collapsed part of the infected lungs with the intention of closing the cavities (Daniel, 2006). Nonetheless, these invasive early therapies seemed to do little to alleviate the symptoms, and are now deemed dangerous and controversial. Albert Calmette and Camille Guérin, inspired by Edward Jenner’s discovery, that humans could be immunised against smallpox following cowpox infection, began developing a vaccine against *M. tuberculosis* using *M. bovis*, the aetiological agent of bovine TB. In 1921, after successful attenuation of the strain, the Bacille Calmette-Guérin (BCG) vaccine was administered to humans (Calmette, 1928) and remains the only vaccine in use

today regardless of reports on its variable efficacy (Brewer & Colditz, 1995; Colditz *et al.*, 1994).

1.3. Pathogenesis of tuberculosis

Transmission of *M. tuberculosis* begins with the inhalation of infective droplet nuclei expelled from the respiratory tract of an active TB sufferer. The nasopharynx and the upper respiratory tract trap larger particles; however, droplets with a diameter as large as 5µm may enter the alveoli, whereby they are ingested by the alveolar macrophages (Lurie, 1950). Receptor-mediated phagocytosis of the invading bacteria involves several major host cell surface receptors, such as, complement receptors (CR1, CR2, and CR3), mannose receptors (MR), surfactant protein receptors, CD14, and scavenger receptors (Ernst 1998). Following phagocytosis, the bacteria continue to reside within the membrane-bound vacuole called the phagosome, which matures to form the phagolysosome (Figure 1.1). This process subjects the internalised bacilli to attack from hydrolytic enzymes delivered by the lysosome. These initial microbicidal defenses may destroy the invading bacilli, yet some are able to evade this outcome by inhibiting the maturation process of the phagosome, as well as modulating the internal environment allowing logarithmic growth, leading to lysis of the immune cell. The released bacteria, chemoattractants, and cellular debris draw in other macrophages and monocytes from the bloodstream. The logarithmic bacterial growth terminates when T-lymphocytes, attracted by interleukin-8, arrive at the lesions. The lesions then undergo caseous necrosis due to the amplified immune response, resulting in a build up of acidic necrotic material in the centre, predominantly made up of macrophage debris (Dannenberg & Rook, 1964; Dannenberg & Sugimoto, 1976). This acidic, anoxic environment does not support bacterial growth, although the bacteria can survive in the destroyed tissue. Eventually, the copious amounts of released antigen stimulate the cell-mediated immune response; cytokines activate macrophages, which are then capable of killing bacilli ingested

from the edges of the lesion. In most cases the disease enters a period latency with the formation of a granulomatous lesion, named a ‘tubercle’.

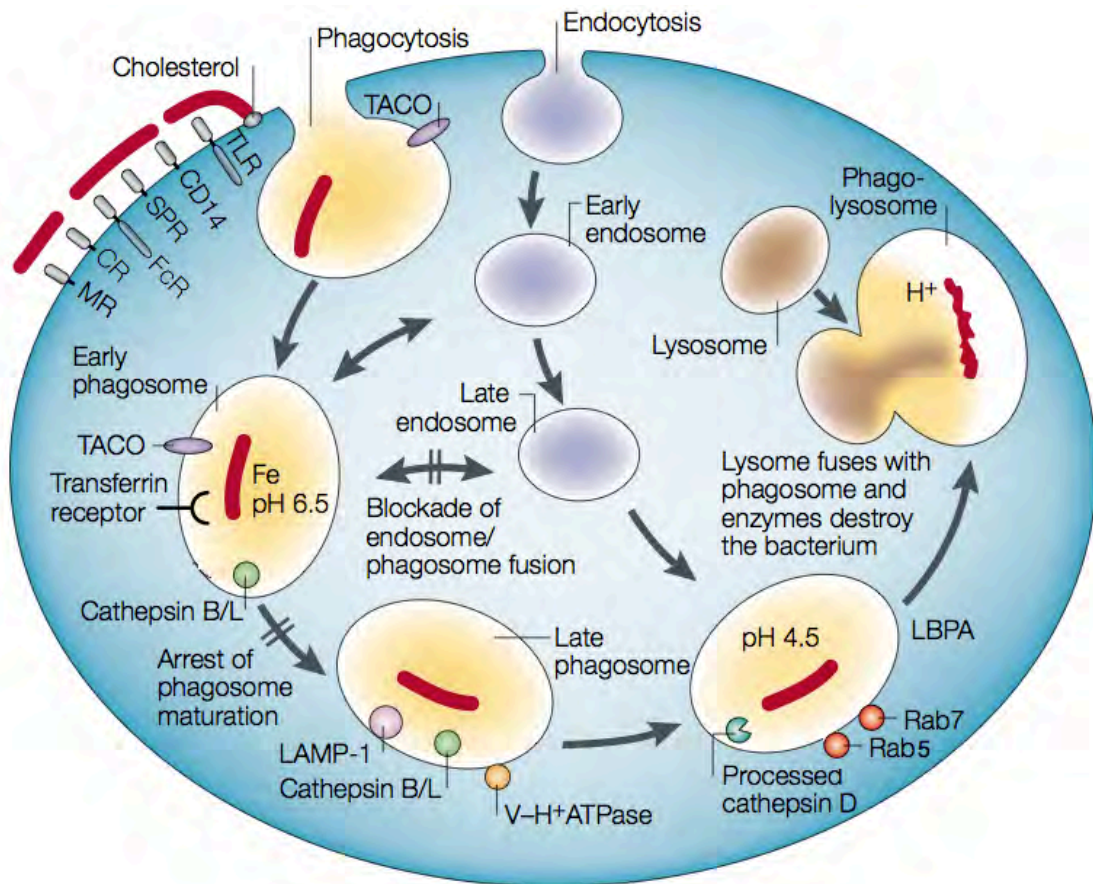


Figure 1.1: The intracellular existence of *M. tuberculosis*. This figure illustrates the influence of *M. tuberculosis* on the phagosome and endosome maturation processes. Specialised cell types — the so-called ‘professional’ phagocytes, engulf larger particles. Numerous cell-surface receptors participate in the interaction between *M. tuberculosis* and the macrophages, facilitated by Cholesterol. *M. tuberculosis* resides in a phagosome, the maturation of which is inhibited at an early stage. The early mycobacteria-containing phagosome retains tryptophan-aspartate containing coat protein TACO, which apparently prevents its further maturation. *M. tuberculosis* inhibits phagosomal acidification (which normally occurs *via* recruitment of V_o-H⁺ ATPase) and prevents fusion with the endosomal pathway. Rab5 is involved in regulation of the fusion with vesicles of the endosomal-lysosomal pathway. Phagosomal maturation is not always successfully halted, allowing some phagosomes to mature into phagolysosomes. Phagosomal maturation is promoted in activated macrophages, particularly after stimulation by IFN- γ . CR, complement receptor; FcR, receptor for the constant fragment of immunoglobulin; LAMP-1 lysosomal-associated membrane protein 1; LBPA, lysobiphosphatic acid; MR, mannose receptor; Rab5 and Rab7, members of the small GTPase family; SPR, surfactant protein receptor; TACO, tryptophane, aspartate-containing coat protein; TLR, Toll-like receptor; V-H⁺ATPase, vacuolar ATP-dependent proton pump (Adapted from Kaufmann, 2001).

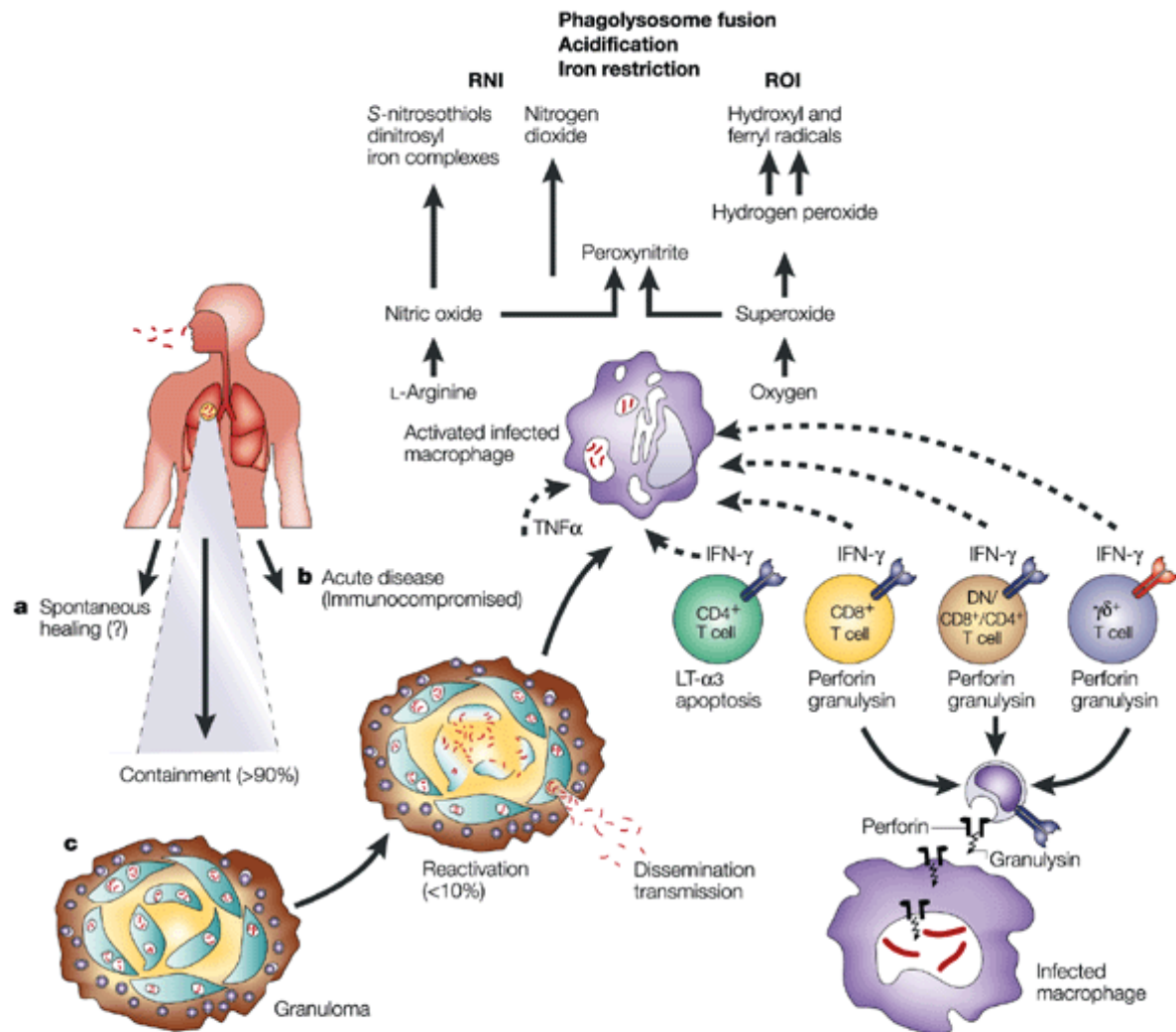


Figure 1.2 Overview of TB infection and host defence. There are three potential outcomes of infection of the human host in *M. tuberculosis*. **a)** The frequency of spontaneous healing is unknown, but is assumed to be rare **b)** Disease progression immediately after infection in the immunocompromised host. **c)** In the majority of cases, mycobacteria are initially contained and disease progresses later due to reactivation. The granuloma is the major site of infection, which develops from infected macrophages that become surrounded by lymphocytes. Effector T cells (CD4⁺ and CD8⁺ T cells, and double-negative or CD4/CD8 single-positive T cells that recognise antigen presented by CD1) and macrophages participate in the control of TB. Crucial macrophage activators interferon-γ (IFN-γ) and tumour-necrosis factor-α (TNF-α) are produced by T cell and macrophages respectively. Macrophage activation permits phagosomal maturation and the production of antimicrobial molecules such as reactive nitrogen intermediates (RNI) and reactive oxygen intermediates (ROI). LT-3, lymphotoxin-3 (Adapted from Kaufmann, 2001).

It is estimated that only 1 in 10 infected individuals will go on to develop clinical symptoms due to reactivation of TB, and the lifetime risk of this is 5-10% (Figure 1.2). The strongest risk factor for reactivation of TB is an impaired immune system, for instance, as a result of HIV infection, malnutrition, advanced malignancy or old age (Kaufmann, 2001). HIV infected individuals have a 7-10% annual risk of latent disease progressing into active TB. Their incompetent immune cells ingest the bacilli from the edges of the caseous regions, yet they are unable to halt growth, thus the delayed-type hypersensitivity response continues to destroy tissue. This results in lymphohematogenous dissemination, whereby escaping bacteria are free to form multiple lesions throughout the body (Kaufmann, 2001; Raupach & Kaufmann, 2001).

1.4. Epidemiology of tuberculosis

By the mid 20th century, with the onset of improved public health services, the BCG vaccine and the use of specific drug therapies, TB prevalence had declined dramatically in industrialised countries, so much so, that the disease was considered to be close to elimination. The resurgence of TB occurred during the 1980s, exacerbated by several factors, such as the HIV/AIDS pandemic, the variable effectiveness of the BCG vaccine, lax drug adherence resulting in the emergence of multi-drug resistant strains (MDR-TB) and increased immigration from developing countries where TB has continued to be endemic (Figures 1.3 & 1.4). In fact, the concept of TB's imminent eradication cannot be further from reality (Murray & Salomon, 1998). In 1993 the World Health Organisation declared TB a global emergency, estimating that a third of the world's population are infected, equating to 2 billion people. With 8 million new cases reported each year and 2 million fatalities annually, *M. tuberculosis* is the biggest global killer amongst infectious diseases (Dye & Raviglione, 2005). These alarming statistics and the emergence of MDR-TB strains and extensively-

drug resistant (XDR-TB) strains have highlighted the urgency for the development of newer, more efficient antimicrobial agents (Blanchard, 1996; Pablos-Mendez *et al.*, 1998).

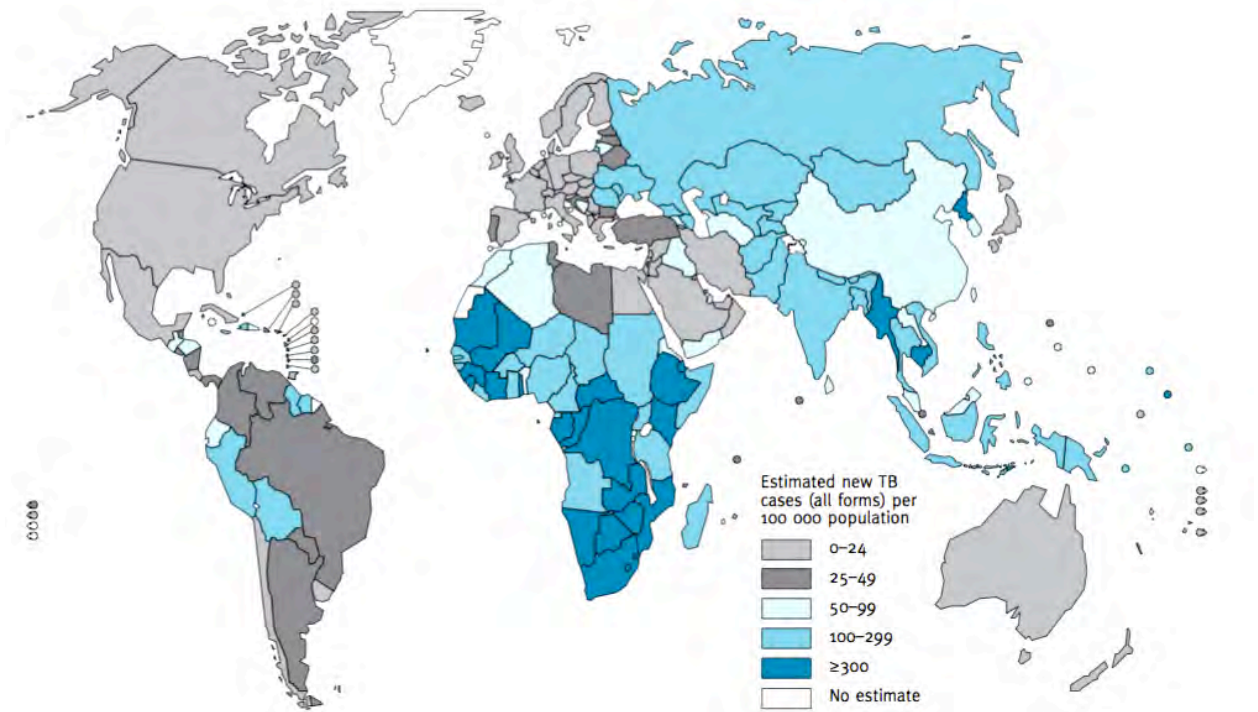


Figure. 1.3: Estimated TB incidence rates in the year 2009 (WHO, 2010).

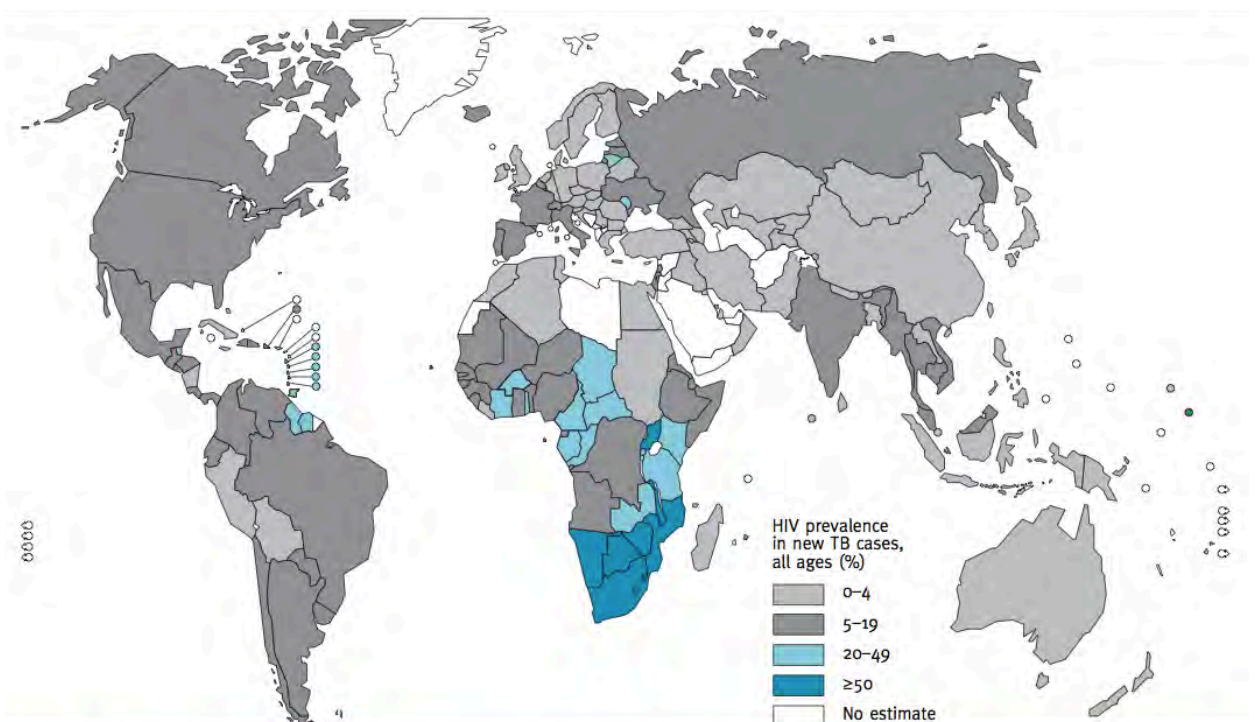
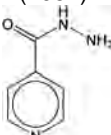
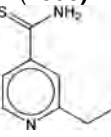
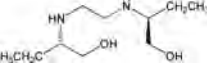
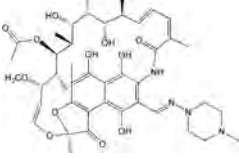
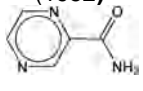
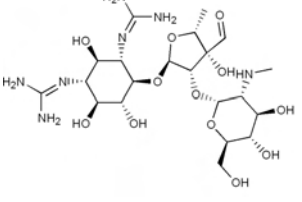


Figure. 1.4: Estimated HIV prevalence in new TB cases in the year 2009 (WHO, 2010).

1.5. TB drug treatments

The most commonly used TB drug regimens include the so-called front-line drugs, rifampicin (RIF), isoniazid (INH), pyrazinamide (PZA) and ethambutol (EMB) as shown in Table 1.2.

Table 1.2: Commonly used TB drugs and their targets. Adapted from Kremer & Besra, (2002); Nachega & Chaisson, (2003).

Drug	Drug mechanism of action	Genes involved in resistance	Function of gene
Isoniazid (INH) (1952) 	Inhibition of mycolic acid biosynthesis and other multiple effects on DNA, lipids, carbohydrates and NAD metabolism	<i>katG</i> <i>inhA</i> <i>ndh</i> <i>oxyR-aphC</i>	Catalase-peroxidase Enoyl-Acp reductase NADH dehydrogenase II Alkyl hydroperoxidase
Ethionamide (ETH) (1956) 	Inhibition of mycolic acid biosynthesis	<i>ethA</i> <i>inhA</i>	Flavin mono-oxygenase Enoyl-Acp reductase
Ethambutol (EMB) (1961) 	Inhibition of cell wall arabinogalactan (AG) biosynthesis	<i>embCAB</i>	Arabinosyltransferases
Rifampicin (RIF) (1966) 	Inhibition of transcription	<i>rpoB</i>	RNA polymerase
Pyrazinamide (PYR) (1952) 	Acidification of cytoplasm and de-energising the membrane	<i>pncA</i>	Nicotinamidase/pyrazinamide
Streptomycin (STREP) (1944) 	Inhibition of protein synthesis	<i>rpsL</i> <i>rrs</i>	S12 ribosomal protein 16S rRNA

In cases where INH resistance has occurred, streptomycin (STRP) is used as a replacement, although it is not preferred since there is a higher toxicity and a high incidence of STRP-resistant TB. The most effective drug regimen is endorsed by the WHO and is called Directly Observed Treatment, Short-course (DOTS), developed to fully supervise those patients deemed high-risk for non-drug adherence. This course consists of a 6-month treatment plan, where the initial phase is 2 months, involving the administration of INH, RIF, EMB and PZA. The remaining four months is known as the continuation phase, during which time different regimens may be followed depending on any resistance profiles, but generally involves taking RIF and INH (Farmer & Kim, 1998).

1.5.1. TB Drug resistance

The global problem of TB has been worsened by the development of drug resistant *M. tuberculosis* strains and is generally attributed to poor compliance with treatment. Lax drug adherence is associated with either lengthy duration of TB therapy, the tendency of patients to feel free of previous disease-like symptoms before course completion, therapy termination due to certain side effects, or unreliable drug supplies, all of which have accelerated MDR- and XDR-TB strains (Munro *et al.*, 2007). MDR-TB is defined as TB that is resistant to at least INH and RIF, the two most powerful first-line anti-TB drugs. Treatment in the case of MDR-TB can exceed 2 years, in comparison to drug-sensitive TB, which can be effectively treated with a 6-month regimen, thus significantly increasing costs and side effects. The incidence rates are increasing with 424,000 cases in 2004, up from 273,000 in 2000 (Aziz *et al.*, 2006; Zignol *et al.*, 2006), and a mortality rate of 27% in those infected with MDR-TB compared to 18% for drug-sensitive TB infections (World Health Organisation (WHO) 2007). XDR-TB has now disturbingly emerged; defined as MDR-TB that has developed additional resistance to three injectable second-line drugs (aminoglycosides) and one of the fluoroquinolones (CDC, 2006; World Health Organisation (WHO) 2007). Worryingly,

XDR-TB has been detected in 45 countries as disclosed by the WHO/IUATLD report for 2008, and is untreatable so far. This shows that control of drug-resistant TB incidence is somewhat inadequate, especially in regions with a high prevalence of HIV cases, where TB-HIV co-infections increase the susceptibility to re-infection, relapse and treatment failure (Nations *et al.*, 2006; Omerod, 2005). Therefore, there is a necessity to discover new specific antimicrobial compounds against *M. tuberculosis*.

1.6. The mycobacterial cell wall

The compositional complexity of the mycobacterial cell wall (Figure 1.5) distinguishes *Mycobacterium* species from the majority of other prokaryotes. Classified as Gram-positive organisms, their envelopes do in fact share notable features with Gram-negative cell walls, such as an outer permeability barrier acting as a pseudo-outer membrane (Brennan & Nikaido, 1995; Minnikin, 1982). Much of the early structural definition of the cell wall was conducted in the 1960s and 1970s (Lederer *et al.*, 1975; Petit *et al.*, 1969; Adam *et al.*, 1969). Minnikin, in 1982, proposed the currently accepted structural model for the cell wall architecture that was later supported by McNeil and Brennan (McNeil & Brennan, 1991; Minnikin, 1982; Minnikin *et al.*, 2002) and numerous further investigations (Besra & Brennan, 1995; Brennan & Nikaido, 1995; Minnikin, 1991; Nikaido *et al.*, 1993).

The structural features of the cell envelope can be divided into three major components;

1. the plasma membrane
2. the mycolyl-arabinogalactan-peptidoglycan (mAGP) complex (Besra & Brennan, 1997), consisting of three covalently linked macromolecules, peptidoglycan (PG), arabinogalactan (AG) and hydrophobic mycolic acids which decorate the non-reducing terminus of the arabinan domains

3. lipoarabinomannan (LAM), lipomannan (LM), non-covalently bound lipids and glycolipids.

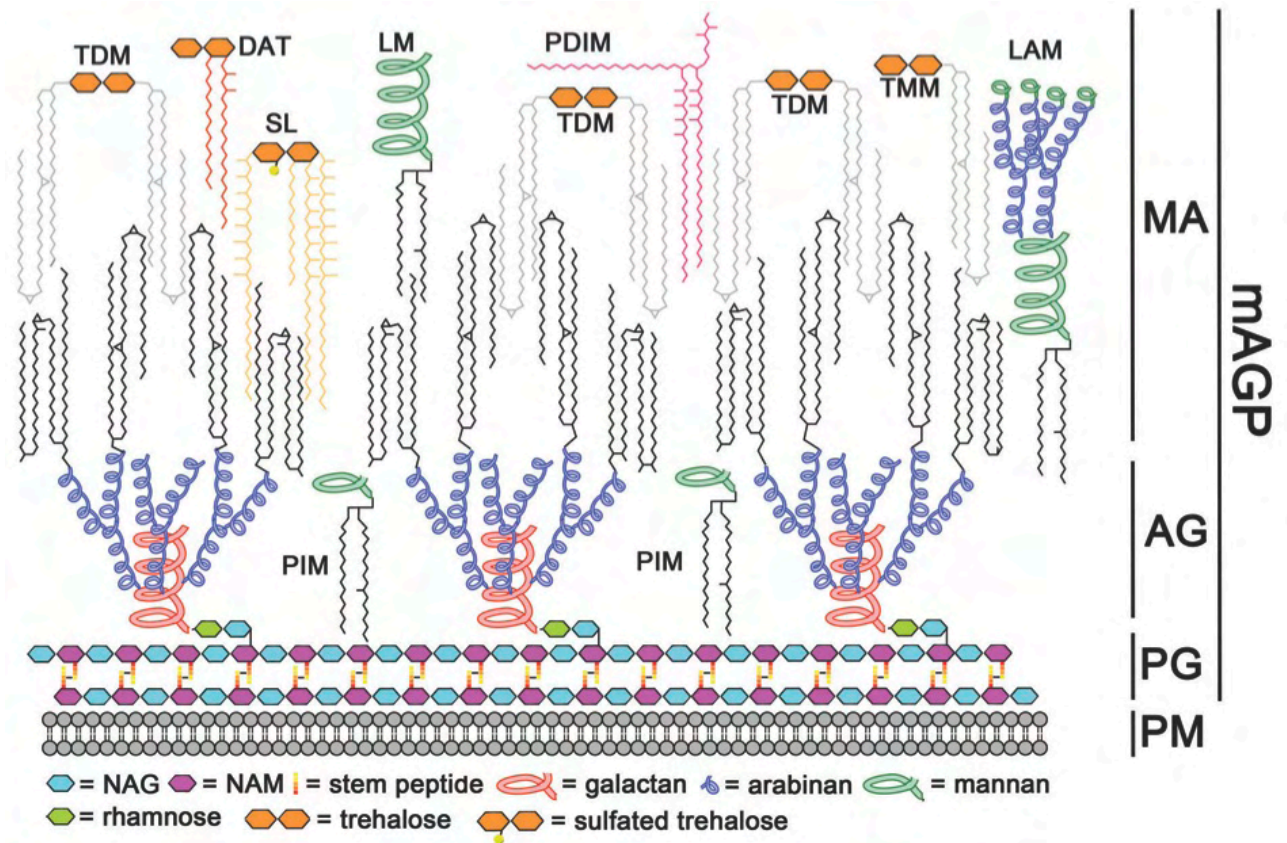


Figure 1.5: Schematic model of the mycobacterial cell wall. The major structural features of the cell wall of *M. tuberculosis* as proposed by Minnikin *et al.* (2002) and modified from Dmitriev *et al.* (2000). The cell envelope consists of a plasma membrane, a cell wall core, an outer membrane and a capsule. Lipoarabinomannan (LAM), mycolyl-arabinogalactan-peptidoglycan (mAGP), phthiocerol dimycocerosates (PDIM), peptidoglycan (PG), plasma membrane (PM), sulfated tetra-acyl trehalose (SL), diacyl trehalose (DAT), penta-acyl trehalose (PAT), trehalose monomycolate (TMM), trehalose dimycolate (TDM), N-acetylglucosamine (NAG), N-acetylmuramic acid (NAM), arabinogalactan (AG).

1.6.1. The cell wall of *M. tuberculosis* as a drug target

Mycobacterial diseases are especially problematic to treat owing to this unique cell wall architecture. This tightly packed, lipid rich envelope accounts for the inherent resistance of *M. tuberculosis* to various hydrophilic antimicrobials, as well as lipophilic molecules that have difficulty passing through this highly ordered mycolic acid layer. The cell wall is essential for growth and survival and cell wall inhibitors have been one of the most active agents of chemotherapy, and as such, the majority of front-line drugs target its biosynthesis (Zhang, 2005). Drug regimens employ at least one cell wall biosynthetic inhibitor, for instance INH and ETH, which target mycolic acid biosynthesis or EMB which inhibits arabinan biosynthesis, taken in combination with other chemotherapeutic agents that have intracellular targets (Nikaido & Jarlier, 1991). However, due to the emergence of various drug resistant strains as discussed previously, there is a need for the discovery of novel drug targets and the development of active compounds against them (Heymann *et al.*, 1999; Sreevatsan *et al.*, 1997b; Telenti *et al.*, 1997). In this regard, the biosynthetic machinery of mycobacterial cell wall represents an attractive target and numerous research studies have been and are being conducted, delving into the intricacies of the mycobacterial cell wall assembly (Bhatt *et al.*, 2007b; Bhowruth *et al.*, 2007; Brennan & Crick, 2007; Dover *et al.*, 2008).

1.6.2. Plasma membrane

The plasma membrane acts as a boundary between the cytosol and the periplasmic space, but it also harbours a number of substrates required by cell wall biosynthetic enzymes (Berg *et al.*, 2007), thus playing a crucial role in the biogenesis of the cell wall. A group of glycosylphosphoprenols associated with the plasma membrane have been identified and operate as sugar donor substrates for many of the TB glycosyltransferases. For instance, activated forms of **D**-ribofuranose (Wolucka *et al.*, 1994; Wolucka & de Hoffmann, 1995),

D-mannopyranose (Takayama & Goldman, 1970) and **D**-arabinofuranose (Wolucka & de Hoffmann, 1994; Wolucka *et al.*, 1994) have been identified. Many of the involved glycosyltransferases are either embedded in the lipid bilayer as integral membrane proteins, or associated with the membrane surface by hydrophobic and/or electrostatic interactions. For instance, topology studies of the EmbCAB proteins, the putative arabinofuranosyltransferases revealed 13 transmembrane domains (Telenti *et al.*, 1997). In addition, Alderwick *et al.* (2006b) recently discovered a further arabinofuranosyltransferase AftA, which also contains integral transmembrane spanning domains. It is believed that glycosyltransferases involved in the biosynthesis of the arabinans of both AG and LAM are all integral membrane proteins and are therefore classified as members of the glycosyltransferase family C (GT-C) (Berg *et al.*, 2007). With the exception of phosphatidylinositol mannosides (PIMs), which are constrained to Actinomycetales, the lipid composition of this biomembrane is similar to that of other prokaryotes, suggesting that the general properties of lipid bilayers are applicable for mycobacteria.

1.6.3. Structure and biosynthesis of peptidoglycan

Peptidoglycan (PG) is a complex macromolecular structure situated on the outside of the plasma membrane of almost all eubacteria (Schleifer & Kandler, 1972; van Heijenoort, 2001a, 2001b). Its mesh-like arrangement confers rigidity to the cell, allowing it to withstand osmotic pressure maintaining cell integrity and cellular shape. Relatively little is known about *M. tuberculosis* PG synthesis, although it is generally assumed to be akin to that of *E. coli* (van Heijenoort, 2001a, 2001b), also being classified as A1 γ according to the classification system of Schleifer & Kandler (1972). Mycobacterial PG forms the backbone of the mAGP complex, composed of alternating N-acetylglucosamine (GlcNAc) and modified muramic acid (Mur) residues, linked in a $\beta(1\rightarrow4)$ configuration (Lederer *et al.*, 1975). Unlike *E. coli* PG, the muramic acid residues in *M. tuberculosis* and *M. smegmatis*

for instance, contain a mixture of N-acetyl and N-glycolyl derivatives, whereby the N-acetyl function has been oxidised to a N-glycolyl function to form MurNGly (Mahapatra *et al.*, 2005a; Mahapatra *et al.*, 2005b; Raymond *et al.*, 2005). These additional glycolyl containing residues result in extra hydrogen bonding, strengthening the mesh-like structure (Brennan & Nikaido, 1995), as well as possibly protecting the organism from lysozyme degradation. Tetrapeptide side chains consisting of **L**-alaninyl-**D**-isoglutaminyl-*meso*-diaminopimelyl-**D**-alanine (Petit *et al.*, 1969) cross-link with identical short peptides of neighbouring glycan chains (van Heijenoort, 2007). These cross-links include the expected *meso*-diaminopimelic acid (DAP) and **D**-alanine bond, common to most prokaryotes, but also a high degree of bonds between two residues of DAP (Ghuysen, 1968; Wietzerkin *et al.*, 1974). The proportion of cross-linking in *Mycobacterium* species is 70-80%, significantly more so than *E. coli*, with only 50% (Vollmer, 2004). An additional deviation from *E. coli* PG, is the use of the muramic acid residues as attachment sites for the galactan domain of the arabinogalactan, whereby carbon-6 of some of the muramic acid residues form a phosphodiester bond and are linked to the α -**L**-rhamnopyranose-(1→3)- α -**D**-GlcNAc(1→P) linker unit of AG (Hancock *et al.*, 2002; McNeil *et al.*, 1990).

One model proposed for the three-dimensional topology of the mAGP complex, consistent with the traditional models of PG architecture (Ghuysen, 1968; McNeil & Brennan, 1991), suggests that the PG and the galactan moiety run parallel to the plasma membrane. However, an opposing model put forward by other modeling studies predict that the PG and the AG polymers may in fact be coiled and are thus orientated perpendicular to the plane of the plasma membrane (Dmitriev *et al.*, 2000; Dmitriev *et al.*, 2003). Minnikin and colleagues (2002) proposed that AG as well as LAM form coiled strands and integrate with PG. Although, recent published nuclear magnetic resonance (NMR) data concluded that the PG glycan strand is orthogonal to the plane of the membrane, thus the overall three-dimensional

structure and topology remains open to debate (Meroueh *et al.*, 2006). The biosynthesis of mycobacterial PG is comparable to that of *E. coli* and is shown in Figure 1.6.

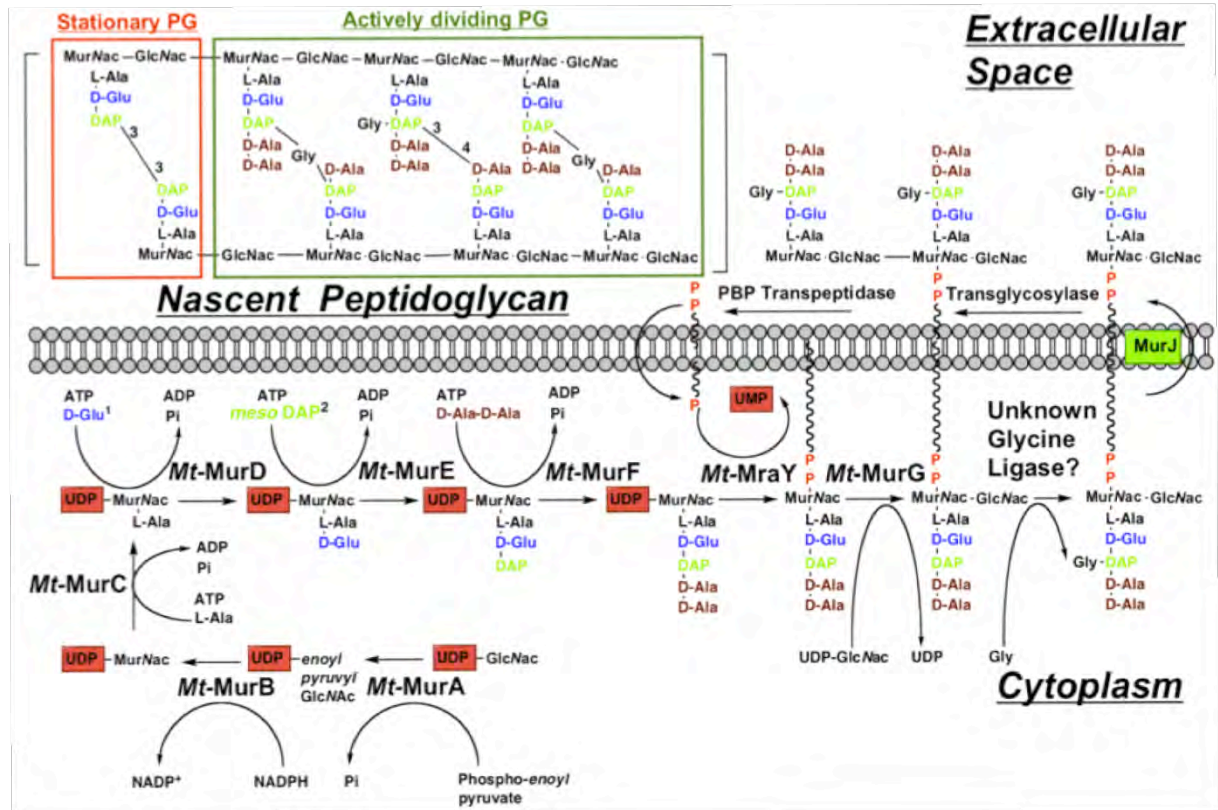


Figure 1.6: Biosynthesis of peptidoglycan in *M. tuberculosis*. The synthesis of the disaccharide-peptide monomer unit is initiated in the cytoplasm, catalysed by six enzymes, MurA to MurF. MurA transfers enolpyruvate from phosphoenolpyruvate to the 3-OH of UDP linked GlcNac, which is reduced to form UDP-MurNac by MurB (De Smet *et al.*, 1999; Goffin & Ghuyssen, 2002). The UDP-MurNac-pentapeptide is then formed via the sequential addition of L-alanine, D-glutamic acid, DAP and a D-alanyl-D-alanine dipeptide, to MurNac, by MurC, MurD, MurE and MurF, respectively (Mahapatra *et al.*, 2000). Lipid I synthesis involves MraY (MurX) transferring the modified MurNac residue to a polyprenyl phosphate carrier lipid, followed by addition of GlcNac by MurG (Ikeda *et al.*, 1991). The product, GlcNac-MurNac(pentapeptide)-diphosphoryl-undecaprenol (Lipid II) is then translocated across the membrane and incorporated into the growing PG by transglycosylases and further modified by transpeptidases (Bhakta & Basu, 2002; Goffin & Ghuyssen, 2002).

1.6.4. Biosynthesis of the linker unit

Mycobacterial viability rests heavily on the structural integrity of the cell wall, thus the attachment of which the AG proper is hinged to the PG layer is pivotal. Amar & Vilkas (1973), initially reported that AG is tethered to PG at intervals by a phosphodiester bond,

supported by the presence of muramyl-6-phosphate in the cell wall preparations from several mycobacterial species (Kanetsuna, 1968; Liu & Gotschlich, 1967). The fundamental question of the chemical nature of this link wasn't answered until 20 years later when oligosaccharides containing galactofuranose (Gal_f) from the galactan domain were isolated along with rhamnose (Rha) residues (McNeil *et al.*, 1990). The further discovery of the disaccharide **L-Rhap-(1→3)-D-GlcNAc** (Figure 1.7) led to the conclusion that these constituents make up the linkage unit and the inference that the GlcNAc is directly attached to the 6-position of a proportion of the muramyl residues of PG (McNeil *et al.*, 1990).

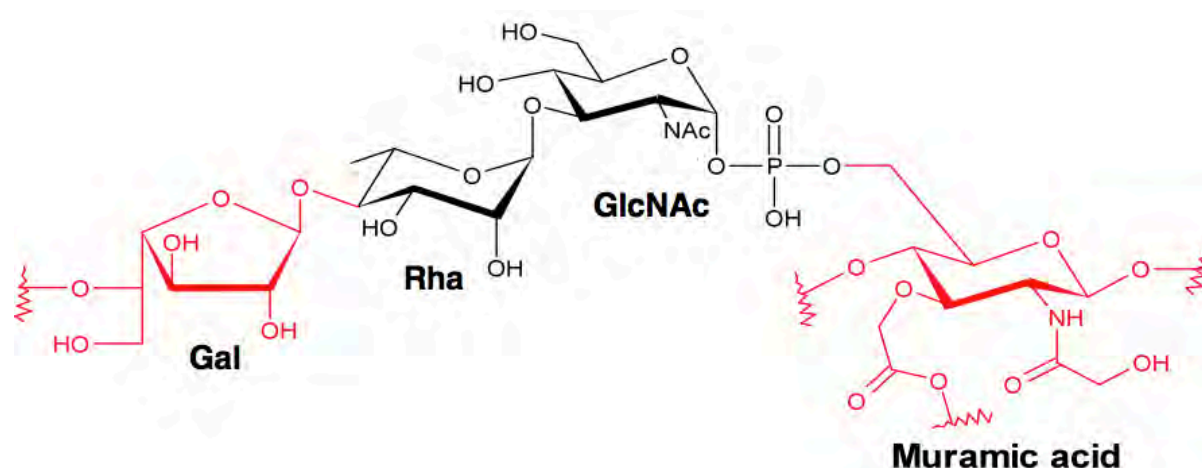


Figure 1.7: The Rha-GlcNAc linker unit. The molecular structure of the LU, the conduit between AG and PG. The reducing end of AG consists of the terminal sequence $\rightarrow 5\text{-D-Galf-(1}\rightarrow 4\text{)-L-Rhap-(1}\rightarrow 3\text{)-D-GlcNAc}$, attached to muramyl-6-P.

The crucial structural role of the linker unit (LU) (Figure 1.7) in the attachment of AG to PG, as well as the presence of **L-Rhamnose**, a sugar absent in humans, makes the biosynthetic machinery of the mycobacterial LU (Figure 1.8) an attractive drug target (Ma *et al.*, 2002). In *M. tuberculosis*, synthesis is initiated on the acceptor decaprenyl-phosphate (Dec-P or C₅₀-P), whereby GlcNAc-phosphate is transferred from UDP-GlcNAc, forming C₅₀-P-P-GlcNAc, referred to as glycolipid 1 (GL-1) (Mikusova *et al.*, 1996). The enzyme formerly known as Rfe (Rv1302, WecA) has been implicated as a decaprenyl-phosphate α -N-acetylglucosaminyltransferase by its significant homology to the *E. coli* WecA protein (Amer

& Valvano, 2002; Dal Nogare *et al.*, 1998), although there are no biochemical data as yet to definitively prove this supposition. The linkage region is completed by the subsequent addition of the Rha residue by the recently defined rhamnosyltransferase, WbbL (Rv3265c), to the 3-position of the GlcNAc of GL-1, forming glycolipid 2 (GL-2) (Figure 1.8) (Mills *et al.*, 2004). The key to these studies was with the successful complementation of an *E. coli* mutant with Rv3265c (*wbbL*) and subsequent restoration of rhamnosyltransferase activity (McNeil, 1999). Moreover, investigations from *M. smegmatis* have highlighted the essentiality of *wbbL* for bacterial viability (Mills *et al.*, 2004).

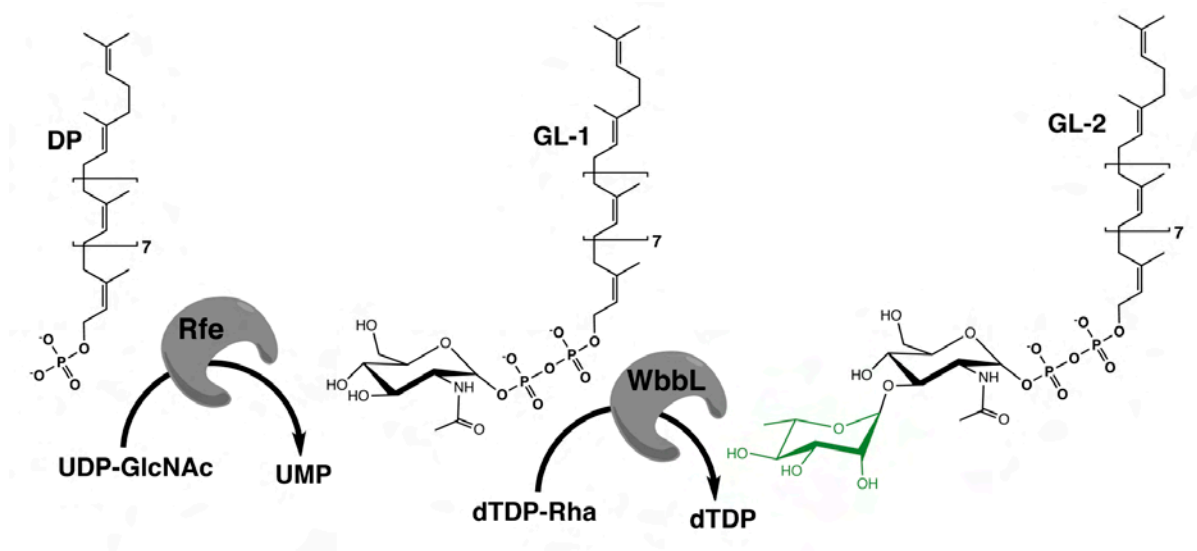


Figure 1.8: Formation of the linker unit - glycolipid-1 (GL-1) and glycolipid-2 (GL-2). α -GlcNAc-1-P is transferred from UDP-GlcNAc to decaprenol (DP) by the GlcNAc-1-phosphate transferase Rfe (Rv1302, WecA), followed by the attachment of a rhamnosyl residue from dTDP-Rha catalysed by WbbL (Rv3265c) (Mills *et al.*, 2004), resulting in Rha-GlcNAc-P-P-decaprenyl.

The *wbbL* gene product utilises the nucleotide donor dTDP-rhamnose for the formation of GL-2, so it stands to reason that the rhamnosyl biosynthetic pathway has come under scrutiny and a number of inhibitors have been described (Babaoglu *et al.*, 2003; Kantardjieff *et al.*,

2004; Ma *et al.*, 2001). Synthesis of dTDP-Rha occurs *via* a linear 4-stage pathway utilising the gene products of *rmlABCD* as depicted in Figure 1.9.

Recognition of the genes involved transpired by comparison to known polysaccharide biosynthetic enzymes found in other bacteria, namely *E. coli* (Ma *et al.*, 1997; Stevenson *et al.*, 1994; Weston *et al.*, 1997). RmlA (Rv0334) sets in motion the sequence of reactions, converting dTTP + α -D-glucose 1-phosphate to dTDP-glucose + PP_i (Ma *et al.*, 1997). The enzyme was cloned from *M. tuberculosis* and transformed into an *E. coli* strain devoid of four TDP-Rha biosynthetic genes. Cellular extract analysis revealed an abundance of α -D-Glc-P thymidyltransferase activity confirming its proposed function (Ma *et al.*, 1997). The product of RmlA activity is then shuttled through three sequential reactions catalysed by dTDP-D-glucose 4,6-dehydratase (Rv3464, RmlB), dTDP-4-keto-6-deoxy-D-glucose 3,5 epimerase (Rv3465, RmlC) and dTDP-Rha synthase (Rv3266, RmlD) (Hoang *et al.*, 1999; Ma *et al.*, 2001; Stern *et al.*, 1999). Li *et al* (2006) demonstrated that *rmlB* and *rmlC* genes are also essential for mycobacterial growth.

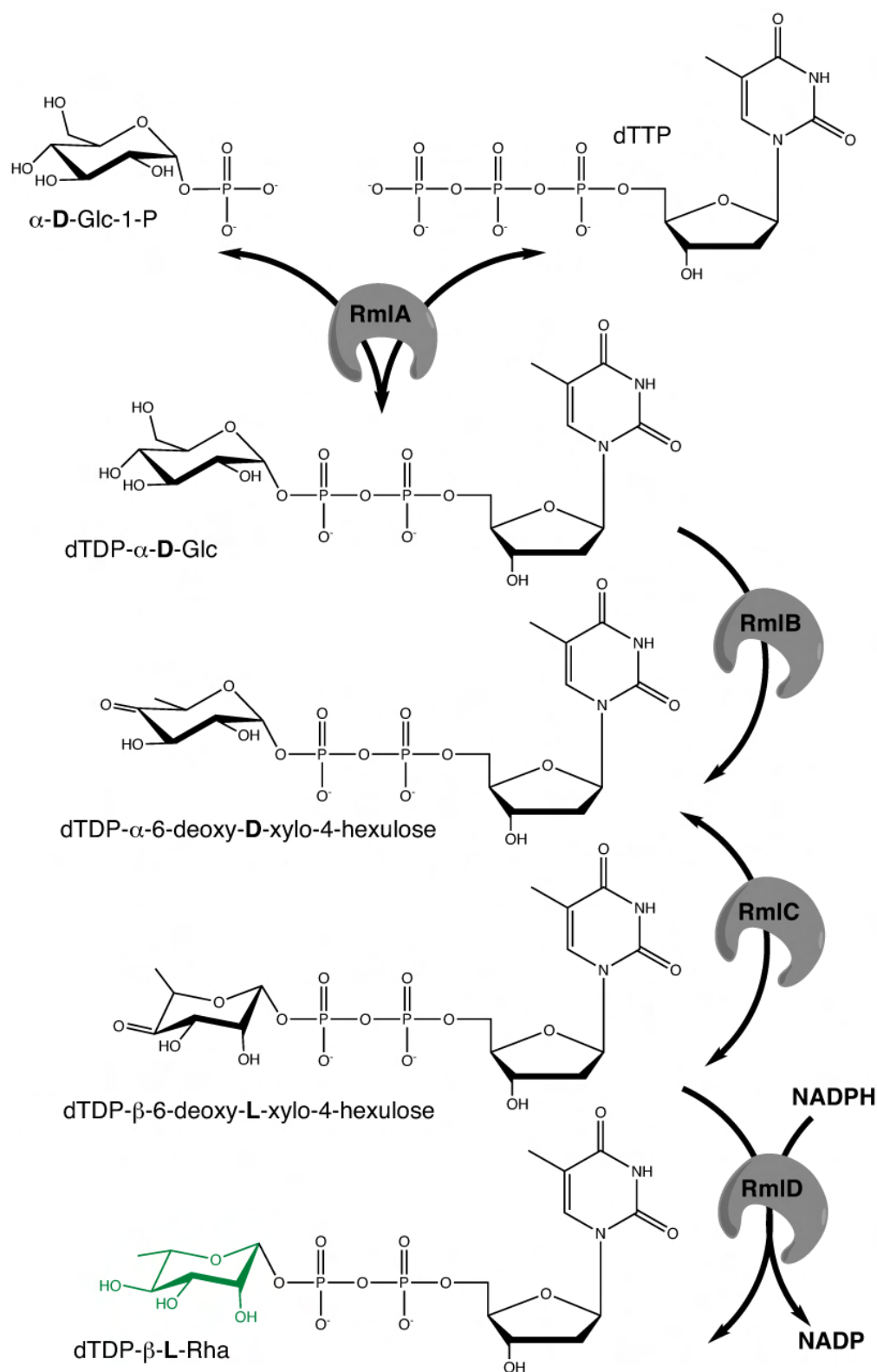


Figure 1.9: Biosynthetic pathway of dTDP-rhamnose. A series of enzymes converts glucose-1-phosphate (α -D-Glc-1-P) to dTDP-Rha. RmlA (Rv0334) = α -D-glucose-1-phosphate thymidyl transferase (Ma *et al.*, 1997), RmlB (Rv3464) = dTDP-D-glucose 4,6-dehydratase (Ma *et al.*, 2001), RmlC (Rv3465) = dTDP-4-keto-6-deoxy-D-glucose (Stern *et al.*, 1999), and RmlD (Rv3266c) = dTDP-rhamnose synthetase (Hoang *et al.*, 1999).

1.6.5. Arabinogalactan

1.6.5.1. Structural features of arabinogalactan

Exclusive to the Actinomycetales, the mAG complex is a key structural component which makes up the bulk of the cell wall (Minnikin *et al.*, 2002). Arabinogalactan (AG), the unique heteropolysaccharide, is covalently tethered to the PG *via* a phosphodiester bond to approximately 10-12% of the muramic acid residues of PG (Amar & Vilkas, 1973; Misaki *et al.*, 1974). Collectively, PG and AG, form a covalently linked network positioned between the plasma membrane and the mycolic acid layer, resulting in an exceptionally robust cell wall. Early work demonstrated that the polymer was composed predominantly of arabinose and galactose (Azuma *et al.*, 1968; Kanetsuna, 1968; Kanetsuna *et al.*, 1969; McNeil *et al.*, 1987; Misaki *et al.*, 1966). Both sugars are in the furanoid ring form, **D**-galactofuranosyl (Galf) and **D**-arabinofuranosyl (Araf), which are extremely rare in nature (McNeil *et al.*, 1987). Detailed characterisation of oligomers generated from partial depolymerisation of per-*O*-alkylated AG and the use of methylation analysis, gas-chromatography-mass spectrometry (GC-MS), fast atom bombardment-mass spectrometry (FAB-MS) and NMR spectroscopy established the detailed structure of this complex and the fact that unlike most bacterial polysaccharides, AG lacks repeating units being composed of a few distinct structural motifs (Besra *et al.*, 1995; Daffé *et al.*, 1990; McNeil *et al.*, 1990; McNeil *et al.*, 1991; Vilkas *et al.*, 1973). The use of *endo*-arabinofuranosidases secreted from a *Cellomonas* species provided additional support for the obtained structural data as well as revealing further insights (McNeil *et al.*, 1994). AG consists of a linear galactan composed of 30 linear alternating $\beta(1\rightarrow5)$ and $\beta(1\rightarrow6)$ Galf residues (Abou-Zeid *et al.*, 1982; McNeil *et al.*, 1987; Vilkas *et al.*, 1973), attached to the rhamnosyl residue of the linker unit. Three apparently similar **D**-arabinan chains comprised of 22 or 23 Araf residues are affixed to the C-5 of the $\beta(1\rightarrow6)$ linked Galf (Besra *et al.*, 1995). Recent studies by Alderwick *et al* (2005) ascertained that the arabinan chains are attached specifically to the 8th, 10th and 12th Galf

residue, data congruent with Besra *et al.* (1995) who recognised long stretches of unbranched galactan, leading to the prediction that the chains are attached near the reducing end. It seems that the arabinan domain is present as a highly branched network built on a backbone of $\alpha(1\rightarrow5)$ linked sugars with a number of $\alpha(1\rightarrow3)$ linked residues forming 3,5-Araf branch points (Daffé *et al.*, 1990). Further $\alpha(1\rightarrow5)$ linked Araf sugars are attached subsequent to this branch point with the non reducing ends terminated by $\beta(1\rightarrow2)$ Araf residues. The final structural motif is the distinctive hexa-arabinoside (Ara₆) (McNeil *et al.*, 1994) present as (Araf- $\beta(1\rightarrow2)$ -Araf- $\alpha(1\rightarrow)_2 \rightarrow$ 3,5-Araf- $\alpha(1\rightarrow5)$ -Araf- $\alpha(1\rightarrow5)$), of which two-thirds are mycolated (Figure 1.10).

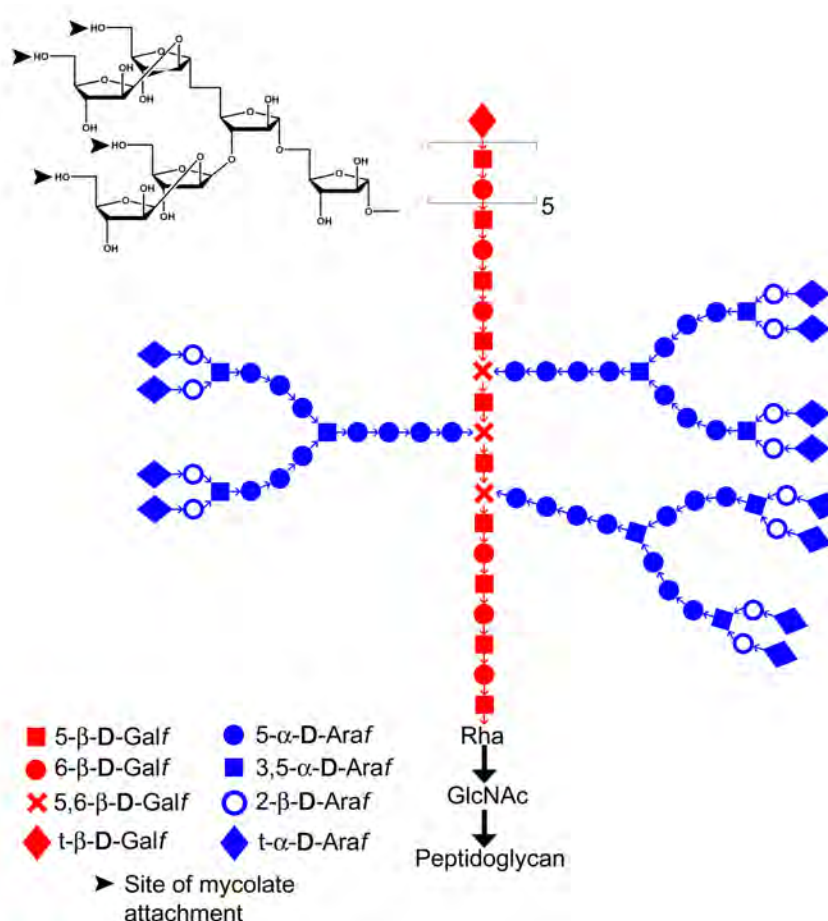


Figure 1.10: Structural features of arabinogalactan. Pictorial representation of the arabinogalactan of *M. tuberculosis* as defined by McNeil *et al.* (1987), Daffé *et al.* (1990), McNeil *et al.* (1994) and Besra *et al.* (1995). Three chains of arabinan are attached to each galactan chain, of which two-thirds are substituted with mycolic acids.

Research emphasis has now shifted somewhat from structural analysis to biosynthesis. The complete sequencing of the mycobacterial genome has provided major impetus in the identification and the study of the enzymes involved in the biosynthesis of this exceptional structure, with the hope of uncovering new drug targets.

1.6.5.2. Synthesis of arabinogalactan biosynthetic precursors

1.6.5.2.1. Galactan precursor synthesis

D-galf residues, the main constituents of the galactan component of the mAGP complex, do not exist in mammalian metabolism, thus their biosynthesis constitutes an appealing target for chemotherapy without any deleterious side effects. Galf residues of the galactan domain are incorporated from the high-energy sugar nucleotide donor UDP-Galf, which is formed *via* two reactions. In *E. coli*, galactosyl residues in the pyranose ring form (UDP-Galp) are synthesised by the action of UDP-glucose 4-epimerase on UDP-glucopyranose (UDP-Glcp), the protein of which is encoded by the *galE* gene (Lemaire & Muller-Hill, 1986). Weston *et al.* (1997) assayed for the reverse reaction in *M. smegmatis* using radiolabeled UDP-Galp and UDP-glucose 4-epimerase activity was observed, of which the purified protein and its N-terminal sequence was shown to be similar to *M. tuberculosis* Rv3634. Conversion of UDP-Galp to the furanose form occurs *via* ring contraction catalysed by the enzyme UDP-galactopyranose mutase (Glf) that was first recognised in *E. coli* (Nassau *et al.*, 1996) and subsequently in *M. smegmatis* and *M. tuberculosis* (Rv3809c) (Weston *et al.*, 1997) and is summarised in Figure 1.11. Allelic exchange experiments of *glf* in *M. smegmatis* highlighted the essentiality of this gene (Pan *et al.*, 2001).

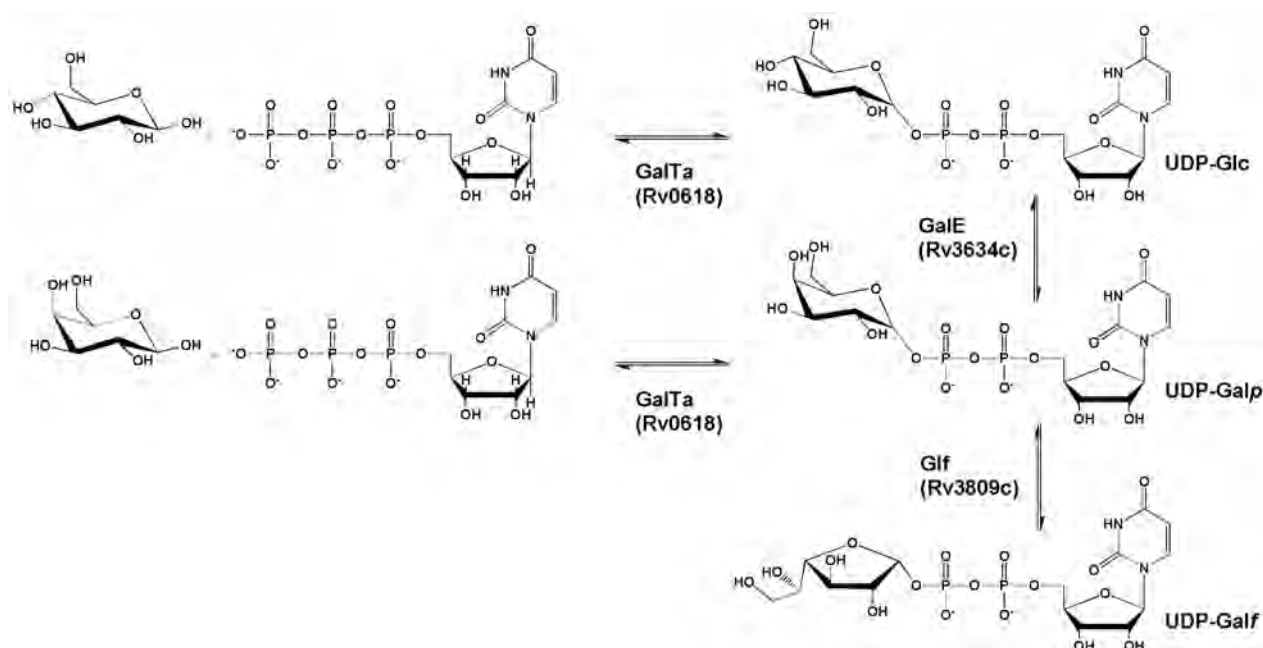


Figure 1.11: Formation of galactan precursors. Adapted from Pan *et al.* (2001). UDP-glucose (UDP-Glc) is converted to UDP-galactopyranose (UDP-Galp), catalysed by UDP-galactopyranose epimerase (Rv3634) (Weston *et al.* 1998). Glf, a UDP-galactopyranose mutase (Rv3809c), subsequently converts UDP-Galp to UDP-Galf.

1.6.5.2.2. Arabinan precursor synthesis

Endeavours to uncover sugar nucleotides of Araf have proven unsuccessful. Arabinan biosynthesis in the Actinomycetales involves β -D-arabinofuranosyl-1-monophosphodecaprenol (DPA), the only known donor of Araf residues (Alderwick *et al.*, 2005; Wolucka *et al.*, 1994; Xin *et al.*, 1997). Synthetically derived DP[^{14}C]A and an array of synthetic acceptors have determined that DPA provides Araf units in the *in vitro* formation of 2-linked and 5-linked arabinofuranosyl linkages present in the arabinans of AG and LAM (Belanger *et al.*, 1996; Lee *et al.*, 1997; Xin *et al.*, 1997). The use of DPA and endogenous acceptors from membrane preparations produced a structure identical to the natural polymer, with equal distribution of radiolabel, highlighting that the lack of 3-linked linkages was not due to another unidentified activated donor and most likely the inability of the $\alpha(1\rightarrow3)$ AraT

to recognise the acceptor. Subsequent assays discovered other DPA dependent AraTs, the so-called “priming” enzyme AftA (Rv3792), was responsible for the addition of the first AraT to the galactan domain, as well as demonstrating conclusively that DPA is the only donor in the related organism *C. glutamicum* (Alderwick *et al.*, 2005).

Due to the important role of DPA, elucidation of its biosynthetic pathway has received much attention. The recognised biosynthesis of such polyprenylphosphate sugars chiefly involves the donation of a glycosyl residue from a sugar nucleotide to the polyprenylphosphate, interestingly the sugar nucleotides of arabinose (UDP-Ara or GDP-Ara) have not been identified. The carbon skeleton of the arabinosyl residues (Figure 1.12) are derived from the non-oxidative pentose shunt (Scherman *et al.*, 1995), after which, ribose 5-phosphate and ATP react with the assistance of a pRpp synthetase to produce pRpp (Wolucka *et al.*, 2008). The 5-phospho- α -**D**-ribose 1-pyrophosphate:decaprenyl phosphate 5-phosphoribosyl transferase (Rv3806c), or UbiA transfers ribose-5-phosphate from pRpp to decaprenylphosphate to form DPPR (Huang *et al.*, 2005). The final stages involve dephosphorylation of DPPR and epimerisation at the C-2 anomeric hydroxyl of the ribose moiety by Rv3790 (DprE1) forming the putative intermediate, decaprenylphosphoryl-2-keto- β -**D**-erythro-pentofuranose (DPK) (Mikusova *et al.*, 2005). Subsequent reduction by Rv3791 (DprE2) results in the completed arabinose donor DPA. Studies on the enzymes involved in the complete pathway to **D**-arabinose await thorough biochemical characterisation.

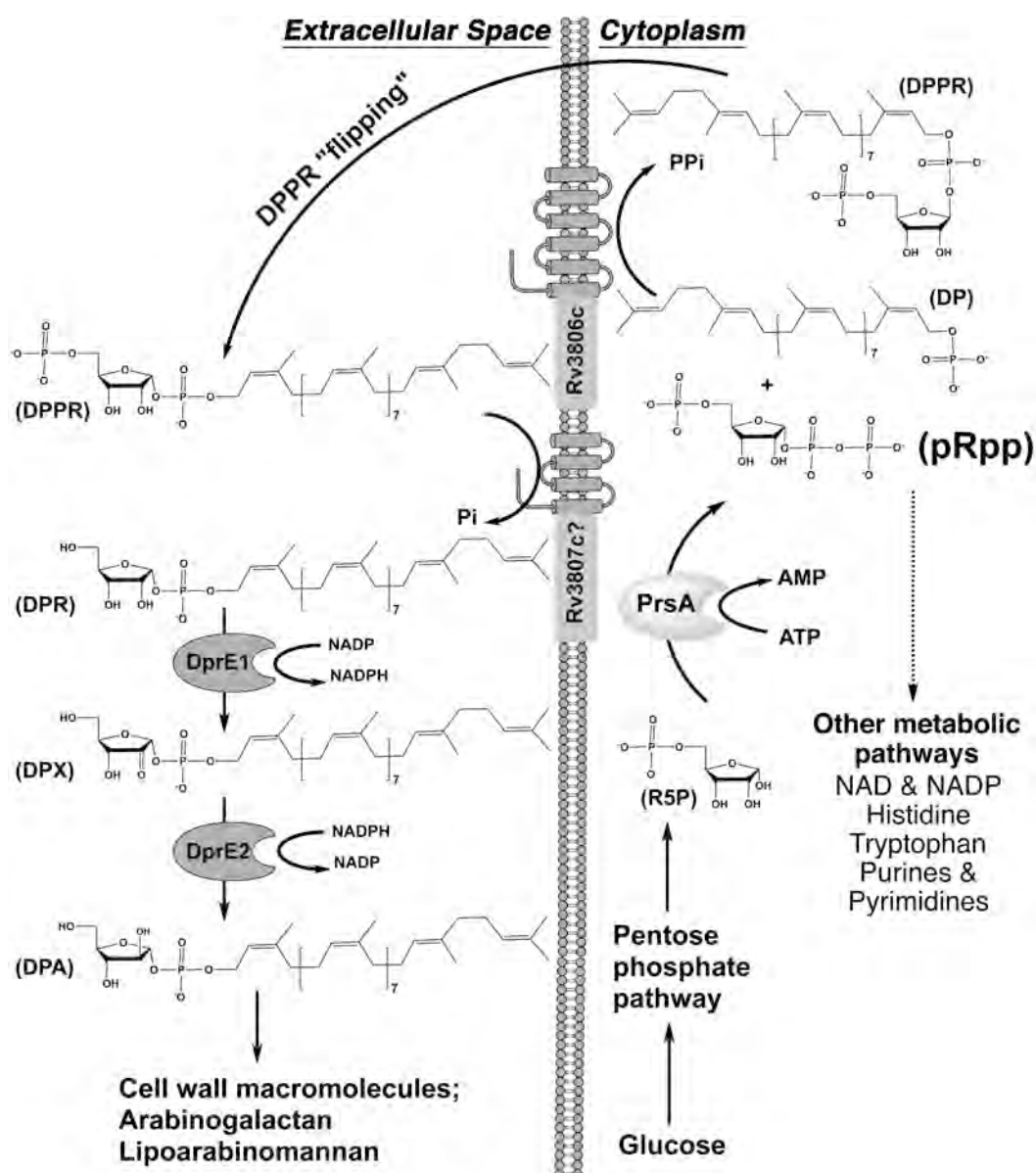


Figure 1.12: Formation of arabinan precursor DPA. The carbon atoms of the Ara_f residues are derived from the pentose shunt pathway. α -D-ribose-5-phosphate (R5P) is then acted on by PrsA a pRpp synthetase, which catalyses the addition of a diphosphate moiety from ATP to the carbon-1-OH (Alderwick *et al.*, 2010). The formation of decaprenylphosphoryl-D-arabinose (DPA) then proceeds with the transfer of ribose-5-phosphate from pRpp to decaprenylphosphate to form decaprenylphosphoryl-5-phosphoribose (DPPR). DPPR then undergoes dephosphorylation to decaprenol-1-monophosphoribose (DPR) and epimerisation of the ribosyl unit at carbon 2-OH position. DprE1 (Rv3790), a FAD-containing oxidoreductase is responsible for oxidising the ribosyl carbon-2-OH producing the keto sugar decaprenol-1-monophosphoryl-2-keto- β -erythro-pentofuranose (DPX). This is the reduced to DPA DprE2 (Rv3791, a decaprenylphosphoryl-2-keto-D-erythropentose reductase (Mikusova *et al.*, 2005).

1.6.5.3. Galactan biosynthesis

The assortment of glycosyl linkages within the galactan moiety leads to the supposition that at least two to four Galf transferases (GalTs) are involved in its biosynthesis (Crick *et al.*, 2001). It was predicted that one GalT could be specifically designed to recognise the LU (C_{50} -P-P-GlcNAc-Rha or GL2) catalysing the $\beta(1\rightarrow4)$ linkage allowing galactan formation to begin and then another to add the following Galf units. Indeed, Mikusova *et al.* (2000, 2006) recognised Rv3782 (Glft1) as the putative GalT responsible for the initial transfer of possibly two Galf residues from UDP-Galf, forming C_{50} -P-P-GlcNAc-Rha-Galf (GL-3) and C_{50} -P-P-GlcNAc-Rha-Galf-Galf (GL-4) (Alderwick *et al.*, 2008; Mikusova *et al.*, 2006).

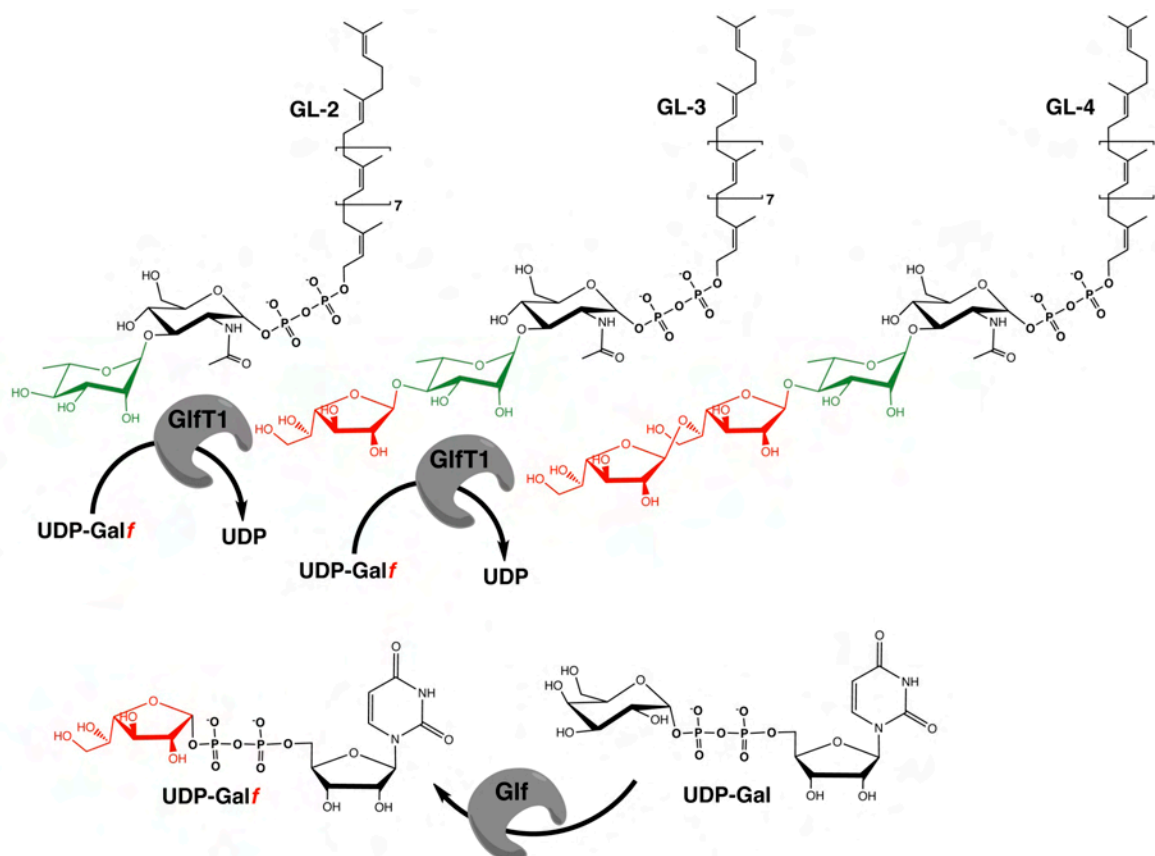


Figure 1.13: Polymerisation of galactan - biosynthesis of GL-4. The first two galactosyl sugars are added to the rhamnosyl residue of the linker unit *via* Glft1 (Rv3782) (Mikusova *et al.*, 2006).

Rv3782 was implicated as a possible GalT due to the observations that there is significant sequence identity with portions of Rv3808c a known GalT (discussed below), which is classified as an inverting glycosyltransferase-2 (GT-2) of the GT-A superfamily. In addition, Rv3782 is also situated in the putative “AG biosynthetic gene cluster” (Mikusova *et al.*, 2006). Kremer *et al.* (2001a) reported the first GalT with the identification of Rv3808c (Glft1) through the use of a novel neoglycolipid acceptor assay, together with UDP-Galf and isolated *E. coli* membranes expressing the aforementioned gene (Kremer *et al.*, 2001a). It was demonstrated that the enzyme has dual functionality, acting both as a UDP-Galf:β-D-(1→5) GalT and the UDP-Galf:β-D-(1→6) GalT, responsible for the polymerisation of approximately 30 Galf residues with alternating β(1→5) and β(1→6) linkages (Kremer *et al.*, 2001; Rose *et al.*, 2006).

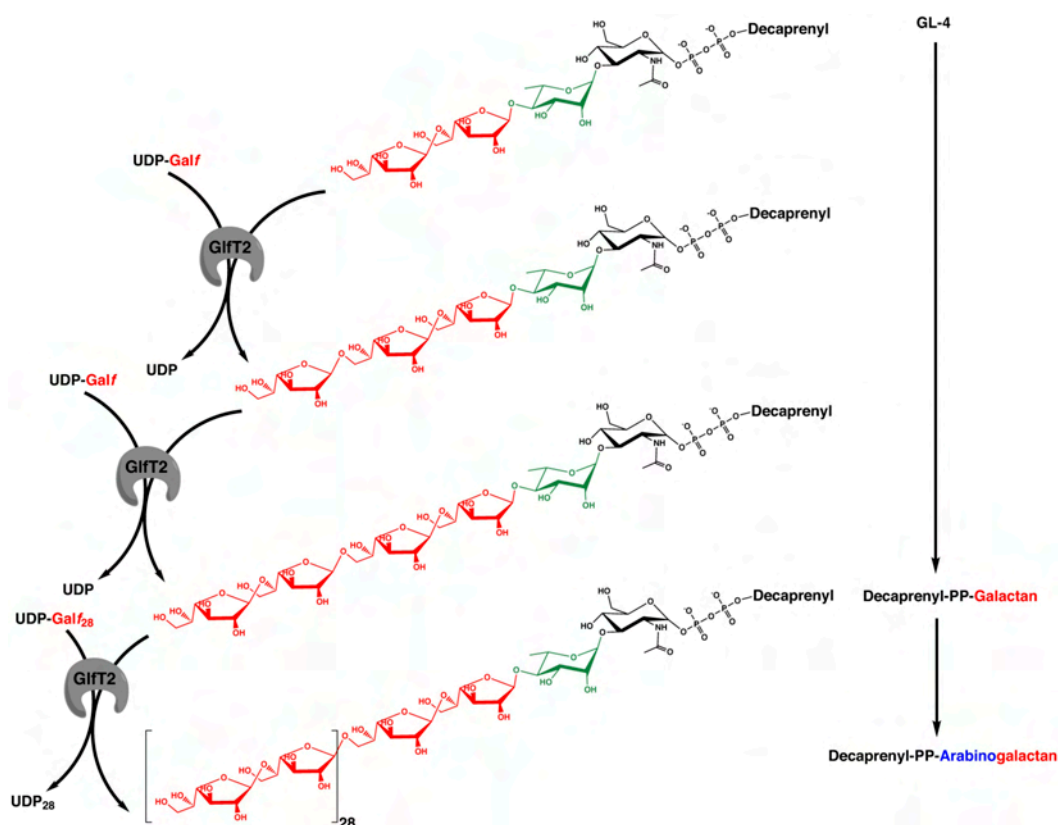


Figure 1.14: Polymerisation of galactan. The bifunctional galactosylfuranosyl transferase GlfT2 (Rv3808c) adds the remaining alternating β(1→5) and β(1→6) galactosyl residues to GL-4.

1.6.5.4. Arabinan biosynthesis

1.6.5.4.1. Ethambutol inhibition and its use in the identification of the Emb proteins

The arabinan homopolymer is a pivotal structure in both AG and LAM, the two major cell wall polysaccharides. Accordingly, it is considered one of the most prominent mycobacterial structures being targeted by the frontline drug EMB ((*S,S'*)-2,2'-(ethylenediimino)di-1-butanol). EMB is a synthetic compound that was first recognised as an anti-mycobacterial agent in 1961 (Thomas, 1961). Early work by Kilburn & Greenberg observed an unanticipated increase in viable cells during the initial four hours after addition of EMB to *M. smegmatis* cultures. It was postulated that large bacillary clusters disaggregated due to a possible reduction in lipid content, which would lead to the apparent increase in colony-forming units (CFU) (Kilburn & Greenberg, 1977). This theory was supported by Takayama and coworkers who conducted a series of early studies into the effects of the EMB on *M. smegmatis*, reporting that inhibition of mycolic acid transfer into the cell wall and the simultaneous accumulation of trehalose-monomycolate (TMM), trehalose-dimycolate (TDM), and free mycolic acids occurred within 15 minutes of drug administration (Kilburn & Takayama, 1981; Takayama *et al.*, 1979). This suggested that the target might be a mycolyltransferase responsible for the transfer of mycolic acids onto the arabinan polymer. However, it was later discovered that the earliest point of drug inhibition occurred during arabinan synthesis demonstrated by the immediate inhibition of incorporated label from [¹⁴C]-glucose into the cell wall **D**-arabinose monomers (Takayama & Kilburn, 1989), whilst synthesis of the galactan of AG remained unaffected (Mikusova *et al.*, 1995). Furthermore, the arabinans of both AG and LAM were disturbed, although inhibition of label into the latter was less pronounced and at a later stage of its biosynthesis (Deng *et al.*, 1995; Mikusova *et al.*, 1995).

The generation of EMB-resistant *M. smegmatis* mutants greatly aided the discovery of the primary EMB target, implicating it as an arabinan specific inhibitor. This was illustrated by Mikusova *et al.*, (1995), who subjected an EMB-resistant strain to sub-inhibitory levels of EMB (10µg/ml) showing that the resistant mutant produced “normal” cell wall AG but a truncated version of LAM due to arabinan inhibition. Extending this observation using higher concentrations of EMB, Khoo *et al.* (1996) reported that the degree of truncation in LAM was dose dependent and at higher concentrations, the arabinan of AG was also impaired. Collectively, these studies indicate that the effects of EMB on the synthesis of both arabinan moieties are uncoupled, and the time difference of inhibition implies that synthesis occurs *via* distinct pathways, involving multiple AraT targets with varying EMB sensitivities. A number of concurrent EMB studies provided evidence of an accumulation of DPA, the source of Araf residues in arabinan biosynthesis, confirming that EMB effects were not due to inhibition of Araf donor synthesis but rather its utilisation (Lee *et al.*, 1995; Wolucka *et al.*, 1994). Taken together, all the evidence points to arabinan polymerisation, specifically the arabinan of AG, as the primary target of EMB.

A major breakthrough in the discovery of the precise EMB cellular target arose through exploitation of a moderately resistant strain from the related *M. avium* species. The genomic library from the aforementioned strain was screened and over-expressed in an otherwise susceptible *M. smegmatis* host, leading to the identification of a resistance conferring region encompassing three complete open reading frames (ORFs), *embR*, *embA* and *embB* (Belanger *et al.*, 1996). Moreover, use of an EMB-sensitive cell-free arabinan biosynthetic assay demonstrated that arabinosyltransferase activity was restored with *embAB* over-expression. Interestingly, neither *embA* or *embB* alone was sufficient to confer multi-copy resistance, thus supporting the supposition that they are translationally coupled forming a multienzyme complex (Belanger *et al.*, 1996). EMB resistance was also used to identify the *embCAB* gene

cluster from *M. smegmatis*, which was subsequently characterised in *M. tuberculosis* and *M. leprae*, all of which possess the same syntenic organisation (Lety *et al.*, 1997; Telenti *et al.*, 1997) and encode homologues of the *embA* and *embB* genes from *M. avium*. Escuyer *et al.* (2001) created individual genetic knockouts in *M. smegmatis*, *embC*, *embA* and *embB*, all of which were viable, with the most profound affects observed in the *embB* mutant. Individual inactivation of *embA*, and *embB* resulted in the diminished incorporation of arabinose into AG, specifically, the terminal disaccharide β -D-Araf-(1 \rightarrow 2)- α -D-Araf, normally situated on the 3-OH of the 3,5-linked Araf residue.

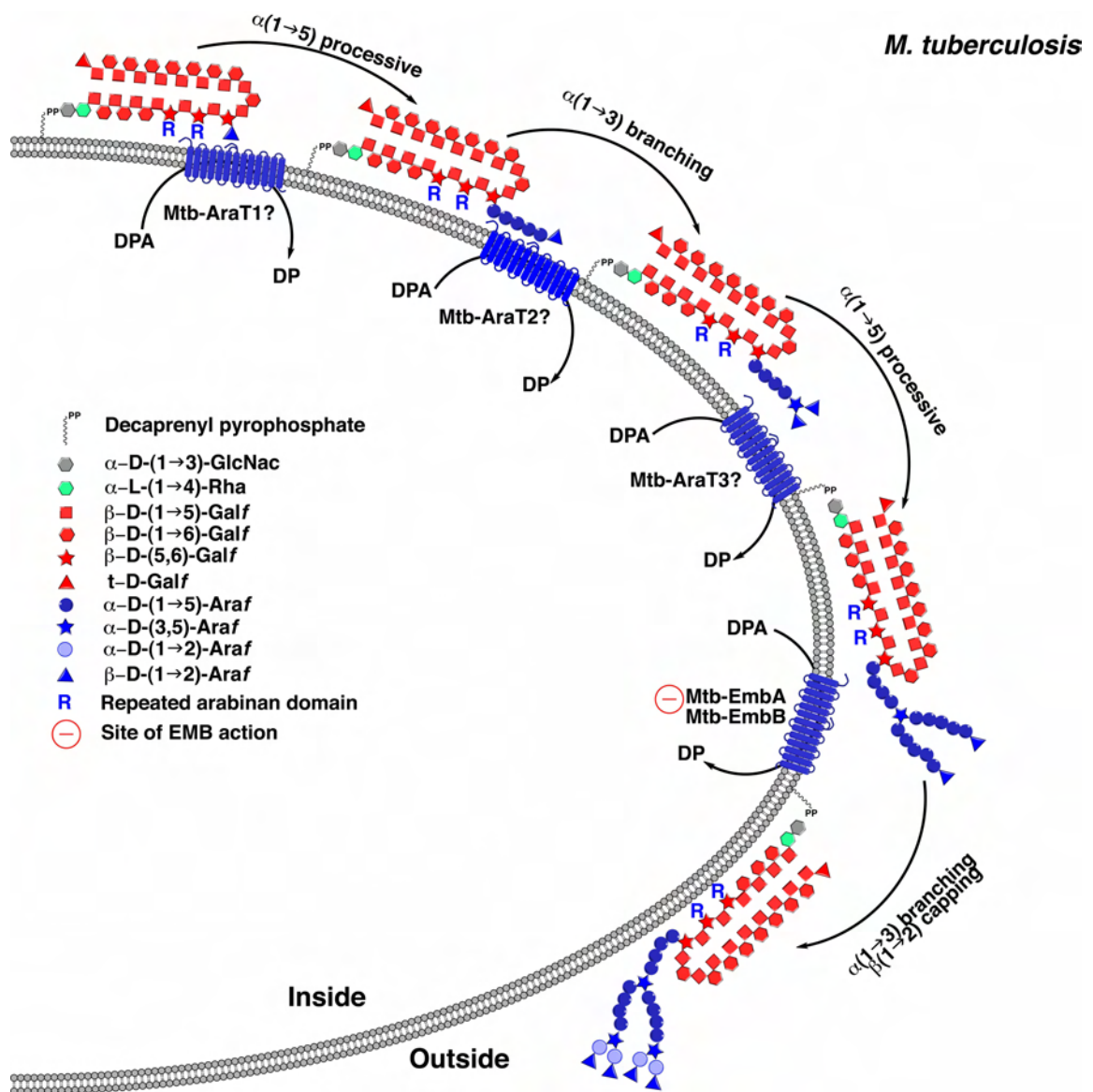


Figure 1.15: Schematic presentation of arabinogalactan biosynthesis.

Thus, a substantial amount of the otherwise Ara₆ motifs were present as terminal linear Ara₄ structures akin to the terminal motif of LAM (Escuyer *et al.*, 2001), also leading to a loss of cell wall bound mycolates. Based on the above observations, it appears that the Emb proteins could be involved in Ara₆ biosynthesis, with the authors suggesting that the EmbA/EmbB proteins could both act as $\alpha(1\rightarrow3)$ AraTs. Indeed, Khasnobis *et al.* (2006), assayed for the putative activity of EmbA/EmbB, using cell-free preparations from wild-type *M. smegmatis* and demonstrated the formation of the non-reducing terminal disaccharide, which were absent in both *embA* and *embB* mutants. Moreover, the transferase activity was re-established upon mixing the membrane preparations from the disrupted strains with wild-type membranes.

1.6.5.4.2. EMB resistance

Identification of the *emb* gene cluster has provided the opportunity to analyse the molecular basis of resistance of mycobacteria to EMB. Telenti *et al.* (1997) demonstrated that high-level resistance to EMB in *M. smegmatis* could be related to either overproduction of the Emb protein(s), a structural mutation in a conserved region of EmbB, or both. A number of reports presented additional genetic evidence for a key role of the EmbB protein in cell wall biosynthesis highlighting the fact it is the most EMB-sensitive protein in the gene cluster (Alcaide *et al.*, 1997). Mutations in EmbB have been recorded in up to 65% of EMB resistant clinical isolates of *M. tuberculosis*, with the majority of mutations present at codon 306 or in the immediate surrounding area (Lety *et al.*, 1997; Ramaswamy *et al.*, 2000). This region is highly conserved amongst mycobacteria and topological analysis of the Emb proteins (Telenti *et al.*, 1997) positioned this EMB resistance-determining region (ERDR) in the second intracellular loop of EmbB (Sreevatsan *et al.*, 1997b). Five distinct mutations have been recognised at codon 306, resulting in a substitution of the wild-type methionine with isoleucine, leucine or valine (Sreevatsan *et al.*, 1997b). Other mutations have been identified

in the second intracellular loop region and the large-C terminal globular region of EmbB (Ramaswamy *et al.*, 2000). It should be noted that there are a number of EMB resistant strains that do not possess ERDR mutations, thus other genes may be involved in EMB resistance.

1.6.5.4.3. Identification of novel arabinofuranosyltransferases and the use of *C. glutamicum* as a model organism

Efforts to generate viable *embA/embB* mutants in *M. tuberculosis* and an *embAB* double mutant in *M. smegmatis* have so far proven unfruitful, highlighting their essentiality (Mills *et al.*, 2004; Pan *et al.*, 2001; Vilcheze *et al.*, 2000). The *Corynebacteriaceae* taxon, as previously discussed, encompasses *Mycobacterium* species as well as *Corynebacterium* species, such as *C. diphtheriae* and *C. glutamicum*. The corynebacteria possess a comparable cell wall core and have previously been shown to serve as a useful model organism in the study of essential orthologous *M. tuberculosis* genes (Gande *et al.*, 2004; Gibson *et al.*, 2003; Radmacher *et al.*, 2005). Centred on this observation, Alderwick *et al.* (2005) successfully constructed a *C. glutamicum* mutant with its singular *emb* gene disrupted (Cg-*emb*). *Corynebacterium* are deemed the archetype of *Corynebacteriaceae* since they maintain a low frequency of gene duplications and modifications, thus it is reasonable that *C. glutamicum* possesses only one *emb* gene. Surprisingly, Cg-*emb* exhibited higher identity to *embC*, even though *C. glutamicum* lacks an elaborately arabinosylated LM product (Dover *et al.*, 2004; Tatituri *et al.*, 2007a). Chemical analyses of the tolerable Cg-*emb* deletion mutant revealed an almost total loss of cell wall arabinan, except terminal *t*-Araf residues decorating the galactan backbone (Alderwick *et al.*, 2005). Moreover, EMB treatment of wild-type *C. glutamicum* produced an identical profile to that of the mutant, illustrating that Cg-*emb* is indeed the target of EMB and furthermore, there is another AraT responsible for “priming” the galactan backbone. Disruption of the decaprenyl transferase orthologue Cg-*ubiA*, involved in formation of the lipid-linked sugar donor DPA, resulted in total ablation of Araf

residues indicating that the unidentified AraT was also DPA dependent (Alderwick *et al.*, 2005).

By virtue of DPA's role as the only arabinose donor, it follows that all of the AraTs will be dependent on this polyprenyl-linked sugar. The Emb proteins, although novel, possess membrane topologies consistent with other glycosyltransferases (GTs) that use lipid-linked precursors, and do not resemble the more typical nucleotide-diphosphate (NDP) sugar donor requiring GTs. The Carbohydrate-Active enZymes (CAZy) have classified GTs into approximately 87 families with 3 large structural superfamilies, GT-A, GT-B and GT-C (Berg *et al.*, 2007; Unligil and Rini, 2000; Liu and Mushegian, 2003). GT-A and GT-B are NDP-sugar utilising, predominantly soluble and peripheral membrane proteins. The GT-C superfamily embody polyprenyl-linked sugar donor dependent, integral membrane proteins, all of which contain 8-13 predicted transmembrane (TM) domains, with typically low sequence similarity, but a conserved amino acid motif, called the DxD motif, generally positioned in the first or second predicted extracytoplasmic loop. The modified DxD motif (e.g., DxE, ExD, DDx, DEx, or EEx) lies upstream of a conserved proline motif, both of which are located in the same predicted loop and have been so called the "GT-C motif" (Berg *et al.*, 2007). The actual mechanism is unknown but this motif may be responsible for the binding of a lipid-linked sugar donor and/or catalytic activity. The Emb proteins have been classified as GT-Cs, comprising approximately 1100 amino acids and 12-13 TM spanning regions (Berg *et al.*, 2005). Considering the other putative AraTs will utilise the same substrate, it follows that they will share these structural similarities.

1.6.5.4.4. Identification and functional role of AftA

The identity of the novel “priming” AraT, arabinofuranosyltransferase AftA (Rv3792), which is responsible for priming the 8th, 10th and 12th Galf residues for further attachment of $\alpha(1\rightarrow5)$ -linked Araf units, was addressed by Alderwick *et al.* (2006b).

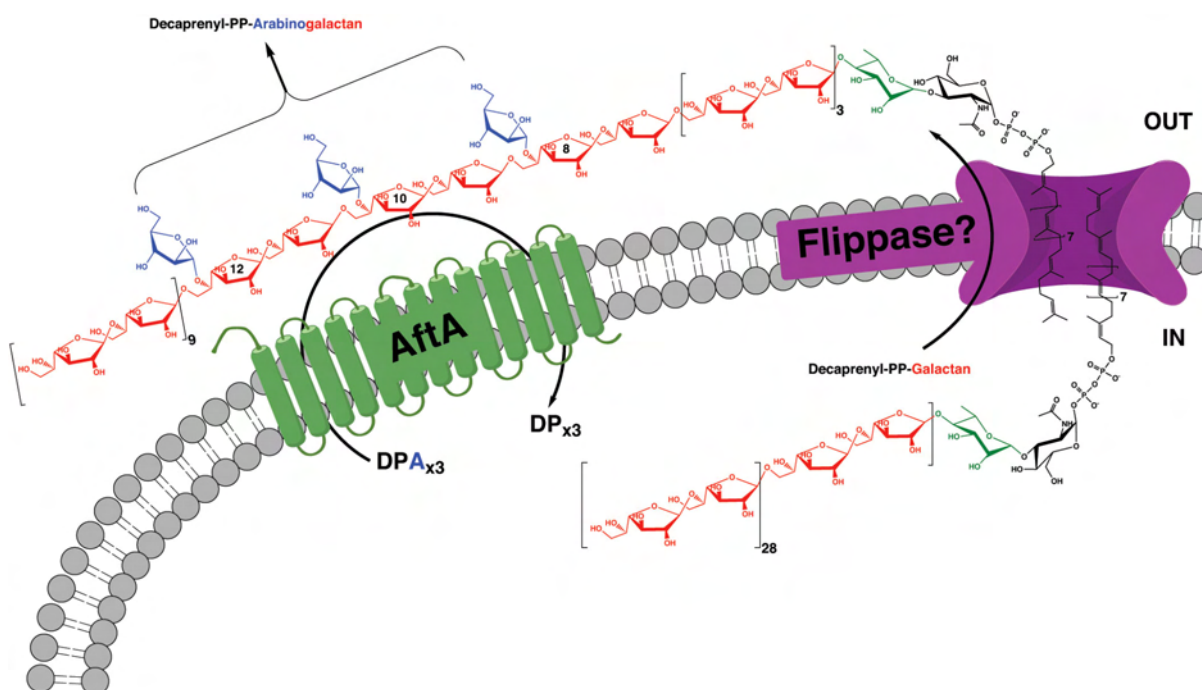


Figure 1.16: Early arabinogalactan formation. The biosynthesis of the arabinan of AG is initiated by AftA (Rv3792), an integral membrane protein responsible for priming the decaprenyl-PP-galactan for further elaboration by arabinosyltransferases (Alderwick *et al.*, 2005). The Araf residues derived from DPA are affixed to the carbon-5 hydroxyl of the 8th, 10th and 12th β -(1 \rightarrow 6) linked Galf residues of the galactan chain.

Genome comparisons of the *Corynebacterianae* *emb* locus revealed a highly conserved gene situated after the DPPR epimerising enzymes and adjacent to *embC*. Although AftA proteins show no significant sequence identity to the Emb proteins, they do possess a notably similar domain organisation and localisation to that of EmbC, with an array of conserved amino acids comparable to the GT-C motif. Contrary to the Emb proteins, AftA only encodes for 643 amino acids with 11 predicted TM domains; however, it is proposed to contain an Emb analogous C-terminal region directed towards the periplasm. AftA is essential for *M. tuberculosis* (Sasseti *et al.*, 2003); hence its orthologue was successfully disrupted in *C.*

glutamicum producing a cell wall lacking Araf units (Alderwick *et al.*, 2005). Furthermore, *E. coli* membranes expressing *M. tuberculosis* AftA exhibited AraT activity, specifically transferring arabinose from DPA to a galactan acceptor, which was shown to be EMB resistant (Alderwick *et al.*, 2006b).

1.6.6. Mycolic acids

Mycolic acids and their homologs have been defined as high molecular weight α -alkyl, β -hydroxy fatty acids (Asselineau & Lederer, 1950). These fatty acids differ in length across species, consisting of 70-90 carbons in mycobacteria (Goodfellow & Minnikin, 1981; Lechevalier *et al.*, 1986) and 22-38 carbons in their corynebacterial counterparts, the corynomycolic acids. In *M. tuberculosis*, these long chain fatty acids are extremely hydrophobic, containing a meromycolate chain (up to C₅₆) with a saturated α -side chain (C₂₄-C₂₆). Studies have shown that there are three distinct structural categories of mycolic acids, depending on the chemical modifications present in the meromycolate chain. These include the α -mycolates, which are the most abundant form, containing no oxygenated functional groups in the meromycolate branch and two cyclopropane rings that are in the *cis* configuration (Minnikin *et al.*, 2002; Qureshi *et al.*, 1978; Yuan *et al.*, 1995). Ketomycolates and methoxymycolates on the other hand, are oxygenated species with only one cyclopropane ring in the *cis* and *trans* configuration, respectively (George *et al.*, 1995). The cyclopropane rings contribute to the structural integrity of the cell wall complex (George *et al.*, 1995), and protect the bacillus from oxidative stress by hydrogen peroxide (Yuan *et al.*, 1995). Deletion of the methoxy- and ketomycolates (Dubnau *et al.*, 2000) and removal of the proximal cyclopropane ring of the α -mycolic acids (Glickman *et al.*, 2000) leads to considerable attenuation of virulence in mouse models. Thus, the fine structure of mycolic acids is coupled to the virulence of *M. tuberculosis*.

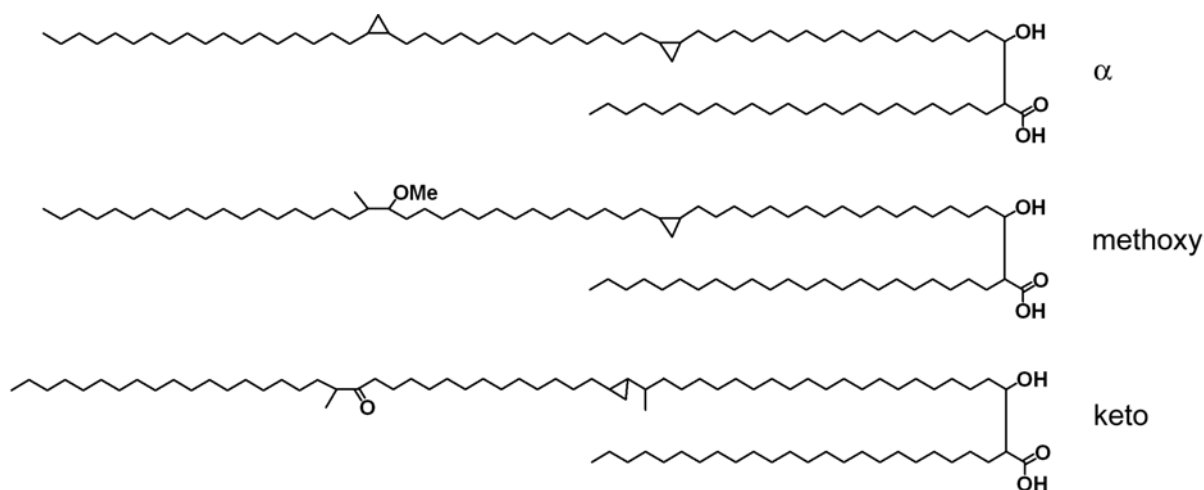


Figure 1.17: Structures of representative mycolic acids from *M. tuberculosis*. Modified from Minnikin *et al.* (2002).

1.6.6.1. Biosynthesis of mycolic acids

The fatty acid synthase-I (FAS-I) and fatty acid synthase-II (FAS-II) pathways are the two systems responsible for the biosynthesis of the mycolic acids (Bloch, 1977; Bloch & Vance, 1977). FAS-I is a multifunctional polypeptide encoded by the gene *fas* (*Rv2524c*) (Smith *et al.*, 2003). This single polypeptide contains all the functional domains required for the generation of short chain acyl-Coenzyme A (acyl-CoA) primers, which are either fed into the FAS-II pathway or become the C₂₆ α -alkyl branch of the mycolic acids. FAS-I begins *de novo* fatty acid synthesis by utilising acetyl-CoA and malonyl-CoA, elongating the acetyl group by two carbons in each cycle (Heath & Rock, 2002). These substrates are only available for the FAS-I pathway upon activation *via* a thioester linkage to the prosthetic group of Coenzyme A. The intermediates remain associated to the polypeptide during the complete process; transacylation passes them from one active site of one domain to the active site of the next in the following sequence: acyltransferase, enoyl reductase, dehydratase, malonyl/palmitoyl transferase, acyl carrier protein (ACP), β -ketoacylreductase and β -keto synthase (Smith *et al.*, 2003).

The FAS-II system is not capable of *de novo* fatty acid synthesis, thus relying on FAS-I for its acyl-CoA substrate. An additional FAS-II substrate is malonyl-AcpM, an activated primer (Kremer *et al.*, 2001; Schaeffer *et al.*, 2001). Malonyl-AcpM is synthesised by the malonyl-CoA:AcpM transacylase mtFabD from malonyl-CoA and phosphopantothienylated *holo*-AcpM. AcpM has the vital role of steering acyl intermediates between enzymes, initially shuttling malonyl-AcpM to an acyl-CoA primer derived from the FAS-I pathway, allowing the two substrates to undergo a condensation reaction catalysed by mtFabH (Choi *et al.*, 2000). The AcpM-acyl precursor, β -ketoacyl-ACP is then reduced by MabA/FabG1 to β -hydroxyacyl-AcpM (Banerjee *et al.*, 1998; Marrakchi *et al.*, 2002), which is subsequently dehydrated by a β -hydroxyacyl-AcpM dehydratase (Rv0636) (Sacco *et al.*, 2007; Brown *et al.*, 2007). InhA, an enoyl-AcpM reductase; the target of the INH, performs the enoyl-reduction, resulting in an AcpM-bound acyl chain, which is now two carbon units longer through the complete enzyme cycle. The cycle is then repeated several times, except for the substitution of mtFabH with the β -ketoacyl-AcpM synthases, KasA (Rv2245) or KasB (Rv2246), which catalyse the condensation of the acyl-AcpM and the new malonyl-AcpM, further elongating the chain by two carbon units (Figure 1.15) (Bhatt *et al.*, 2005; Bhatt *et al.*, 2007; Gao *et al.*, 2003; Kremer *et al.*, 2002a; Schaeffer *et al.*, 2001b; Slayden & Barry, 2002).

The final step in the synthesis of the mycolic acids was proposed by Walker *et al.* (1973) using a *C. diphtheriae* model, and later in *M. tuberculosis* by Takayama & Qureshi (1975). The proposed Claisen-type condensation of C₂₆-S-CoA and meromycolyl-AMP has been described as the final step carried out by Pks13, the type I polyketide synthase family protein. Prior to the participation of Pks13, each meromycolyl-S-AcpM from the FAS-II pathway are converted into meromycolyl-AMP by FadD32 (Triverdi *et al.*, 2004), a specific fatty acyl-AMP ligase.

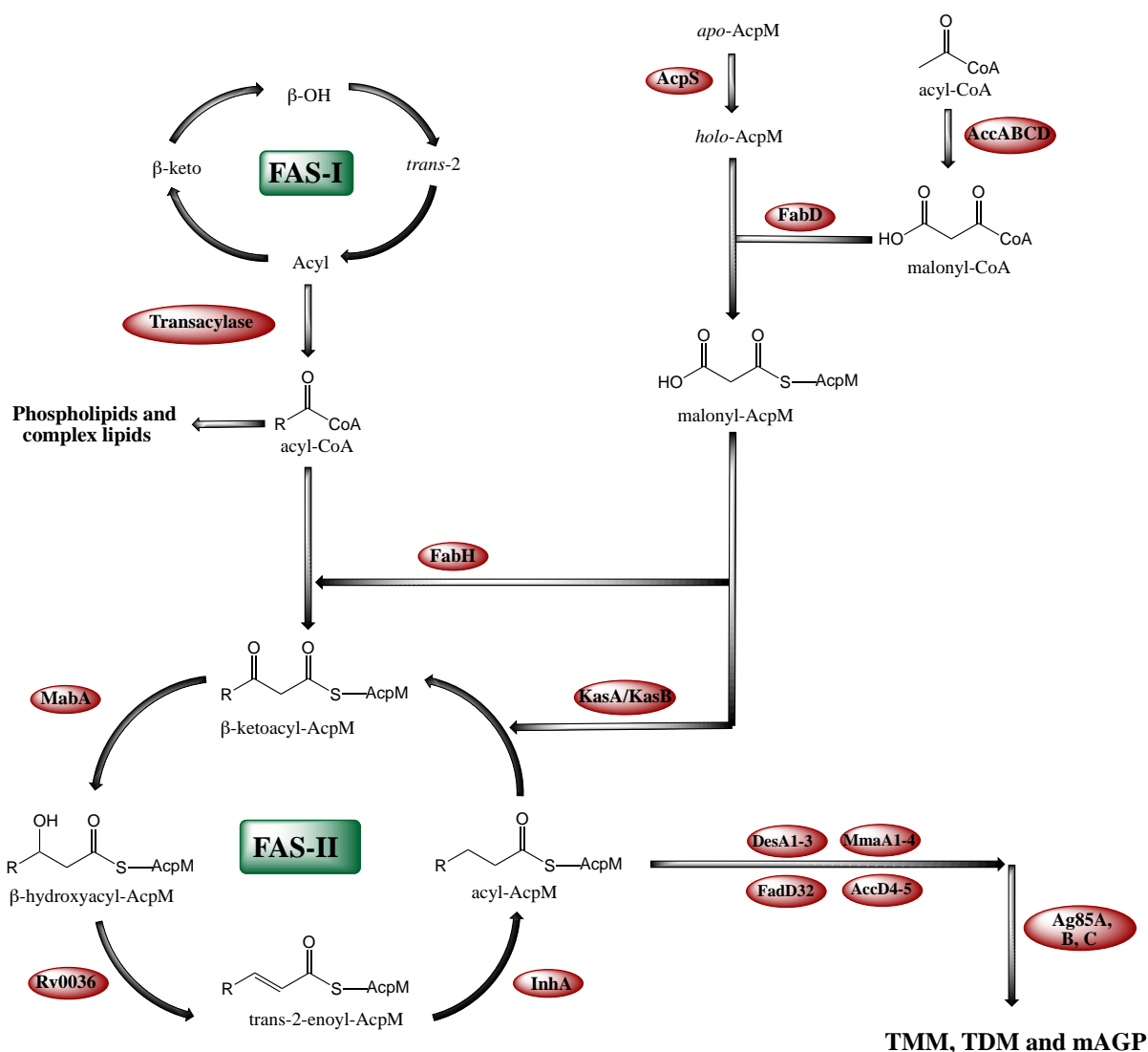


Figure 1.18: Mycolic acid biosynthesis in *M. tuberculosis* (Adapted from Bhowruth *et al.*, 2008). mtFabD converts malonyl-CoA to malonyl-AcpM, which is then ligated by mtFabH to FAS-I derived C₁₄-CoA. The FAS-II system (KasB/A, MabA, InhA, and Rv0636) continues to process the C₁₆ acyl-AcpM product producing mercomycolates (C₅₆). The meromycolic acid precursors are ligated to a FAS-I synthesised C₂₆ fatty acid that constitutes the α-branch of the final mycolic acid. Mycolic acids are then formed *via* the condensation of the α-branch and the meromycolate by polyketide synthase Pks13.

The C₂₆-S-CoA released from FAS-I is carboxylated by AccD4 (Rv3799c) and AccD5 (Rv3280), the acyl-CoA carboxylases, yielding 2-carboxyl-C₂₆-CoA. This is followed by Pks13 thioester binding of the two substrates, C₅₂-meromycolyl and 2-carboxyl-C₂₆-acyl group to the N-terminus and C-terminus PPB domains, respectively (Takayama *et al.*, 2005). Subsequent reactions occur generating the mature C₇₈-mycolate (Lea-Smith *et al.*, 2007) (as

shown in Figure 1.18). A series of mycolyltransferases are believed to be involved in the transfer of mycolic acids to their outer cell wall position. Mycolates are also present in free, solvent-extractable trehalose conjugates TMM and TDM (Asselineau & Lederer, 1950; Minnikin, 1982; Minnikin *et al.*, 2002), of which TMM is present both intra- and extracellularly, leading to the possible implication that it is responsible for the transport of extracellular mycolates and mycolyl components of the mAGP (Takayama *et al.*, 2005). TMM, a key precursor for the biosynthesis of TDM is dephosphorylated and translocated across the membrane, whereby three mycolyltransferases Ag85A, Ag85b and Ag85c synthesise TDM and transfer mycolic acids to the arabinan termini (Belisle *et al.*, 1997; Takayama *et al.*, 2005).

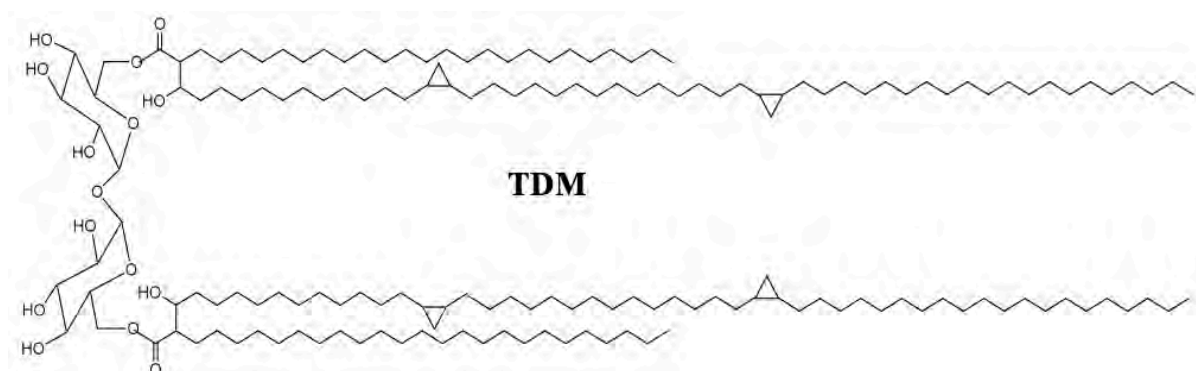


Figure 1.19: Structure of TDM

1.6.7. Structural features of lipoarabinomannan (LAM) and related biosynthetic precursors (LM and PIMs)

The mycobacterial cell wall's core framework, the mAGP complex, provides a template for the insertion of an abundance of mannosylated molecules, such as lipoarabinomannan (LAM) and its structurally related glycolipids, lipomannan (LM) and phosphatidylinositol mannosides (PIMs) (Besra *et al.*, 1997; Brennan & Ballou, 1967; Brennan & Ballou, 1968b; Brennan & Nikaido, 1995; Hill & Ballou, 1966; Morita *et al.*, 2004). These highly complex immunomodulatory lipoglycans are found ubiquitously in the envelopes of all mycobacterial

species, non-covalently associated to the plasma membrane and/or the mycolic acid layer *via* a conserved phosphatidyl-*myo*-inositol (PI) anchor (Hunter & Brennan, 1990), which extends to the exterior of the cell wall (Besra & Brennan, 1997; Belanger & Iamine, 2000; Nigou *et al.*, 2003). LAM is composed of numerous structural domains, the aforementioned PI anchor, as well as a polysaccharidic backbone consisting of **D**-mannan and **D**-arabinan and several distinct capping motifs.

1.6.7.1. Phosphatidyl-*myo*-inositol mannosides (PIMs)

The PI linker is based on a *sn*-glycero-3-phospho-(1-**D**-*myo*-inositol) unit, whereby, the glycerol phosphate component is attached to the L-1-position of *myo*-inositol (Ballou *et al.*, 1963; Ballou & Lee, 1964) and mannopyranosyl (*Manp*) residues decorate positions C-2 and C-6 of the inositol ring, constituting phosphatidylinositol dimannoside (PIM₂). This anchor shows a high degree of heterogeneity with regard to its multiple acylation states, with four potential sites, two of which are present on the glycerol unit, one on the *Manp* unit linked to C-2 of *myo*-inositol and the fourth at the C-3 position of *myo*-inositol (Brennan & Ballou, 1968; Khoo *et al.*, 1995). Ac₁PIM₂ and Ac₁PIM₆ are the major PIM species, existing as a diacylglycerol with a further fatty acid attached to the *Manp* residue at C-2 of *myo*-inositol. Ac₂PIM₂ and Ac₂PIM₆ also exist, but Ac₁PIM₂ is believed to be the preferred precursor upon which higher PIM_{s(3-6)} are built, as well as LAM, and its arabinose-free counterpart LM (Chatterjee *et al.*, 1992a).

1.6.7.2. Characterisation of LM and LAM

The mannan of LM and LAM is an extension of the PIMs, containing on average 20-30 residues, emanating from the C-6 position of the inositol ring (Chatterjee *et al.*, 1991; Khoo *et al.*, 1996). This $\alpha(1\rightarrow6)$ -linked mannan backbone is adorned with single *Manp* sugars at

C-2 of the occasional $\alpha(1\rightarrow6)$ -linked mannose in all mycobacterial species examined, with the exception of *M. chelonae*, which contains C-3-linked branching (Guerardel *et al.*, 2002).

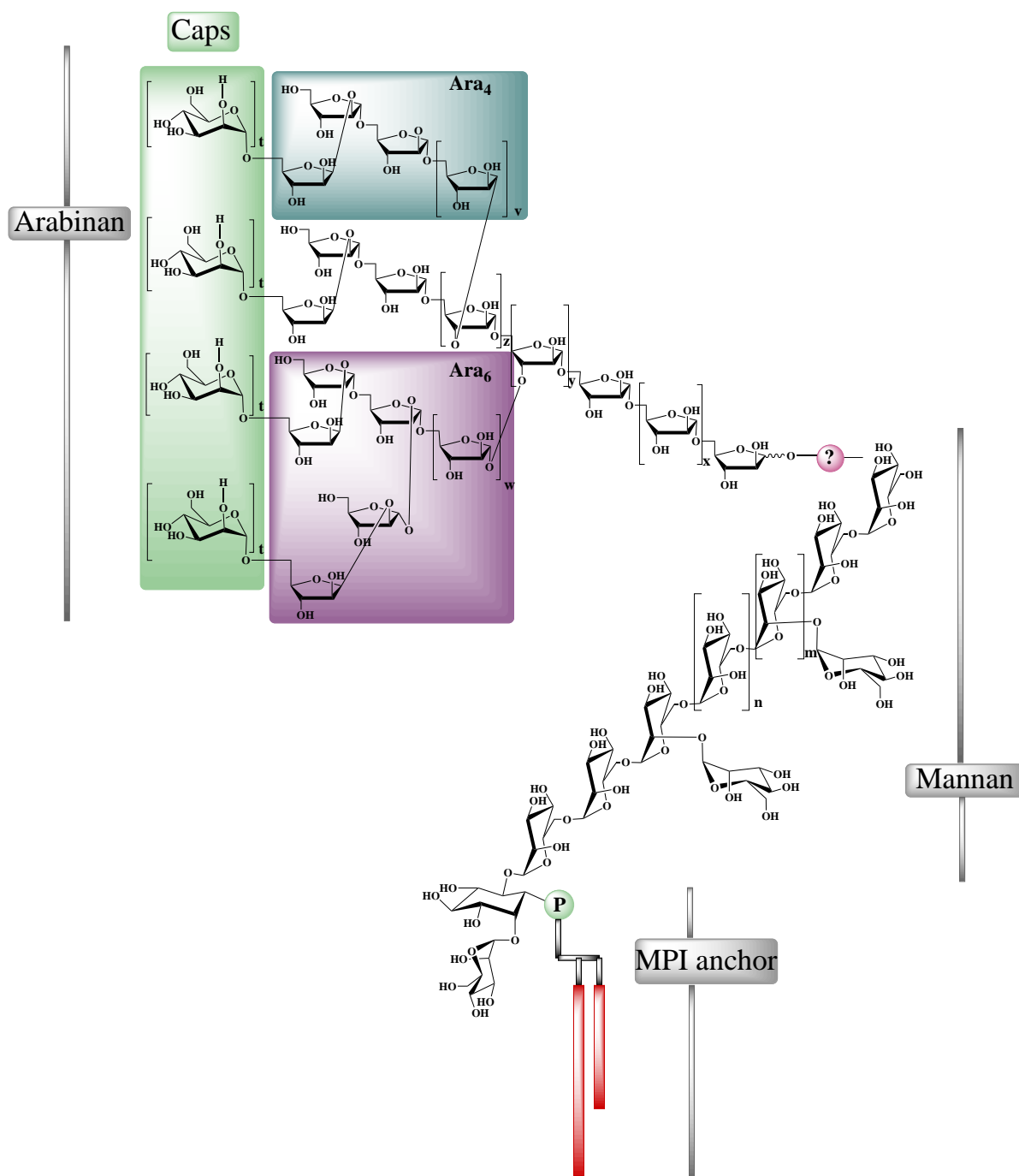


Figure 1.20: Current structural model of mycobacterial LAM. The MPI anchor is linked to a mannann backbone with a $\alpha(1\rightarrow6)$ Man_p core branched frequently at the 2-position with a single α -Man_p. Attached to the mannann core is an arabinan domain (approximately 50–70 residues in total). The point of attachment of arabinan to the mannann has not been elucidated. The non-reducing termini of the arabinan are capped with species specific sugars (Lee *et al.*, 2005).

LM is further glycosylated with an arabinan domain similar to, but more variable than, that in AG. Shi *et al.* (2006) identified the occurrence of an Ara₁₈₋₂₂ motif in *M. smegmatis* that resembled the internal structure of the arabinan of AG, however, the terminal extensions at the non-reducing end varied. The basic structure of the polymer consists of a linear $\alpha(1\rightarrow5)$ -linked arabinosylfuranosyl backbone with branched hexa-Araf (Ara₆) and linear tetra-Araf (Ara₄) terminal moieties (Chatterjee *et al.*, 1991; 1993), equating to between 50-80 Araf residues (Khoo *et al.*, 1996).

1.6.7.3. Characterisation of LAM capping

Mycobacterial species differ in the nature and extent of the capping motifs modifying the nonreducing termini of the arabinan chains, specifically, the $\beta(1\rightarrow2)$ -linked terminal Araf units. To date, three structural families have been recognised, mannose capped LAM (Man-LAM), PI capped LAM (PI-LAM) and non capped LAM (Ara-LAM), of which “Man-caps” are an important feature of the LAM of pathogenic species or slow growing mycobacteria, such as *M. tuberculosis*, *M. bovis*, *M. bovis BCG*, *M. leprae*, *M. avium*, *M. xenopi*, *M. marinum*, and *M. kansasii*. The caps may be present as single Man_p capping residues, di or tri-mannosides, of which di-mannosides predominate. (Delmas *et al.*, 1997; Guerardel *et al.*, 2003). Fast growing mycobacteria such as *M. smegmatis* and *M. fortuitum* possess PI caps, and *M. chelonae* is the only known example of Ara-LAM.

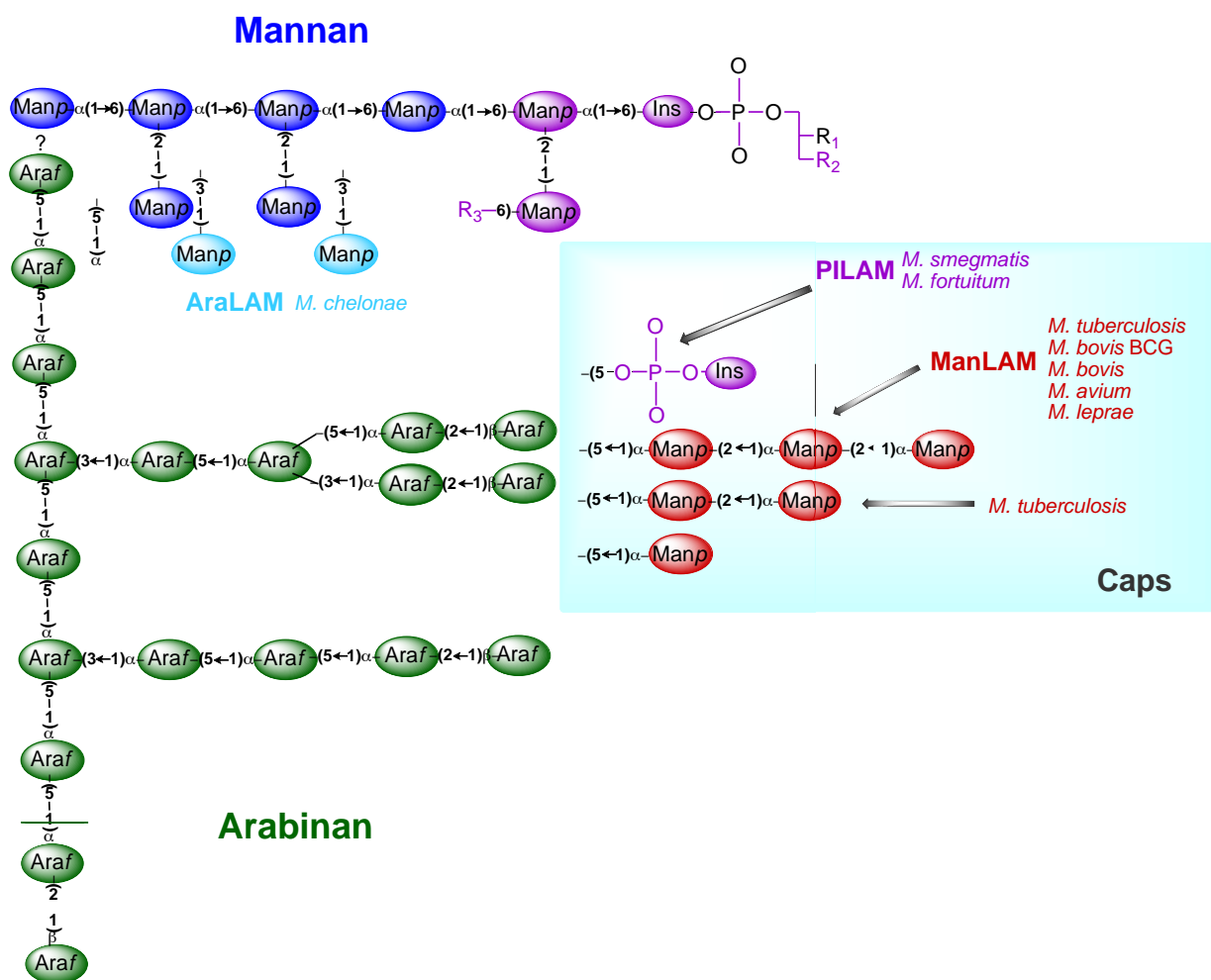


Figure 1.21: Structural model of mycobacterial ManLAM, PILAM and AraLAM highlighting the different capping motifs found in all mycobacterial LAM. The non-reducing termini of arabinan are decorated with species specific sugars; 1–3 mannose units in *M. tuberculosis* and *M. bovis*, phosphatidylinositol in *M. smegmatis* (Nigou *et al.*, 2003).

1.6.7.4. Biosynthesis of PIMs, LM and LAM

1.6.7.4.1. Synthesis of precursors

1.6.7.4.2. GDP-Man_p biosynthesis

Mannose is a key component in numerous cell wall and intracellular molecules present in mycobacteria, including the mannolipids PIMs, LM and LAM and has been shown to be essential for the growth and viability of *M. smegmatis* (Patterson *et al.*, 2003). Mycobacteria can obtain mannose *via* two distinct pathways (Figure 1.21). The first relies on phosphorylation by a hexokinase (Rv2702) to produce mannose-6-phosphate from exogenously obtained mannose (Hsieh *et al.*, 1996). The second is carried out by ManA (Rv3255c), a phosphomannose isomerase (PMI), which synthesises mannose-6-phosphate by converting fructose-6-phosphate obtained from the glycolytic pathway. Patterson *et al.* (2003), demonstrated the essentiality of PMI *in vitro* in an *M. smegmatis* mutant, which was unable to synthesise mannose-containing molecules in the absence of an extracellular source of mannose (Patterson *et al.*, 2003). Mannose-6-phosphate is subsequently converted into mannose-1-phosphate by a phosphomannomutase (PMM) encoded by *manB* (Rv3257c) (McCarthy *et al.*, 2005). Indeed, accumulation of PIMs, LM, and LAM was observed in a *M. smegmatis* strain overexpressing *M. tuberculosis* ManB, which intimates its role in the biosynthesis of these mannolipids (McCarthy *et al.*, 2005). Finally, mannose-1-phosphate is modified by GDP-mannose pyrophosphorylase, ManC (Rv3264c) to GDP-Man_p the nucleotide sugar donor of mannose (Ma *et al.*, 2001; Ning & Elbein, 1999).

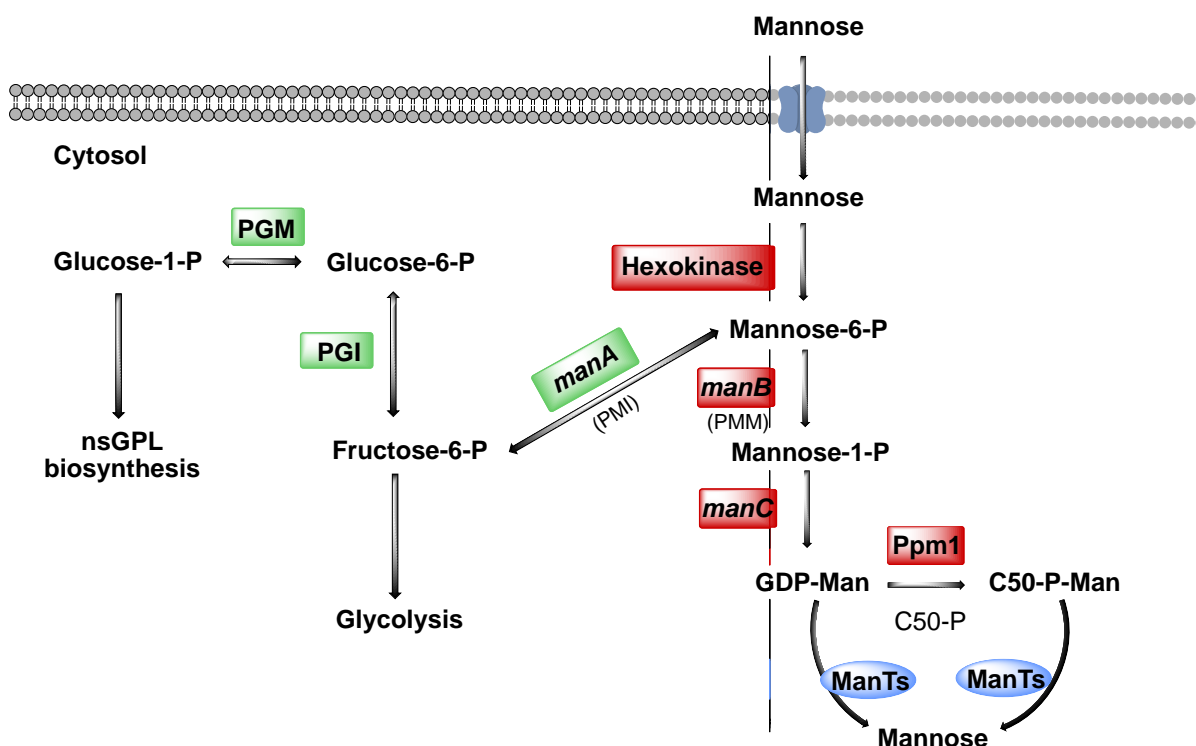


Figure 1.22: Pathway of mannose biosynthesis in mycobacteria. Two sugar donors are accessible to mycobacteria, GDP-Man and C₅₀-P-Man (DPM), playing a separate role in mannan biosynthesis. Abbreviations: P = phosphate. Adapted from McCarthy *et al.* (2005) and Patterson *et al.* (2003).

1.6.7.4.3. β -D-Mannosyl-1-monophosphoryldecaprenol (PPM) biosynthesis

Takayama & Goldman (1970) presented initial reports characterising mannosylipids potentially involved in mannan biosynthesis. They identified a C₅₀-polyprenol based mannosylipid (C₅₀-P-Man) in *M. tuberculosis*, followed by the characterisation of a *M. smegmatis* specific alkali stable, C₃₅-octahydroheptaprenyl-phospho-mannose (C₃₅-P-Man) (Takayama & Goldman, 1970). It was later demonstrated by Besra *et al.* (1997) that Ac₁PIM₂ is specifically extended by the addition of Manp residues from the alkali-stable sugar donor, polyprenol-monophosphomannose (PPM), to form higher PIMs and linear LM. Gurucha *et al.* (2002) identified a polyprenol monophosphomannose synthase, Rv2051 (Ppm1) from *M. tuberculosis* by means of a combined genomics and biochemical approach, derived from similarities to the known eukaryotic dolichol monophosphomannose (DPM) synthases

(Gibson *et al.*, 2003; Gurcha *et al.*, 2002). It was discovered that PPM is generated from GDP-Man and the corresponding polyprenol phosphate *via* Ppm1. Therefore the PPM synthase is a key enzyme in the generation of PPM, which is subsequently utilised in the biosynthesis of LM and LAM, thus making it a potential drug target.

1.6.7.4.4. Synthesis of PI

Phosphatidyl-*myo*-inositol (PI) is the component upon which PIMs, LM and LAM are built and is the linkage to the plasma membrane. The initial step in the synthesis of PI is the phosphorylation of diacylglycerol (DAG) by a DAG Kinase (Rv2252) to form phosphatidic acid (Owens *et al.*, 2006; Salman *et al.*, 1999). A CDP-DAG synthase (Rv2881c), activates phosphatidic acid with CTP forming cytidine diphosphate-diacylglycerol (CDP-DAG) (Nigou & Besra, 2002b), which later reacts with *Myo*-inositol forming PI. Recently, the gene encoding the PI synthase (Rv2612c) was identified and shown to be essential in *M. tuberculosis* (Jackson *et al.*, 2000).

1.6.7.5. Biosynthesis of PIMs

The currently accepted model for PIM biogenesis follows a linear pathway $\text{PI} \rightarrow \text{PIM}_2 \rightarrow \text{PIM}_4 \rightarrow \text{PIM}_6$ (Figure 1.23). In *M. tuberculosis* PimA (Rv2601) catalyses the glycosylation of PI by the transference of Man_p from GDP-Man_p to the 2-position of PI forming PIM₁ (Kordulakova *et al.*, 2002), which is subsequently acylated by Rv2611c at the 6-position (Kordulakova *et al.*, 2003). A Rv2611c mutant of *M. smegmatis* exhibited severe growth defects and accumulation of non-acylated PIM₁ and PIM₂. Furthermore, in a cell-free assay utilising membrane preparations from *M. smegmatis*, overexpression of Rv2611c increased the incorporation of [¹⁴C]-palmitate into PIMs (Kordulakova *et al.*, 2003). Both of these enzymes are part of a conserved gene cluster of six ORFs in an operon, which is present in all members of *Corynebacterineae* (Cole & Barrell, 1998; Cole *et al.*, 1998).

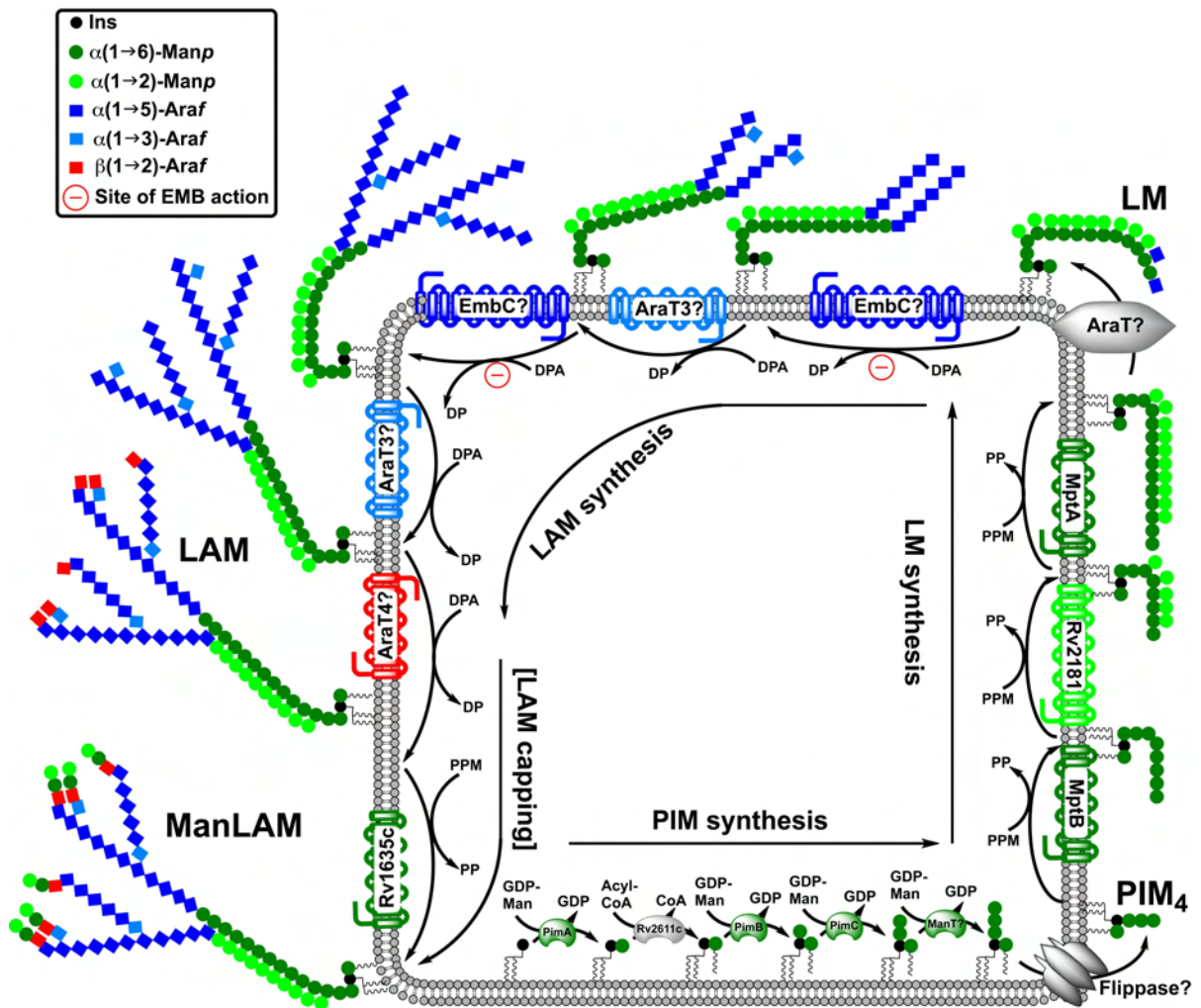
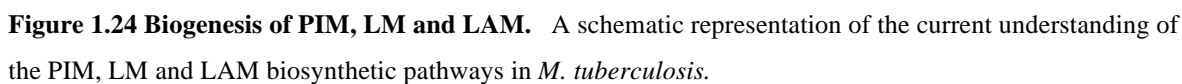


Figure 1.23: Pictorial depiction of PIM, LM and LAM biosynthesis. The three first mannosylations of PI in biosynthesis of PIMs involve the GDP-Man dependent PimA, PimB, and PimC, which are believed to occur on the cytoplasmic face of the plasma membrane. Rv2611c is responsible for the acylation of PIM₁. PIM₃ or PIM₄ is translocated across the bilayer by an unidentified flippase, where it then acts as a substrate for PimE towards biosynthesis of the polar PIM₆ and as a precursor in the formation of LM. The ManT(s) involved in the synthesis of the mannan backbone of LM (MptA and MptB) are believed to be C₅₀-P-Man dependent, as was suggested for Rv2181, the α 1,2-ManT responsible for the LM branching. LAM is generated *via* the further elaboration of LM with Araf units forming an arabinan domain. As yet, only the EmbC protein has been recognised, but the exact activity remains to be ascertained.

PimB (Rv0557) was originally proposed as an α -D-mannose- $\alpha(1\rightarrow6)$ -phosphatidyl-*myo*-

inositol-mannopyranosyltransferase (PimB) responsible for the formation of Ac₁PIM₂ through the transference of mannose from GDP-Man_p to Ac₁PIM₁ (Schaeffer *et al.*, 1999). However, it was later found that disruption of *pimB* in *M. tuberculosis* did not affect the biogenesis of PIMs (Torrelles *et al.*, 2009) suggesting that either complementary activities existed in the form of gene duplications or PimB is responsible for another function (Kremer *et al.*, 2002a). Recent investigations have identified Rv2188c, now termed PimB', as the protein involved in the second mannosylation step responsible for Ac₁PIM₂ formation (Lea-Smith *et al.*, 2008; Mishra *et al.*, 2008b; Mishra *et al.*, 2009). Indeed, work carried out by Tatituri *et al.* (2007) demonstrated PimB's role in the biosynthesis of a novel mannlipid, ManGlcAGroAc₂ and a LM-like molecule in *C. glutamicum*, and has since been renamed MgtA (Tatituri *et al.*, 2007b). Ac₁PIM₂ can remain unmodified, accumulating as an end product or be acylated to Ac₂PIM₂ and/or mannosylated forming the higher PIMs (Ac₁PIM₃-Ac₁PIM₆/Ac₂PIM₃-Ac₂PIM₆), or LM and LAM. Research using cell free extracts has identified the mannosyltransferase PimC from *M. tuberculosis* strain CDC1551 implicating it as the ManT responsible for Ac₁PIM₃ /Ac₂PIM₃ formation from Ac₁PIM₂ /Ac₂PIM₂ (Kremer *et al.*, 2002a). However, a *M. bovis* BCG *pimC* deletion mutant continued to produce normal levels of PIMs/ LM/LAM implying redundancy of genes or compensatory pathways (Kremer *et al.*, 2002b). In fact, there is no strong homologue of *pimC* in *M. tuberculosis* H₃₇Rv or *M. smegmatis*, thus it remains to be identified along with the ManT accountable for α(1→6) mannosylation of Ac₁/Ac₂PIM₃ yielding Ac₁/Ac₂PIM₄. This product is believed to be an intermediate at the branch point at which polar PIMs and LM/LAM biosynthesis diverges (Mishra *et al.*, 2008a; Morita *et al.*, 2004; Morita *et al.*, 2006). It is proposed that up until this branch point, mannose residues have been provided by the nucleotide-derived sugar substrate GDP-Man, characterising the earlier ManTs as members of the GT-A/B superfamily of glycosyltransferases. It has been hypothesised that Ac₁/Ac₂PIM₄ is translocated across the plasma membrane, where it becomes available for Rv1159 (PimE), the recently identified

$\alpha(1\rightarrow2)$ -mannopyranosyltransferase which utilises the polyprenylphosphate sugars PPM/C₅₀-P-Man as a substrate, adding an $\alpha(1\rightarrow2)$ -Man_p residue resulting in the synthesis of Ac₁/Ac₂PIM₅ (Morita *et al.*, 2006). This transition to the GT-C superfamily of glycosyltransferases, which utilise polyprenylphosphate sugars (Liu & Mushegian, 2003), has been supported by a number of inhibition studies in which amphomycin, an inhibitor of the mannose donor PPM/C₅₀-P-Man, was shown to halt the synthesis of PIM₄-PIM₆ (Besra *et al.*, 1997; Morita *et al.*, 2006) and effect elongation and branching of LM and LAM (Morita *et al.*, 2006). The biosynthesis of the final product Ac₁/Ac₂PIM₆ has not been deduced, although the involvement of PimE cannot be ruled out.



1.6.7.6. Biosynthesis of LM and LAM

1.6.7.6.1. The role of MptA, MptB and Rv2181

The mannan of LM/LAM is believed to be an extension of the PIMs, specifically Ac₁/Ac₂PIM₄, and is composed of a linear $\alpha(1\rightarrow6)$ mannan backbone, punctuated occasionally at C-2 with single $\alpha(1\rightarrow2)$ -linked mannoses, resulting in a mannan of approximately 25-30 residues (Figure 1.24) (Chatterjee *et al.*, 1991; Khoo *et al.*, 1996). Mishra *et al.* (2007, 2008a) recently identified two $\alpha(1\rightarrow6)$ mannopyranosyltransferases, mannopyranosyltransferase A and B, named MptA and MptB, using *C. glutamicum* as a model organism. It was elucidated that MptA (NCgl2093 and *M. tuberculosis* homolog, Rv2174) are concerned with the biosynthesis of the distal end of the $\alpha(1\rightarrow6)$ mannan backbone of LM (Mishra *et al.*, 2007; Kaur *et al.*, 2007) and MptB (Rv1459c) is involved in the synthesis of the proximal end of the mannan backbone. A reduction in $\alpha(1\rightarrow6)$ -mannopyranosyltransferase activity, with complete loss of LM and LAM, was observed in a MptB-deletion mutant in *C. glutamicum*. Further evidence from cell free *C. glutamicum* assays utilising C₅₀-P-Manp and expressing Rv1459c and/or its *M. smegmatis* homologue MSMEG_3120 showed that these enzymes possess $\alpha(1\rightarrow6)$ -mannopyranosyltransferase activity. However, *M. tuberculosis* and *M. smegmatis* MptB proteins are unable to complement the *C. glutamicum* Δ mptB mutant, suggesting substrate specificity differences. It is proposed that MptB catalyses the addition of further Manp residues (12-15 sugars) to Ac₁PIM₄, which has been transported across the plasma membrane by an as yet unidentified flippase (Mishra *et al.*, 2008a).

Kaur *et al.* (2006) recently identified the putative integral membrane proteins, MSMEG4250 in *M. smegmatis* and Rv2181 in *M. tuberculosis* as potential polyprenol-dependent glycosyltransferases based on shared characteristics with previously identified enzymes. A knock-out of MSMEG4250 in *M. smegmatis* possessed a truncated version of LAM with a

decrease in the number of $\alpha(1\rightarrow2)$ -Manp branching residues and altered growth with an inability to synthesise LM. Complementation of the mutant with the corresponding ortholog of *M. tuberculosis* (Rv2181) restored normal LM/LAM synthesis. However, regulation of LM and LAM biosynthesis in *M. smegmatis* appears to differ somewhat with *M. tuberculosis*, as *M. tuberculosis* Δ Rv2181 produced truncated versions of LM and Man-LAM (Kaur *et al.*, 2008).

Table 1.3: Genes involved in biosynthesis of LAM and related glycoconjugates (Mishra *et al.*, 2009)

Protein	Function	Role	References
PgsA (Rv2612c)	PI synthase	PI synthase	Jackson <i>et al.</i> 2000
PimA (Rv2610c)	Synthesis of PIM1	$\alpha(1\rightarrow2)$ -Mannopyranosyltransferase	Kordulakova <i>et al.</i> 2003
Rv2611c	Synthesis of Ac1/Ac2PIM1	Acyl transferase	Kordulakova <i>et al.</i> 2003
PimB (Rv2188c)	Synthesis of Ac1/Ac2PIM2	$\alpha(1\rightarrow6)$ -Mannopyranosyltransferase	Lea-Smith <i>et al.</i> 2008; Mishra <i>et al.</i> , 2008; 2009
MgtA (Rv0557)	Synthesis of Gl-X and Ac1/Ac2PIM2	$\alpha(1\rightarrow6)$ -Mannopyranosyltransferase	Tatituri <i>et al.</i> 2007a; Mishra <i>et al.</i> , 2008
PimC (RvD2-ORF1)	Synthesis of Ac1/Ac2PIM3	$\alpha(1\rightarrow6)$ -Mannopyranosyltransferase	Kremer <i>et al.</i> , 2002
PimE (Rv1159)	Synthesis of Ac1/Ac2PIM5	$\alpha(1\rightarrow2)$ -Mannopyranosyltransferase	Morita <i>et al.</i> , 2006
MptB (Rv1459c)	Synthesis of proximal mannan backbone <i>i.e.</i> Ac1/Ac2PIM12-17	$\alpha(1\rightarrow6)$ -Mannopyranosyltransferase	Mishra <i>et al.</i> , 2008
MptA (Rv2174)	Synthesis of distal mannan backbone <i>i.e.</i> Ac1/Ac2PIM22-25	$\alpha(1\rightarrow6)$ -Mannopyranosyltransferase	Mishra <i>et al.</i> , 2007.
MptC (Rv2181)	Adds $\alpha(1\rightarrow2)$ -Manp units on mannan backbone, and also adds second mannose cap on ManLAM	$\alpha(1\rightarrow2)$ -Mannopyranosyltransferase	Kaur <i>et al.</i> , 2008; 2010
EmbC (Rv3793)	Involved in the synthesis of $\alpha(1\rightarrow5)$ -arabinan backbone	$\alpha(1\rightarrow5)$ -Arabinofuranosyltransferase	Zhang <i>et al.</i> , 2003
AftC (Rv2673)	Adds AraF on $\alpha(1\rightarrow5)$ -arabinan backbone in $\alpha(3\rightarrow5)$ -direction	$\alpha(1\rightarrow3)$ -Arabinofuranosyltransferase	Birch <i>et al.</i> , 2010
AftD (Rv0236c)	Either adds $\alpha(1\rightarrow3)$ -AraF units to the non-reducing end of $\alpha(1\rightarrow5)$ -arabinan branch or synthesize	$\alpha(1\rightarrow3)$ or $\alpha(1\rightarrow5)$ -Arabinofuranosyltransferase	Skovierova <i>et al.</i> , 2009
CapA (Rv1635c)	Adds first mannose cap on ManLAM	$\alpha(1\rightarrow5)$ -Mannopyranosyltransferase	Appelmelk <i>et al.</i> , 2008

1.6.7.7. Arabinan biosynthesis in lipoarabinomannan

1.6.7.7.1. The role of EmbC

LAM is generated *via* the further elaboration of LM with Araf units forming an arabinan domain akin to that found in AG (Besra *et al.*, 1997). The linkage pattern of Araf residues and the Ara₆ non-reducing end are also present in AG (as discussed in section 1.6.5.1); however, the arabinans also differ in a number of ways. Firstly, LAM also contains a linear tetra-arabinoside (Ara₄) as well as the Ara₆ motif, with a major difference being that the non-reducing end of the LAM arabinan is substituted with α -mannosyl residues rather than with mycolic acids (Chatterjee *et al.*, 1992b). The arabinan structure is also more variable in LAM, with a recent study suggesting that the precise Ara₁₈ arrangement is not always present, but rather chains of differing lengths extend from the interior 3,5-Araf residues (Shi *et al.*, 2006). It is theorised that at least five distinct arabinofuranosyltransferases are required for the generation of mature LAM, based on the linkages present; as yet only the EmbC protein has been recognised, but the exact activity remains to be ascertained (Zhang *et al.*, 2003). Although EmbC is an essential enzyme in *M. tuberculosis* (Goude *et al.*, 2008), inactivation of the gene in *M. smegmatis* produced a viable mutant, with lack of arabinosylation in LAM but AG remained largely unaffected (Escuyer *et al.*, 2001; Zhang *et al.*, 2003). This knockout strain did possess two to three single Araf residues secured to the mannan backbone, suggesting the existence of an additional AraT, analogous to the priming enzyme AftA (Zhang *et al.*, 2003). However, despite extensive analyses, the arabinan chain attachment sites have not been defined (Chatterjee & Khoo, 1998).

The EmbC protein is predicted to contain 13 transmembrane helices and a modified DxD motif, which is expected to play a role in carbohydrate binding and is thus classified as a member of the GT-C super-family of integral membrane glycosyltransferases (Berg *et al.*, 2005). The characteristic GT-C motif of EmbC may be responsible for the chain elongation

of $\alpha(1\rightarrow5)$ -Araf residues, where the arabinan units are linked to each other creating 3,5- α -Araf branches on 5-linked chains or by transferring the residues directly on to the mannan backbone (Berg *et al.* 2005). Thus, *embC* inhibition appears to be parallel to the *emb* mediated inhibition of arabinosylation of galactan in corynebacterial AG, conferring the $\alpha(1\rightarrow5)$ transferase activity. Point mutations introduced into the conserved proline motif proximal to the large carboxyl-terminal globular region, resulted in the biosynthesis of shorter arabinan domains thus this region seems to control chain length extension of the arabinan domain of LAM (Shi *et al.*, 2006).

1.6.7.8. Mannose - capping of LAM

The arabinan domain of LAM is further modified by the addition of α -mannosyl residues, resulting in capping with either one, two or three Man_p residues. The total extent of capping is about 70%, with a di-mannoside cap being the most abundant (Chatterjee *et al.*, 1992; Chatterjee *et al.*, 1993). It is predicted that synthesis would require at least two ManTs, one that should recognise the arabinan domain and thus add the primary $\alpha(1\rightarrow5)$ -mannose and a further ManT for the elongation of this mannose with a second $\alpha(1\rightarrow2)$ -mannose. Mannose-capped LAM (Man-LAM) is a feature of all pathogenic strains of the *Mycobacterium* genus and is, hence, responsible for some of the immuno-modulatory properties of these strains (Briken *et al.*, 2004). Subtractive genomics of the *M. tuberculosis* genome, with those species of the genus that do not contain mannose-capped LAM, such as *M. smegmatis*, highlighted the GT-C enzyme Rv1635c (Dinadayala *et al.*, 2006). A transposon mutant strain of *M. tuberculosis* CDC1551 with an ineffective copy of *MT1671* (*Rv1635c*), did indeed produce LAM devoid of Man_p capping (Dinadayala *et al.*, 2006). Moreover, an *M. smegmatis* strain expressing *MT1671* resulted in a hybrid LAM, possessing single mannose caps. Further studies supported this finding, with *Rv1635c* mutants in *M. marinum* and *M. bovis* BCG showing that *Rv1635c* encoded for a mannopyranosyltransferase involved in the addition of

the first Manp residue on the non-reducing arabinan termini of LAM (Appelmelk *et al.*, 2008). More recently, Kaur *et al.* (2008) have shown that Rv2181c possesses varied substrate specificity, capable of adding $\alpha(1\rightarrow2)$ -Manp residues onto the mannan backbone, as well as the non-reducing end of LAM in combination with Rv1635c (Kaur *et al.*, 2008).

1.6.7.9. Immunomodulatory properties of LAM & LM

LAM and related lipoglycans are not only essential for mycobacterial growth and survival (Haite *et al.*, 2005; Kovacevic *et al.*, 2006), but have also been implicated in a broad spectrum of immunomodulatory activities. During the last decade, investigators have studied LAM and LM isolated from a multitude of mycobacterial organisms with various capping motifs, hoping to gain insight into the nature of these host-pathogen interactions and the importance of these complex heteropolysaccharides in pathogenesis (Dao *et al.*, 2004; Garton *et al.*, 2002; Gibson *et al.*, 2003; Gibson *et al.*, 2004; Gibson *et al.*, 2005; Maeda *et al.*, 2003; Quesniaux *et al.*, 2004a, 2004b).

The ability of mycobacteria to persist in host tissues is central to the disease. One strategy for survival is phagosomal maturation inhibition (Armstrong & Hart, 1971; Nguyen & Pieters, 2005; Russell, 2001); another is the suppression of the cell-mediated host immune response after infection. Several studies using purified LAM have highlighted a major role for this lipoglycan in both of these phenomena.

1.6.7.9.1. Phagosome maturation arrest

ManLAM has been implicated in inhibition of phagosome maturation (Jo, 2008; Quesniaux *et al.*, 2004a) and infection induced apoptosis (Rojas *et al.*, 2000). Man-LAM blocks the increase of macrophage cytosolic Ca^{2+} that normally occurs upon infection, thereby inhibiting Ca^{2+} /calmodulin-dependent PI3-kinase hVPS34 (Chua and Deretic, 2004; Malik *et*

al., 2001; Vergne *et al.*, 2004a, 2004b). PI3-Kinase is necessary for the production of PI3-phosphate on the phagosomal membrane, which is subsequently involved in the recruitment of the Rab5 effector EEA1 to the early endosome. This is required for the delivery of lysosomal components from the trans-Golgi network (TGN) to the phagosome and regulation of fusion with vesicles of the endosomal-lysosomal pathway, as discussed in section 1.3 (Simonsen *et al.*, 1999; Vergne *et al.*, 2003). ManLAM is able to suppress cytosolic Ca^{2+} -increase and therefore restrict generation of PI3-phosphate (Fratti *et al.*, 2003; Vergne *et al.*, 2003b). Indeed, Fratti *et al.* (2001) reported that ManLAM-coated beads behaved similarly to *M. bovis* BCG LAM, in that they resided in early endosomes that failed to recruit EEA1. Thus, *M. tuberculosis* ManLAM may contribute to the maturation arrest of bacillus-containing phagosomes by virtue of its ability to attenuate hVPS34 and to inhibit EEA1 recruitment. The inhibition of Ca^{2+} increase appears to be specific for ManLAM, as LAM, lacking terminal mannose capping, from non-pathogenic *Mycobacterium* does not affect Ca^{2+} levels (Vergne *et al.*, 2003). At present, the mechanism by which ManLAM alters Ca^{2+} fluxes remains to be established (figure 1.25).

It has also been reported that p38 mitogen-activated protein kinase (p38 MAPK) contributes to phagosome maturation arrest in a way distinct from the inhibition of cytosolic Ca^{2+} increase. ManLAM has been implicated as a trigger for an increase in p38 MAPK activation, which contributes to phagosome maturation arrest through modulation of EEA1 recruitment (Fratti *et al.*, 2003) and downstream trafficking events. However, Welin *et al.* (2008) recently published contrasting results demonstrating that ManLAM did not effect p38 MAPK activation.

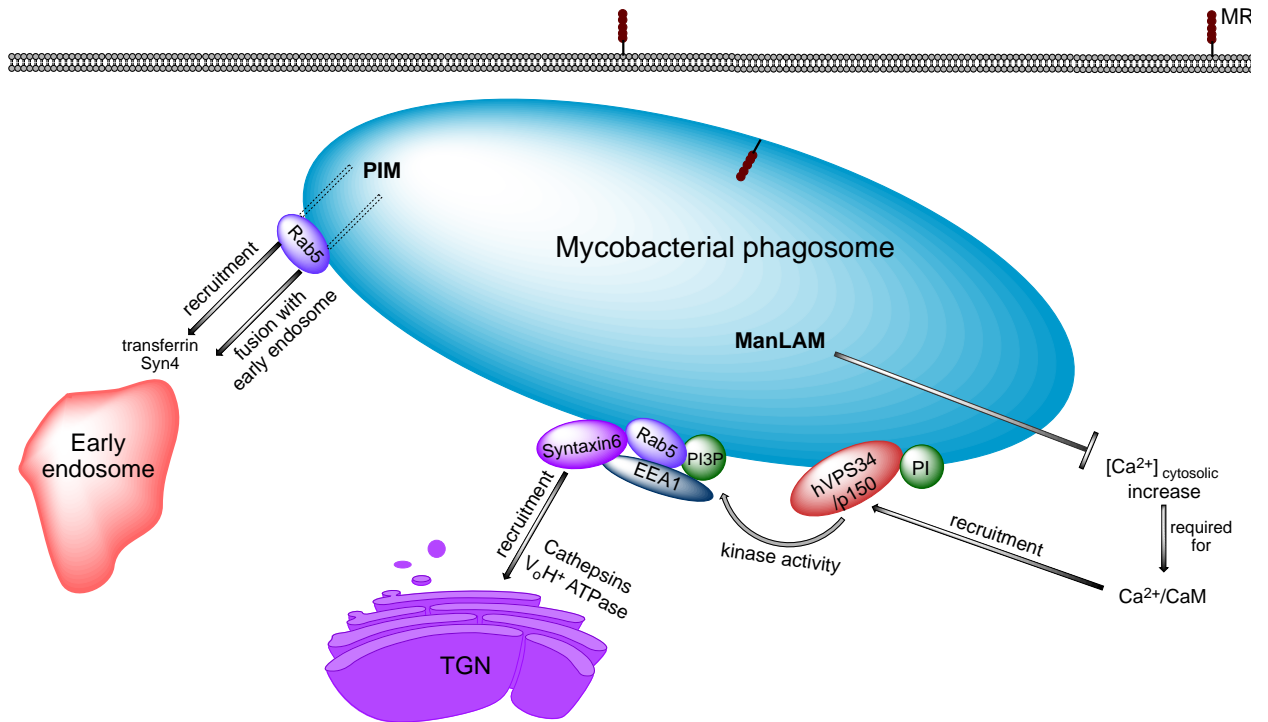


Figure 1.25: The role of ManLAM and PIMs in phagosome maturation arrest. Fusion with early endosomes required for nutrient acquisition is promoted by PIMs. ManLAM inhibits lysosomal fusion and acidification by inhibiting cytosolic- Ca^{2+} increase and thereby blocks the successive steps of hVPS34 kinase activity at the phagosomal membrane, the recruitment of Rab5, EEA1 and Syn6 to the phagosome, and the delivery of cathepsins and VoH^+ ATPase. TGN = *trans*-Golgi network, CaM = calmodulin, PI(3P) = phosphatidylinositol (3-phosphate), Syn = syntaxin, EEA1 = early endosome autoantigen.

Another process of maturation arrest involves the incorporation of ManLAM, *via* its GPI anchor, into so-called lipid rafts or membrane rafts of the macrophage cell membrane. These are cholesterol and glycosphingolipid-rich domains that act as docking sites for cell signalling processes (Welin *et al.*, 2008). The insertion of ManLAM is reported to reorganise the phagosomal membrane in such a way as to disrupt access to the molecules essential for maturation (Hayakawa *et al.*, 2007). The overall effect is that the mycobacteria can survive in their self-created phagosomal niche.

In contrast to ManLAM, its biosynthetic precursor LM does not affect phagolysosomal development (Kang *et al.*, 2005; Vergne *et al.*, 2004b). PIMs, however, have been found to specifically stimulate early endosomal fusion through incorporation into the membrane rafts

and thus competitively inhibiting insertion of LAM (Welin *et al.*, 2008). Therefore PIM generates a bypass mechanism allowing endosome fusion necessary for nutrient delivery to the bacilli residing in the phagosome (Kelley and Schorey, 2003; Vergne *et al.*, 2004b). Torrelles *et al.* (2006), reported that the MR has a high affinity for higher-order PIMs (PIM₅ and PIM₆) while lower-order PIMs (PIM₂) are not recognised. Thus, although ManLAM and PIMs influence the phagosome maturation by distinct mechanisms, both may involve ligation to the mannose receptor (MR) (Vergne *et al.*, 2004b).

1.6.7.9.2. Lipoglycan interaction with the host cell

While LM is mainly associated with toll-like receptor (TLR)-signalling, the higher-order PIMs and ManLAM are recognised by the C-type lectins DC-SIGN and the macrophage MR (Tailleux *et al.*, 2005). Both C-type lectins show comparable recognition specificities for the mannosylated glycolipids, and, as receptors CD14 and pulmonary surfactant protein (SP)-A and SP-D also bind ManLAM (Ernst, 1998; Pugin *et al.*, 1994; Sidobre *et al.*, 2000; Torrelles *et al.*, 2008), interactions of mycobacteria with all these pattern recognition receptors may enhance or dampen inflammatory signals and thereby determine the nature of the immune response. Anti-inflammatory signaling, *via* the interaction of the glycolipids with the host immune system, can be regarded as strategies of mycobacteria to escape immune surveillance (Torrelles & Schlesinger, 2010), but may be also vital in prevention of an exaggerated inflammatory response (Jo, 2008).

1.6.7.9.3. LAM and the Mannose receptor

The ManLAM-mediated phagosome maturation delay is dependent on the MR present on the macrophage membrane. Indeed, Kang *et al.* (2005) demonstrated the reversal of delayed phagolysosome fusion by use of a MR-blocking antibody alongside LAM-coated

microspheres. Further supporting evidence was presented by Ferguson *et al.* (2006), demonstrating that coating *M. tuberculosis* with the mannose cap binding C-type lectin surfactant protein D (SP-D), increases phagolysosome fusion in infected macrophages.

Given that the macrophage MR only recognises the mannose-capped ManLAM and not AraLAM or PILAM (Schlesinger *et al.*, 1994), this is further evidence that ligation to the macrophage MR is required for the phagosome maturation block, which appears to be restricted to the more virulent *Mycobacterium* species. This receptor is distinguished by the fact that it mediates the engulfment of microbes without necessarily inciting a proinflammatory response and thereby has long been postulated to enhance early intracellular survival of the microbe. This receptor has also been implicated in intracellular trafficking of LAM to the late endosomal compartments for loading onto CD1b molecules for LAM presentation to T cells (Prigozy *et al.*, 1997). Some species of PIMs expressed by *M. tuberculosis* have been shown to engage the MR and illicit an MR-dependent delay in phagolysosome fusion (Torelles *et al.*, 2006), whereas PILAM and AraLAM did not effect maturation (Kang *et al.*, 2005).

1.6.7.9.4. Modulation of DC-SIGN activity

Immature DCs are seeded throughout peripheral tissues to act as sentinels against invading pathogens. Indeed, immature DCs internalise *M. tuberculosis* derived LAMs and present these structures *via* the CD1b-presentation pathway to LAM specific T cells. DC-SIGN has a high affinity for mannose-containing carbohydrates. It was demonstrated by Geitjenbeek *et al.* (2003), that mycobacteria specifically target DC-SIGN through ManLAM to impair DC maturation and to induce production of the anti-inflammatory cytokine IL-10. These conditions promote immunosuppression.

DC-SIGN only recognises LAM if it is mannose-capped (Geitjenbeek *et al.*, 2003; Maeda *et al.*, 2003) and it has been shown to have a strong affinity for increasing chain lengths of

$\alpha(1\rightarrow2)$ -linked mannosyl residues (Koppel *et al.*, 2004). Unsurprisingly, PIM₅ and PIM₆ are recognized by DC-SIGN with a higher affinity than lower order PIMs, most likely due to terminal $\alpha(1\rightarrow2)$ -linked mannosyl residues similar to the mannose cap of ManLAM (Boonyarattanakalin *et al.*, 2008; Driessen *et al.*, 2009). On the other hand, a BCG mutant producing a mannose-cap devoid LAM still bound DC-SIGN to the same extent as wild-type BCG (Appelmek *et al.*, 2008); thus, other DC-SIGN ligands must be present in the mycobacterial cell envelope.

ManLAM binding to LPS-activated DCs increases the secretion of pro-inflammatory IL-12 and IL-6 as well as IL-10 (Gringhuis *et al.*, 2009); therefore, this suggests that DC-SIGN binding may function primarily in the protection of the host (Ehlers, 2009).

1.6.7.9.5. Toll-like receptors

PILAM and LM stimulate innate immunity *via* signaling through TLR2, which differs from that of ManLAM. TLR2 signalling has been demonstrated for PI-anchored mannosylated lipoglycans; however, it is dependent on their degree of acylation and mannosylation (Doz *et al.*, 2007; Gilleron *et al.*, 2006; Nigou *et al.*, 2008). For instance, lipoglycan-induced signaling occurs *via* the TLR1/TLR2-heterodimer complex, which recognises tri-acylated lipoglycans (Elass *et al.*, 2005; Gilleron *et al.*, 2006; Nigou *et al.*, 2008). The degree of mannosylation also affects the ability of the lipoglycan to activate TLR2, with a higher level of activation accompanying an increasing length of mannan chain (Nigou *et al.*, 2008). LM presents the largest accessible mannan chain, since it does not possess a masking arabinan domain; it did indeed show increased TLR2-signalling (Quesniaux *et al.*, 2004b), although this activity is restricted to the tri- and tetra-acylated forms (Ac₁/Ac₂-LM) (Doz *et al.*, 2007; Gilleron *et al.*, 2006). Ac₁/Ac₂PIM₂, PILAM and AraLAM have been shown to be poor inducers of TLR2-signalling in comparison to LM and Ac₁/Ac₂PIM₆ (Nigou *et al.*, 2008), highlighting the need for a large unmasked mannan chain. Vignal *et al.* (2003) also presented

supporting evidence, showing that in contrast to LM, neither AraLAM from *M. chelonae* nor ManLAM and Ac₁/Ac₂PIM₂ from *M. kansasii* mediate a TLR2-dependent activation (Vignal *et al.*, 2003). Moreover, chemical degradation of the arabinan domain of ManLAM from *M. kansasii* restored its ability to induce cytokine secretion *via* TLR2, which suggests that the arabinan domain prevents proper interaction of ManLAM with TLR2 (Vignal *et al.*, 2003). This was confirmed in this thesis (Chapter 3) in which LAM containing a truncated arabinan domain from a *M. smegmatis* AftC knock-out mutant, showed enhanced TLR2-signalling as compared to wild-type LAM (Birch *et al.*, 2010). Overall, the data indicate that LM, and in a minor respect PIM₆, are the only significant TLR2-ligands from this group of mycobacterial lipoglycans.

1.7. Project aims

Mycobacterial diseases are especially problematic to treat owing to the unique lipid-rich cell wall architecture. The cell wall is essential for growth and survival and the majority of front-line drugs target its biosynthesis (Zhang, 2005). In particular, EMB and INH inhibit biosynthesis of arabinan and mycolic acids, respectively. Nonetheless, the global problem of TB has been worsened in recent years by the emergence of MDR- and XDR-TB cases, leading to a necessity to discover novel drug targets and specific antimicrobial compounds against them (Sreevatsan *et al.*, 1997b; Telenti *et al.*, 1997). In this regard, the biosynthetic machinery of the mycobacterial cell wall and associated lipoglycans represent attractive targets (Bhatt *et al.*, 2007b; Bhowruth *et al.*, 2007; Brennan & Crick, 2007; Dover *et al.*, 2008).

The structural basis of the arabinan of both AG and LAM is now well defined (Besra *et al.*, 1995; Daffé *et al.*, 1990; McNeil *et al.*, 1990), conversely, aspects of its biosynthesis remained poorly resolved. Upon commencing this study, only EmbA, EmbB and the newly identified AftA were implicated in AG arabinan biosynthesis and only EmbC as the AraT involved in LAM biosynthesis (Alderwick *et al.*, 2006; Mikusova *et al.*, 1995; Zhang *et al.*, 2003). Given that the arabinan domains utilise several different Ara α linkages clearly suggests that additional AraTs must be required to form a fully matured arabinan. All of these recognised AraTs are classified as members of the GT-C superfamily of integral membrane proteins. Liu and Mushegian (2003) identified members of this superfamily, representing potential candidates involved in the biosynthesis of cell wall related components. The major hindrance for the study of these genes, adopting a “reverse-genetics” approach, is the essentiality of arabinan in *M. tuberculosis*. For instance, a direct knock out *embA*, *embB* or *embC* resulted in non-viable mutants of *M. tuberculosis*. Furthermore, the study of *M. tuberculosis* has posed a formidable challenge as a result of its long generation time,

fastidious growth requirements, and high risk of contagion. *M. smegmatis* and *C. glutamicum* share similar genomic organization and cell wall biosynthetic machinery, and are nonpathogenic, fast-growing organisms that can tolerate deletion of some cell wall biosynthetic genes that are essential in *M. tuberculosis* (Alderwick *et al.*, 2005b; Alderwick *et al.*, 2006c; Gande *et al.*, 2004). The aim of this thesis was to study the direct effects of *Corynebacteriaceae* glycosyltransferases which represent the orthologous genes and enzymes of *M. tuberculosis*, in the model organisms *C. glutamicum* and *M. smegmatis*. More specifically:

- Bioinformatic investigation of the published *Corynebacterineae* genomes using comparative genomics to identify putative glycosyltransferases involved in cell wall AG and LAM biosynthesis.
- Deletion of selected genes from *M. smegmatis* and *C. glutamicum* that encode putative GT-C glycosyltransferases involved in AG and LAM biosynthesis.
- Subsequent phenotypic characterization of strains deleted of putative GT-C glycosyltransferase encoding genes which includes
 - Carbohydrate and lipid chemical compositional analysis of purified cell wall material.
 - Biochemical investigation into consequential effects of AraT activity in isolated membranes using a range of neoglycolipid acceptor analogues.

Chapter 2

2. Identification and characterisation of AftB and AftC arabinotransferases involved in arabinogalactan biosynthesis

2.1. Introduction

TB is currently the leading cause of mortality from a single infectious agent, responsible for 1.8 million fatalities annually, as well as latently infecting a third of the world's population. Mycobacterial diseases, such as TB and leprosy, consequently still represent a global health problem (Gupta *et al.*, 2001). For instance, the recent emergence of MDR-TB strains and, more recently, XDR-TB clinical isolates (Singh *et al.*, 2007; Zignol *et al.*, 2006), has prompted the need for new drugs and drug targets. The causative agent of these diseases, *M. tuberculosis* and *M. leprae*, respectively, are members of the *Corynebacteriaceae*, a group of atypical Gram-positive bacteria characterised by an intricate cell envelope (Besra *et al.*, 1995; McNeil *et al.*, 1990; McNeil *et al.*, 1991).

This distinctive mycobacterial cell envelope is composed of three macromolecules, LAM, mycolyl-AG and PG (Besra *et al.*, 1995; Chatterjee *et al.*, 1991; McNeil *et al.*, 1990; McNeil *et al.*, 1991). The galactan domain of AG is linked to PG via a specialised “linker unit”, **L**-Rhap-(1→4)- α -**D**-GlcNAc, and its distal arabinan domain to mycolic acids, forming mAGP complex (Besra *et al.*, 1995; McNeil *et al.*, 1990; McNeil *et al.*, 1991). The arabinan domain contains α (1→5), α (1→3) and β (1→2) Araf linkages, arranged in several distinct structural motifs (Alderwick *et al.*, 2005b; Besra *et al.*, 1995; Daffé *et al.*, 1990). The non-reducing arabinan termini of AG consists of *t*-Araf, 2-Araf, 5-Araf, and 3,5-Araf residues arranged into a characteristic terminal Ara₆ motif, with the 5-OH of the *t*-Araf and 2-Araf residues representing sites of mycolylation (McNeil *et al.*, 1991). The packing and ordering of mycolic acids within the mAGP and additional lipids within the outer envelope results in a highly impermeable barrier (Minnikin *et al.*, 2002), which is essential for bacterial survival.

It is interesting to note that several front-line anti-tubercular drugs, such as ethambutol (EMB) (Belanger *et al.*, 1996; Takayama & Kilburn, 1989; Telenti *et al.*, 1997) and isoniazid (INH) (Banerjee *et al.*, 1994; Winder & Collins, 1970), target aspects of the biosynthesis of the mAGP complex.

The structural basis of AG is now well defined (Besra *et al.*, 1995; Daffé *et al.*, 1990; McNeil *et al.*, 1990), conversely, aspects of its biosynthesis remain poorly resolved. The biosynthesis of AG involves the formation of a linear galactan chain, with alternating $\beta(1\rightarrow5)$ and $\beta(1\rightarrow6)$ -**D**-galactofuranosyl (Galf) residues of approximately 30 residues in length, from the specialised ‘linker unit’, **L**-Rhap-(1 \rightarrow 4)- α -**D**-GlcNAc (Kremer *et al.*, 2001; Mikusova *et al.*, 2000), attaching the AG to the PG *via* the C-6 of some of the MurNGly residues. MALDI-TOF MS analyses of per-*O*-methylated AG of *C. glutamicum*, deleted of its single arabinofuranosyltransferase *Cg-emb*, revealed that the 8th, 10th and 12th Galf residue possessed singular Ara_f residues (Alderwick *et al.*, 2005b). These specific Ara_f residues were recently shown to be transferred by a specialised arabinofuranosyltransferase AftA, whose gene in all *Corynebacteriaceae* analysed to date is adjacent to the *emb* cluster (Alderwick *et al.*, 2006c). These initial Ara_f residues “prime” the galactan backbone for further attachment of $\alpha(1\rightarrow5)$ linked Ara_f residues. These reactions require the arabinofuranosyltransferase activities of Mt-EmbA and Mt-EmbB, or Cg-Emb, respectively; these are also targets of EMB (Alderwick *et al.*, 2005b; Radmacher *et al.*, 2005; Telenti *et al.*, 1997), which eventually result in mature AG.

Disruption of either *embA* or *embB*, in *M. smegmatis*, produced an impairment of the terminal Ara₆ motif, resulting in a linear terminal motif (Escuyer *et al.*, 2001). The Emb and AftA proteins utilise the specialised sugar donor, β -**D**-arabinofuranosyl-1-monophosphoryl-

decaprenol (DPA) (Lee *et al.*, 1995b; Lee *et al.*, 1997; Wolucka *et al.*, 1994b), and is a characteristic feature found only in *Corynebacteriaceae* (Alderwick *et al.*, 2006a; Huang *et al.*, 2005; Mikusova *et al.*, 2005). In addition, these proteins also belong to the GT-C superfamily of integral membrane glycosyltransferases (Liu & Mushegian, 2003). A recent topological analysis of Cg-Emb (Seidel *et al.*, 2007c), together with a mutational study of Mt-EmbC (Berg *et al.*, 2005), revealed for the first time a clear domain organisation of these proteins. The glycosyltransferase DDX signature is evident in the extracellular loop which connects helices III-IV and the chain elongation “Pro-motif”, is in the extracellular loop connecting helices XIII-XIV (Berg *et al.*, 2005).

It is interesting to note that the arabinan domain of AG utilises several different Araf linkages, which suggests that additional arabinofuranosyltransferases must be required to form a fully matured AG. Moreover, initial Araf residues at branching sites could require specialised arabinofuranosyltransferases, as already observed for AftA (Alderwick *et al.*, 2006c). Clearly additional arabinofuranosyltransferases still remain to be identified in *Corynebacteriaceae*. Liu and Mushegian (2003) identified fifteen members of the GT-C superfamily, representing candidates involved in the biosynthesis of cell wall related glycans and lipoglycans in *M. tuberculosis*. In order to study the direct effects of *Corynebacteriaceae* arabinofuranosyltransferases, we have attempted to identify and delete genes, which represent the orthologous genes and enzymes of *M. tuberculosis*, in the model organisms *C. glutamicum* and *M. smegmatis*. The study of *M. tuberculosis* has posed a formidable challenge as a result of its long generation time, fastidious growth requirements and high risk of contagion. *M. smegmatis* and *C. glutamicum*, on the other hand, are non-pathogenic, fast-growing organisms that can tolerate deletion of some cell wall biosynthetic genes that are essential in *M. tuberculosis* (Alderwick *et al.*, 2005b; Alderwick *et al.*, 2006c; Gande *et al.*, 2004). Herein, we present the identification of two novel arabinofuranosyltransferases of the

GT-C superfamily, arabinofuranosyltransferase B (AftB) and arabinofuranosyltransferase C (AftC). The latter is responsible for the transfer of *Araf* residues from DPA to the arabinan domain to form $\alpha(1\rightarrow3)$ -linked *Araf* residues, which result in the branched arabinan domain distal to the non-reducing terminal Ara_6 motif characteristic of mycobacterial AG. AftB is responsible for the transfer of *Araf* residues from DPA to the arabinan domain to form terminal $\beta(1\rightarrow2)$ linked *Araf* residues, which marks the “end-point” for AG arabinan biosynthesis before decoration with mycolic acids.

2.2. Results

2.2.1. Genome comparison of the *aftB* locus

With the recent identification of AftA as a novel arabinofuranosyltransferase present in *Corynebacteriaceae* (Alderwick *et al.*, 2006c), and based on the fact that it is present in a highly conserved cell wall locus (Alderwick *et al.*, 2006c), we concentrated our studies to identify other cell wall related genes. Subsequently, we identified Rv3805c (Figure 2.1A), which is located in close proximity to the antigen 85 complex-encoding genes *fbpA* and *fbpD* (Belisle *et al.*, 1997). Furthermore, Rv3805c is likely to form an operon together with *ubiA*, which is required for prenyl transfer to 5-phosphoribose pyrophosphate (PRPP) to form decaprenylphosphoryl-5-phosphoribose (DPPR), before conversion to DPA (Huang *et al.*, 2005; Mikusova *et al.*, 2005), and *glfT*, which is responsible for establishing the galactan backbone of AG (Kremer *et al.*, 2001; Mikusova *et al.*, 2000). The apparent fundamental function of *aftB* is indicated by the fact that the genome organisation of this particular region is syntenic in *Corynebacteriaceae*, including all *Mycobacterium* and *Corynebacterium* species analysed to date (Figure 2.1A, B) and also in *Norcardia farcinica* IFM 10152 and *Rhodococcus* sp. RHA1.

The gene product of Rv3805c, termed AftB, is predicted to form nine transmembrane (TM) spanning helices, in its amino-terminal part, whereas a 237 amino acid carboxy-terminal part is directed towards the periplasm (Figure 2.1C). Interestingly, AftB shows no obvious sequence similarity to the previously identified arabinofuranosyltransferases, such as Emb (Alderwick *et al.*, 2005b) and AftA (Alderwick *et al.*, 2006c), although the topology, with the C-terminus directed towards the periplasmic side, is to some degree comparable. However, the intragenomic similarity of the AftB proteins is very high, even for the most distant pairs, *M. tuberculosis* and *C. diphtheriae*, exhibiting 33% identity over the entire length of

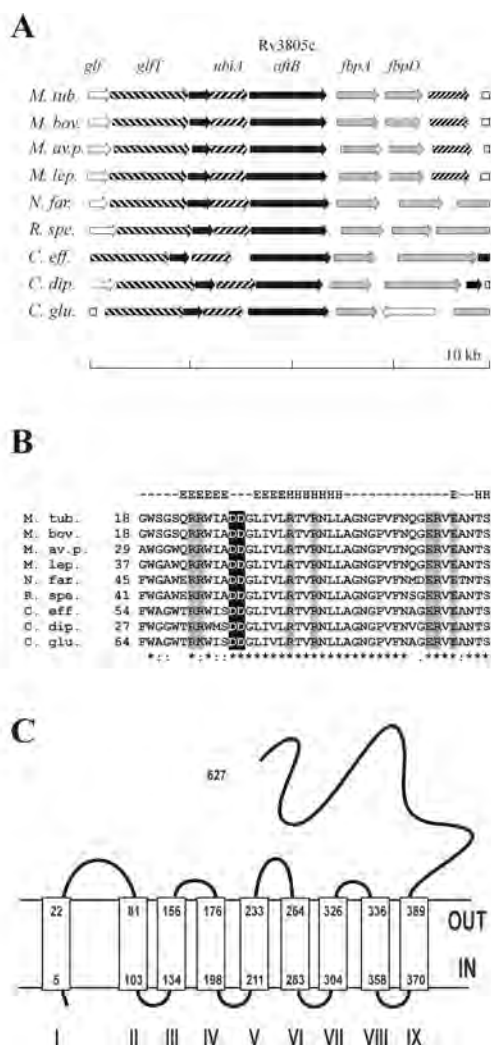


Figure 2.1: Comparison of the *aftB* locus within *Corynebacteriaceae*. **A)** The locus consists in *M. tuberculosis* (*M. tub.*) of *aftB* with the upstream located *ubiA* gene product catalysing prenylation of 5-phosphoribose pyrophosphate (PRPP) (Huang *et al.*, 2005)), and *glfT* (Kremer *et al.*, 2001) and UDP-Galp mutase enzyme *glf* (Pan *et al.*, 2001). Downstream of *aftB* the genes *fbpA*, and *fbpD* are located which encode mycolyltransferases (Belisle *et al.*, 1997). The organisation of these genes is largely retained in a number of *Corynebacteriaceae* indicative for a basic functional unit. In *N. farcinica* (*N. far.*), a third paralogous mycolyltransferase is present, and in *C. glutamicum* (*C. glu.*) a transposon is inserted between the two mycolyltransferases. Orthologous genes are shaded accordingly. *M. bovis* (*M. bov.*), *M. avium paratuberculosis* (*M. av. p.*), *M. leprae* (*M. lep.*), *Rhodococcus* sp. RHA1 (*R. spe.*), *C. efficiens* (*C. eff.*), and *C. diphtheriae* (*C. dip.*). **B)** Partial sequence comparison of the first loop region of AftB. The conserved charged residues possibly involved in glycosyltransferase activity are shaded in grey, and the adjacent aspartate residues possibly directly involved in glycosyl transfer are in white on black background (Liu & Mushegian, 2003). On top are the predicted structural properties of the peptide with E indicating β -sheet, and H α -helix structure. **C)** Topology of Mt-AftB based on dense alignment surface (DAS) analysis (Cserzo *et al.*, 1997). The membrane spanning helices are given in Roman numbers, and their amino acyl residues in Arabic.

the proteins. Even stronger conservation is found in the first periplasmic loop region (Figure 2.1B), exhibiting a modified motif of the GT-C superfamily of glycosyltransferases consisting of two adjacent aspartic acid residues (Liu & Mushegian, 2003). Also, the periplasmic loop regions following helix V and VII are strongly conserved, which may play a role in presenting the nascent arabinose domain to the catalytic glycosyltransferase site. Taken together, the features of AftB and the locus where the gene is localised suggests that it represents a glycosyltransferase involved in AG biosynthesis.

2.2.2. Construction of *C. glutamicum*Δ*aftB*

In an attempt to delete *aftB* in *C. glutamicum* the non-replicative plasmid pK19mobsacBΔ*aftB* was constructed carrying sequences adjacent to Cg-*aftB*. The vector was introduced into *C. glutamicum* and in several electroporation assays kanamycin resistant clones were obtained, indicating integration of pK19mobsacBΔ*aftB* into the genome by homologous recombination (Figure 2.2A). The *sacB* gene enables for positive selection of a second homologous recombination event, which can result either in the original wild-type genomic organisation or in clones deleted of *aftB* (Schafer *et al.*, 1994). Forty-eight clones exhibiting the desired phenotype of vector-loss (Kan^S, Suc^R) were analysed by PCR and twenty-one of them were found to have Cg-*aftB* excised. These numbers indicate that the loss of Cg-*aftB* is apparently not a serious disadvantage for viability, in contrast with Cg-*aftA*, where deletion was rather difficult to obtain (Alderwick *et al.*, 2006c). As a result, one clone was subsequently termed *C. glutamicum*Δ*aftB* and confirmed by PCR to have Cg-*aftB* deleted, whereas controls with *C. glutamicum* wild type and genes adjacent to Cg-*aftB* resulted in the expected amplification products (Figure 2.2A).

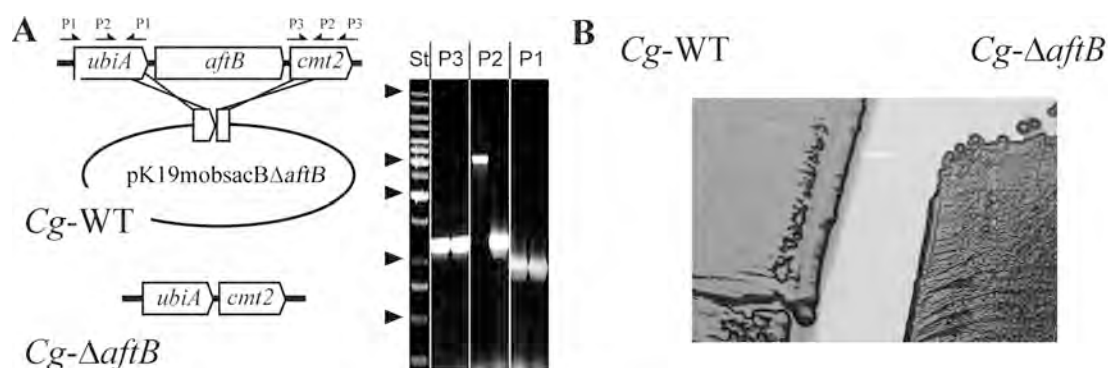


Figure 2.2: Construction and characteristics of *C. glutamicum*Δ*aftB*. **A)** Genomic illustration of *Cg-aftB* with its adjacent genes *ubiA* and *cmt2*, which is the orthologue of mycobacterial *fbpA*, and the strategy to delete *Cg-aftB* using the deletion vector pK19mobsacBΔ*aftB*. This vector carries 18 nucleotides of the 5′-end of *Cg-aftB* and 36 nucleotides of its 3′-end thereby enabling the in-frame deletion of almost the entire *Cg-aftB* gene. The arrows marked P2 locate the primers used for the PCR analysis to confirm the absence of *Cg-aftB*. Primers P1 were used to detect *ubiA*, and P3 to detect *cmt2*. Distances are not drawn to scale. The results of the PCR analysis are shown on the right, where the results obtained with the corresponding primer pairs are marked accordingly. Samples were applied pair wise with the amplification products obtained from the wild type applied in the left lane, and that of the deletion mutant in the right lane. St marks the standard, where the arrowheads are located at 10, 3, 2, 1, and 0.5 kb, respectively. **B)** Phenotype of *C. glutamicum*Δ*aftB* cells spread on BHI medium and incubated for 3 days. On the left is shown wild type *C. glutamicum* (*Cg-WT*) and on the right the deletion mutant *C. glutamicum*Δ*aftB* (*Cg-ΔaftB*). The picture shows an area of about 1.5 cm square.

2.2.3. *In vitro* growth analysis of *C. glutamicum*Δ*aftB*

Growth of wild type *C. glutamicum* and *C. glutamicum*Δ*aftB* were compared in BHI medium as well as salt medium CGXII (Eggeling & Bott, 2005). Both strains exhibited comparable growth rates and the final cell densities reached were comparable. Single colonies of the deletion mutant appeared less glossy. In streak-outs on BHI plates, the surface of the deletion mutant appeared rough with a coarsely granular surface, as compared to wild type *C. glutamicum* (Figure 2.2B). Taken together *C. glutamicum*Δ*aftB* possesses only a slight growth defect, under the conditions assayed, indicating a degree of tolerance to the deletion of *Cg-aftB*. Complementation of *C. glutamicum*Δ*aftB* with either pMSX-*Cg-aftB* or pMSX-Mt-*aftB* restored the mutant to a wild type phenotype. For the purpose of significance, *C.*

*glutamicum*Δ*aftB* complemented with Mt-*aftB* was used throughout this investigation to study the corresponding mutant phenotype; however, similar results were also obtained with *C. glutamicum*Δ*aftB* complemented with Cg-*aftB*.

2.2.4. Analysis of cell wall associated lipids and bound corynomycolic acid

The initial qualitative investigations involved the analysis of cell wall associated lipids and release of bound corynomycolic acids as corynomycolic acid methyl esters (CMAMEs) following by TLC analysis. Analysis of free lipids from other previously identified cell wall mutants, such as *C. glutamicum*Δ*emb* (Alderwick *et al.*, 2005b) and *C. glutamicum*Δ*aftA* (Alderwick *et al.*, 2006c), highlighted an apparent increase in trehalose monocorynomycolate (TMCM) indicating a defect in cell wall biosynthesis. This phenotype was also consistently observed for the *aftB* deletion mutant (Figure 2.3). Quantitative free lipid analysis used [¹⁴C]-acetate labeled cultures and equal loading of radioactivity based on the extractable free lipids for *C. glutamicum*, *C. glutamicum*Δ*aftB* and the complemented *C. glutamicum*Δ*aftB* pMSX-Mt-*aftB* strains. Typically, *C. glutamicum* exhibited the known free lipid profile for wild type *C. glutamicum*, including phospholipids (3945 cpm), TMCM (3217 cpm), trehalose dicorynomycolate (TDCM) (8619 cpm) and non-polar lipids migrating at the solvent front (8753 cpm) (Figure 2.3, lane 1). In contrast, following equivalent loading of radioactivity and quantitative analysis by phosphoimager analyses, *C. glutamicum*Δ*aftB* possessed an approximate significant three-fold increase in TMCM (10185 cpm) and a decrease in TDCM (6539 cpm), phospholipids (1275 cpm) and non-polar lipids (5439 cpm) (Figure 2.3, lane 2). Complementation of *C. glutamicum*Δ*aftB* with pMSX-Mt-*aftB*, reverted the deletion mutant back to a phenotype similar to the wild type, TMCM (3331 cpm), TDCM (9123 cpm), phospholipids (4011 cpm) and non-polar lipids (8901 cpm) (Figure 2.3, lane 3).

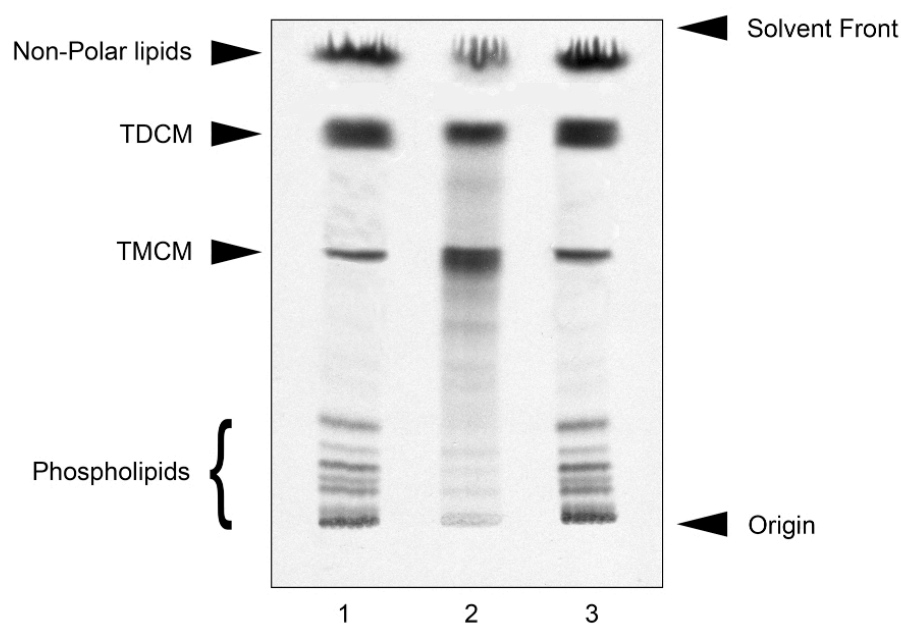


Figure 2.3: Quantitative analysis of extractable [^{14}C]lipids from *C. glutamicum*, *C. glutamicum* Δ *aftB* and *C. glutamicum* Δ *aftB* pMSX-Mt-*aftB*. Lipids were extracted from cells by a series of organic washes as described in “Materials and methods”. An aliquot (25,000 cpm) from each strain was subjected to TLC using silica gel plates (5735 silica gel 60F₂₅₄, Merck) developed in $\text{CHCl}_3/\text{CH}_3\text{OH}/\text{H}_2\text{O}$ (60:16:2, v/v/v) and either charred using 5% molybdophosphoric acid in ethanol at 100 °C to reveal the extracted lipids and compared to known standards (Alderwick *et al.*, 2005; Gande *et al.*, 2004) or quantified using a phosphorimager following exposure to Kodak X-Omat film for 24 h. The TLC-autoradiogram is representative of 3 independent experiments. Lane 1, *C. glutamicum*; lane 2, *C. glutamicum* Δ *aftB*; and lane 3, *C. glutamicum* Δ *aftB* pMSX-Mt-*aftB*.

To relate the above growth phenotypic changes of *C. glutamicum* Δ *aftB* to its cellular composition, *C. glutamicum* Δ *aftB* and *C. glutamicum* Δ *aftB* pMSX-Mt-*aftB*, along with wild type *C. glutamicum*, were analysed for arabinogalactan esterified corynomycolic acids released from the above [^{14}C]-delipidated cells. As expected, the wild type exhibited a typical profile of CMAMEs (Figure 2.4, lane 1, 28562 cpm), whereas these products were significantly reduced in *C. glutamicum* Δ *aftB* (Figure 2.4, lane 2, 8947 cpm). In addition, complementation of *C. glutamicum* Δ *aftB* with pMSX-Mt-*aftB* (Fig. 2.4, lane 3, 27523 cpm) led to the restoration of normal ‘levels’ of cell wall bound corynomycolic acids. These results suggested that Mt-*aftB* was involved in a key aspect of arabinan biosynthesis, whereby

deletion perturbs tethering of corynomycolic acids to AG, but not as severely as in *C. glutamicum* Δemb and *C. glutamicum* $\Delta aftA$ mutants (Alderwick *et al.*, 2005b; Alderwick *et al.*, 2006c).

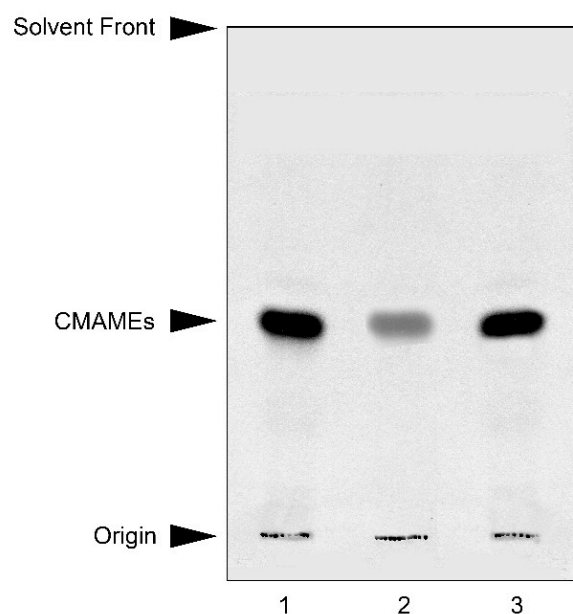


Figure 2.4: Quantitative analysis [^{14}C]CMAMEs from *C. glutamicum*, *C. glutamicum* $\Delta aftB$ and *C. glutamicum* $\Delta aftB$ pMSX-Mt-*aftB*. The bound [^{14}C]corynomycolic acids from [^{14}C] delipidated extracts were released by the addition of TBAH at 100 °C overnight and methylated as described in “Materials and Methods”. A 5% aliquot from each strain was subjected to TLC using silica gel plates (5735 silica gel 60F₂₅₄, Merck) developed in petroleum ether/acetone (95:5, v/v) and either charred using 5% molybdophosphoric acid in ethanol at 100 °C to reveal [^{14}C]CMAMEs and compared to known standards (Alderwick *et al.*, 2005; Gande *et al.*, 2004)) or quantified using a phosphorimager following exposure to Kodak X-Omat film for 24 h. The TLC-autoradiogram is representative of 3 independent experiments. Lane 1, *C. glutamicum*; lane 2, *C. glutamicum* $\Delta aftB$; and lane 3, *C. glutamicum* $\Delta aftB$ pMSX-Mt-*aftB*.

2.2.5. Cell wall glycosyl compositional and linkage analysis of cell walls

Alditol acetate derivatives of highly purified mAGP from *C. glutamicum*, *C. glutamicum* $\Delta aftB$ and *C. glutamicum* $\Delta aftB$ pMSX-Mt-*aftB* were prepared for glycosyl

compositional analysis. All strains exhibited a similar Ara:Gal ratio of 3.7:1. However, glycosyl linkage analysis of per-*O*-methylated alditol acetate derivatives of mAGP extracted from these strains highlighted an obvious difference in linkage profiles (Figure 2.5).

All glycosyl linkages could be accounted for in wild type *C. glutamicum* (Figure 2.5A) as described previously (Alderwick *et al.*, 2005b; Alderwick *et al.*, 2006c), however, mAGP from *C. glutamicum* Δ *aftB* was devoid of $\beta(1\rightarrow2)$ Araf linkages (Figure 2.5B). Complementation of *C. glutamicum* Δ *aftB* with pMSX-Mt-*aftB* restored the $\beta(1\rightarrow2)$ Araf linkage thus reverting the deletion mutant to a wild type phenotype (Figure 2.5C). Further to this, we analysed the cell wall glycosyl composition of *C. glutamicum* Δ *aftB* complemented with either pMSX-Mt-*aftB*-D29A or pMSX-Mt-*aftB*-D30A. Each of these complemented strains exhibited a phenotype identical to that of *C. glutamicum* Δ *aftB*, with a complete loss of 2-Araf linkages.

As confirmed by SDS-PAGE (Figure 2.6) the Mt-AftB muteins are synthesised *in vivo* and the failure to establish the $\beta(1\rightarrow2)$ Araf linkage is therefore most likely due to a catalytically inactive AftB, thus highlighting the importance of these particular aspartic acid residues in enzyme function.

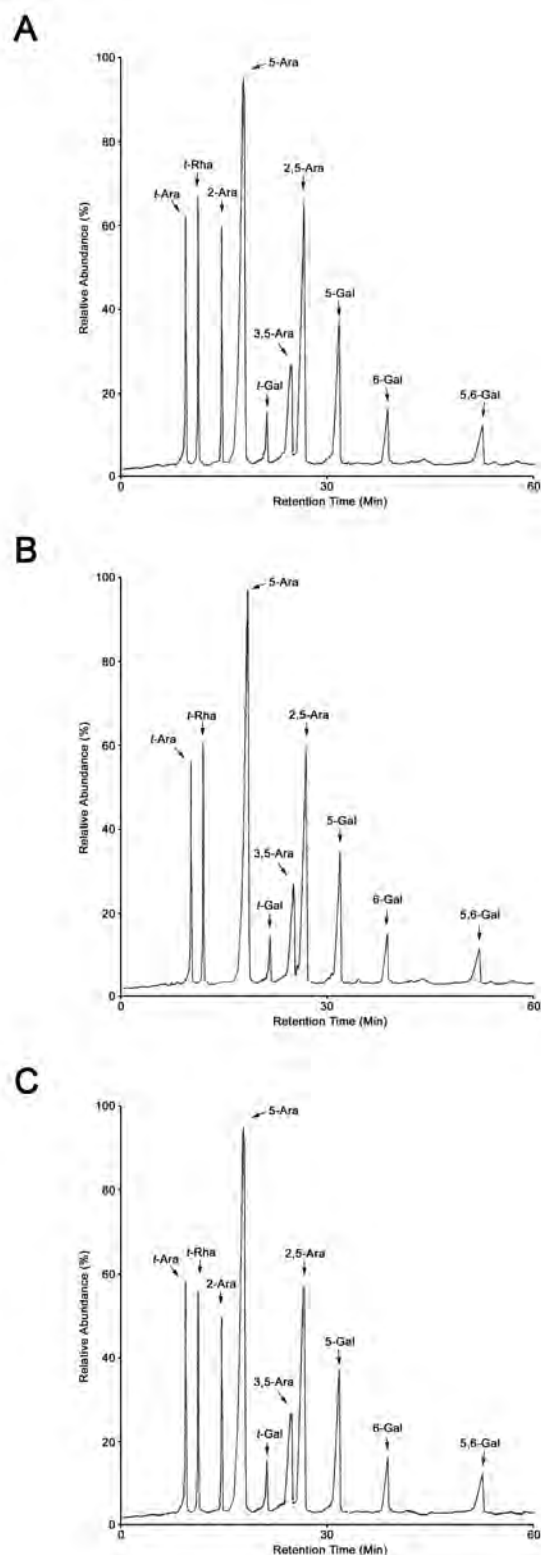


Figure 2.5: Glycosyl linkage analysis of cell walls of *C. glutamicum* (A), *C. glutamicum*Δ*aftB* (B), *C. glutamicum*Δ*aftB* pMSX-Mt-*aftB* (C). Cell walls were per-*O*-methylated, hydrolysed using 2M TFA, reduced and per-*O*-acetylated. The resulting partially per-*O*-methylated, per-*O*-acetylated glycosyl derivatives were analysed by GC/MS as described previously (Alderwick *et al.* 2005; Besra *et al.*, 1995; Daffé *et al.*, 1990).

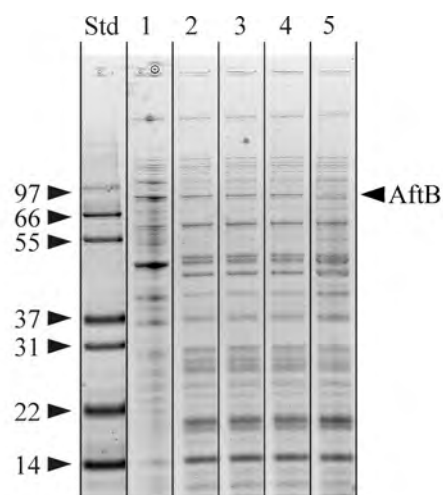


Figure 2.6. Formation of Mt-AftB in *C. glutamicum*. Extracts of *C. glutamicum* Δ *aftB* expressing His-tagged *M. tuberculosis* AftB and AftB muteins were subjected to Ni²⁺-NTA chromatography and analysed by SDS-PAGE. Lane 1, 20 μ g of clarified extract of *C. glutamicum* Δ *aftB* pMSX-Mt-*aftB* prior to chromatography. Lane 2-5 received the entire protein isolated from a 2 L culture of the respective recombinant strain via Ni²⁺-NTA chromatography, which was approximately 20 μ g in each case. Lane 2 *C. glutamicum* Δ *aftB* pMSX-Mt-*aftB*; lane 3, *C. glutamicum* Δ *aftB* pMSX-Mt-*aftB*-D29A; lane 4, *C. glutamicum* Δ *aftB* pMSX-Mt-*aftB*-D30A; and lane 5, *C. glutamicum* Δ *aftB* pMSX (control). Standards (Std) along with their molecular weights in kDa are shown. The expected molecular weight for Mt-AftB is 72 kDa and the faint band at this location in lanes 2-4 is shown by an arrow and was verified by peptide mass fingerprinting as *M. tuberculosis* AftB.

2.2.6. Endogenous *in vitro* arabinofuranosyltransferase activity of *C. glutamicum*, *C. glutamicum* Δ *aftB* and *C. glutamicum* Δ *aftB* complemented with Mt-*aftB* and product analysis.

We assessed the capacity of membrane preparations from *C. glutamicum*, *C. glutamicum* Δ *aftB* and *C. glutamicum* Δ *aftB*, complemented with pMSX-Mt-*aftB*, to catalyse arabinofuranosyltransferase activity in the presence of an exogenous synthetic α -D-Araf-(1 \rightarrow 5)- α -D-Araf-*O*-C₈, neoglycolipid acceptor (Lee *et al.*, 1997) and DP[¹⁴C]A (Lee *et al.*, 1998). TLC analysis of the products, when assayed with wild type *C. glutamicum* membranes, resulted in the formation of two products (A and B) (Figure 2.7A) when analysed by TLC (Figure 2.7B). The enzymatic synthesis of products A and B are consistent with previous studies (Lee *et al.*, 1997) using mycobacterial membrane preparations resulting in trisaccharide products as a result of the addition of α (1 \rightarrow 5) and β (1 \rightarrow 2) linked Araf residues to the disaccharide acceptor (Figure 2.7A) (Lee *et al.*, 1997). Addition of EMB in several experiments, even at high concentrations of up to 1 mg/ml to the reaction mixture, resulted in the complete loss of only product A. However, when assays were performed using

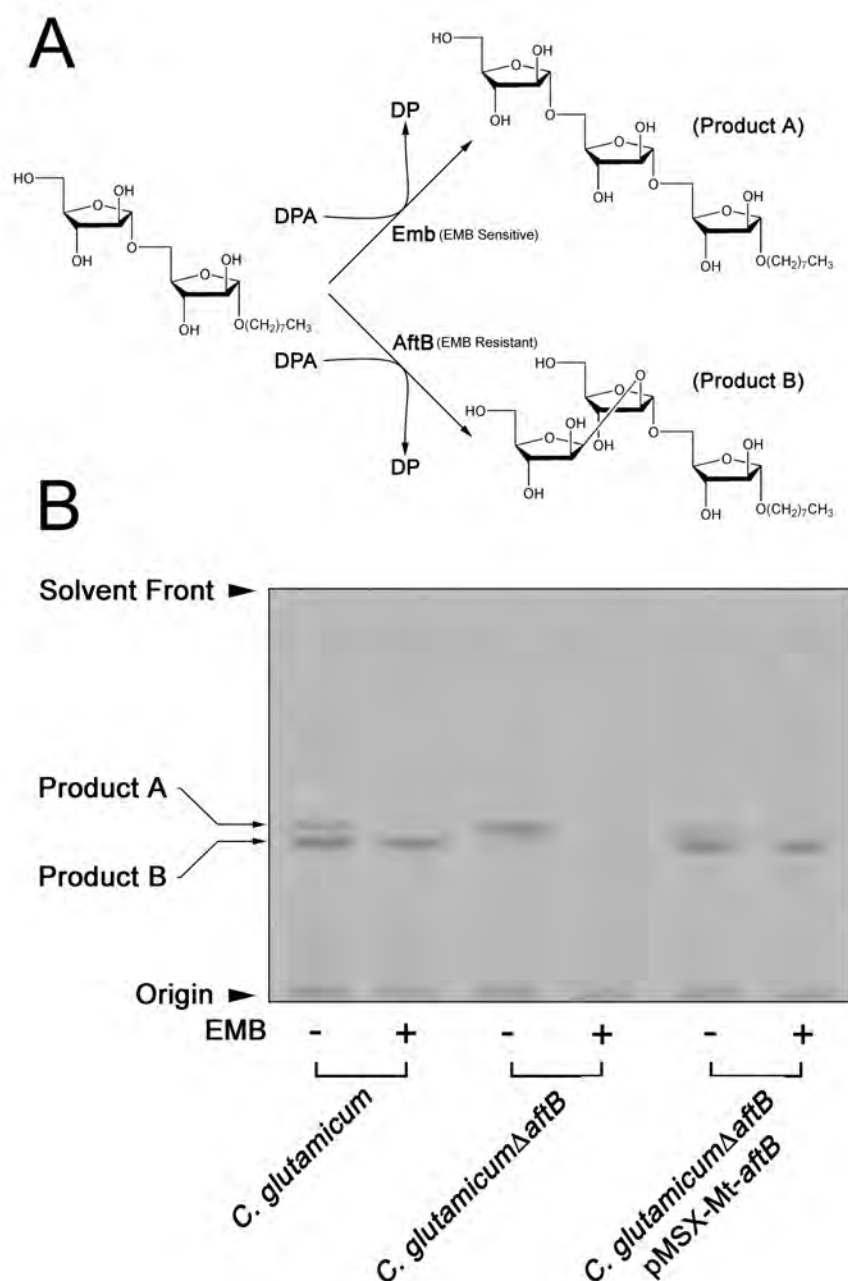


Figure 2.7: Arabinofuranosyltransferase activity in membranes prepared from *C. glutamicum*, *C. glutamicum* Δ *aftB* and *C. glutamicum* Δ *aftB* pMSX-Mt-*aftB*. A, Biosynthetic reaction scheme of products formed in arabinofuranosyltransferase assays using α -D-Araf-(1 \rightarrow 5)- α -D-Araf-O-C₈. B, Arabinofuranosyltransferase activity was determined using the synthetic α -D-Araf-(1 \rightarrow 5)- α -D-Araf-O-C₈ acceptor in a cell-free assay as described previously (Lee *et al.*, 1997). The products of the assay were resuspended prior to scintillation counting and subjected to TLC using silica gel plates (5735 silica gel 60F₂₅₄, Merck) in CHCl₃:CH₃OH:H₂O:NH₄OH (65/25/3.6/0.5, v/v/v/v) with the reaction products visualised by autoradiography.

Membranes, prepared from *C. glutamicum* Δ *aftB*, only a single band migrating to a position akin to that of product A could be observed and no product formation could be identified upon the addition of 100 μ g/ml of EMB (Figure 2.7B). Membranes prepared from *C. glutamicum* Δ *aftB*, complemented with pMSX-Mt-*aftB*, restored product A and B formation back to that of the wild type (Figure 2.7B) and only product B was synthesised when EMB (up to 1 mg/ml) was added to the reaction mixture.

2.2.7. ES-MS and GC/MS analysis of product A and B

Newly synthesised products A and B prepared using *C. glutamicum* treated with EMB and *C. glutamicum* Δ *aftB* membranes, as described above, were further characterised. ES-MS analysis of the reaction products A and B extracted through preparative TLC (Figure 2.8A), revealed a strong molecular ion m/z 549.3 ($M+Na^+$), which corresponds to a trisaccharide product Araf-(1 \rightarrow ?)-Araf-(1 \rightarrow 5)- α -D-Araf-*O*-C₈. GC/MS analysis of the partially per-*O*-methylated, per-*O*-acetylated alditol acetate derivative of product A, synthesised in assays with *C. glutamicum* Δ *aftB* membranes revealed the addition of only an α (1 \rightarrow 5) linked Araf residue (Figure 2.8B and Figure 2.7A) (Lee *et al.*, 1997). However, GC/MS analysis of the partially per-*O*-methylated, per-*O*-acetylated alditol acetate derivative of product B, synthesised in enzyme assays utilising membranes from *C. glutamicum* and EMB, identified the new glycosyl linkage as a β (1 \rightarrow 2)-linked Araf residue (Figure 2.8C and Figure 2.7A). By analogy, this new glycosidic linkage corresponds to a terminal β (1 \rightarrow 2) linked Araf residue (Lee *et al.*, 1997). Finally, the results clearly establish, both from *in vivo* and *in vitro* experiments, that Mt-AftB catalyses the addition of a β (1 \rightarrow 2) Araf unit, and that this enzyme is resistant to EMB (Figure 2.7B).

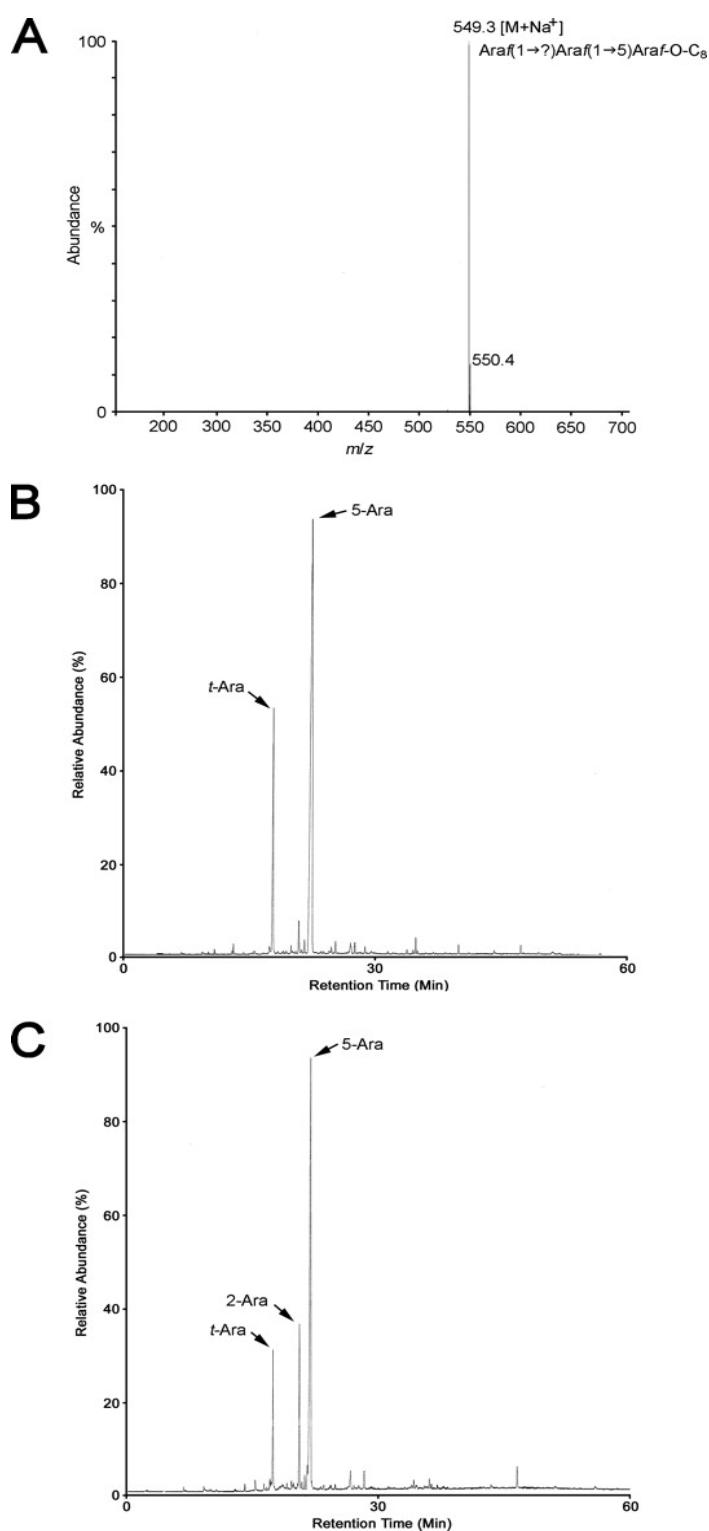


Figure 2.8: ES-MS and GC/MS characterisation of products A and B. **A**, ES-MS analysis of products from assays containing membranes prepared from *C. glutamicum* treated with EMB and *C. glutamicum*Δ*aftB*. **B**, GC/MS analysis of the partially per-*O*-methylated, per-*O*-acetylated alditol acetate derivative of product A obtained from assays containing membranes prepared from *C. glutamicum*Δ*aftB*. **C**, GC/MS analysis of the partially per-*O*-methylated, per-*O*-acetylated alditol acetate derivative of product B obtained from assays containing membranes and EMB prepared from *C. glutamicum*.

2.2.8. Genome comparison of the AftC locus

In silico analysis of one of the putative glycosyltransferases of *M. tuberculosis*, Rv2673, highlighted that orthologues are present in a range of species belonging to the sub-order *Corynebacterianeae*, including the families *Mycobacteriaceae*, *Corynebacteriaceae* and *Nocardiaceae* (Figure 2.9A).

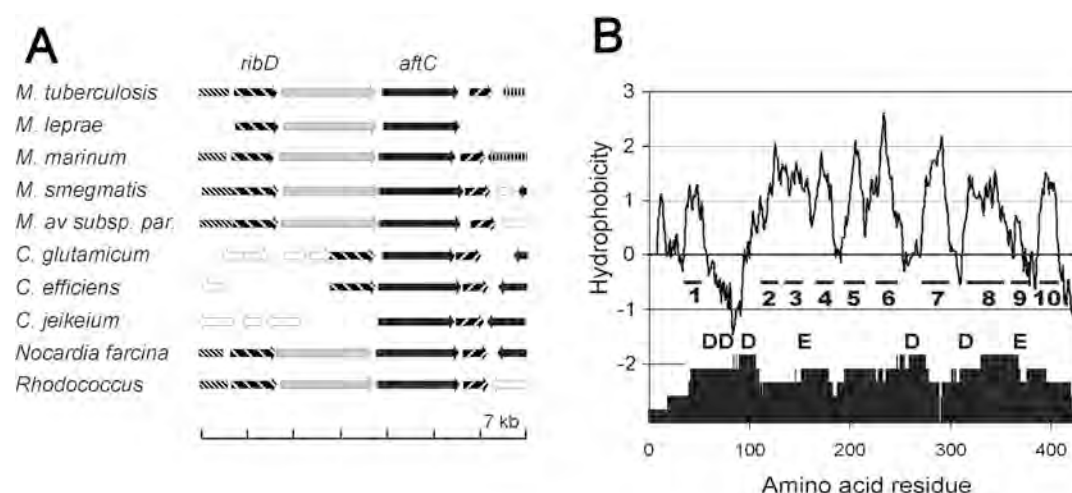


Figure 2.9: Comparison of the *aftC* locus within the *Corynebacterianeae*. **A)** The locus in the bacteria analysed consists of *aftC* which in *M. tuberculosis* has the locus tag Rv2673 and in *C. glutamicum* NCgl1822. The genomic region displayed encompasses 7 kb, and orthologous genes are highlighted accordingly. Abbreviations: *M. marinum*, *Mycobacterium marinum*; *M. av subsp. par.*, *Mycobacterium avium subsp. paratuberculosis*; *C. efficiens*, *Corynebacterium efficiens*; *C. jeikeium*, *Corynebacterium jeikeium*; *Nocardia farcina*, *Nocardia farcina* IFM 10152; *Rhodococcus*, *Rhodococcus* sp. strain RHA1. **B)** AftC is a hydrophobic protein predicted to span the membrane 10 times and the transmembrane helices are numbered accordingly. The lower part of the figure shows the degree of conservation of the orthologues given in A as analysed by the DIALIGN method (Brudno *et al.*, 2003). Also shown is the approximate position of the fully conserved aspartyl and glutamyl residues.

Furthermore, the organisation of the gene locus is largely retained. The adjacent genes are largely of unknown function. *RibD* encodes a bifunctional deaminase-reductase domain, followed by a gene product containing a hydrolase domain, which is however absent in *Corynebacterium*, and downstream of Rv2673 a domain of unknown function is present. The wide distribution of Rv2673, its syntenic organisation, and the fact that it is retained even in

M. leprae, strongly indicates a fundamental function of its product. According to our experimental analysis we annotated this gene arabinofuranosyltransferase C (*aftC*).

AftC of *M. tuberculosis* is 433 amino acid residues long. It is a hydrophobic protein and is predicted to possess 10 transmembrane-spanning segments (Figure 2.9B). However, in contrast to AftA, AftB or EmbC, it is characterised by the absence of a periplasmic carboxyterminal extension. The amino acid sequence among the *Corynebacteriaceae* is very well conserved, and there are 43% identical residues shared by the *M. tuberculosis* and *C. glutamicum* proteins. The degree of conservation is particularly high in the loop regions, for instance between helix 1 and 2, 3 and 4, or 6 and 7 (Figure 2.9B). The fully conserved aspartyl and glutamyl residues, which we propose to be involved in catalysis or substrate binding, are located in the first extended loop region (Liu & Mushegian, 2003) as demonstrated earlier with AftB. Interestingly, the long transmembrane helix 8 is well conserved and it is within this region that there is a strong identity to a membrane protein of *Vibrio parahaemolyticus* (CpsG). Furthermore, this gene is located in a gene cluster involved in the biosynthesis of a capsular polysaccharide within this pathogen (Guvener & McCarter, 2003).

2.2.9. Construction and growth of mutants

In order to delete *aftC* and study possible consequences, we generated a null mutant of *M. smegmatis* *mc*²155 *MSMEG2785* (homologue of *Rv2673*) using specialised transduction (Figure 2.10A). In contrast to our *C. glutamicum* studies (see below), growth of *M. smegmatis*Δ*aftC*, in comparison to *M. smegmatis*, was poor in liquid media (Figure 2.10B) and sensitive to the addition of Tween-20 on agar plates (>0.005%). In addition, on solid media, *M. smegmatis*Δ*aftC* had a smooth appearance in comparison to the typical crenulated colony morphology found for wild type *M. smegmatis* (Figure 2.11). Complementation of *M.*

*smegmatis*Δ*aftC* with either pMV261-Ms-*aftC* or pMV261-Mt-*aftC* restored the mutant to a wild type phenotype (Figure 2.10B).

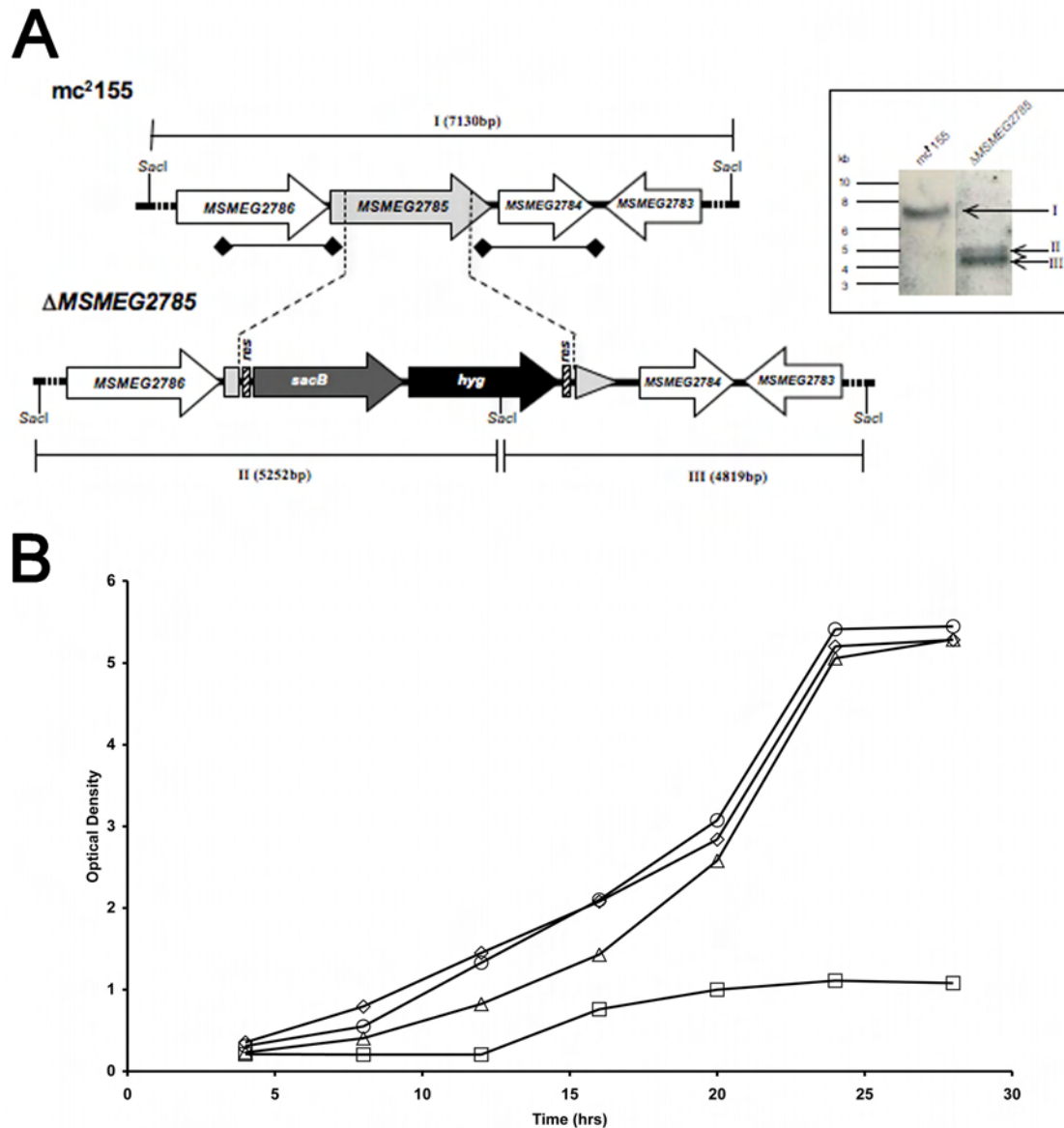


Figure 2.10: Generation of a *MSMEG2785* null mutant. **A)** A map of the *MSMEG2785* region in the parental *M. smegmatis* strain and its corresponding region in the Δ*MSMEG2785* mutant. *res*, γδ resolvase site; *hyg*, hygromycin resistance gene from *Streptomyces hygroscopicus*; *sacB*, sucrose counter-selectable gene from *Bacillus subtilis*. Digoxigenin-labelled probes were derived from ~1kb upstream and downstream flanking sequences that were used to construct the knockout plasmid, and are indicated by thick lines with square ends. *SacI* digested bands expected in a Southern blot are indicated in roman numerals with sises in brackets. The inset shows the Southern blot of *SacI* digested genomic DNA from the two strains with expected bands indicated by arrows. **B)** Growth of wild type of *M. smegmatis* (◇), *M. smegmatis*Δ*aftC* (□), *M. smegmatis*Δ*aftC* pMV261-Ms-*aftC* (Δ), and *M. smegmatis*Δ*aftC* pMV261-Mt-*aftC* (○) on TSB medium.

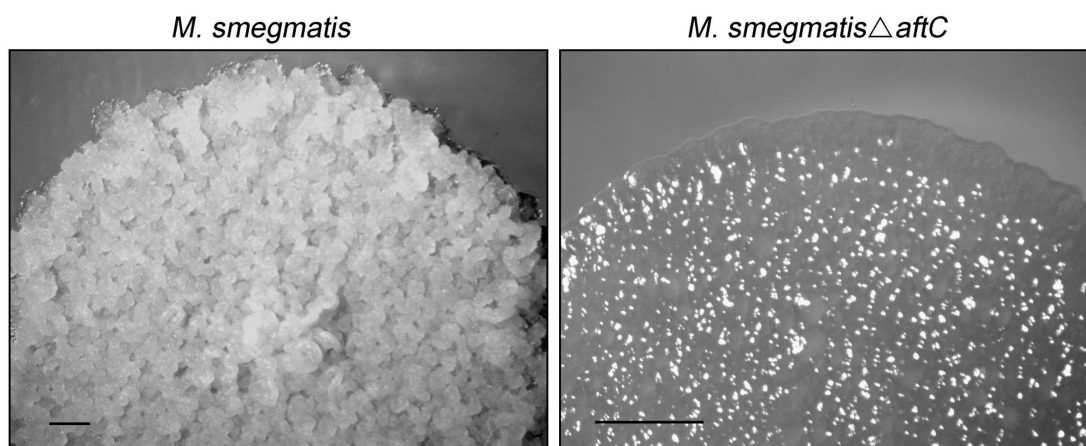


Figure 2.11: Colony morphology of wild-type *M. smegmatis* and *M. smegmatis* Δ *aftC* on TSB-agar plates. Black bar represents 1 mm.

To study the function of the corynebacterial AftC the non-replicative plasmid pK19mobsacB Δ *aftC* was constructed. This was used to transform *C. glutamicum* to kanamycin resistance, indicating integration in its chromosome (Figure 2.12). Loss of vector was obtained by selection for sucrose-resistance yielding clones with *aftC* deleted. A PCR analysis with primer pairs P5 and P6 resulted in the expected fragment of 2160 bp for the wild type and of 1065 bp for the deletion mutant, which was termed *C. glutamicum* Δ *aftC* (Figure 2.12A). In contrast to *M. smegmatis* Δ *aftC*, the growth of the *C. glutamicum* Δ *aftC* mutant on the salt medium CGXII possessed only a slightly reduced growth rate of 0.32 h^{-1} , whereas, that of the wild type *C. glutamicum* was 0.39 h^{-1} (Figure 2.12B).

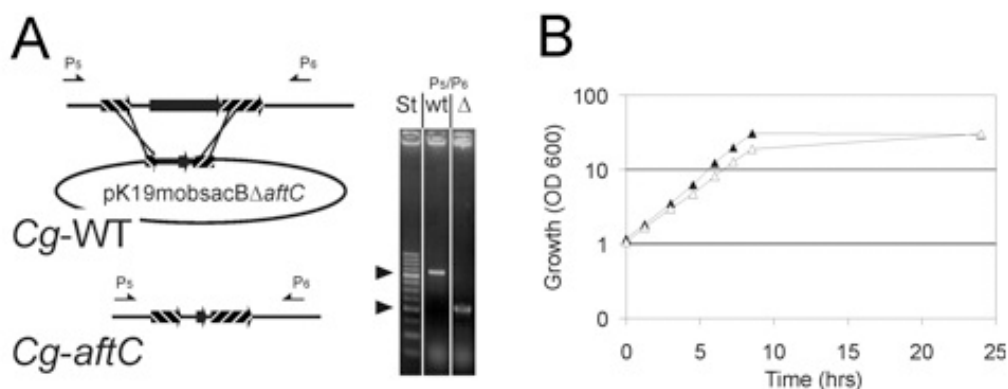


Figure 2.12: Strategy to delete *Cg-aftC* using the deletion vector *pK19mobsacBΔaftC*. **A)** This vector carries 18 nucleotides of the 5' end of *Cg-aftC* and 36 nucleotides of its 3' end thereby enabling the in-frame deletion of almost the entire *Cg-aftC* gene. The arrows marked P5 and P6 locate the primers used for the PCR analysis to confirm the absence of *Cg-aftC*. Distances are not drawn to scale. The results of the PCR analysis with the primer pair P5/P6 are shown on the right. Amplification products obtained from the wild type (wt) were applied in the middle lane and that of the deletion mutant in the right lane. 'St' marks the standard, where the arrowheads are located at 1 and 0.5 kb. **B)** Growth of the wild type of *C. glutamicum* (▲) and *C. glutamicumΔaftC* (Δ) on salt medium CGXII with glucose as carbon source.

2.2.10. Analysis of cell wall bound mycolic acids

To study the function of mycobacterial AftC deletion, defatted cells were analysed qualitatively for AG esterified mycolic acids from an equivalent starting amount of biomass for each strain, due to differences in growth rate (Figure 2.12B). As expected, *M. smegmatis* exhibited a typical profile of α , α' and epoxy-mycolic acid methyl esters (MAMEs), whereas, these products were drastically reduced in *M. smegmatisΔaftC* (Figure 2.13). In addition, complementation of *M. smegmatisΔaftC* with either pMV261-*Ms-aftC* or pMV261-*Mt-aftC* (Figure 2.13), led to the restoration of normal 'levels' of cell wall bound mycolic acids. These results demonstrated that *Ms-aftC* and *Mt-aftC* are involved in a key aspect of arabinan biosynthesis, whereby deletion substantially perturbs tethering of mycolic acids to AG.

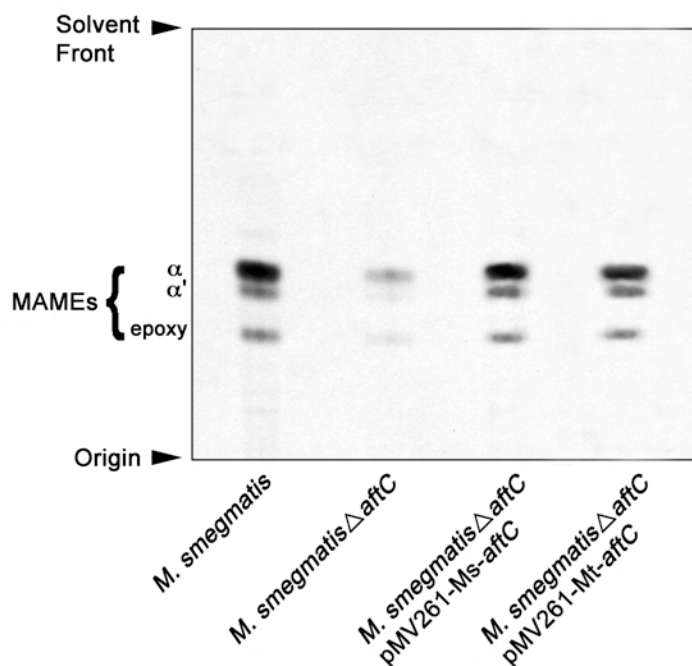


Figure 2.13: Analysis of cell wall bound MAMES from *M. smegmatis*, *M. smegmatis* Δ *aftC*, *M. smegmatis* Δ *aftC* pMV261-Ms-*aftC* and *M. smegmatis* Δ *aftC* pMV261-Mt-*aftC*. The bound mycolic acids from an equivalent amount of freeze-dried cells (100 mg), which were initially de-lipidated using two consecutive extractions of $\text{CHCl}_3:\text{CH}_3\text{OH}:\text{H}_2\text{O}$ (10/10/3; v/v/v/v) at 50°C for 4 h, were released by the addition of tetra-butylammonium hydroxide at 100°C overnight, and methylated as described in the “Materials and methods” Chapter 6. An equivalent aliquot from each strain was subjected to TLC using silica gel plates (5735 silica gel 60F₂₅₄, Merck), and developed in petroleum ether/acetone (95:5, v/v) and charred to reveal MAMES and compared to known standards (Gande *et al.*, 2004).

In contrast to the mycolic acid studies performed with the mycobacterial AftC deletion mutant, *C. glutamicum* Δ *aftC* cells were analysed quantitatively for AG esterified corynomycolic acids due to similar growth rates between strains (Figure 2.11B). Wild type *C. glutamicum* exhibited the known profile of corynomycolic acid methyl esters (CMAMES, 35,345 cpm) (Figure 2.14), whereas, cell wall bound CMAMES were significantly reduced in *C. glutamicum* Δ *aftC* (8023 cpm). The above data were reassuring, as the qualitative (*M. smegmatis* Δ *aftC*) and quantitative (*C. glutamicum* Δ *aftC*) analyses were comparable in terms of a reduction in cell wall bound mycolic acids (Figure 2.13 and Figure 2.14). Importantly,

these results have also shown that *Cg-afuC* is involved in a key aspect of arabinan biosynthesis, whereby deletion perturbs tethering of corynomycolic acids to AG.

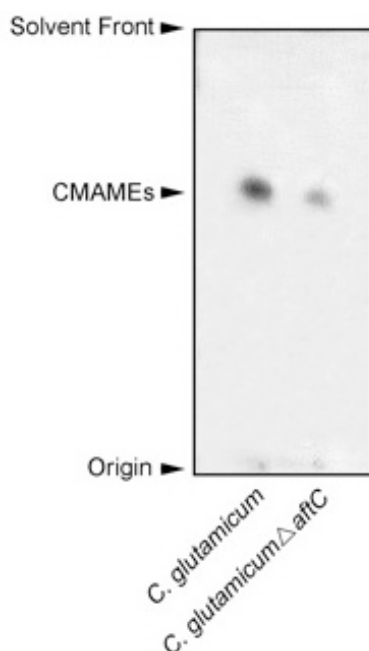


Figure 2.14: Analysis of cell wall bound CMAMES from *C. glutamicum* and *C. glutamicum* Δ *afuC*. The bound [14 C]-labeled corynomycolic acids from de-lipidated [14 C]-labeled cell of pulse-labeled 5 ml cultures were released by the addition of tetra-butyl ammonium hydroxide at 100°C overnight and methylated as described in the “Materials and methods”. An equivalent aliquot from each strain was subjected to TLC/autoradiography using silica gel plates (5735 silica gel 60F₂₅₄, Merck), and developed in petroleum ether/acetone (95:5, v/v) reveal CMAMES and compared to known standards.

2.2.11. Glycosyl compositional analysis of cell walls from *M. smegmatis*, *M. smegmatis* Δ *afuC* and complemented strains

The cell wall core (mAGP) was prepared from *M. smegmatis* and *M. smegmatis* Δ *afuC* as described (Alderwick *et al.*, 2005b; Besra *et al.*, 1995; Daffé *et al.*, 1990) and the ratio of Ara to Gal in mAGP determined by gas chromatography (GC) analysis of alditol acetates (Alderwick *et al.*, 2005b; Besra *et al.*, 1995; Daffé *et al.*, 1990) (Figure 2.15). The glycosyl compositional analysis revealed an Ara:Gal ratio of 2.45:1 for *M. smegmatis*. The *M.*

smegmatis Δ *aftC* yielded an AG with a significant reduction in cell wall Ara with an Ara:Gal ratio of 0.45:1. Complementation of *M. smegmatis* Δ *aftC* with either pMV261-*Ms-aftC* or pMV261-*Mt-aftC*, restored the Ara:Gal ratio to that of the wild type *M. smegmatis* (Figure 2.15, Ara:Gal, 2.40:1).

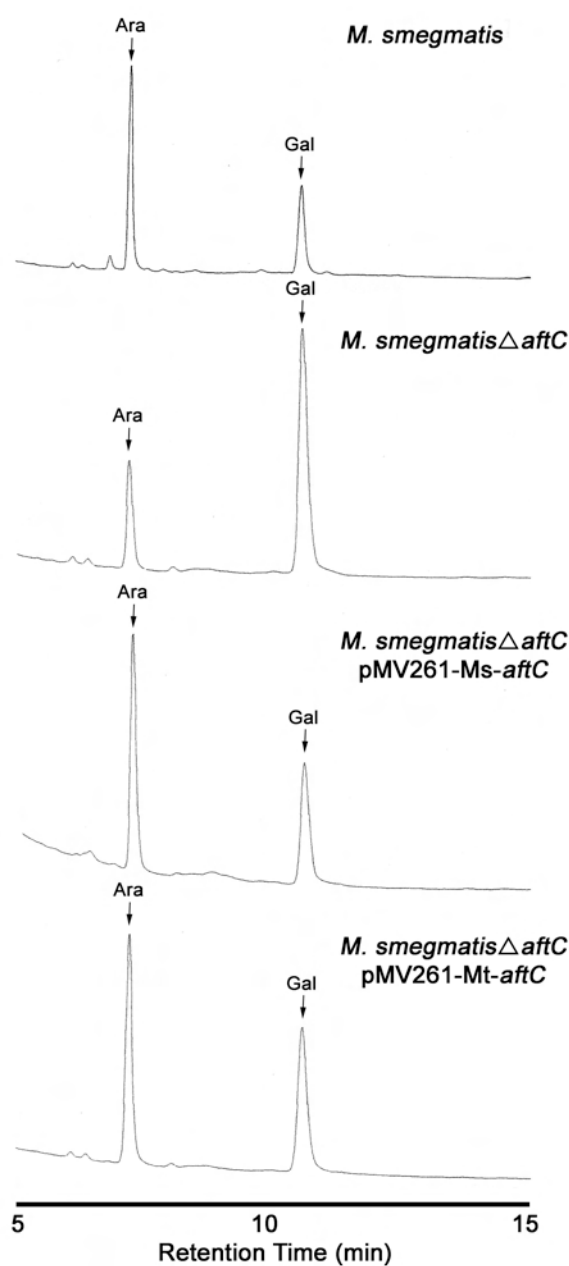


Figure 2.15: GC analysis of cell walls of *M. smegmatis*, *M. smegmatis* Δ *aftC*, *M. smegmatis* Δ *aftC* pMV261-*Ms-aftC* and *M. smegmatis* Δ *aftC* pMV261-*Mt-aftC*. Samples of purified cell walls were hydrolysed with 2M TFA, reduced, per-*O*-acetylated and analysed as described under “Materials and Methods” (Alderwick *et al.*, 2005b; Besra *et al.*, 1995).

2.2.12. Glycosyl linkage analysis of cell walls

Gas chromatography mass spectrometry (GC/MS) analysis of per-*O*-methylated alditol acetate derivatives prepared from *M. smegmatis* and *M. smegmatis* Δ *aftC* indicated the complete absence of 3,5-Araf branching residues, with a significant reduction in *t*-Araf, 2-Araf and 5-Araf-linkages (Figure 2.16). Complementation of *M. smegmatis* Δ *aftC* with either plasmid encoding Ms-*aftC* or Mt-*aftC* restored the glycosyl linkage profile to that of wild type *M. smegmatis* (Figure 2.16). These results demonstrate that MSMEG2875 and Rv2673, are functionally equivalent and are involved in the synthesis of 3,5-Araf branching residues. The GC/MS profiles of per-*O*-methylated alditol acetate derivatives of *C. glutamicum* and *C. glutamicum* Δ *aftC* are shown in Figure 2.17 with *C. glutamicum* Δ *aftC* also clearly devoid of 3,5-Araf branching residues.

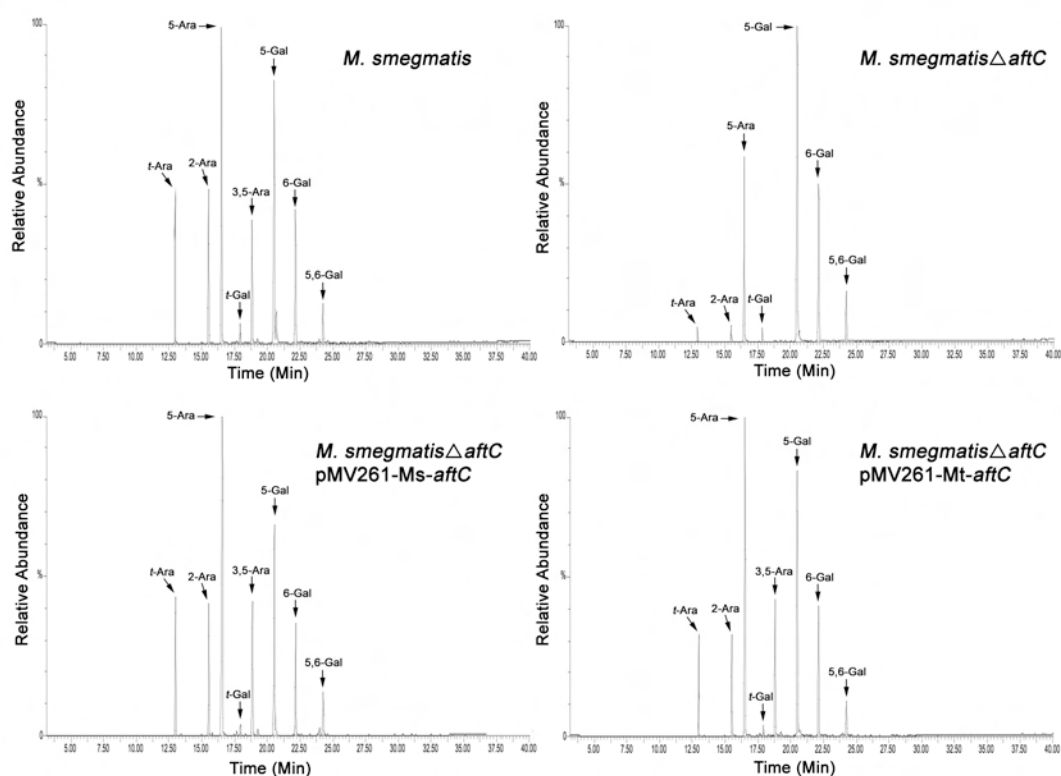


Figure. 2.16: GC/MS analysis of cell walls of *M. smegmatis*, *M. smegmatis* Δ *aftC*, *M. smegmatis* Δ *aftC* pMV261-Ms-*aftC* and *M. smegmatis* Δ *aftC* pMV261-Mt-*aftC*. Per-*O*-methylated cell walls were hydrolysed with 2M TFA, reduced, per-*O*-acetylated and analysed as described under “Materials and methods” (Alderwick *et al.*, 2005b; Besra *et al.*, 1995).

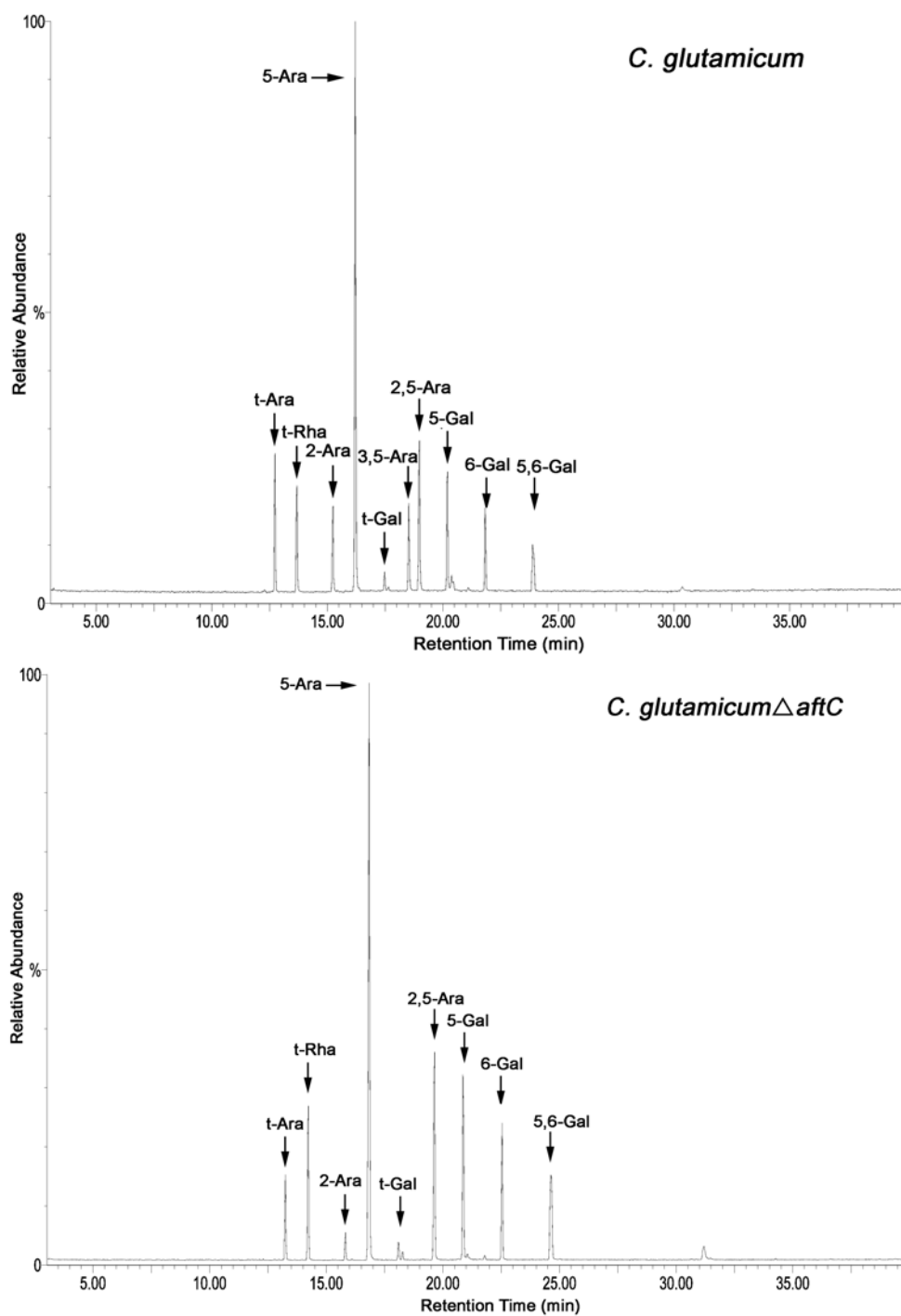


Figure 2.17: GC and GC/MS analysis of cell walls of *C. glutamicum* and *C. glutamicum*Δ*aftC*. Samples of either purified cell walls or per-*O*-methylated, hydrolysed using 2M TFA, reduced, per-*O*-acetylated and analysed as described under “Materials and methods”.

2.2.13. *In vitro* arabinofuranosyltransferase activity with extracts of *M. smegmatis*, *M. smegmatis* Δ *aftC* and complemented strains

Initial attempts to develop an *in vitro* assay using either purified recombinant expressed AftC or *E. coli* membranes expressing *aftC*, have thus far proved unsuccessful, probably due to the hydrophobic nature of the protein. In an alternative approach, we assessed the capacity of membrane preparations from *M. smegmatis*, *M. smegmatis* Δ *aftC* and *M. smegmatis* Δ *aftC* complemented with pMV261-Mt-*aftC* to catalyse arabinofuranosyltransferase activity in the presence of exogenous synthetic acceptors (Lee *et al.*, 1997; Seidel *et al.*, 2007b).

We first assessed whether *M. smegmatis* Δ *aftC* was deficient in $\alpha(1\rightarrow5)$ and $\beta(1\rightarrow2)$ arabinofuranosyltransferase activity, using an α -**D**-Araf-(1 \rightarrow 5)- α -**D**-Araf-*O*-(CH₂)₇CH₃ (Ara₂) synthetic acceptor (Lee *et al.*, 1997) and DP[¹⁴C]A as a sugar donor based on an established assay format for determining $\alpha(1\rightarrow5)$ and $\beta(1\rightarrow2)$ arabinofuranosyltransferase activities (Lee *et al.*, 1998). TLC/autoradiographic analysis of the products, which were only synthesised in the presence of Ara₂, when assayed with *M. smegmatis* membranes resulted in the formation of two products (A and B) (Figure 2.18A and B). The enzymatic synthesis of products A and B are consistent with previous studies using mycobacterial (Lee *et al.*, 1997) membrane preparations resulting in trisaccharide products as a result of $\alpha(1\rightarrow5)$ and $\beta(1\rightarrow2)$ Araf linkages to the Ara₂ acceptor (Figure 2.18A) (Lee *et al.*, 1997). Addition of EMB in several experiments, even at high concentrations of up to 1 mg/ml, to the reaction mixture, resulted in a decrease in only the *in vitro* synthesised α -**D**-[¹⁴C]Araf-(1 \rightarrow 5)- α -**D**-Araf-(1 \rightarrow 5)- α -**D**-Araf-*O*-(CH₂)₇CH₃ product A (Figure 2.18A and B). Assays performed with membranes from *M. smegmatis* Δ *aftC* and the pMV261-Mt-*aftC* complemented strain using the Ara₂ synthetic acceptor gave a similar profile to that of wild type *M. smegmatis* (Figure 2.18B). The data clearly show that the *M. smegmatis* Δ *aftC* strain possesses comparable levels of EMB-sensitive $\alpha(1\rightarrow5)$ and EMB-resistant $\beta(1\rightarrow2)$ arabinofuranosyltransferase activity.

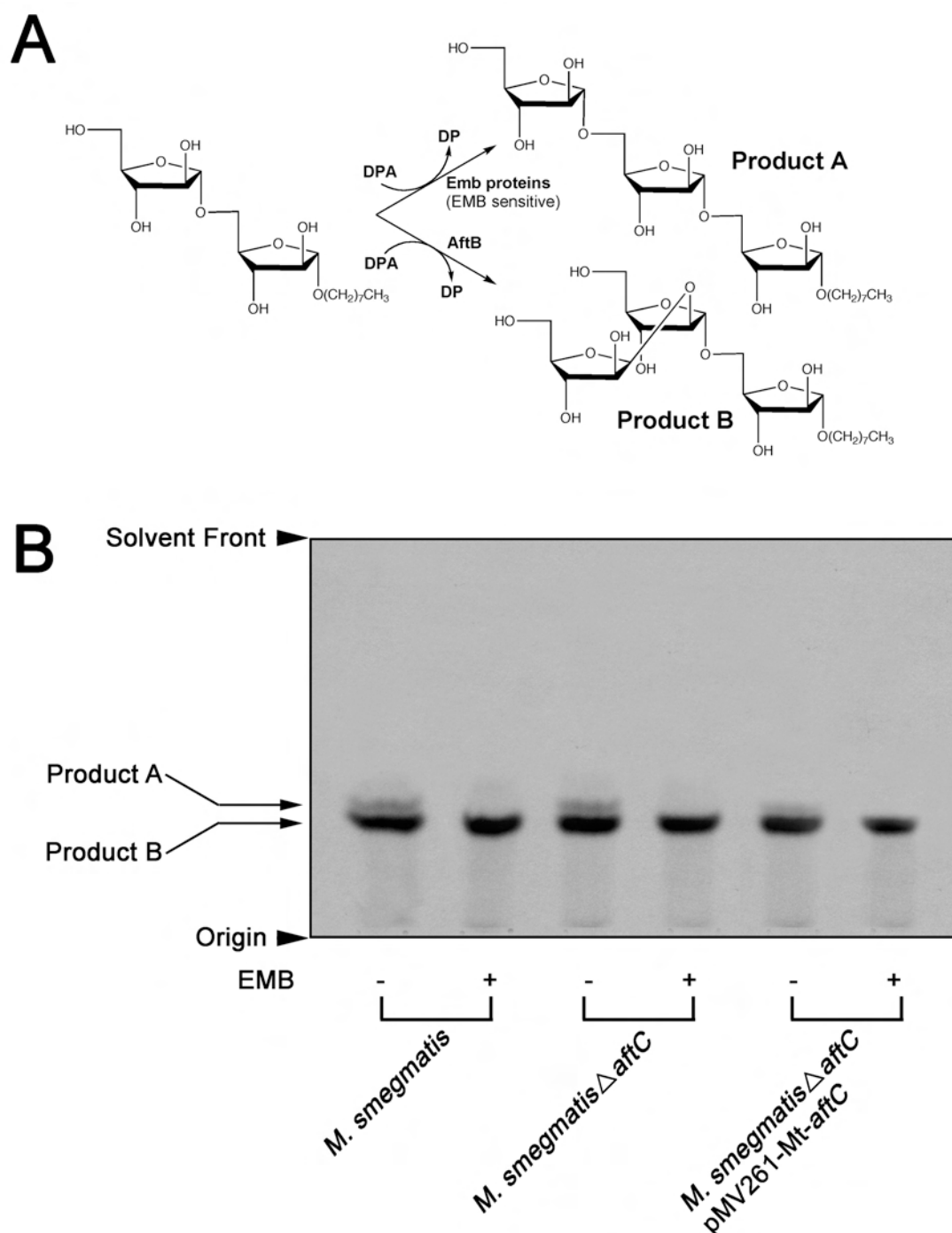


Figure 2.18: Arabinofuranosyltransferase activity utilising an Ara₂ acceptor and membranes prepared from *M. smegmatis*, *M. smegmatis*Δ*aftC* and *M. smegmatis*Δ*aftB* pMV261-Mt-*aftC*. **A)** Biosynthetic reaction scheme of products A and B formed in arabinofuranosyltransferase assays using the neoglycolipid Ara₂ acceptor. **B)** Arabinofuranosyltransferase activity was determined using the synthetic Ara₂ acceptor in a cell-free assay with and without EMB (1 mg/ml) as previously described (Lee *et al.*, 1997). The products of the assay were resuspended prior to scintillation counting (10 %) and the remaining subjected to TLC using silica gel plates (5735 silica gel 60F₂₅₄, Merck) in CHCl₃:CH₃OH:H₂O:NH₄OH (65/25/3.6/0.5, v/v/v/v) with the reaction products visualised by autoradiography. The TLC autoradiogram is representative of several independent experiments.

We then developed an arabinofuranosyltransferase assay using the synthetic acceptor α -**D**-Araf-(1 \rightarrow 5)- α -**D**-Araf-(1 \rightarrow 5)- α -**D**-Araf-(1 \rightarrow 5)- α -**D**-Araf-(1 \rightarrow 5)- α -**D**-Araf-*O*-(CH₂)₈NH₂ (Ara₅) (See figure 2.20B) and DP[¹⁴C]A as a sugar donor (Lee *et al.*, 1998). TLC/autoradiographic analysis of the products, which are only synthesised in the presence of Ara₅, when assayed with *M. smegmatis* membranes resulted in the formation of a single product X (Figure 2.19A) through the transfer of a single [¹⁴C]Araf residue, with a retardation factor (*R_f*) consistent with a synthetic Ara₆ acceptor (Appelmelk *et al.*, 2008) standard (Figure 2.19B). Interestingly, addition of EMB in several experiments, even at high concentrations of up to 1 mg/ml to the reaction mixture did not inhibit the synthesis of this *in vitro* synthesised [¹⁴C]Araf-Ara₅ (Figure 2.19A, Product X), illustrating that the Ara₅ acceptor was not extended *via* an EMB-sensitive α (1 \rightarrow 5) arabinofuranosyltransferase. Interestingly, membranes prepared from the *M. smegmatis* Δ *aftC* strain were unable to synthesise the *in vitro* product to the same level of activity that was observed with wild type membranes prepared from *M. smegmatis* (Figure 2.19A). This was not surprising, since our earlier *in vivo* and *in vitro* studies would have expected residual Ara₆ product formation, considering that *M. smegmatis* Δ *aftC* possesses β (1 \rightarrow 2) arabinofuranosyltransferase activity. Assays performed with membranes from the *M. smegmatis* Δ *aftC* pMV261-Mt-*aftC* complemented strain, gave a similar profile to that of wild type *M. smegmatis* (Figure 2.19).

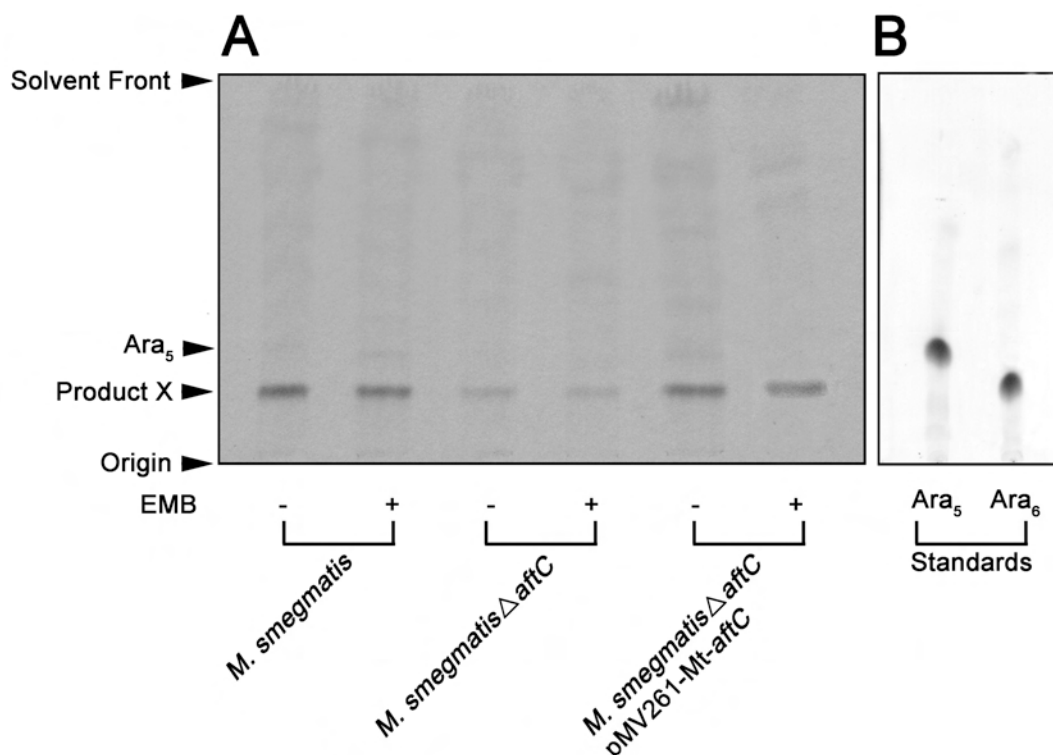


Figure 2.19: Arabinofuranosyltransferase activity utilising an Ara₅ acceptor and membranes prepared from *M. smegmatis*, *M. smegmatis*Δ*aftC* and *M. smegmatis*Δ*aftC* pMV261-Mt-*aftC*. **A)** AraT activity was determined using the synthetic Ara₅ acceptor in a cell-free assay with and without EMB (1mg ml⁻¹). The products reflective of three independent enzymes and assayed were resuspended prior to scintillation counting (10%) and the remaining subjected to TLC using silica gel plates (5735 silica gel 60F254 Merck) in isopropanol/actetic acid/water 8/1/1 v/v/v), with the reaction product X visualised with autoradiography. The TLC autoradiogram is representative of three different independent experiments. **B)** Ara₅ and Ara₆ (Appelmek *et al.*, 2008) acceptor standards were subjected to TLC as above, and the reaction products were visualised by staining with α -naphthol followed by charring.

To establish that the Ara₅ acceptor is being utilised by two different arabinofuranosyltransferases, presumably establishing $\beta(1\rightarrow2)$ and $\alpha(1\rightarrow3)$ linkages, assays similar to that used before were scaled up and product X extracted and purified through preparative TLC for each membrane preparation. GC/MS analysis of the partially per-*O*-methylated, per-*O*-acetylated alditol acetate derivatives of product X in assays preformed with *M. smegmatis* membranes revealed the addition of $\beta(1\rightarrow2)$ (R_t 15.52 min; m/z 129, 130, 161, 190) and $\alpha(1\rightarrow3)$ (R_t 15.83 min; m/z 118, 129, 130, 190, 202, 233) linked Ara_f residues (Figure 2.20A and B). Therefore, the product migrating below Ara₅ and co-incident

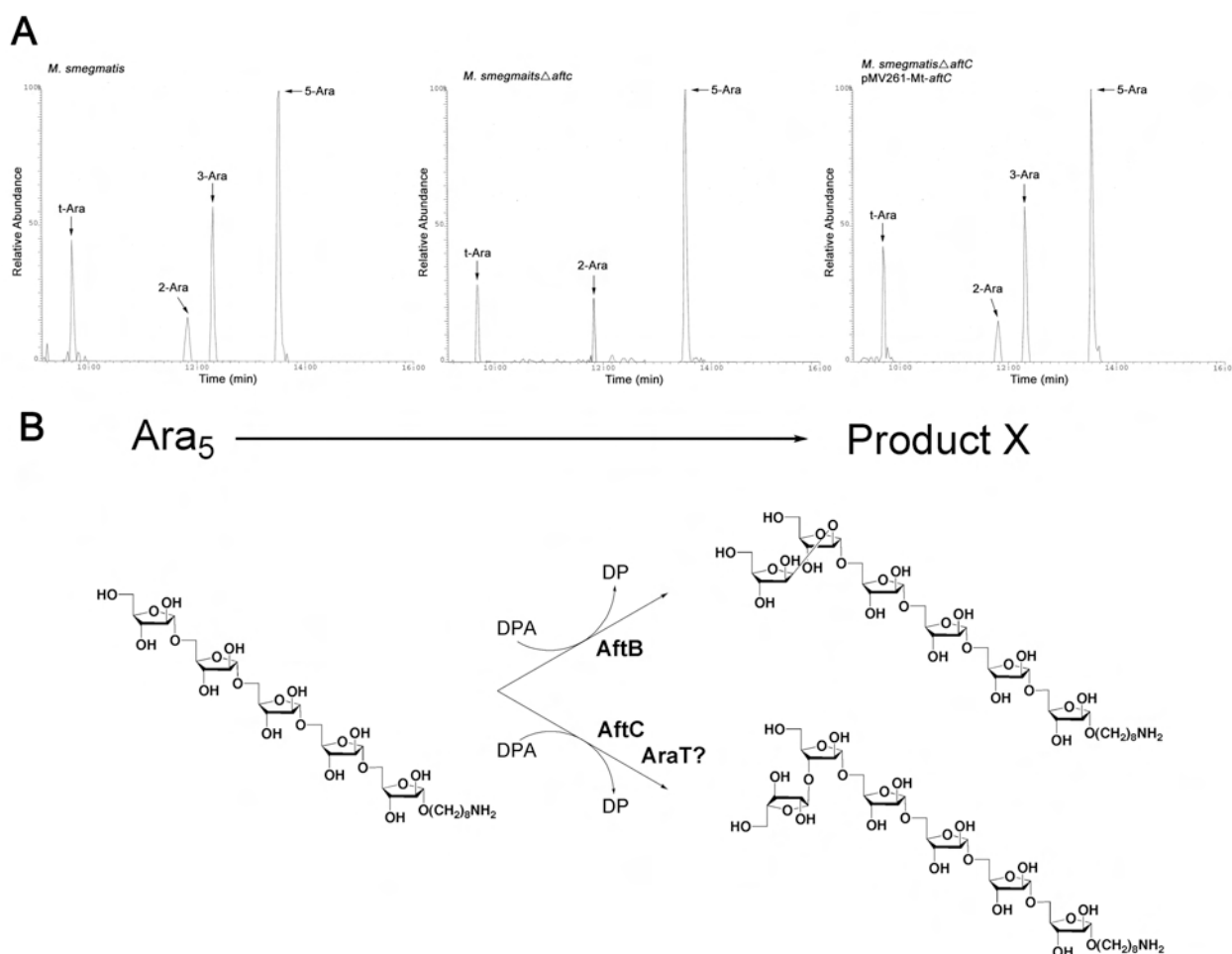


Figure 2.20: GC/MS characterisation of *in vitro* synthesised product X from the arabinofuranosyltransferase assays utilising the Ara₅ acceptor. **A)** GC/MS analysis of the partially per-*O*-methylated, per-*O*-acetylated alditol acetate derivative of product X obtained from assays containing membranes prepared from either *M. smegmatis*, *M. smegmatis*Δ*aftC* or *M. smegmatis*Δ*aftB* pMV261-Mt-*aftC*. **B)** Panel illustrates the structure(s) of product X.

with the Ara₆ acceptor standard on TLC (Figure 2.19A and B) is in fact a mixture of two products. The addition of β(1→2)-linked Ara_f residues can be attributed to the function of AftB. The presence of α(1→3)-linked Ara_f residues in this assay using an Ara₅ acceptor clearly highlights the role of a novel arabinofuranosyltransferase(s) capable of functioning in an α(1→3) capacity. Importantly, there is a complete removal of α(1→3) activity when the Ara₅ acceptor is incubated with membranes prepared from *M. smegmatis*Δ*aftC* (Figure

2.20A). However, $\beta(1\rightarrow2)$ activity is clearly present in *M. smegmatis* Δ *aftC* (Figure 2.20A). In addition, *M. smegmatis* Δ *aftC* complemented with pMV261-Mt-*aftC* restores $\alpha(1\rightarrow3)$ arabinofuranosyltransferase activity to wild type *M. smegmatis* (Fig 2.20A). The results clearly establish both from *in vivo* and *in vitro* experiments that AftC catalyses the addition of an $\alpha(1\rightarrow3)$ -Araf unit *via* an $\alpha(1\rightarrow3)$ arabinofuranosyltransferase and that this enzyme is also resistant to EMB (Figure 2.19A).

2.2.14. Discussion

The mAGP represents one of the most important cell wall components of the *Corynebacteriaceae* and is essential for the viability of *M. tuberculosis* (Gande *et al.*, 2004; Mills *et al.*, 2004; Pan *et al.*, 2001; Vilcheze *et al.*, 2000). It is therefore not surprising that one of the most effective anti-mycobacterial drugs, EMB, targets its synthesis through inhibition of AG biosynthesis. However, the emergence of MDR-TB and XDR-TB has accelerated the need to discover new drug targets (Brennan & Nikaido, 1995). One of the strategies is to identify genes involved in AG biosynthesis. This strategy was previously used to identify the presence of a new “priming” enzyme, now termed AftA, which would link the initial Araf unit with the C-5 OH of a $\beta(1\rightarrow6)$ linked Galf of a pre-synthesised galactan core (Alderwick *et al.*, 2005b).

Although, the previously described Emb (Alderwick *et al.*, 2005b) and AftA (Alderwick *et al.*, 2006c) are arabinofuranosyltransferases, the proteins cannot functionally replace each other. Thus, despite some functional relationship, these glycosyltransferases have inherent specific features, as evident from the insensitivity of AftA towards EMB. The single Cg-Emb (Alderwick *et al.*, 2005b; Radmacher *et al.*, 2005) and Mt-Emb proteins are sensitive towards EMB (Belanger *et al.*, 1996; Telenti *et al.*, 1997). The number of arabinofuranosyltransferases that are required for mycobacterial arabinan biosynthesis has been a matter of speculation to date, depending on how the arabinan chains are assembled. The primary structure of AG (Besra *et al.*, 1995; Daffé *et al.*, 1990) would suggest at least five distinct arabinofuranosyltransferases are required for the complete formation of AG. Interestingly, *M. smegmatis* *embA* and *embB* mutants were found to possess reduced amounts of the non-reducing terminal disaccharide β -D-Araf-(1 \rightarrow 2)-a-D-Araf and result in the removal of the dominant terminal non-reducing Ara₆ branched motif in the mutant being

replaced by a linear Ara₄ motif. The authors of this study concluded that the *M. smegmatis* *embA* and *embB* mutants result in a lack of 3-arm branching off the main $\alpha(1\rightarrow5)$ -arabinan chain proximal to the non-reducing and attachment site of mycolic acids in AG (Escuyer *et al.*, 2001). Initially, it was proposed that the β -**D**-Araf-(1 \rightarrow 2)- α -**D**-Araf disaccharide was assembled using EmbA and EmbB. However, the identification of AftB in this study and the development of an *in vitro* assay (Lee *et al.*, 1997) suggests that EmbA/B act as $\alpha(1\rightarrow5)$ arabinofuranosyltransferases.

This study has identified Rv3805c, which has now been termed AftB, as a novel retaining arabinofuranosyltransferase, and is likely to form a new family which is distinct from the inverting arabinofuranosyltransferase enzymes (EmbA, B, C, and AftA) in GT-83/85 families (Coutinho & Henrissat, 1999). More precisely, AftB adds to the non-reducing end of the arabinan domain of AG $\beta(1\rightarrow2)$ Araf residues, as shown through both *in vivo* and *in vitro* experiments. For instance, incubation of membranes prepared from *C. glutamicum* with DP[¹⁴C]A and the disaccharide neoglycolipid acceptor resulted in the appearance of two trisaccharide products (A and B), which equate to the transfer of both $\alpha(1\rightarrow5)$ and $\beta(1\rightarrow2)$ Araf residues, respectively. Through further chemical characterisation of the products by TLC, ES-MS, and glycosyl linkage analyses, an $\alpha(1\rightarrow5)$ linked trisaccharide product could only be identified in assays conducted with membranes prepared from *C. glutamicum* Δ *aftB*. This clear loss of $\beta(1\rightarrow2)$ Araf activity corroborates the cell wall analysis of the *C. glutamicum* Δ *aftB* mutant, where the loss of $\beta(1\rightarrow2)$ linked Araf residues could also be observed. We also attempted to inhibit AftB activity by incubation of the assay components in the presence of high concentrations of EMB (up to 1 mg/ml), a known inhibitor of the Emb proteins in *M. tuberculosis* and *C. glutamicum*. In doing so, analysis of the corresponding products synthesised from *C. glutamicum* membranes following EMB

treatment clearly show evidence of an EMB resistant $\beta(1\rightarrow2)$ arabinofuranosyltransferase activity and an EMB sensitive $\alpha(1\rightarrow5)$ arabinofuranosyltransferase activity. In addition, since it has previously been established that the EMB-resistant AftA introduces the priming Ara_f residue at the 8th, 10th and 12th Gal_f residue of the galactan backbone, it can be concluded that the bulk $\alpha(1\rightarrow5)$ Ara_f stems of AG represent the primary target of EMB. It is interesting to note that EMB resistance is simply not due to AftB being a retaining arabinofuranosyltransferase, in contrast to the inverting arabinofuranosyltransferase Mt-EmbA and Mt-EmbB, since AftA, which is also an inverting arabinofuranosyltransferase, is also EMB resistant (Alderwick *et al.*, 2006c). It is noteworthy that deletion of *aftB* in *C. glutamicum* results in only a weak phenotype (Figure 2.2B). In *M. tuberculosis*, mycolic acids are attached to the terminal $\beta(1\rightarrow2)$ Ara_f and penultimate $\alpha(1\rightarrow5)$ Ara_f residue of the Ara₆ motif of AG (McNeil *et al.*, 1991). This appears to be similar in *C. glutamicum* since, in the absence of terminal $\beta(1\rightarrow2)$ Ara_f residues, mycolic acids are still bound to AG, thus emphasizing, in this respect, the cell wall similarity of these bacteria. However, in *C. glutamicum* a maximal 5% of the mycolic acids are covalently attached to AG (Puech *et al.*, 2001), whereas this value is about 10% in *M. tuberculosis* (McNeil *et al.*, 1991). The fact that the *aftB* deletion mutant of *C. glutamicum* possesses less AG bound mycolic acids, also results in an increased abundance of TCM. This situation can be entirely different in *M. tuberculosis* due to the essentiality of *aftB* in *M. tuberculosis* (Sasseti *et al.*, 2003) and requires further investigation.

A modified scheme for terminal cell wall arabinan biosynthesis in *Corynebacteriaceae* is presented in Figure 2.21. It is possible that the AftB protein is responsible for the successive addition of two $\beta(1\rightarrow2)$ Ara_f residues at a 3,5-Ara_f branched residue. Although, this may be a reasonable inference from the *in vivo* structural work with the *aftB* deletion strain, it has not

been completely verified by our *in vitro* assay. Therefore, it is formally possible that the AftB-dependent addition of one $\beta(1\rightarrow2)$ Araf residue is required, before a second GT-C related arabinofuranosyltransferase adds the second terminal $\beta(1\rightarrow2)$ Araf residue as shown in Figure 2.21.

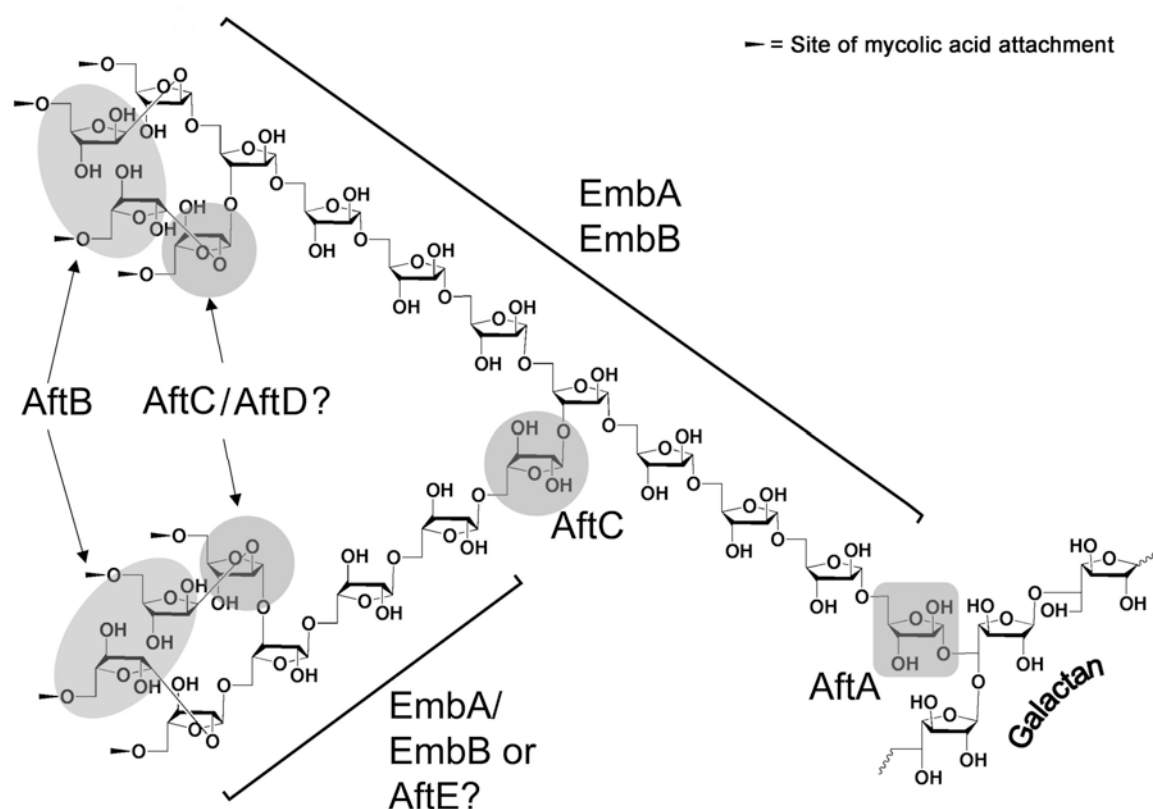


Figure 2.21: Proposed mycobacterial arabinan biosynthesis and the role of AftB and AftC. For reasons of simplicity it is shown that one of the $\beta(1\rightarrow2)$ linked Araf residues is added by AftB, whilst the second $\beta(1\rightarrow2)$ linked Araf residue may be catalysed by AftB or *via* an unknown GT-C arabinofuranosyltransferase (AftD), presumably closely related to AftB.

This study has also identified MSMEG2785 (also Rv2673 and NCgl1822), which we have termed AftC, as a novel branching arabinofuranosyltransferase. More precisely, AftC

catalyses the addition of $\alpha(1\rightarrow3)$ Araf residues as shown through both *in vivo* and *in vitro* experiments, ultimately resulting in 3,5-Araf residues after further $\alpha(1\rightarrow5)$ extension, characteristic of AG. For instance, incubation of membranes prepared from *M. smegmatis* with DP[^{14}C]A and a linear $\alpha(1\rightarrow5)$ -Ara₅ neoglycolipid acceptor resulted in the synthesis of an Ara₆ product. Further chemical characterisation of the product, by glycosyl linkage analysis, established that the $\alpha(1\rightarrow5)$ -Ara₅ acceptor was extended *via* an EMB resistant $\alpha(1\rightarrow3)$ arabinofuranosyltransferase, giving rise to 3-linked Araf residues and corroborating our earlier cell wall analysis of the *M. smegmatis* ΔaftC mutant. Since, it is now established that only $\alpha(1\rightarrow5)$ arabinofuranosyltransferase(s) are EMB-sensitive it can be further speculated that EmbA and EmbB function in the assembly of the linear $\alpha(1\rightarrow5)$ arabinan segments as presented in Figure 2.21. This is in accordance with previous data (Besra *et al.*, 1995; Daffé *et al.*, 1990) and phenotypes of EmbA and EmbB (Escuyer *et al.*, 2001; Zhang *et al.*, 2003) and Cg-Emb (Alderwick *et al.*, 2005b) mutants. It is clear that further studies are required to establish the precise role of EmbA and EmbB in mycobacteria.

The analysis of the *M. smegmatis* ΔaftC mutant to date and based on the Ara:Gal ratio would suggest that the residual arabinan segment in the mutant consists of approximately five Araf residues: $\beta\text{-D-Araf-(1}\rightarrow\text{2)-}\alpha\text{-D-Araf-(1}\rightarrow\text{5)-}\alpha\text{-D-Araf-(1}\rightarrow\text{5)-}\alpha\text{-D-Araf-(1}\rightarrow\text{5)-}\alpha\text{-D-Araf-}$ located at three branches on the galactan chain (Alderwick *et al.*, 2005b; Besra *et al.*, 1995). This is consistent with the recent primary structure of AG (Bhamidi *et al.*, 2008), with a ‘non-variable’ terminal non-reducing Ara₁₇ motif, introduction of a 3,5-Araf residue distal to this non-reducing end by AftC and further extension by a linear $\alpha(1\rightarrow5)$ Araf domain (Figure 2.21). The latter appears to be variable (up to 12/13 residues). However, based on *M. smegmatis* ΔaftC and the subsequent Ara:Gal compositional analysis, a dominant Ara₂₂/Ara₂₃ motif would be consistent with recent (Bhamidi *et al.*, 2008) and previous (Besra *et al.*,

1995) structural data on AG and this is represented in terms of biosynthetic considerations in Figure 2.21.

The arabinofuranosyltransferases of the Emb family (EmbC, EmbA and EmbB) (Belanger *et al.*, 1996; Berg *et al.*, 2005; Escuyer *et al.*, 2001; Telenti *et al.*, 1997), AftA (Alderwick *et al.*, 2006c), AftB and AftC, possess some sequence similarity. This relates to a modified glycosyltransferase motif, which is defined in the GT-C glycosyltransferase superfamily as either DXD, EXD, DDX, or DEX (Liu & Mushegian, 2003). The most distant is probably AftA with only one negatively charged D residue, however possessing an adjacent polar Q residue (Alderwick *et al.*, 2006c). In AftB there are two adjacent D residues (Figure 2.1B), which due to our mutational study are likely to be directly involved in glycosyl hydrolysis and transfer. Also, the high number of charged amino acid residues of the strongly conserved loop region following the first TM helix might contribute to the proper orientation of substrates at the catalytic centre. The glycosyltransferase motif of arabinofuranosyltransferases so far identified is always located in a periplasmic loop region, which connects TM III-IV in EmbC, TM III-IV in AftA, and TM I-II in AftB (Figure 2.1B & C). A further feature common of the Emb, AftA and AftB proteins is that they consist of an N-terminal region, which has a number of hydrophobic segments spanning the TM, and a large C-terminal domain, which in Emb has been demonstrated to be located towards the periplasmic side (Seidel *et al.*, 2007c). The number of TMs is different amongst these proteins, but the involvement of these TMs could be considered as being important for the translocation of DPA, the lipid linked substrate of these glycosyltransferases. The weak structural identities of the membrane embedded part of the arabinofuranosyltransferases, indicates that transport and presentation of DPA to the catalytic site might be different for these enzymes. A "Pro-motif" as identified in the Emb proteins (Berg *et al.*, 2005) is not present in AftB and AftA. This motif is typical for polysaccharide co-polymerases and is

assumed to control the chain length in polysaccharide biosynthesis. Its absence in AftA and AftB seems plausible, since these enzymes add only singular Araf residues, but the Emb proteins presumably add a number of $\alpha(1\rightarrow5)$ linked Araf residues to form the inner chain of the AG domain.

To conclude, AftB and AftC represent novel arabinofuranosyltransferases in *Corynebacteriaceae*, such as *M. tuberculosis*, which are responsible for the addition of the terminal $\beta(1\rightarrow2)$ linked Araf residues and branching $\alpha(1\rightarrow3)$ Araf residues, respectively. The genomic organisation in the genomes of the *Corynebacteriaceae* sequenced is intriguing, revealing high synteny of the *M. tuberculosis* *aftB* and *aftC* locus to the maps of all other *Mycobacterium* and *Corynebacterium* species. The identification of new cell wall biosynthetic drug targets is of great importance, especially with the emergence of MDR-TB and XDR-TB. These newly discovered DPA dependent arabinofuranosyltransferases represent, along with straightforward *in vitro* enzyme assays, promising candidates for further exploitation as potential drug targets.

Chapter 3

3. Identification and characterisation of a crucial branching $\alpha(1\rightarrow3)$ arabinofuranosyltransferase involved in LAM biosynthesis

3.1. Introduction

TB affects a third of mankind and causes 1.7 million fatalities annually (Dye *et al.*, 2006). The spread of TB has been facilitated in recent decades, due to the susceptibility of HIV infected individuals to *Mycobacterium tuberculosis* (Kaye & Frieden, 1996). The problem has been compounded by the emergence of MDR-TB and XDR-TB strains (Shah *et al.*, 2007). *M. tuberculosis* resides within the family of *Corynebacteriaceae*. A common feature of this family is that they possess an unusual cell wall architecture dominated by an essential heteropolysaccharide termed AG, which is linked to both mycolic acids and peptidoglycan, forming the mAGP complex (Besra *et al.* 1995; Daffé *et al.*, 1993; McNeil *et al.*, 1991). The formation of the arabinan domain of AG results from the subsequent addition of Ara_f residues by a set of unique AraTs. The front line drug EMB has been shown to target at least three AraTs (EmbA, EmbB and EmbC) (Belanger *et al.*, 1996; Telenti *et al.*, 1997), but shows no inhibitory effects against the other recently identified cell wall AraTs, such as AftA (Alderwick *et al.*, 2006), AftB (Chapter 2) and AftC (Chapter 2). In the previous chapter, we successfully deleted *MSMEG2785* (*Ms-aftC*) (Birch *et al.*, 2008), and showed that this leads to expression of a severely truncated AG structure with branching defects in its arabinan domain.

Apart from AG, mycobacteria contain several other glycoconjugates. LAM, which contains an arabinan domain that is structurally similar to that of AG, is a major component of the cell wall. It consists of a core mannan domain covalently linked to a mannosyl-phosphatidyl-*myo*-inositol anchor, which makes it structurally similar to its biochemical precursor LM (Berg *et al.*, 2007; Besra *et al.*, 2007; Morita *et al.*, 2004). Both LAM and LM exhibit

immunomodulatory functions that may influence the host immune response (Jozefowski *et al.*, 2007). Species-specific differences in the “capping-motifs” of the non-reducing termini of the arabinan domain, for which three variants exist, i.e. AraLAM, PI-LAM and ManLAM (Gilleron *et al.*, 1997; Khoo *et al.*, 1995; Khoo *et al.*, 2001; Nigou *et al.*, 1997; Nigou *et al.*, 1999), have been shown to be important for this function.

The arabinan domain of LAM is attached to an, as yet unidentified, region of the mannan backbone and is thought to be synthesised in a similar manner to that of arabinan found in AG (Berg *et al.*, 2007; Besra *et al.*, 2007; Morita *et al.*, 2004). To date, only one AraT has been implicated in the biosynthesis of LAM. This enzyme, EmbC, has also been shown to be targeted by EMB, but to a lesser extent than the cell wall core AraTs, EmbA and EmbB (Mikusova *et al.*, 1995; Zhang *et al.*, 2003). The formation of the arabinan domain of LAM requires an $\alpha(1\rightarrow3)$ AraT in a similar manner to AG, thus resulting in the branched motif of LAM. Here we investigated the potential role of AftC in LAM biosynthesis. By structural analysis of LAM from a *M. smegmatis* Δ *aftC* mutant we demonstrate that AftC carries dual functionality and is responsible for introducing 3,5-Araf branches into LAM, in addition to AG. Furthermore, we show, by treating an *M. smegmatis* Δ *aftC* mutant with EMB, that EmbC is involved in the very early steps of the LAM arabinan core synthesis and that truncation of this domain modulates the immunological properties of the molecule.

3.2. Results

3.2.1. Effects of *aftC* inactivation on LM/LAM biosynthesis

M. smegmatis wild type (WT) (Figure 3.1, Lane 1) and *M. smegmatis* Δ *aftC* lipoglycans (Figure 3.1, Lanes 2-4) were purified using conventional methods (Nigou *et al.*, 1997), resulting in the recovery of a highly purified lipoglycan with an intermediate size between *M. smegmatis* LAM and LM, now termed AftC-LAM (Figure 3.1, Lane 3). Complementation of *M. smegmatis* Δ *aftC* with *Ms-aftC* restored the lipoglycan profile to WT *M. smegmatis* (Figure 3.1, Lane 5). Plasmid borne *Mt-aftC* also resulted in complementation of the mutant (Figure 3.1, Lane 6). The molecular weight of AftC-LAM was investigated by negative-ion matrix assisted laser desorption ionization time-of-flight (MALDI-TOF) mass spectrometry (MS). The mass of WT-LAM and AftC-LAM exhibited broad unresolved peaks centered at m/z 15000 and 8000, respectively, indicating a weight decrease of ~7 kDa for the mutant LAM (Figure 3.2, A and B).

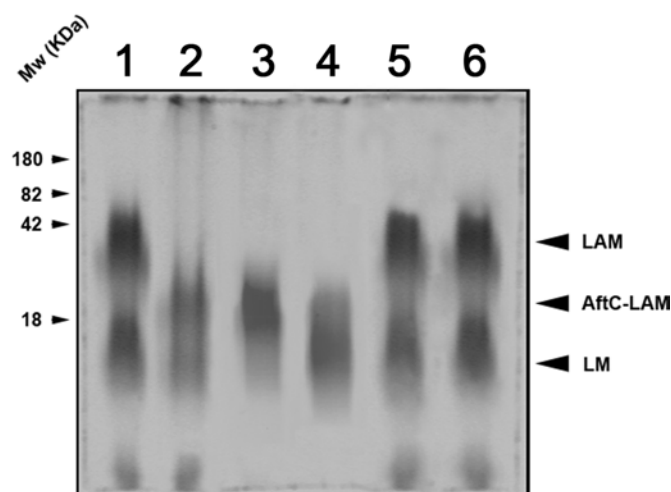


Figure 3.1: SDS-PAGE analysis of lipoglycans extracted from *M. smegmatis* and *M. smegmatis* Δ *aftC*. Lane 1, lipoglycans extracted from *M. smegmatis*; Lane 2, lipoglycans extracted from *M. smegmatis* Δ *aftC*; Lane 3, purified AftC-LAM from *M. smegmatis* Δ *aftC* and Lane 4, purified LM from *M. smegmatis* Δ *aftC*; Lane 5, lipoglycans extracted from *M. smegmatis* Δ *aftC* pMV261-*Ms-aftC* and Lane 6, lipoglycans extracted from *M. smegmatis* Δ *aftC* pMV261-*Mt-aftC*.

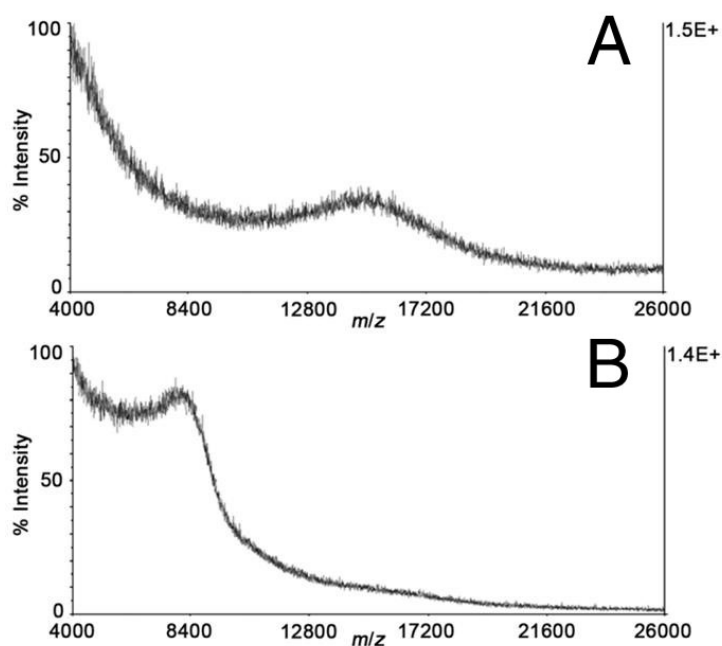


Figure 3.2: MALDI-TOF-MS analysis of purified WT-LAM (A) and AftC-LAM (B) extracted from *M. smegmatis* and *M. smegmatis* Δ *aftC* respectively. MALDI-TOF-MS spectra were acquired in the linear negative mode with a delayed extraction using 2,5-dihydrobenzoic acid as a matrix.

3.2.2. Structural characterisation of AftC-LAM

The ratio of Ara to Man in WT-LAM and AftC-LAM was determined using gas chromatography (GC) of alditol acetate derivatives (Birch *et al.*, 2008) (Figure 3.3, A and C). WT-LAM, had a molar ratio of Ara:Man of 2.7:1, which is consistent with previously reported data (Zhang *et al.*, 2003), whereas for AftC-LAM the Ara:Man ratio was 0.59:1 (Figure 3.3, A and C). Complementation of *M. smegmatis* Δ *aftC* with either *Ms-aftC* or *Mt-aftC*, restored the Ara:Man ratio to that of the wild type LAM (Fig. 3.3, E and G). In *M. smegmatis*, LAM consists approximately of 71 Ara, 27 Man, and 1 Ins units (Petzold *et al.*, 2005; Zhang *et al.* 2003). The loss of 7kDa for AftC-LAM equates to 45 Ara residues, suggesting that AftC-LAM contains one or more short arabinan domains of up to ~16 Ara residues.

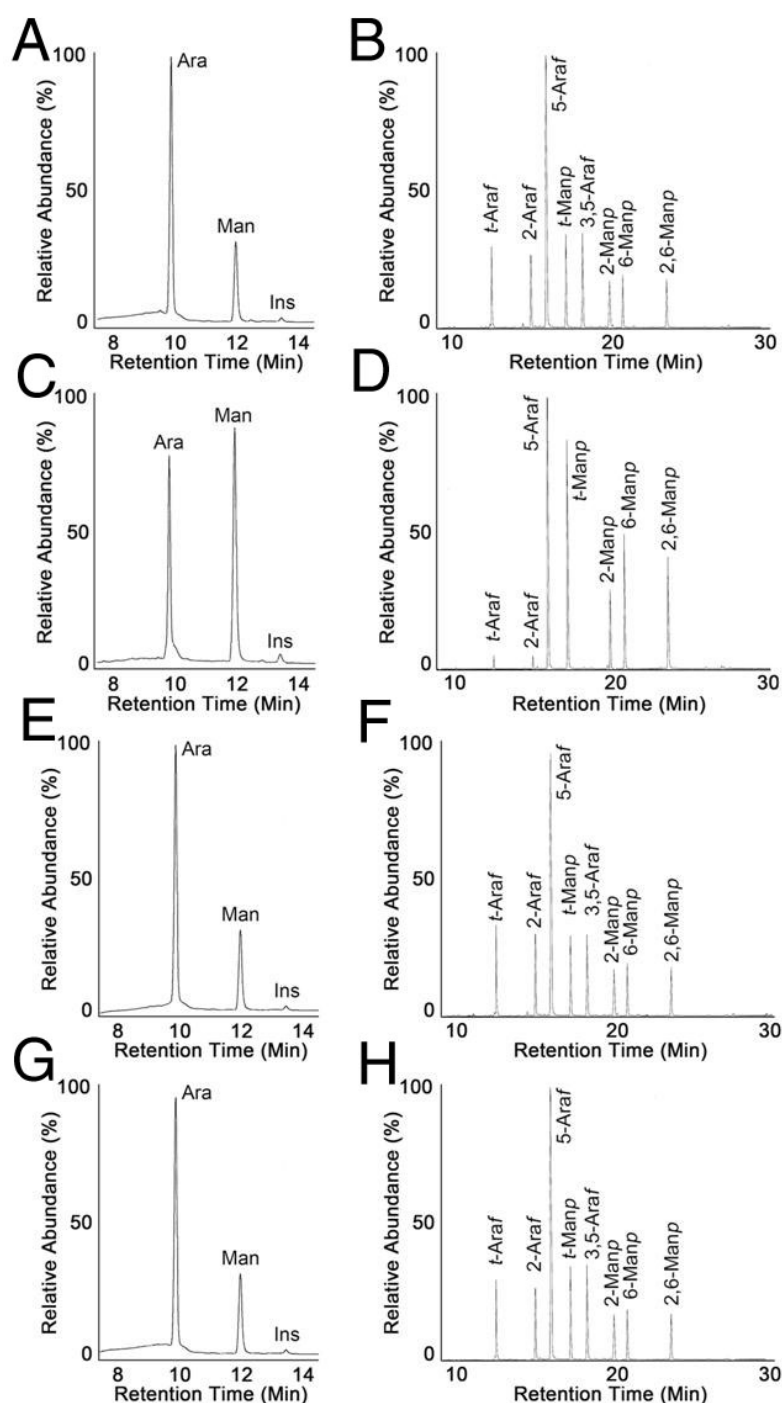


Figure 3.3: GC and GC/MS analysis of purified lipoglycans extracted from *M. smegmatis* (A and B), *M. smegmatis* $\Delta aftC$ (C and D), *M. smegmatis* $\Delta aftC$ pMV261- *Ms-aftC* (E and F), and *M. smegmatis* $\Delta aftC$ pMV261-*Mt-aftC* (G and H). The glycosyl composition of lipoglycans extracted were analyzed by GC after derivatization to alditol acetates. Glycosyl linkage analysis was performed after per-*O*-methylation and derivatization to partially per-*O*-methylated alditol acetates. Briefly, lipoglycan samples were per-*O*-methylated using dimethyl sulfinyl carbanion, hydrolyzed using 2 M TFA, reduced using NaBD₄, and per-*O*-acetylated. The resulting per-*O*-methylated alditol acetates were solubilized in CHCl₃ before analysis by GC/MS.

The ^1H -NMR spectrum of WT-LAM (Figure 3.4A) was much more complex than the anomeric region of AftC-LAM (Figure 3.4B). Indeed, the AftC-LAM 1D ^1H spectrum exhibits three major well-defined resonances characterised by several overlapping resonances arising from six different classes of glycosidic residues.

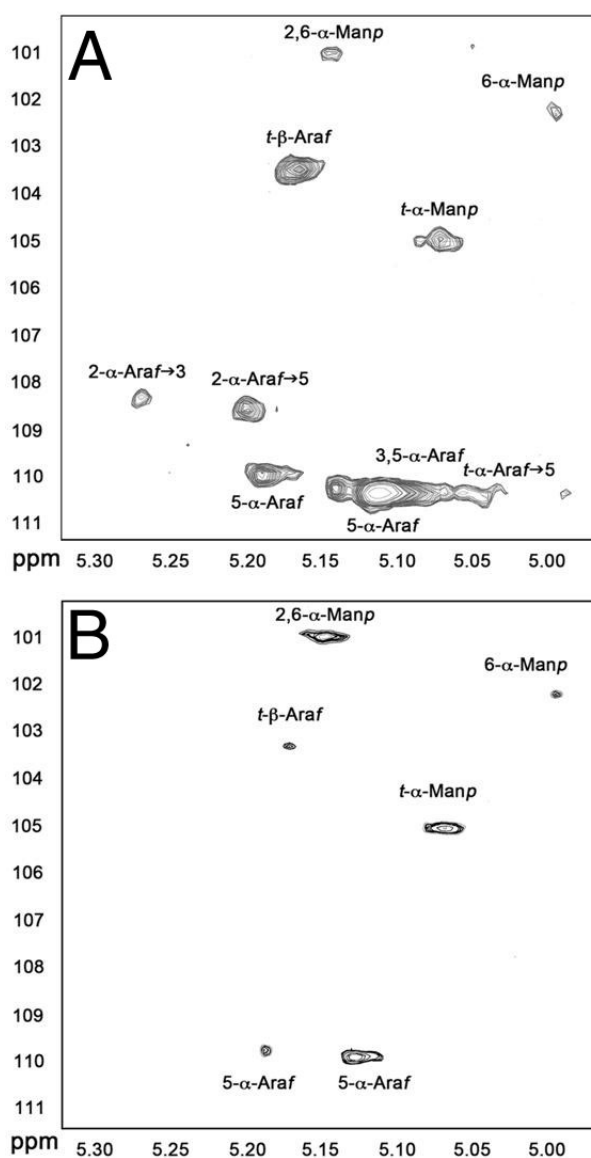


Figure 3.4: Two-dimensional NMR spectra of WT-LAM and AftC-LAM purified from *M. smegmatis* and *M. smegmatis* Δ *aftC*. Structural characterisation of WT-LAM A) and AftC-LAM B). ^1H , ^{13}C HSQC NMR spectra were acquired in D_2O at 313K. Expanded regions (δ ^1H : 5.0-5.30, δ ^{13}C : 101-111) are shown.

Based on our data for WT-LAM and previously published work (Nigou *et al.*, 1997), the ^{13}C resonance at $\delta 101$ ppm that correlated to an anomeric proton at $\delta 5.15$ ppm with a $^1J_{\text{H1,C1}}$ coupling constant of approximately 170 Hz was assigned as 2,6-Manp. The resonances at $\delta 105$ and $\delta 102.3$, correlating to protons at $\delta 5.07$ and $\delta 4.90$ were assigned as *t*-Manp and 6-Manp, respectively. The *t*- β -Araf residues corresponded to $\delta 103.4$ with ^1H at $\delta 5.16$. The well-separated spin systems for 2- α -Araf attached to the 3-position (2- α -Araf \rightarrow 3, $\delta 108.2$, $\delta 5.27$ ppm) and 5-position (2- α -Araf \rightarrow 5, $\delta 108.5$, $\delta 5.20$) of the 3,5-Araf were also visible in the spectra of WT-LAM. Several spin systems were observed ($\delta 110.3$ and $\delta 5.19$ ppm, $\delta 110.3$ and $\delta 5.14$ ppm and $\delta 110.3$ and $\delta 5.11$ ppm) assigned to 5- α -Araf in different chemical environments, with one overlapping set of 3,5- α -Araf ($\delta 110.2$ - $\delta 5.12$) for WT-LAM. As reported two distinct chemical shifts of *t*- α -Araf could occur for the respective arms of a branched 3,5- α -Araf, as observed for 2- α -Araf \rightarrow 3 and 2- α -Araf \rightarrow 5 (Nigou *et al.*, 1997). In AftC-LAM (Figure 3.4B) the resonances associated with the mannan core (*t*-Manp, 6-Manp and 2,6-Manp) are conserved but resonances associated with Araf residues are notably less abundant. In particular, 2- α -Araf \rightarrow 3 is absent and the complex set of signals for the different 5- α -Araf are now much more simplified due to the loss of 3,5- α -Araf (Figure 3.4B). GC/MS of per-*O*-methylated alditol acetate derivatives confirmed this result in that it showed an unaltered glycosidic linkage profile for the mannan backbone of both WT- and AftC-LAM and a complete loss 3,5-Araf and significant reduction in *t*-Araf, 2-Araf and 5-Araf-linkages for the latter LAM (Figure 3.3 B and D). Complementation of *M. smegmatis* ΔaftC with either *Ms-aftC* or *Mt-aftC* restored the glycosyl linkage profile to that of WT (Figure 3.3, F and H), demonstrating that MSMEG2785 (*Ms-aftC*) and Rv2673 (*Mt-aftC*) are functional orthologues. Overall, the compositional analysis suggests that, as compared to WT-LAM, AftC-LAM has an unaltered mannan domain composed of an $\alpha(1\rightarrow6)$ -Manp backbone substituted by *t*-Manp units at O-2 positions, and to which is attached one or more short

$\alpha(1\rightarrow5)$ -linked linear arabinan chain (in total representing approximately 12-15 Araf units) terminating in a single $\beta(1\rightarrow2)$ Ara residue (Figure 3.5).

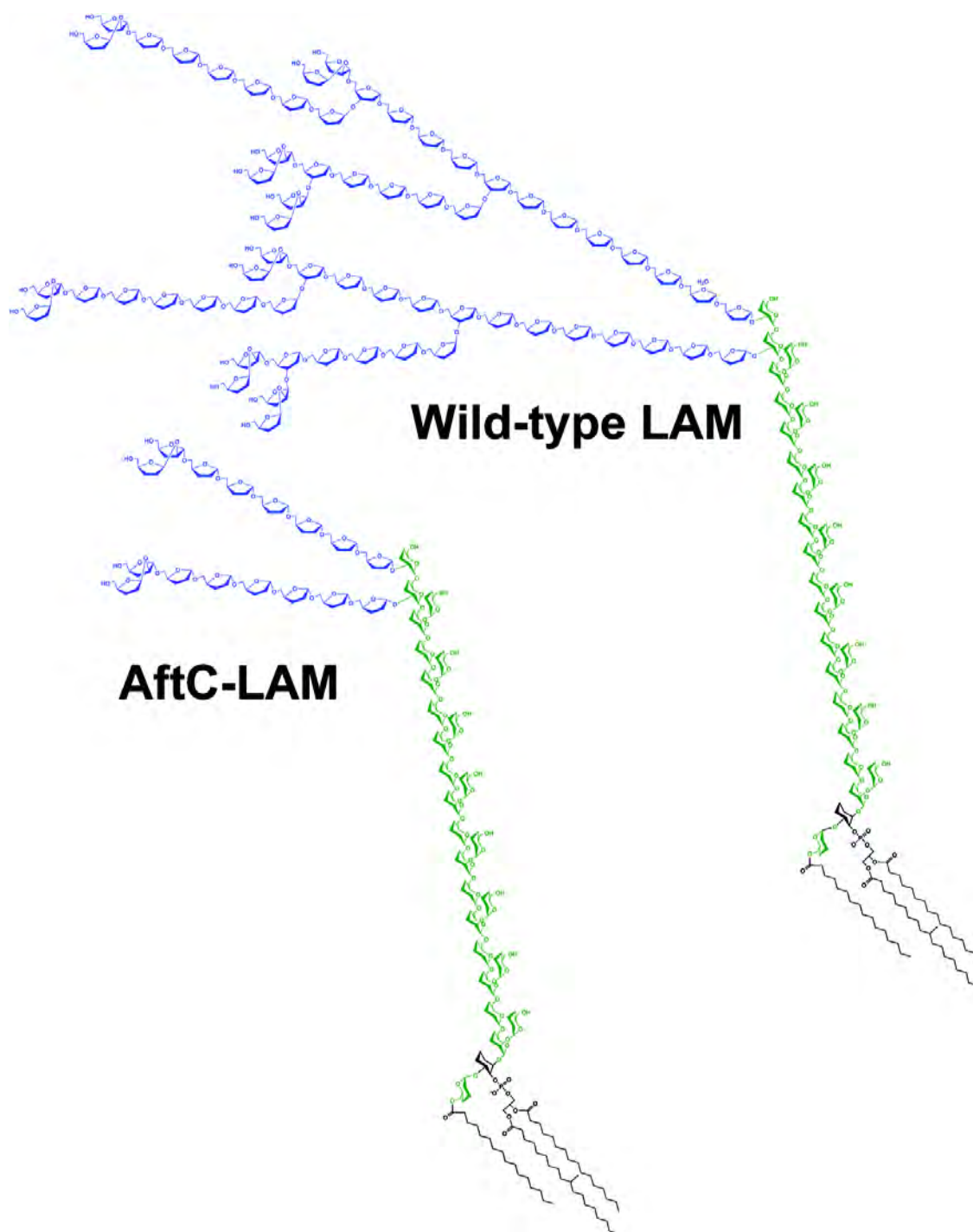


Figure 3.5: Structural representation of WT-LAM and AftC-LAM. Mannose and arabinose residues are displayed in green and blue, respectively. Lipoglycans are represented in their triacylated form and capping motifs have been removed for clarity.

3.2.3. Effect of ethambutol on AftC-LAM formation

EMB blocks cell wall arabinan biosynthesis by targeting the Emb proteins (Belanger *et al.*, 1996; Telenti *et al.*, 1997). Although EmbC is known to be involved in LAM arabinan biosynthesis (Zhang *et al.*, 2003), its precise role is as yet inconclusive. We exploited the phenotype of *M. smegmatis* Δ *aftC* and the structural properties of AftC-LAM to investigate this role. For this, we treated [14 C]-glucose labeled cultures of *M. smegmatis* with sub-inhibitory concentrations of EMB, extracted the lipoglycans and performed a radiochemical quantification of [14 C]-incorporated sugars. SDS-PAGE analysis of the [14 C]-LM/LAM pool of WT *M. smegmatis* revealed 2 broad bands corresponding to LAM and LM migrating to their expected sizes (Figure 3.6A, Lane 1) and an Ara:Man ratio of 1.2:1 (Figure 3.6B, Lane 1). Subsequent analysis of the [14 C]-LM/LAM lipoglycan pool from *M. smegmatis* Δ *aftC*, resulted in labeling of AftC-LAM and LM (Figure 3.6A, Lane 2) and an Ara:Man ratio of 0.5:1 (Figure 3.6B, Lane 2). Addition of EMB at 0.5 μ g ml $^{-1}$ resulted in a decrease in the size of the AftC-[14 C]-LAM, an accumulation of [14 C]-LM (Figure 3.6A, Lane 3) and a corresponding change in the Ara:Man ratio of 0.3:1 (Figure 3.6B, Lane 3). Since AftC-LAM contains an intact mannan core, the only possible effect of EMB, is by directly inhibiting EmbC activity (addition of the terminal β (1 \rightarrow 2) Ara f residues by AftB is insensitive to EMB (Alderwick *et al.*, 2006)), thus showing its involvement in the very early stages of LAM arabinan biosynthesis and inhibition of an α (1 \rightarrow 5) AraT. Notably, we observed that residual [14 C]-Ara labeling always remained upon EMB treatment (Figure 3.6B, Lane 3), suggesting that another AraT possibly adds the first Ara f residue to LM, akin to AftA in AG biosynthesis (Alderwick *et al.*, 2006).

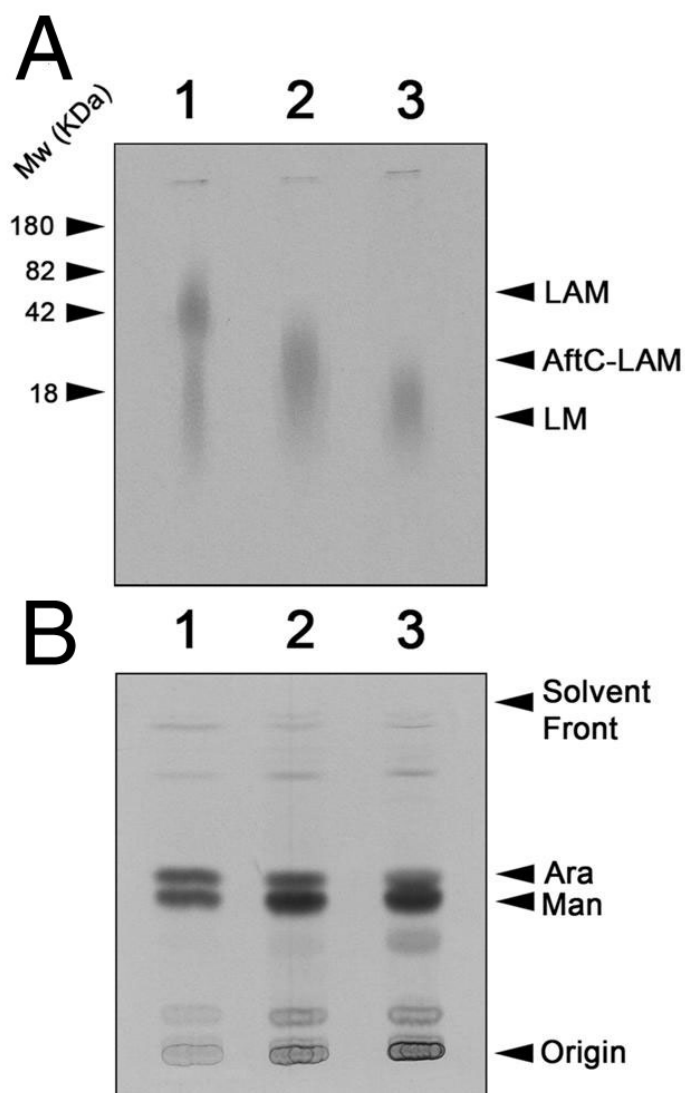


Figure 3.6: SDS-PAGE **A)** and total sugar analysis **B)** of $[^{14}\text{C}]$ -labeled lipoglycans extracted from *M. smegmatis* and *M. smegmatis* Δ *aftC* treated with EMB. Growing cultures of *M. smegmatis* and *M. smegmatis* Δ *aftC* were labeled with $[^{14}\text{C}]$ -glucose and their lipoglycans extracted and analysed by SDS-PAGE (**A**). Lane 1, *M. smegmatis*, Lane 2, *M. smegmatis* Δ *aftC* and Lane 3, *M. smegmatis* Δ *aftC* + 0.5 $\mu\text{g ml}^{-1}$ EMB. The above lipoglycans were hydrolysed in 2 M TFA and analysed by TLC to determine the total sugar composition (**B**). Lane 1, *M. smegmatis*, Lane 2, *M. smegmatis* Δ *aftC* and Lane 3, *M. smegmatis* Δ *aftC* + 0.5 $\mu\text{g ml}^{-1}$ EMB.

3.2.4. AftC-LAM displays pro-inflammatory properties

LMs, in contrast to LAMs, are potent pro-inflammatory lipoglycans (Doz *et al.*, 2007; Nigou *et al.*, 2008; Quesniaux *et al.*, 2004b; Vignal *et al.*, 2003). This difference has been attributed

to the presence of the arabinan domain in LAM which masks the “bioactive” mannan core (Guerardel *et al.*, 2002; Vignal *et al.*, 2003). To investigate the consequence of the *aftC* mutation on the pro-inflammatory activity of LAM, we compared WT- and AftC-LAM for release of TNF- α by human THP1 cells. Consistent with earlier studies (Vignal *et al.*, 2003), truncated AftC-LAM, as compared to WT-LAM, exhibited an increased pro-inflammatory activity (Figure 3.7A). LM is a known agonist for TLR2 (Briken *et al.*, 2004). Therefore, we investigated the ability of WT- and AftC-LAM to activate this receptor. HEK293 cells expressing TLR2 were stimulated with increasing amounts of LAM after which TLR2-dependent IL-8 production was determined. As shown in Figure 3.7B, AftC-LAM induced a much stronger TLR2 activation than did WT-LAM (~10-fold). This result demonstrates that the presence of the full-length arabinan domain somehow hampered TLR2 activation. Previously, it has been reported that immune stimulatory activity of some *M. smegmatis* LAM preparations may have been caused by lipopeptide contamination (Nigou *et al.*, 2008). To investigate this issue, both WT and AftC-LAM were pre-treated with H₂O₂ (a procedure that inactivates lipopeptides (Morr *et al.*, 2002; Zahringer *et al.*, 2008)), after which they were re-tested for their activity on HEK293 TLR2 cells. As shown in Figure 3.7, pre-treatment with H₂O₂ substantially reduced the activity of both WT- and AftC-LAM. However, in contrast to WT-LAM, which lost all of its activity, a substantial part of the activity arising from AftC-LAM was sustained for up to 168 h of treatment (Figure 3.7C). This was not due to the inactivation of the H₂O₂ itself, since addition of fresh H₂O₂ after 96 h did not further reduce the activity (Figure 3.7C). Therefore, we conclude that both LAM preparations were probably contaminated with lipopeptides to a certain extent. Nevertheless, inactivation of these molecules with H₂O₂, clearly demonstrated that AftC-LAM was able to activate TLR2, whereas WT-LAM (PILAM) became completely inactive for concentrations up to 100 μ g/ml (Figure 3.7D).

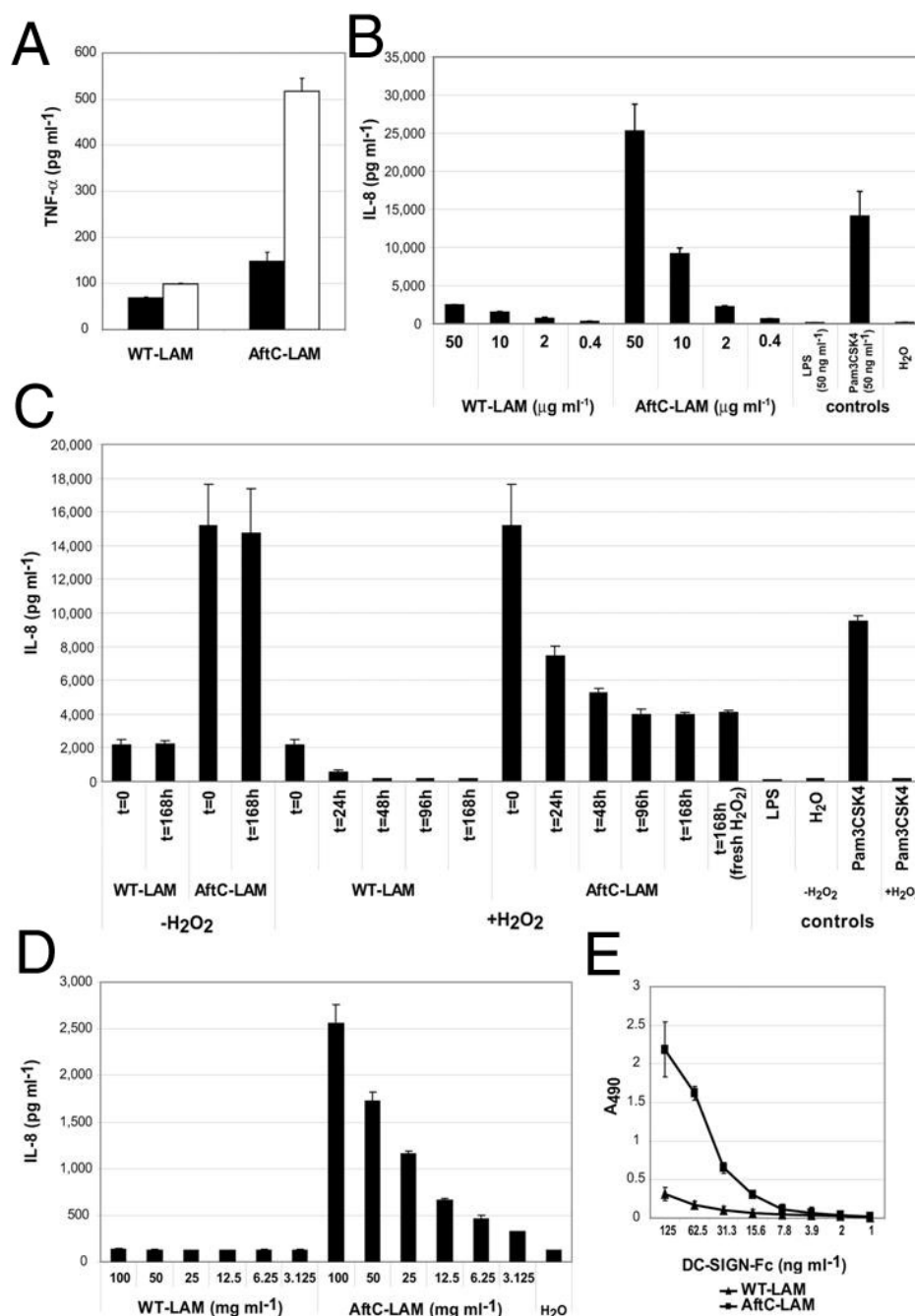


Figure 3.7: TNF- α production by human THP-1 cells and IL-8 production by HEK293 TLR-2 cells in response to WT-LAM and AftC-LAM. A) Human THP-1 cells were incubated with 1 μ g ml⁻¹ (black bars) or 10 μ g ml⁻¹ (white bars) WT- or AftC-LAM. TNF- α was quantified after 24 h by ELISA. (B-D) HEK293 cells transfected with TLR2 were stimulated with: B) increasing amounts of WT- or AftC-LAM, with LPS (50 ng ml⁻¹), with Pam₃CSK₄ (50 ng ml⁻¹) or with H₂O as a negative control; C) 50 μ g ml⁻¹ of WT- or AftC-LAM (with and without 1% hydrogen peroxide (\pm H₂O₂) for the indicated time period), with LPS (50 ng ml⁻¹), Pam₃CSK₄ (50 ng ml⁻¹) (\pm H₂O₂ for 48 h) or with H₂O as a negative control; D) with increasing amounts of WT- or AftC-LAM (treated with H₂O₂ for 168 h). In all cases, cells were stimulated for 24 h at 37°C, after which the supernatants were harvested and analysed for IL-8 by ELISA. E) Binding of DC-SIGN-Fc to WT- (▲) or AftC-LAM (■) as determined by ELISA. Absorption was measured at 490 nm. In all panels, data are expressed as the mean \pm s.d. from 1 representative of 3 independent experiments.

To determine whether the increased pro-inflammatory activity of AftC-LAM indeed coincided with a more exposed mannan domain, the ability of WT- and AftC-LAM to interact with an Fc construct harboring the extracellular domain of the C-type lectin DC-SIGN was investigated. DC-SIGN is highly expressed on dendritic cells and recognises high-mannose structures (Appelmelk *et al.*, 2003; Feinberg *et al.*, 2001) including LM (Pitarque *et al.*, 2005) but not PILAM (Maeda *et al.*, 2003). As shown in Figure 3.7E, the reactivity of DC-SIGN-Fc towards AftC-LAM was stronger as compared to the reactivity against WT-LAM, demonstrating that the mannan core of AftC-LAM was more accessible.

3.2.5. Discussion

The data described unequivocally demonstrate that AftC is responsible for introducing 3,5-Araf branching in the LAM arabinan domain of *M. smegmatis* and proposes a new model for LAM biosynthesis (Figure 3.8). Furthermore, we show, for the first time, that EmbC is involved in the very early stages of LAM arabinan biosynthesis and that with the truncation of the arabinan domain LAM gains the ability to activate TLR2. Although the structure of the arabinan domain of LAM is well understood, less is known of the enzymes involved in its biosynthesis. One important reason is that *C. glutamicum*, a preferred model organism to study mycobacterial AG and LM biosynthesis (Alderwick *et al.*, 2006; Seidel *et al.*, 2007; Birch *et al.*, 2008) does not produce a convoluted LAM, as present in mycobacteria. During our investigation of various putative GT-C glycosyltransferases, we deleted *msmeg2785* (AftC) from *M. smegmatis*, which resulted in a phenotype that displayed a severely truncated AG (Chapter 2) (Birch *et al.*, 2008). In this chapter, we re-visited this mutant in an attempt to investigate the potential role of AftC in LAM biosynthesis. Chemical analysis revealed that LAM isolated from the *aftC* mutant contained an unaltered mannan core, but with one or more simple arabinan moieties of approximately 12-16 Araf units composed of $\alpha(1\rightarrow5)$ -linkages terminating in a single $\beta(1\rightarrow2)$ fashion. It is reasonable to conclude from our data that AftC is not involved in early arabinan LAM biosynthesis, since a more pronounced truncation of LAM would then be expected. AftC has dual functionality, in terms of its involvement in the biosynthesis of both AG and LAM. Attempts to generate an *aftC* deficient strain of *M. tuberculosis* has thus far proved unsuccessful, highlighting the essentiality of *aftC* in *M. tuberculosis* (Sasseti *et al.*, 2003) and the species' intolerance to cell-wall changes. Hence, AftC represents an excellent drug target.

EmbC has long been implicated in the biosynthesis of mycobacterial LAM and has been shown to be a target of the front line drug EMB (Mikusova *et al.*, 1995; Zhang *et al.*, 2003). However, speculation around its precise enzymatic function has remained controversial. By utilising the unique phenotype of *M. smegmatis* Δ aftC, we now provide unequivocal evidence that EmbC is an $\alpha(1\rightarrow5)$ AraT, which is inhibited by EMB (Figure 3.8).

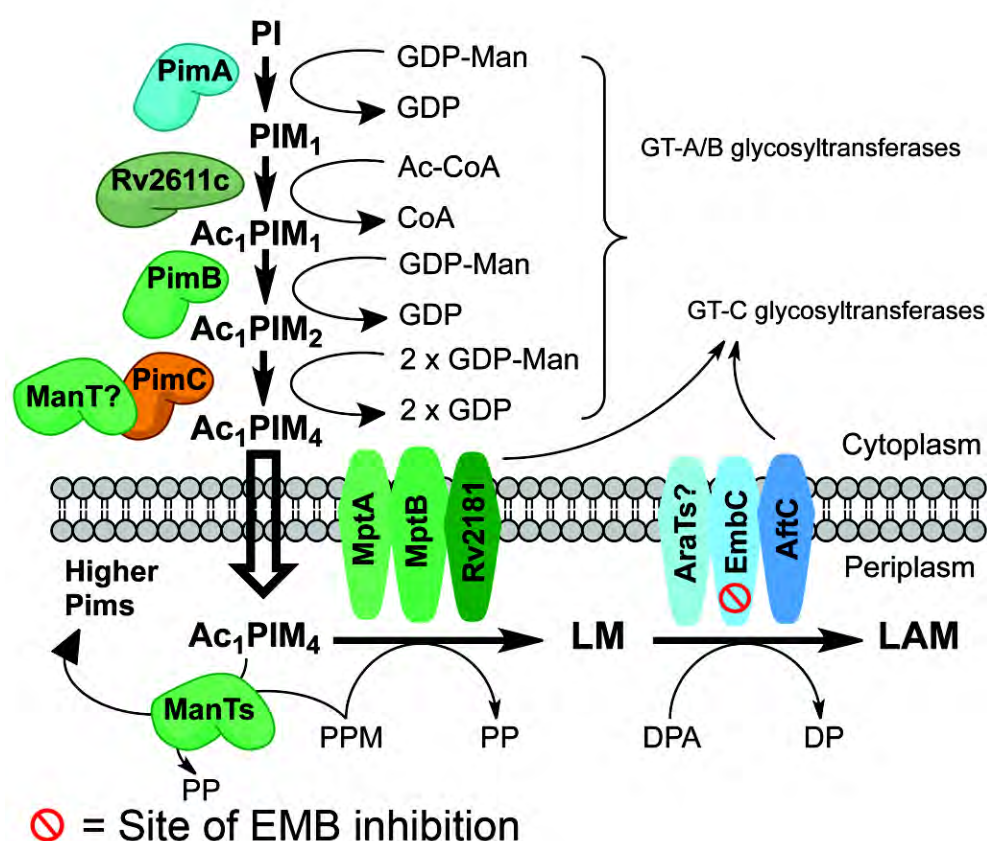


Figure 3.8: Mycobacterial LAM biosynthesis and the role of AftC. The GT-A/B family of glycosyltransferases perform sequential glycosidic transfer of mannose residues utilising the high energy nucleotide GDP-Man, to a PI based anchor in the cytoplasm. The GT-C family of glycosyltransferases then continue LM and LAM biosynthesis by elaborating Ac₁PIM₄ with mannose and arabinose residues. MptA, MptB and Rv2181 are the only known ManTs involved in core mannan biosynthesis, for which they utilise the lipid linked substrate polyprenylphosphomannose (PPM) as the sugar donor. Decaprenyl-1-monophosphoarabinose (DPA) is utilised by an unknown AraT to prime LM at an, as yet, unidentified position. EmbC and AftC are the other two identified AraTs which mature the final LAM molecule before species specific capping occurs.

We now propose a working model, whereby an as yet unidentified GT-C AraT, primes the mannan backbone with singular Araf residues in much the same way as AftA primes the galactan backbone of AG (Alderwick *et al.*, 2006). Subsequently, EmbC extends the arabinan chain in an $\alpha(1\rightarrow5)$ fashion before AftC branches the polysaccharide with an $\alpha(1\rightarrow3)$ Araf residue and the domain is further matured by a combination of AraTs including AftC, AftB and perhaps other as yet unidentified enzymes (Figure 3.8).

Several mycobacterial cell-wall lipoglycans are pro-inflammatory stimuli of the host immune response. Both LM and LAM are members of a family of mycobacterial lipoglycans that all contain a conserved MPI anchor (Briken *et al.*, 2004). Interestingly, LM, besides being a potent inducer of pro-inflammatory cytokines, also displays strong anti-inflammatory properties and represses lipopolysaccharide (LPS)-induced cytokine responses in macrophages (Quesniaux *et al.*, 2004b). Recently, by making use of LM preparations, separated by their degree of acylation, it was demonstrated that these pro- and anti-inflammatory properties are, at least in part, dependent on the degree of acylation (Doz *et al.*, 2007; Gilleron *et al.*, 2006). Whereas, tri- and tetra-acylated LM forms displayed strong pro-inflammatory properties, mono- and di-acylated molecules did not (Gilleron *et al.*, 2006). Besides the degree of acylation, additional structural features of MPI-anchored lipoglycans determine their biological activity. Recently, it was shown that the chain length of the mannan core of MPI-anchored lipoglycans directly correlated with their ability to activate TLR2 (Nigou *et al.*, 2008). Whereas lipoglycans with short oligomannopyranosyl backbones, such as the PIMs, were marginally active, the TLR2-activating potency of lipoglycans with longer backbones, i.e. LM, was strongly enhanced (Nigou *et al.*, 2008). In addition to mannan chain length, the type of substitution of the mannan core was found to be critical, with activity being retained in the case of Manp substitutions but absent when the core was substituted with Araf residues (Nigou *et al.*, 2008). This was evidently clear for

mycobacterial LAMs, which carry a bulky arabinan domain. Although their LM core would in principal allow for TLR2 activation, the LAMs were found to be inactive (Nigou *et al.*, 2008). The assumption that the arabinan domain is directly involved in “silencing activity” is further sustained by the observation that chemical degradation of the arabinan domain restores the pro-inflammatory properties of LAM (Vignal *et al.*, 2003). Our results are in agreement with these findings as AftC-LAM, which expresses a severely truncated arabinan domain, exhibited an increased pro-inflammatory activity (Figure 3.7). Since WT and AftC-LAM did not differ in their pattern of acylation or core mannan composition, the increased pro-inflammatory activity must be directly related to the shortening of the arabinan domain. Exactly how the arabinan domain prevents TLR activation is currently not fully understood. One thought is that the arabinan domain exerts its inhibitory effect by steric hindrance (Vignal *et al.*, 2003). Although several lines of evidence point to this direction, the exact mechanism and the level at which this occurs remains unclear. In several mycobacterial species, the non-reducing termini of the branched arabinan domain are modified by capping motifs consisting of either oligomannosyl, i.e. ManLAMs, or PILAM units such as in *M. smegmatis* (Khoo *et al.*, 1995). Whereas reports on the immune stimulatory properties of ManLAMs are consistent and unambiguously demonstrate that these types of LAMs are inactive (Nigou *et al.*, 2008; Vignal *et al.*, 2003), some controversy exists on the activity of PILAMs. Early reports demonstrate that PILAM is pro-inflammatory and signals *via* TLR2 (Chatterjee *et al.*, 1992; Gilleron *et al.*, 1997; Tapping *et al.*, 2003; Underhill *et al.*, 1999; Vignal *et al.*, 2003). However, the mechanism by which a low degree of inositol-phosphate capping would confer this pro-inflammatory activity has never been explained. One hypothesis is that the *myo*-inositol-phosphate motif in the MPI-anchored lipoglycans may mimic the inositol-phosphate caps on PILAMs thereby conferring activity. However, the notion that the unsubstituted PI caps are unlikely to mimic the acylated MPI anchor plus the

observation that PIMs are only marginally active, clearly demonstrate that the PI motif alone does not confer activity (Vignal *et al.*, 2003). Interestingly, in a more recent study, Nigou *et al.* (2008) demonstrated that highly purified PILAMs from *M. smegmatis* and *M. fortuitum* were equivalent in activity to ManLAMs. Therefore, in contrast to what was previously suggested, the authors concluded that the presence of PI caps did not make LAM pro-inflammatory and they suggested that the activity in earlier experiments was probably due to lipopeptide contamination. Even though contaminant lipopeptides may not be detected by the current analytical methods, trace amounts of these molecules (<0.1%) are enough to influence the outcome of much more sensitive biological assays. We therefore determined the effect of H₂O₂ treatment on the TLR2-stimulating activity of both WT and AftC-LAM. As shown in Figure 3.7C, treatment with H₂O₂ severely reduced the activity of WT-LAM (PILAM) suggesting that the earlier observed activity was indeed due to lipopeptide contamination. In contrast, although the activity of AftC-LAM was also substantially reduced, a stable part of the activity was insensitive to H₂O₂ treatment (Figure 3.7C). Although, we cannot exclude that H₂O₂ also acts on LAM and may thereby abrogate its activity, the observation that the residual activity of AftC-LAM stabilised after 4 days of treatment, instead of gradually declining further, argues against this notion. Furthermore, H₂O₂ treatment fully inactivated the lipopeptide Pam₃CSK₄, demonstrating that inactivated lipopeptides do not display any residual activity (Figure 3.7C). Overall, these data strongly suggest that the pro-inflammatory activity observed in some PILAM preparations was indeed the result of contaminating lipopeptides. Nevertheless, based on these experiments, we conclude that truncation of the arabinan domain by the *aftC* mutation resulted in an increased pro-inflammatory activity of AftC-LAM.

Chapter 4

4. Identification of a rhamnopyransolyltransferase (RptA) which utilises a novel decaprenolphosphorhamnose substrate

4.1. Introduction

A particularly interesting feature of *C. glutamicum* is the presence of terminal rhamnopyranose (*t*-Rhap) residues attached to the C2 position of $\alpha(1\rightarrow5)$ linked Ara_f residues in the arabinan domain of AG (Alderwick *et al.*, 2005). The biological function of these residues remains to be clarified, nevertheless, they are a feature of the corynebacterial cell wall and the biosynthesis of which, needs to be addressed. The current paradigm of AG biosynthesis follows a linear pathway, which is built upon a decaprenyl pyrophosphate lipid carrier. The unique disaccharide linker and galactan domain is synthesised by a variety of GT-A and GT-B family of glycosyltransferases, all of which utilise a nucleotide diphosphate activated sugar substrate for transferase activity. It has been hypothesised (Alderwick *et al.*, 2007; Alderwick *et al.*, 2006; Berg *et al.*, 2007), that a major shift in the biosynthetic machinery takes place upon the initiation of arabinan polymerisation. AftA, Emb, AftC and AftB all belong to the GT-C family of glycosyltransferases and all of which utilise DPA as the sole lipid activated phospho-sugar donor for arabinose transfer into the cell wall. Since, *t*-Rhap residues are present in the arabinan component of the cell wall, the enzyme(s) responsible for its addition are likely to belong to the GT-C family of glycosyltransferase, and through deduction, one which utilises a lipid-phosphate derived rhamnose substrate, similar to DPA. Herein, we present the putative protein NCgl0543 as a distinct *t*-rhamnopyranosyltransferase of the GT-C superfamily, which is responsible for the transfer of *t*-Rhap residues to the arabinan domain to form the branched 2,5-linked Ara_f motifs of *C. glutamicum*. In addition, we have identified a novel decaprenol-mono-phosphorylrhamnose and discuss its role in substrate presentation for AG biosynthesis in *C. glutamicum*.

4.2. Results

4.2.1. Genome comparison of the NCgl0543 (*rptA*) locus

An examination of the genome sequence of *C. glutamicum* revealed that there are fourteen glycosyltransferases of the GT-C family. The function of AftA has been identified (Alderwick *et al.*, 2006), AftB, AftC, MptA (Mishra *et al.*, 2007), and that of MptB (Mishra *et al.*, 2008) which act as membrane-bound glycosyltransferases using polyprenylated-phospho-arabinosyl- and mannosyl-sugar donors, respectively, in the synthesis of AG and LAM. The above mentioned genes are also present in *M. tuberculosis* illustrating that they are required to build the elementary cell wall structure of the *Corynebacteriaceae* (Dover *et al.*, 2004).

An, as yet, uncharacterised GT-C glycosyltransferase of *C. glutamicum* is encoded by the putative protein NCgl0543. Orthologues of this gene, with identities exceeding 34%, are present in *C. glutamicum* R, *Corynebacterium efficiens*, *Corynebacterium glucuronalyticum* (ATCC 51867), and *Corynebacterium amycolatum* SK46, the latter two saprophytic organisms being human skin pathogens (Letek *et al.*, 2006; Tauch *et al.*, 2008). The genomic organisation surrounding NCgl0543 is largely syntenic and is preceded by a putative tRNA pseudouridine synthase and downstream of NCgl0543 is a membrane protein of unknown function (pfam class DUF690). There are no orthologues of NCgl0543 present in *Corynebacterium diphtheriae*, *Corynebacterium jeikeium* nor *Corynebacterium urealyticum* DSM 7109 (Cerdano-Tarraga *et al.*, 2003; Tauch *et al.*, 2005; Tauch *et al.*, 2008).

NCgl0543 of *C. glutamicum* is a large polytopic membrane protein of 799 amino acid residues and is predicted to possess 13 transmembrane-spanning helices (TMH) (Figure 4.1A). It is further characterised by a periplasmic carboxyterminal extension of 237 aa, similar to the C-terminal features of AftA (Alderwick *et al.*, 2006), AftB, and the Emb

proteins (Alderwick *et al.*, 2006; Berg *et al.*, 2005; Seidel *et al.*, 2007; Telenti *et al.*, 2007). A particularly highly conserved region is present at the end of the long loop connecting TMH 3 and TMH 4. This region is schematically shown in Figure 4.1A, as is part of its sequence (Figure 4.1B). This sequence resembles the glycosyltransferase GT-C family DXD motif (Liu & Mushegian, 2003), as it contains a number of basic and acidic residues, with the latter being shown in mutational studies to be essential for glycosyltransferase activity using polyprenylated phospho-sugar donors (Berg *et al.*, 2007; Seidel *et al.*, 2007b).

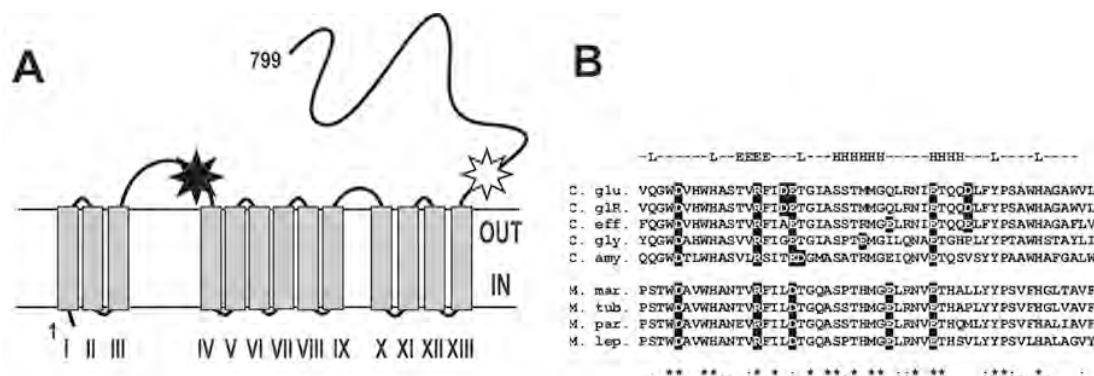


Figure 4.1: Hypothetical spatial organisation and partial sequence of the putative protein NCgl0543. A) The hypothetical schematic organisation of the putative protein NCgl0543 is shown spanning the membrane 13 times with the carboxy terminal end consisting of 237 amino acids and located in the periplasm. Also shown is the long loop of 168 amino acids connecting TMH 3 and TMH 4. The black star locates the putative glycosyltransferase region given in B and the white star a conserved region, and also present in the putative protein Rv3779, in the periplasmic part of the protein. **B)** Illustrates the part of the loop region, where acidic and basic residues are highlighted. Although, the overall topology of the *M. tuberculosis* putative protein Rv3779 and its orthologs are somewhat different to that of the corynebacterial proteins, the loop region is strongly conserved in the *Corynebacteriaceae* and this is indicated for selected mycobacterial species underneath the sequence alignment. Shown are aa 127 - 188 of the *M. tuberculosis* sequence, and aa 184 - 235 of the *C. glutamicum* sequence. On top of the sequence comparison the predicted secondary structure is given, with L indicating a loop region, H a helical structure, and E an extended sheet structure. The abbreviations are as follows: *C. glu.*, *Corynebacterium glutamicum* ATCC13032; *C. glR.*, *Corynebacterium glutamicum* strainR; *C. eff.*, *Corynebacterium efficiens*; *C. gly.*, *Corynebacterium glucuronalyticum*; *C. amy.*, *Corynebacterium amycolatum*; *M. mar.*, *Mycobacterium marinum* (ATCC BAA-535); *M. tub.*, *Mycobacterium tuberculosis*; *M. par.*, *Mycobacterium paratuberculosis*; *M. lep.*, *Mycobacterium leprae*.

4.2.2. Construction of *C. glutamicum* Δ rptA

In an attempt to delete NCgl0543 in *C. glutamicum*, the non-replicative vector pK19mobsacB Δ NCgl0543 was constructed. This was introduced into *C. glutamicum* via electroporation and kanamycin-resistant clones obtained indicating integration in the chromosome by homologous recombination (Schafer *et al.*, 1994). Using the sucrose resistance provoked by the *sacB* gene a second homologous recombination event was selected. A total of 9 clones were analysed by PCR and in 2 of them a wild type reversion at the NCgl0543 locus was restored, whereas a deletion of NCgl0543 was obtained in the 7 remaining clones. These numbers indicate that loss of NCgl0543 is not detrimental to cell growth or viability. As a result, and based on the results described below, one clone was subsequently termed *C. glutamicum* Δ rptA and confirmed by PCR to have Cg-rptA deleted, whereas controls with *C. glutamicum* wild type resulted in the expected larger amplification product.

4.2.3. In vitro growth phenotype of *C. glutamicum* Δ rptA

Growth of wild-type *C. glutamicum* and *C. glutamicum* Δ rptA was compared in liquid mineral salt medium CGXII and rich medium BHIS (Eggeling & Bott, 2005). Both strains exhibited comparable growth rates of $0.36 \pm 0.03 \text{ h}^{-1}$ on mineral salt medium CGXII and $0.60 \pm 0.05 \text{ h}^{-1}$ on rich medium BHIS. Thus, *C. glutamicum* Δ rptA does not exhibit an apparent growth defect indicating some degree of tolerance to the deletion of Cg-rptA. For further analyses, *C. glutamicum* Δ rptA was transformed with a plasmid encoding Cg-rptA, as well as with a plasmid encoding Rv3779 of *M. tuberculosis* to result in *C. glutamicum* Δ rptA pVWEx-Cg-rptA and *C. glutamicum* Δ rptA pVWEx-Rv3779.

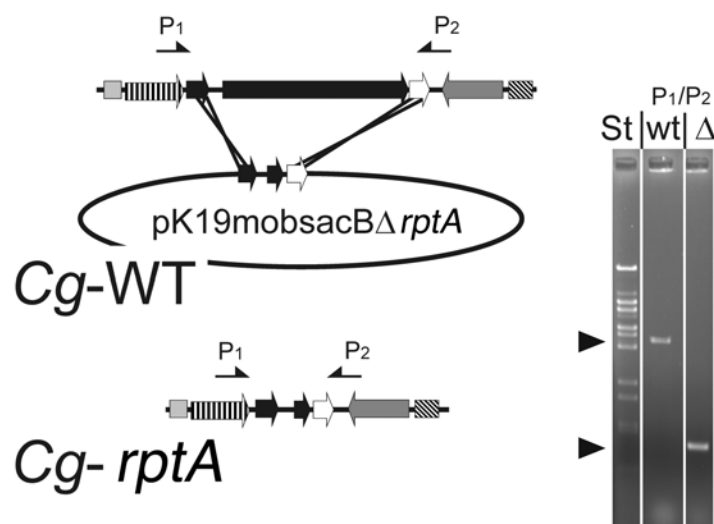


Figure 4.2: Strategy to delete *Cg-rptA* using the deletion vector pK19mobsacBΔ*rptA*. This vector carries 18 nucleotides of the 5' end of *Cg-rptA* and 36 nucleotides of its 3' end thereby enabling the in-frame deletion of the entire *Cg-rptA* gene. The arrows marked P1 and P2 locate the primers used for the PCR analysis to confirm the absence of *Cg-rptA*. Distances are not drawn to scale. The results of the PCR analysis with the primer pair P1/P2 are shown on the right. Amplification products obtained from the wild type (wt) were applied in the middle lane and that of the deletion mutant in the right lane. 'St' marks the standard.

4.2.4. Glycosyl compositional analysis of cell walls from *C. glutamicum*, *C. glutamicum*Δ*rptA*, *C. glutamicum*Δ*rptA* pVWEx-*Cg-rptA*, and *C. glutamicum*Δ*rptA* pVWEx-Rv3779

To study the function of a corynebacterial *rptA* deletion mutant, defatted cells were analysed quantitatively for AG esterified corynemycolic acids. Wild type *C. glutamicum* exhibited the known profile of CMAMES as previously described (Alderwick *et al.*, 2005). Furthermore, cell wall bound CMAMES were not significantly altered in *C. glutamicum*Δ*rptA*, which is contrary to the deletion of other GT-C glycosyltransferases in *C. glutamicum* (Alderwick *et al.*, 2005; Alderwick *et al.*, 2006). Analysis of cell wall associated lipids in several independent experiments highlighted no change in the lipid profiles of the *Cg-rptA* deletion mutant compared to that of *C. glutamicum*. This was confirmed quantitatively through [¹⁴C]acetate labeling of cultures and equal loading of radioactivity of extractable free lipids

from *C. glutamicum*, *C. glutamicum* Δ *rptA* and the complemented *C. glutamicum* Δ *rptA* strain using plasmid pVWEx-Cg-*rptA*. These results demonstrate that, unlike Cg-*emb* or Cg-*aftA* (Alderwick *et al.*, 2005; Alderwick *et al.*, 2006), Cg-*rptA* has little or no involvement in the structure or biosynthesis of cell wall bound/extractable lipids in *C. glutamicum*.

The cell wall core (mAGP) was prepared from *C. glutamicum* and *C. glutamicum* Δ *rptA* as described (Alderwick *et al.*, 2005; Besra *et al.*, 1995; Daffé *et al.* 1990) and the ratio of Rha, Ara to Gal in mAGP determined by gas chromatography (GC) analysis of alditol acetates (Alderwick *et al.*, 2005; Besra *et al.*, 1995; Daffé *et al.* 1990 (Figure 4.2). The glycosyl compositional analysis of wild type *C. glutamicum* revealed a relative molar ratio of Rha:Ara:Gal of 21:71:31 which is in accordance with previous data (Alderwick *et al.*, 2005) (Figure 4.2). The *C. glutamicum* Δ *rptA* mutant yielded a molar ratio of Rha:Ara:Gal (1:71:31), with a significant reduction in Rha content and no relative change in the Ara:Gal ratio (Figure 4.2). Complementation of *C. glutamicum* Δ *rptA* with pVWEx-Cg-*rptA* restored the Rha:Ara:Gal ratio to that of wild type *C. glutamicum* (Figure 4.2). Interestingly, complementation with pVWEx-Rv3779 did not complement and yielded a phenotype identical to that of *C. glutamicum* Δ *rptA*.

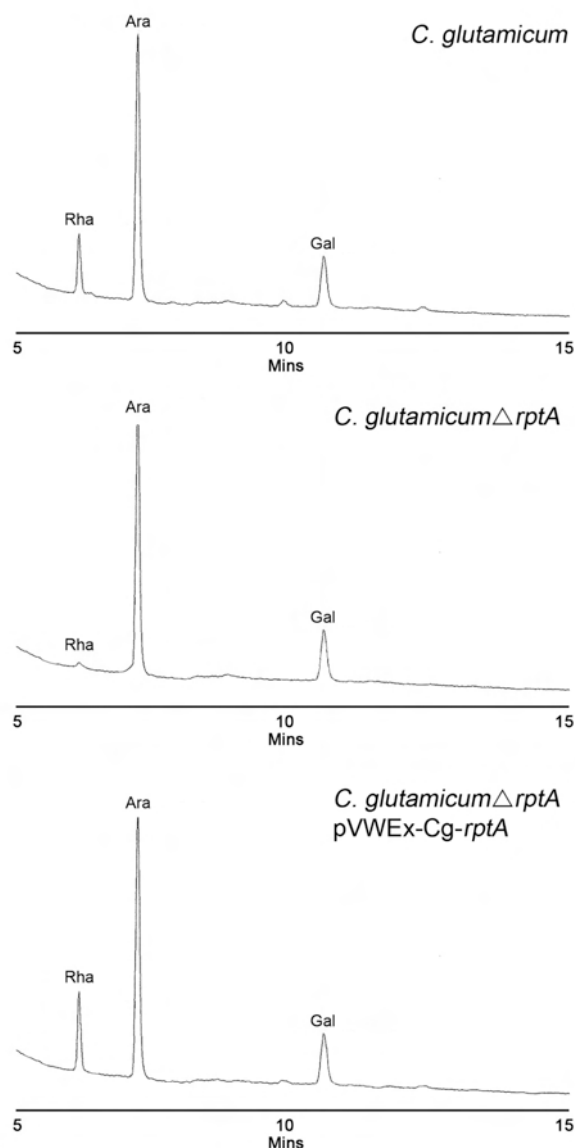


Figure 4.3: GC analysis of cell walls of *C. glutamicum*, *C. glutamicum* Δ *rptA* and *C. glutamicum* Δ *rptA* pVWEx-Cg-*rptA*. Samples of purified cell walls were hydrolysed with 2M TFA, reduced, per-*O*-acetylated and analysed as described under “Materials and Methods” (Alderwick *et al.*, 2005; Besra *et al.*, 1995). Abbreviations: Ara, arabinose; Gal, galactose; Rha, rhamnose.

4.2.5. Glycosyl linkage analysis of cell walls from *C. glutamicum*, *C. glutamicum* Δ *rptA*, *C. glutamicum* Δ *rptA* pVWEx-Cg-*rptA*, and *C. glutamicum* Δ *rptA* pVWEx-Rv3779

Gas chromatography mass spectrometry (GC/MS) analysis of per-*O*-methylated alditol acetate derivatives prepared from *C. glutamicum* and *C. glutamicum* Δ *rptA* indicated a loss of *t*-linked Rha_p residues with a corresponding loss of 2,5-linked Ara_f residues (Figure 4.4).

Complementation of *C. glutamicum* Δ *rptA* with plasmid-encoded pVWEx-Cg-*rptA* restored the glycosyl linkage profile to that of wild type *C. glutamicum* (Figure 4.4). Furthermore, as demonstrated by our total sugar analysis and cell wall sugar linkage analysis, Rv3779 was unable to complement *C. glutamicum* Δ *rptA* by pVWEx-Rv3779. These results demonstrate that the putative protein NCgl0543 is involved in the biosynthesis of *C. glutamicum* AG through the addition of *t*-Rhap residues to the C2 position of the 5-linked backbone domain of specific Ara β residues.

4.2.6. Recognition of a rhamnose lipid-linked sugar donor, decaprenyl-P-rhamnose

Initial assays involved wild type membranes from *C. glutamicum* and either UDP-[¹⁴C]GlcNAc, dTDP-[¹⁴C]Rha, UDP-[¹⁴C]Gal or pl[¹⁴C]Rpp as sugar donors for AG biosynthesis. Samples of the radioactive lipids from each assay were applied to TLC plates which were then developed in CHCl₃/CH₃OH/NH₄OH/H₂O (65:25:0.5:3.6) and autoradiograms obtained (Figure 4.5).

As expected a series of polar glycolipids (GL-1 to -4) were observed corresponding to GlcNAc-P-polyprenyl (GL-1), Rha-GlcNAc-P-polyprenyl (GL-2), Gal-Rha-GlcNAc-P-polyprenyl (GL-3), Gal-Gal-Rha-GlcNAc-P-polyprenyl (GL-4) and DPA/DPR consistent with previous studies utilising *M. smegmatis* membranes (Mikusova *et al.*, 1996). Interestingly, the inclusion of dTDP-[¹⁴C]-Rha also resulted in the synthesis of a more apolar rhamnose-labeled lipid X product, in comparison to GL-2-4 (Figure 4.5).

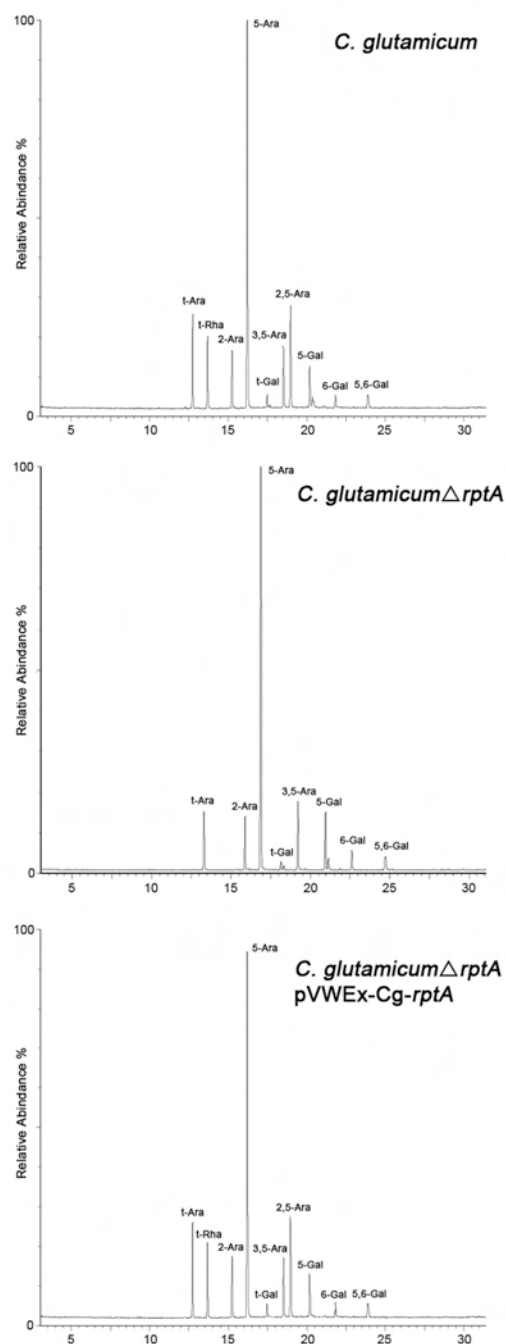


Figure 4.4: GC/MS analysis of cell walls of *C. glutamicum*, *C. glutamicum*Δ*rptA* and *C. glutamicum*Δ*rptA* pVWEx-Cg-*rptA*. Samples of per-*O*-methylated cell walls were hydrolysed with 2M TFA, reduced, per-*O*-acetylated and analysed as described under “Materials and Methods” (Alderwick *et al.*, 2005; Besra *et al.*, 1995)

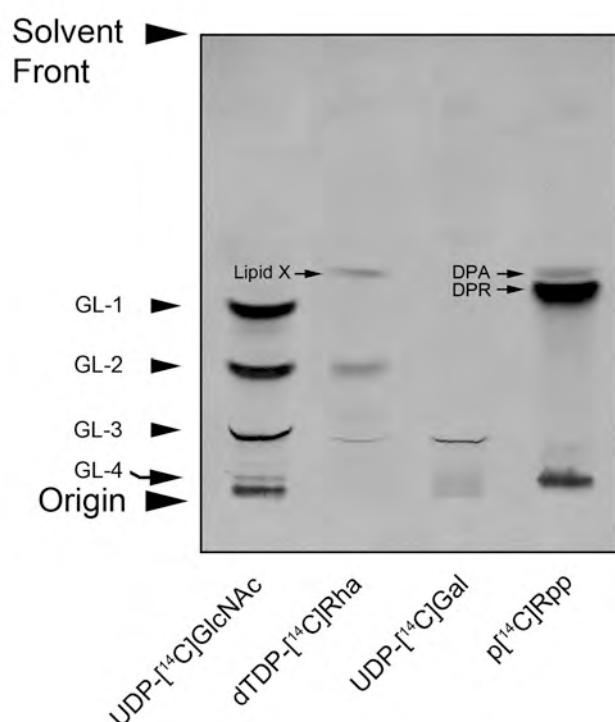


Figure 4.5: Analysis of $[^{14}\text{C}]$ GlcNAc, $[^{14}\text{C}]$ Rha, $[^{14}\text{C}]$ Gal and $[^{14}\text{C}]$ Ara labeled glycolipids in *C. glutamicum*. Membranes from *C. glutamicum* were prepared, mixed with decaprenyl-1-monophosphate and labeled with either UDP- $[^{14}\text{C}]$ GlcNAc, dTDP- $[^{14}\text{C}]$ Rha, UDP- $[^{14}\text{C}]$ Gal or p- $[^{14}\text{C}]$ Rpp. Radiolabeled glycolipids were extracted, analysed by TLC and visualised by autoradiography as described in “Materials and Methods”. Abbreviations: GL-1, GlcNAc-P-P-polyprenyl; GL-2, Rha-GlcNAc-P-P-polyprenyl; GL-3, Gal-Rha-GlcNAc-P-P-polyprenyl; GL-4, Gal-Gal-Rha-GlcNAc-P-P-polyprenyl; Lipid-X, putative decaprenol-1-monophosphate-rhamnopyranose; DPA, β -D-arabinofuranosyl-1-monophosphoryldecaprenol; DPR, β -D-ribofuranosyl-1-monophosphoryldecaprenol.

This lipid X was sensitive to acid and resistant to mild-base treatment indicating that this product was also a polyprenyl-P based lipid. Importantly, an increase in the synthesis of lipid X, based on TLC and densitometry, was found when assays were repeated with membranes prepared from *C. glutamicum* Δ rptA (lipid X, 4300 cpm) compared to *C. glutamicum* (lipid X, 3057 cpm), indicating that lipid X was probably the lipid-linked sugar donor for the GT-C glycosyltransferase RptA in this study (Figure 4.6). Furthermore, the synthesis of lipid X was unaffected by the addition of tunicamycin (*C. glutamicum* lipid X, 3222 cpm; *C.*

glutamicum Δ *rptA* lipid X, 4203 cpm) which inhibits GlcNAc phosphotransferase activity of Rv1302, thus leading to a marked decrease in GlcNAc-P-polyprenyl (GL-1) and higher GLs (e.g. >GL-2) (Figure 4.6).

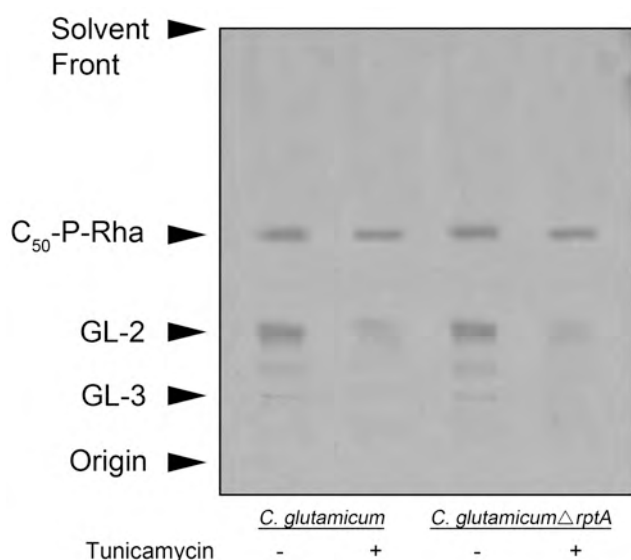


Figure 4.6: Analysis of [14 C]Rha base stable lipids in *C. glutamicum* and *C. glutamicum* Δ *rptA* and the effect of tunicamycin. Membranes from *C. glutamicum* and *C. glutamicum* Δ *rptA* were prepared, mixed with decaprenol-1-monophosphate and labeled with dTDP-[14 C]Rha. [14 C]Rha-labeled glycolipids were extracted, analysed by TLC and visualised by autoradiography as described in “Materials and Methods”. Abbreviations: GL-1, GlcNAc-P-P-polyprenyl; GL-2, Rha-GlcNAc-P-P-polyprenyl; GL-3, Gal-Rha-GlcNAc-P-P-polyprenyl; GL-4, Gal-Gal-Rha-GlcNAc-P-P-polyprenyl; Lipid-X, putative decaprenol-1-monophosphate-rhamnopyranose.

The basic assay mixture was scaled-up containing cold dTDP-Rha and the lipid X extracted for subsequent characterisation by treatment with mild base. Negative-ion electro-spray mass spectrometry (ES-MS) revealed a major signal ($M-H$) $^{-}$ at m/z 777 for decaprenyl phosphate (Figure 4.7A inset), and a product ion at m/z 924 corresponding to decaprenyl-P-rhamnose (Figure 4.7A). We also observe mass ions at m/z 934 and m/z 936, which could indicate 5 and 6 fully saturated isoprene units out of a possible 10. Similar observations have previously been reported in other *Corynebacteriaceae* glycolipids, such as the apparent mycolate transporter Myc-PL (Besra *et al.*, 1994). Altogether, the above dTDP-Rha labeling, sensitivity to acid, resistance to base and to tunicamycin, and analysis by ES-MS, confirmed

that lipid X was prenylated-P-rhamnose (Figure 4.7B), and is therefore the likely substrate of the membrane bound rhamnosyltransferase RptA.

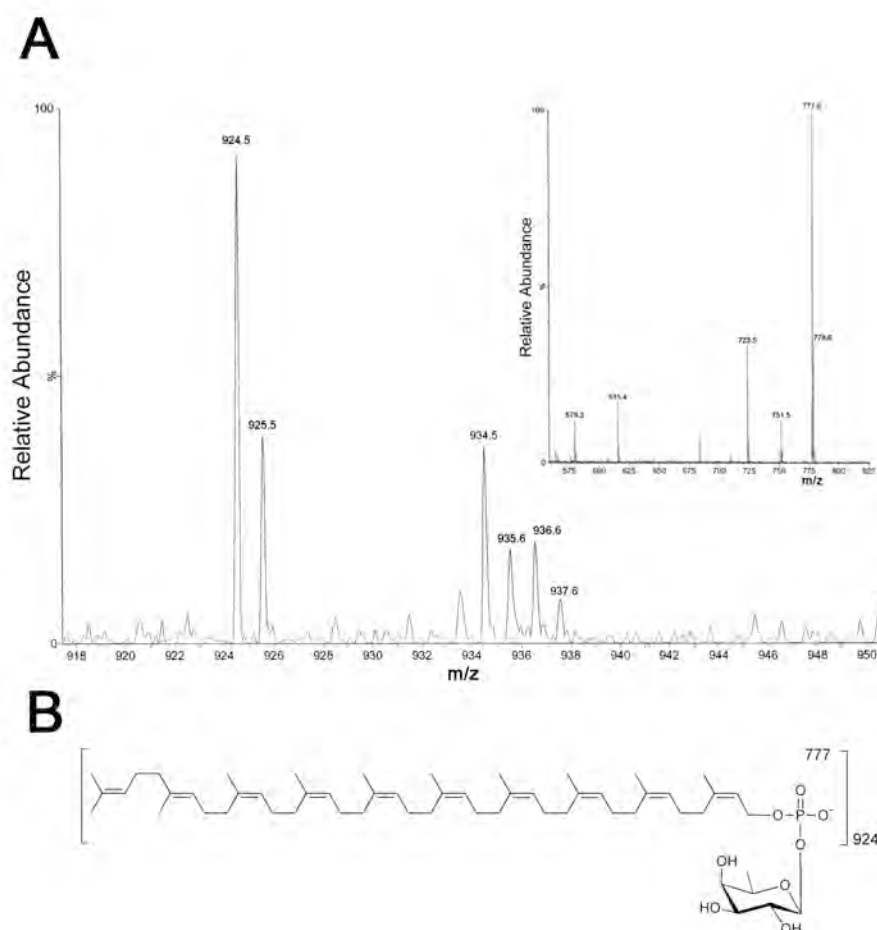


Figure 4.7: Mass spectrometry analysis and identification of decaprenyl-1-monophosphorylrhamnose. A) Electrospray mass spectrometry (in the negative mode) of decaprenyl-1-phosphorylrhamnose. **B)** Structure of decaprenyl-1-phosphorylrhamnose.

4.3. Discussion

It is clear, from this present study, that *Cg-rptA* is non-essential and is involved in the addition of *t*-Rhap residues to a 5-linked Ara_f backbone giving rise to branched 2,5-linked Ara_f residues. We also report a Rha:Ara molar ratio of 21:71 in *C. glutamicum* AG (Figure 4.3), which equates to approximately 7 *t*-Rhap residues per arabinan tricosamer. This significant amount of rhamnose in the cell wall must not be dismissed, and more so, the functional significance must be elucidated. Rhamnose is present in the cell walls of many Gram-positive bacteria such as *Staphylococcus*, *Streptococcus*, *Bacillus* and *Pseudomonas* (Weidnemaier & Peschel, 2008). In *Pseudomonas aeruginosa*, L-rhamnose is present in the form of mono or di substituted rhamnolipids, and these virulence factors are thought to act by disrupting lipid membranes by acting as a surfactant (Van Delden & Iglewski, 1998). In other Gram-positive bacteria, rhamnose is present in the cell wall as part of the carbohydrate moieties of teichoic acids and other cell-wall glycopolymers (Baddiley, 1972). However, since *C. glutamicum* is non-pathogenic, the introduction of *t*-Rhap residues is probably related to either (i) structural integrity or (ii) a mechanism to cap and end arabinan synthesis and provide a control point for the extent of mycolation of the "terminal" arabinan units.

Cg-rptA shares approximately 40% sequence similarity with the putative *M. tuberculosis* protein Rv3779. Although, the total length of the proteins differ by 133 aa, there are remarkable structural similarities, such as the high identity at the sequence level in the GT-C loop, which is located between TMH 3 and 4 in *C. glutamicum* (Figure 4.1) and TMH 4 and 5 in *M. tuberculosis* Rv3779. This loop is followed by 10 TMHs in *C. glutamicum*, which are present and similarly arranged in the *M. tuberculosis* orthologue. Interestingly, within the final periplasmic region, there is also a similar stretch of aa residues indicated as an open star in Figure 4.1A. Since the carboxy terminal periplasmic domain is suggested to play a role in

substrate recognition, which in the case of the GT-C glycosyltransferases is a growing polysaccharide, we speculate that both Cg-RptA and the putative Rv3779 protein recognise a related substrate, such as an arabinan oligosaccharide and distinct sugar donors, since the putative protein, Rv3779, failed to complement *C. glutamicum*Δ*rptA*.

NCgl0543 is part of the *rfb* locus and its genomic organisation is well retained in *Corynebacteriaceae*. Orthologues of this locus, which include *rfbE*, NCgl0197, NCgl0195, *rfbD* (NCgl0198), are present in *C. glutamicum*. RfbE has similarity to an ATP-dependent export carrier and is tentatively annotated as being a polysaccharide export ATP-binding protein, and *rfbD* as a polysaccharide export ABC transporter permease (Cole *et al.*, 1998). We have found that the galactosyltransferase NCgl0195 (Alderwick *et al.*, 2008; Mikusova *et al.*, 2006) is essential in *C. glutamicum* and is involved in GL-3 and GL-4 biosynthesis. Due to the function of Cg-RptA, and its similarity to the putative protein Rv3779, we speculate that the *rfb* locus is essential for polysaccharide biosynthesis and resultant export to the periplasm.

The biosynthesis of high energy nucleotide derived sugar substrates of *Corynebacteriaceae* glycosyltransferases, such as UDP- α -D-Galf (Weston *et al.*, 1997), dTDP-Rhap (Ma *et al.*, 1997) has been well characterised. These substrates are utilised by GT-A/B glycosyltransferases in the cytoplasm of the cell to form a preliminary linear galactan polysaccharide before being exported to the periplasm, by an as yet unidentified flippase. At this point, further polysaccharide biosynthesis employs glycosyltransferases belonging to the GT-C family which make use of prenylated phosphosugar substrates (Liu & Mushegian, 2003; Berg *et al.*, 2007). In *Corynebacteriaceae*, decaprenol (C₅₀) and, to a lesser extent octahydroheptaprenol (C₃₅), are the predominant lipid carriers for peptidoglycan, arabinogalactan and mannan biosynthesis. Decaprenyl phosphate is glycosylated by

arabinose and ribose to form β -**D**-arabinofuranosyl-1-monophosphoryldecaprenol (DPA) and β -**D**-ribofuranosyl-1-monophosphoryldecaprenol (DPR), respectively (Wolucka *et al.*, 1994). It is also glycosylated by mannose to form β -**D**-mannosyl-1-monophosphoryldecaprenol (DPM or PPM) (Gurcha *et al.*, 2002; Yokoyama & Ballou, 1989) and glucose to form β -**D**-glucosyl-1-monophosphoryldecaprenol (GPM) (Schultz & Elbein, 1974). To date, this is the first report of a GT-C rhamnosyltransferase (RptA). Furthermore, this is also the first report of a rhamnosylated monophosphodecaprenol, which is the substrate for RptA and novel with respect to DPA, DPR and DPM. Finally, the discovery of Cg-rptA has shed new light on the glycosyltransferases which are key to building the cell wall AG of Corynebacteriaceae.

Chapter 5

5. Conclusion and future work

M. tuberculosis is a major cause of illness and death worldwide and with the advent of MDR- and XDR-TB strains discovery of new chemotherapeutic agents is paramount (Brennan & Nikaido, 1995). Mycobacteria have an intricate cell wall and maintenance of its integrity is essential for the survival of the bacilli, and as such, numerous anti-tubercular drugs target its biosynthetic machinery. One such drug, EMB, inhibits synthesis of the arabinan, which forms an integral component of AG and LAM, the two dominating heteropolysaccharides located in the mycobacterial cell wall. In this regard, the last two decades have seen considerable effort concentrated towards the elucidation of the enzymes involved with in their biosynthetic pathways.

The number of arabinofuranosyltransferases that are required for mycobacterial arabinan biosynthesis has been a matter of speculation to date depending on how and where the arabinan chains are assembled. In terms of AG, the primary structure (Besra *et al.*, 1995; Daffé *et al.*, 1990) would suggest at least five distinct arabinofuranosyltransferases are required for the complete formation of the three AG arabinan domains. The availability of the complete genome sequence of *M. tuberculosis* H37Rv, as well as the decoding of other Actinomycetales genomes such as *C. glutamicum* proved crucial in forming our experimental hypothesis. Carrying out comparative genomic analysis of *Corynebacterineae* genome sequences, and employing surrogate experimental model systems such as *C. glutamicum* and *M. smegmatis*, has enabled us to study the molecular genetics of mycobacterial cell wall biosynthetic processes, which are otherwise essential in *M. tuberculosis*. This strategy was previously used to identify the presence of a new “priming” enzyme, now termed AftA, which would link the initial Ara_f unit with the C-5 OH of a $\beta(1\rightarrow6)$ linked Gal_f of a pre-synthesised galactan core (Alderwick *et al.*, 2005b).

The studies reported in this thesis have identified Rv3805c, which has now been termed AftB, as a novel retaining arabinofuranosyltransferase, which adds to the non-reducing end of the arabinan domain of AG $\beta(1\rightarrow2)$ Araf residues. Deletion of its orthologue *NCgl2780* in the closely related species *C. glutamicum* produced a viable mutant with a decreased abundance of cell wall bound mycolic acids, consistent with a partial loss of mycolylation sites. Glycosyl linkage analysis of arabinogalactan revealed the complete loss of terminal $\beta(1\rightarrow2)$ linked Araf residues which was fully restored upon complementation with a plasmid expressing Cg-AftB or Mt-AftB but not with muteins of Mt-AftB, where the two adjacent aspartic acid residues, which have been suggested to be involved in glycosyltransferase activity, were replaced by alanine. In addition, the use of *C. glutamicum* and *C. glutamicum* Δ *aftB* in an *in vitro* assay utilizing the sugar donor DPA together with a neoglycolipid acceptor as substrate, confirmed AftB as a terminal $\beta(1\rightarrow2)$ arabinofuranosyltransferase, which was also insensitive to EMB.

Interestingly, Escuyer *et al.* (2001) reported, *M. smegmatis* *embA* and *embB* mutants possessing reduced amounts of the non-reducing terminal disaccharide β -D-Araf-(1 \rightarrow 2)- α -D-Araf, resulting in the absence of the dominant terminal non-reducing Ara₆ branched motif in the mutant being replaced by a linear Ara₄ motif. The authors of this study concluded that the *M. smegmatis* *embA* and *embB* mutants result in a lack of 3-arm branching off the main $\alpha(1\rightarrow5)$ -arabinan chain proximal to the non-reducing and attachment site of mycolic acids in AG (Escuyer *et al.*, 2001), leading to the supposition that the β -D-Araf-(1 \rightarrow 2)- α -D-Araf disaccharide was assembled using EmbA and EmbB.

The results presented in this thesis do not reflect the proposed roles of the known AraTs propounded by Escuyer *et al.* (2001), in fact the complete biochemical and molecular characterisation of AftB in this study and the development of an *in vitro* assay (Lee *et al.*,

1997) suggests that EmbA/B may act as $\alpha(1\rightarrow5)$ arabinofuranosyltransferases, although further definitive characterisation is required. Due to the inherent absence of a LAM-like molecule in *C. glutamicum*, we were unable to determine the involvement of Mt-AftB in both AG and LAM arabinan biosynthetic pathways. In terms of future studies, it would be interesting to generate an *aftB* mutant in *M. smegmatis* to assess whether or not AftB has dual functionality, with regard to LAM biosynthesis, and is responsible for $\beta(1\rightarrow2)$ capping in LAM, akin to our studies of *M. smegmatis* AftC (see below).

In addition, our current studies have also identified MSMEG2785 (Rv2673 and NCgl1822), which we have termed AftC, as a novel branching arabinofuranosyltransferase. *In vivo* and *in vitro* experiments demonstrated that AftC catalyses the addition of $\alpha(1\rightarrow3)$ Araf residues, ultimately resulting in 3,5-Araf residues after further $\alpha(1\rightarrow5)$ extension, characteristic of AG. It was shown that incubation of membranes prepared from *M. smegmatis* with DP[^{14}C]A and a linear $\alpha(1\rightarrow5)$ -Ara₅ neoglycolipid acceptor resulted in the synthesis of an Ara₆ product. Further chemical characterisation of the product by glycosyl linkage analysis established that the $\alpha(1\rightarrow5)$ -Ara₅ acceptor was extended *via* an EMB resistant $\alpha(1\rightarrow3)$ arabinofuranosyltransferase, giving rise to 3-linked Araf residues. Since, it is now established that only $\alpha(1\rightarrow5)$ arabinofuranosyltransferase(s) are EMB-sensitive it can be further speculated that EmbA and EmbB function in the assembly of the linear $\alpha(1\rightarrow5)$ arabinan segments. This is in accordance with previous data (Besra *et al.*, 1995; Daffé *et al.*, 1990) and phenotypes of EmbA and EmbB (Escuyer *et al.*, 2001; Zhang *et al.*, 2003) and Cg-Emb (Alderwick *et al.*, 2005b) mutants. It is clear that further studies are required to establish the precise role of EmbA and EmbB in mycobacteria.

Given that *M. smegmatis* possesses a LAM structure similar to *M. tuberculosis*, and the arabinan domain is structurally similar to that of AG, we investigated the potential dual

functionality of AftC. The formation of the arabinan domain of LAM requires an $\alpha(1\rightarrow3)$ AraT resulting in the branched motif of LAM. By structural analysis of LAM from a *M. smegmatis* Δ *aftC* mutant, we demonstrated that AftC carries dual functionality and is responsible for introducing 3,5-Araf branches into LAM, in addition to AG. Furthermore, it was shown by treating an *M. smegmatis* Δ *aftC* mutant with EMB, that EmbC is involved in the very early steps of the LAM arabinan core synthesis and that truncation of this domain modulated the immunological properties of the molecule. AftC-LAM exhibited enhanced pro-inflammatory activity due to its ability to activate TLR2, thus further work using this truncated LAM could shed light on the structure-function relationship of TLR2 activation by mycobacterial lipoglycans. It would be interesting to examine whether the generation of *aftC* mutants in *M. bovis* BCG and *M. marinum* is in fact feasible and if these could be used in infection studies involving mice and zebrafish, respectively.

This study also characterised a further ORF from *C. glutamicum* encoding a distinct *t*-rhamnopyranosyltransferase from the GT-C superfamily of glycosyltransferases, now termed RptA. Disruption of *NCgl0543* in *C. glutamicum* and subsequent biochemical and molecular analyses demonstrated that the enzyme is responsible for the transfer of *t*-Rhap residues to the arabinan domain to form the branched 2,5-linked Araf motifs of *C. glutamicum*. The introduction of *t*-Rhap residues is probably related to either structural integrity or a mechanism to cap and end arabinan synthesis, providing a control point for the extent of mycolation of the "terminal" arabinan units. Cg-*rptA* shares approximately 40% sequence similarity with the putative *M. tuberculosis* protein Rv3779 and there are remarkable structural similarities, such as the high identity at the sequence level in the GT-C loop. Interestingly, within the final periplasmic region, there is also a similar stretch of amino acid residues and given that the carboxy terminal periplasmic domain is suggested to play a role in substrate recognition, we speculated that both Cg-RptA and the putative Rv3779 protein

recognise a related substrate, such as an arabinan oligosaccharide but utilising distinct sugar donors, since the putative protein, Rv3779, failed to complement *C. glutamicum* Δ rptA. A recent investigation by Scherman *et al.* (2009) presented evidence that Rv3779 exhibited polyprenyl-phosphomannopyranose synthase activity. However, a very recent investigation carried out in the same laboratory presented conflicting data, which clearly establishes Rv3779 as a polyprenyl-phospho-*N*-acetylgalactosamine transferase, the enzyme responsible for modifying the interior 3,5-Araf branch motifs by the addition of terminal GalN units (Skovierova *et al.*, 2010). Based on the findings reported in this thesis for RptA (Chapter 4), the latter is the more likely role of Rv3779 since its natural substrate is polyprenyl-phospho-*N*-acetylgalactosamine (polyprenyl-P-GalNAc) for which the equivalent is polyprenyl-P-Rhap in *C. glutamicum* (Chapter 4). Furthermore, the absence of GalN units in the AG of *M. smegmatis* correlates with a clear lack of a Rv3779 homolog in the *M. smegmatis* genome. Our apparent negative observation of a clear phenotypic change upon over expression of Rv3779 in *M. smegmatis* and the inability of Rv3779 to complement the *C. glutamicum* Δ rptA mutant, presents conclusive evidence that *C. glutamicum* and *M. tuberculosis* share similar AG modifying activities. The role of GalN modifications in the AG of *M. tuberculosis* remains unknown.

As noted previously, glycosyltransferases involved in galactan and early PIM biosynthesis utilise high-energy sugar donor substrates and belong to the GT-A/B family present in the cytoplasm of the cell. Upon transition from galactan to arabinan biosynthesis, and early PIM to higher PIM biosynthesis, there is a change to GT-C family of glycosyltransferases, which make use of polyprenol phosphate substrates (Liu & Mushegian, 2003; Berg *et al.*, 2007). With this in mind and the fact that rhamnosyl residues are most likely added in the periplasm, we set about looking for lipid linked sugar donor akin to DPA (Wolucka *et al.*, 1994) and

DPM (Gurcha *et al.*, 2002; Yokoyama & Ballou, 1989). This is the first report of a rhamnosylated monophosphodecaprenol, which is the substrate for RptA.

To conclude, AftB and AftC represent novel AraTs in *Corynebacteriaceae*, which are responsible for the addition of the terminal $\beta(1\rightarrow2)$ linked Ara f residues and branching $\alpha(1\rightarrow3)$ Ara f residues into arabinan, respectively. The identification of new cell wall biosynthetic drug targets is of great importance, especially with the emergence of MDR-TB and XDR-TB. Since AftB and AftC are EMB insensitive, these newly discovered DPA dependent AraTs represent promising candidates for further exploitation as potential drug targets. The disruption of the biosynthesis of mycobacterial AG and LAM formation by small molecule inhibition would potentially have a catastrophic effect on the structural integrity, composition and permeability of the TB cell wall. The molecular mechanism and biochemistry of the GT-C superfamily of glycosyltransferases are poorly understood. Considering that 80% of all pharmacological drug targets are located in the cytoplasmic membrane of cells, further investigation into these polytopic membrane bound enzymes is warranted. It is envisaged that the studies reported in this thesis could be expanded in terms of future experiments exploring: (i) over expression of recombinant arabinofuranosyltransferases, (ii) the development of a sensitive and selective AraT assay suitable for high-throughput screening of a chemical library, (iii) X-ray crystallographic structural studies, and (iv) *in silico* drug design.

Chapter 6

6. Materials and Methods

6.1. Chemicals, reagents and growth conditions

All chemicals and solvents were purchased from Sigma-Aldrich (Dorset, UK), Biorad (CA, USA) and Fischer Chemicals (UK) unless otherwise stated, and were of AnalR grade or equivalent. Enzymes were obtained from Sigma-Aldrich (Dorset, UK), Roche (Lewes, UK) or New England Biolabs (Boston, USA) and were of the highest grade available.

6.2. Bacterial growth conditions

C. glutamicum ATCC 13032 and *E. coli* DH5 α mc^r were grown in Luria-Bertani broth (LB, Difco) at 30°C and 37°C, respectively. The recombinant strains generated in this thesis were grown on complex brain–heart infusion medium LBHIS (5 g tryptone, 5 g NaCl, 2.5 g yeast extract, 18.5 g brain heart infusion (Difco), and 90.1 g sorbitol per litre). Kanamycin and ampicillin were used at a concentration of 50 μ g/ml. The minimal medium CGXII was used for *C. glutamicum* (Eggeling & Bott, 2005). Samples for lipid and cell wall analysis were harvested after reaching an OD 3, followed by a saline wash and freeze drying.

M. smegmatis strains were grown in tryptic soy broth (TSB; Difco), containing 0.05% Tween 80 (TSBT). *M. smegmatis* and mycobacteriophages were also propagated on Middlebrook 7H9 broth (Difco), supplemented with 0.2% glycerol and 0.05% Tween 80. For phage infection experiments Tween 80 was omitted in all media. Solid media were made by adding 1.5% agar to the above-mentioned broths. The concentrations of antibiotics used for *M. smegmatis* were 100 μ g/ml for hygromycin and 20 μ g/ml for kanamycin.

6.2.1. Construction of *C. glutamicum* mutants

6.2.1.1. Construction of *C. glutamicum*Δ*aftB* and complementing strains

M. tuberculosis H37Rv DNA was obtained from the NIH Tuberculosis Research Materials and Vaccine Testing Contract at Colorado State University. All mutant strains in *C. glutamicum* were constructed at Institute for Biotechnology Research Centre, Juelich, Germany.

The vectors made were pMSX-Cg-*aftB* (NCgl2780), pMSX-Mt-*aftB* (Rv3805c), and pK19mobsacΔ*aftB* (NCgl2780). To enable deletion of Cg-*aftB*, cross-over PCR was applied to generate the fragments carrying fused sequences adjacent to the gene in question. Cross-over PCR was applied with primer pairs AB and CD (Table 1.4) and *C. glutamicum* genomic DNA as template. Both amplified products were used in a second PCR with primer pairs AD to generate a fragment consisting of sequences adjacent to Cg-*aftB*, which was blunt end-ligated with SmaI-cleaved pK19mobsacB. All plasmids were confirmed by sequencing. The chromosomal deletion of Cg-*aftB* was performed, using two rounds of positive selection (Schafer *et al.*, 1994), and its successful deletion was verified by use of different primer pairs. Plasmid pMSX-Mt-*aftB* and pMSX-Cg-*aftB* were introduced into *C. glutamicum*Δ*aftB* by electroporation with selection to kanamycin resistance (25 µg/ml).

To express *M. tuberculosis* *aftB* in *C. glutamicum*, the primer pair EF was used, with the restriction sites NdeI and XhoI underlined, using *M. tuberculosis* H37Rv chromosomal DNA as a template. The purified PCR fragment was ligated with accordingly digested pMSX to give pMSX-Mt-*aftB*. pMSX was prepared from pEKEx2 (Eikmanns *et al.*, 1991) to generate a derivative providing an appropriate ribosome binding site together with a C-terminal His tag. It was created by the individual cleavage of pEKEx2 with NdeI and XhoI, each followed by Klenow treatment and religation. The intermediate construct was SalI/DraI-cleaved,

treated with mung bean nuclease, and ligated with the XbaI/MroI fragment from pET22b, which before use was treated with the Klenow fragment to eventually yield pMSX. To overexpress *Cg-afb*, the primer pair GH was used to amplify *C. glutamicum afb*, which was ligated with NdeI- and XhoI-cleaved pMSX to generate pMSX-*Cg-afb*.

Table 1.4: Primers used for the generation of knock-out mutants and complemented strains.

Primer name	Sequences (5'→3')
A	ACGCCAAGCTTTGCTAGTCGCTGCGTTTGGTTC
B	CCCATCCACTAAACACTGGGGGCTAAACGTCATGAG
C	CCCATCCACTAAACACTGGGGGCTAAACGTCATGAG
D	GCCAGTGAATTCGGCGCGCAGCGTTGGTATC
E	GTATGAGCATATGGTCCGGGTCAGCTTGTGG
F	ATTGCCCTCACTCGAGCTCCCGCGGTGGCGGG
G	ATGTGGCCATATGACGTTTAGCCCCAGCGTC
H	TGTTTACTCGAGCTGAGAGCTATATAAAGGTTCTCCGC
I	CGTTAAGCTTCGATCTTGTGATGTGTGGCATCACACG
J	CCCATCCACTAACTTAAACAGCGCCATCAACAACATGG
K	TGTTTAAGTTTAGTGGATGGGTGATCCAACGCACGACCATC
L	GCATGGATCCACGCATACCGAGGGAAAGATCTTC
M	CGTTGAATTCGGTTCCAGTAGCACCTGCGAAAGG
N	CCCATCCACTAACTTAAACACAATCCATAGTGTGCTCAGCATC
O	TGTTTAAGTTTAGTGGATGGGCGGATCCAACGAAGCC
P	GCTTTCTAGAATGCGGGCAACCGCGCAGTGTG
Q	GATGAATCTAGAAAGGGAGATATAGATGCTGACGACACTATG
R	CTACTTTCTAGATTAGTTAGGGACCGTATGCGGC
S	GATAATCTAGAAAGGGAGATATAGGTGGGCCTGTGGTTTCG
T	GCCGTACTTTCTAGACTAGGAGTGTGTTGCTGCG
U	GAACCGCAGGTGTATGAAGCACACGTG
V	GGCAGATTACGCTGCAGTTCTTTCTGCG
MS2785LL	TTTTTTTTCCATAAATTGGATCCGCTGACCGACCTCATC
MS2785LR	TTTTTTTTCCATTTCTTGCGAGCCCGAGCTTGAAGTTG
MS2785RR	TTTTTTTTCCATAGATTGGTTCCTGCTGCTGTCCCTTGG
MS2785RR	TTTTTTTTCCATCTTTTGCGAACTCAGCGGCGATTAC

Site-specific mutations were introduced in *Mt-afb* using appropriate mutagenic primers and pMSX-*Mt-afb* as the double-stranded template (QuikChange kit, Stratagene). After linear amplification of the newly synthesized strands and DpnI digestion of parental strands, plasmids pMSX-*Mt-afb*-D29A and pMSX-*Mt-afb*-D30A were generated carrying the mutations as indicated. All plasmids were verified by sequencing.

6.2.1.2. Construction of *C. glutamicum*Δ*aftC* and complementing strains

The genes analysed were *Rv2673* and *NCgl1505* from *M. tuberculosis* and *C. glutamicum*, respectively, termed *aftC*. To construct the deletion vector pK19mobsacBΔ*aftC* (*NCgl1822*), cross-over PCR was applied with primer pairs IJ and KL and *C. glutamicum* genomic DNA as template. Both amplified products were used in a second PCR with primer pairs IL to generate a 656 bp fragment consisting of sequences adjacent to Cg-*aftC*, which was ligated with BamHI–HindIII-cleaved pK19mobsacB. All plasmids were confirmed by sequencing. The chromosomal deletion of Cg-*aftC* was performed using two rounds of positive selection (Schafer *et al.*, 1994) and its successful deletion was verified by use of two different primer pairs.

6.2.1.3. Construction of *C. glutamicum*Δ*rptA* and complementing strains

The vectors made were pVWEx-Cg-*rptA*, pVWEx-*Rv3779*, and pK19mobsacB*rptA*. To construct the latter deletion vector, crossover PCR was applied with primer pairs MN and OP and *C. glutamicum* genomic DNA as a template. Both amplified products were used in a second PCR with primer pair AD to generate a 587-bp fragment consisting of sequences adjacent to NCgl0543, which was treated with EcoRI and XbaI and ligated with pK19mobsacB to yield pK19mobsacB*rptA*. To enable the expression of NCgl0543, the primer pair QR was used to amplify *rptA* of *C. glutamicum*, which was treated with XbaI and ligated to yield pVWEx-Cg-*rptA*. The primer pair ST was used to amplify *Rv3779* from *M. tuberculosis*. The resulting fragment was treated with XbaI to yield pVWEx-*Rv3779*. The correct orientation and the sequence identities were confirmed for all plasmids by sequencing.

The chromosomal deletion of the *NCgl0543* gene was performed, as described previously, using two rounds of positive selection (Schafer *et al.*, 1994) and its successful deletion was verified by use of primer pair UV. This yielded the expected fragment of 837 bp in the

deletion mutant and was termed *C. glutamicum rptA* and a fragment of 3,179 bp in wild-type *C. glutamicum*.

6.2.2. Construction of *M. smegmatis* mutants

6.2.2.1. Construction of *M. smegmatis*Δ*aftC* and complementing strains

Approximately 1 kb of upstream and downstream flanking sequences of *MSMEG2785* were PCR amplified from *M. smegmatis* mc₂155 genomic DNA using the primer pairs MS2785LL/MS2785LR and MS2785RL/MS2785RR, respectively. Following restriction digestion of the primer incorporated *Van91I* sites, the PCR fragments were cloned into *Van91I*-digested p0004S. The ligation mixture was transformed into *E. coli* Top10 cells and selected on LB agar with hygromycin at 37° overnight. Recovered plasmids were digested with *PacI* and ligated with *PacI*-digested phAE159 to yield the knockout plasmid pDMSMEG2785. The ligated knock-out plasmid and the temperature-sensitive mycobacteriophage phAE159 were then packaged into λ phage heads and transduced into *E. coli* HB101, as described previously (Bardarov *et al.*, 2002), to yield phasmid DNA of the knockout phage phDMSMEG2785. The recovered phasmid was then transformed into *M. smegmatis* via electroporation and cells grown at 30°C for 3 days to yield phage particles. Generation of high titre phage particles involved 200 µl of 0.8 OD_{600nm} culture of *M. smegmatis* mixed into 5 ml molten 7H9 soft agar and overlaid on a basal layer of 7H9 agar. The phage stock was serially diluted (10⁻¹ - 10⁻¹⁰) with MP buffer (50mM Tris.HCl pH7.8, 150mM MgSO₄, 2mM CaCl₂) and 10 µl of each dilution spotted onto the solidified overlay of *M. smegmatis*. Plates were incubated at the permissive temperature of 30°C for 3 days, after which, the plaque forming units were counted and phage titre calculated (pfu = number of pfu in spot x dilution factor x 100). Original phage stock was then diluted to yield approximately 500 plaques *per plate* and mixed with 200 µl *M. smegmatis* in molten 7H9 agar, which was overlaid on solid 7H9 agar.

Plates were incubated at 30°C for 3 days, resulting in a “lacy pattern”. The high titre phage was then collected and filtered through a 0.45µm filter (Stover *et al.*, 1991).

To perform specialized transduction, *M. smegmatis* cultures were grown to an OD_{600nm} 0.8 in 50 ml of TSB (0.05% Tween 80). Harvested cells were then washed three times with 50ml MP buffer and finally resuspended in 5 ml MP buffer. 0.5 ml of cells was then mixed with 0.5 ml of the optimum high titre lysate (10¹⁰ pfu/ml) and incubated overnight at 37°C (Stover *et al.*, 1991; Bardarov *et al.*, 2002). Cells were harvested and resuspended in 25 ml TSB and recovered overnight at 37°C, followed by plating onto TSB agar plates with hygromycin B. Plates were incubated at 37°C for 1-2 weeks. Deletion of *MSMEG2785* in one hygromycin-resistant transductant was confirmed by Southern blot. To enable expression of *MSMEG2785* and *Rv2673*, in the deletion mutant, these were amplified using primer pairs designed for subsequent cloning into the mycobacterial-shuttle vector pMV261 (Stover *et al.*, 1991). All cloned fragments were verified by sequencing.

6.2.2.2. Southern blot analysis

Southern blot analysis was used to confirm gene knock-out mutants and was performed as specified in the Roche Applied Science kit manual. *SacI* digested genomic DNA from *M. smegmatis* wild-type and *M. smegmatis*Δ*aftC* strains were subjected to gel electrophoresis to separate the fragments, producing a laddering effect. In the mutant strain the *aftC* gene had been replaced with a *hyg*^R gene. There were two *SacI* restriction sites in the wild-type and three in the mutant due to the presence of the *hyg*^R gene marker. PCR products of 1 kb of *aftC* left and right flanking regions were used as probes. Following *SacI* digestion, one fragment was observed for wild-type and two fragments for *M. smegmatis*Δ*aftC*. Following gel electrophoresis, the gel was depurinated (0.2M HCL, 15min) and denatured (1.5M NaCl, 0.5M NaOH, 15 min). The gel was then washed to return to pH 7.4 and the DNA

subsequently transferred to positively charged nitrocellulose membrane *via* capillary action with 20 x SSC (3M sodium citrate, pH 7.0). DNA on membrane was then covalently bound by UV-crosslinking. The membrane was finally rinsed with distilled water and air-dried. Probe preparation involved boiling, snap freezing and labeling with digoxigenin-dUTP, using the DIG High Prime DNA labeling and Detection Start Kit (Roche), as described in the kit manual. The membrane was exposed to the probe at 65°C overnight, followed by washing and finally immunodetected with the antibody for 30 min at 25°C. The hybridized probes were visualized with the chemiluminescence.

6.2.3. mAGP purification procedures

After cultivation the thawed *C. glutamicum*/*M. smegmatis* cells were resuspended in phosphate buffered saline containing 2% Triton X-100 (pH 7.2) and disrupted by sonication (MSE Soniprep 150, 12 micron amplitude, 60s ON, 90s OFF for 10 cycles, on ice). The cell debris was centrifuged at 27,000 xg (Besra *et al.*, 1995; Daffé *et al.*, 1990). The pelleted material was extracted three times with 2% SDS in phosphate buffered saline at 95°C for 1 hr to remove associated proteins, successively washed with water, 80% (v/v) acetone in water, and acetone, and finally dried under compressed N₂ to yield a highly purified cell wall preparation (Besra *et al.*, 1995; Daffé *et al.*, 1990).

6.2.3.1. Acid hydrolysis and alditol acetate derivatisation

Cell wall preparations (1 mg) were hydrolysed in 250 µl of 2 M trifluoroacetic acid (TFA) at 120°C for 2 h (Besra *et al.*, 1995; Daffé *et al.*, 1990). After drying under compressed N₂, sugar residues were reduced with 50 µl NaB²H₄ (10 mg/ml in ethanol:1M NH₃ OH (1:1)) and the resultant alditols per-*O*-acetylated using 100µl acetic anhydride with heating at 100 °C for 1 hr. After cooling, the reaction mix was combined with 100µl toluene and dried under compressed N₂. The resulting alditol acetates were partitioned between 2 ml H₂O and 2 ml

CHCl₃, mixed, centrifuged and the organic phase dried under compressed N₂. Alditol acetates were examined by GC as described in section 6.2.4.

6.2.3.2. Glycosidic linkage analysis

Cell wall preparations (10 mg) were suspended in 0.5 ml dimethyl sulfoxide (anhydrous) and 100 µl of 4.8 M dimethyl sulfinyl carbanion (generated by mixing NaH (2.4 g) with anhydrous DMSO (20 ml) and heated at 50°C with stirring for 3 h) (Besra *et al.*, 1995; Daffé *et al.*, 1990). The reaction mixture was stirred at room temperature for 1 hr and then 50 µl of CH₃I was slowly added and the suspension stirred for a further 1 hr. A further 100 µl of 4.8 M dimethyl sulfinyl carbanion and 50 µl CH₃I was added and the process repeated for a total of three times. The reaction mixture was then diluted with an equal volume of water and the entire contents dialysed against 10 L of water, overnight (1000 kDa MWCO Spectra/Por membrane 6, Spectrum labs, UK). The dialysed retentate was dried in a Savant SpeedVac SC110. The resulting per-*O*-methylated cell wall samples were resuspended in 2 ml of H₂O/DMSO (1:1, v/v) and applied to a C₁₈ Sep-Pak cartridge (Alltech, Deerfield, USA), which was pre-equilibrated sequentially with 20 ml ethanol, 5 ml H₂O, 5 ml acetonitrile, 5 ml ethanol and 10 ml H₂O. The material bound to the Sep-Pak was washed with 5 ml H₂O, 8 ml H₂O/acetonitrile (4:1, v/v) and then eluted with 2 ml acetonitrile and 2 ml ethanol, the latter eluants were pooled and dried in a Savant SpeedVac SC110. The per-*O*-methylated cell walls were hydrolysed, reduced and per-*O*-acetylated as described in chapter 6.2.3.1. Per-*O*-methylated and per-*O*-acetylated alditol acetates were examined by GC/MS as described in chapter 6.2.4

6.2.4. GC and GC/MS

GC analysis was performed using a Thermoquest Trace GC 2000. Samples were injected in the splitless mode. The column used was a DB225 (Supelco) ID 0.10 mm, length 10 m and df

0.05 μm . The oven was programmed to hold at an isothermal temperature of 275 °C for a run time of 15 min.

GC/MS was carried out on a Finnigan Polaris/GCQ PlusTM. The column used was a BPX5 (Supleco). Injector temperature was set at 50°C, held for 1 min and then increased to 110°C at 20°C/min. The oven was held at 110°C then ramped to 290°C at 8°C/min and held for 5 min to ensure all the products had eluted from the column. All the data were collected and analyzed using Xcaliber (v.1.2) software.

6.3. Extraction and visualisation of lipids

6.3.1. Cell wall associated lipid extraction

Cells were grown as described in section 6.2, harvested, washed and freeze-dried. Cell wall associated free lipids were extracted twice from 100 mg of dried cells using 2 ml of $\text{CHCl}_3/\text{CH}_3\text{OH}/\text{H}_2\text{O}$ (10:10:3, v/v/v) for 3 hr at 50 °C. Organic extracts were combined with 1.75 ml CHCl_3 and 0.75 ml H_2O , mixed and centrifuged at 1500 x g for 5 mins. The lower organic phase was recovered, back washed twice with 2 ml of $\text{CHCl}_3/\text{CH}_3\text{OH}/\text{H}_2\text{O}$ (3:47:48, v/v/v), dried and resuspended with 200 μl of $\text{CHCl}_3/\text{CH}_3\text{OH}/\text{H}_2\text{O}$ (10:10:3, v/v/v). A 10 μl aliquot was subject to TLC analysis, using silica gel plates (5554 silica gel 60F₂₅₄, Merck) developed in $\text{CHCl}_3/\text{CH}_3\text{OH}/\text{H}_2\text{O}$ (60:16:2, v/v/v). TLC plates were charred, using 5% molybdophosphoric acid (MPA) in ethanol at 100°C to reveal free lipids. MPA was used for the detection of all lipids. Lipid species were revealed by charring the plates with a heat gun. α -Naphthol (α -NAP) was used for the detection of all glycolipids. α -NAP solution was prepared from 6 g of α -naphthol dissolved in 25 ml of sulfuric acid and 450 ml ethanol. Glycolipid species were revealed by gently charring the plates with a heat gun. The Dittmer and Lester reagent was prepared according to the modified procedure of Muthing & Radloff (1998) for the detection of phospholipids and glycopospholipids. Solution A consisted of 40

g molybdenum VI oxide dissolved in 1 L of boiling sulfuric acid, solution B contained 1.7 g of solid molybdenum dissolved into 0.5 L of solution A. Solutions A and B were then mixed with H₂O to give a final solution in the ratio of solution A:solution B:H₂O, 1:1:4. Plates were sprayed with the stain and left to develop for 5 min at room temperature.

6.3.2. Exported (media filtrate) lipid extraction

Exported lipids were analysed in a similar manner to that in *C. glutamicum* cells were cultured as described above. Once the A₆₀₀ reached ~0.5, cultures were labelled with 1 µCi [1,2-¹⁴C]acetic acid (specific activity 50-62 mCi/mmol, GE Healthcare, UK) and further incubated for 8 hr. Cells were harvested by centrifugation at 27,000 x g for 30 min and the supernatant carefully removed and dried using a Savant SpeedVac SC110. The residue was resuspended into 2 ml of CHCl₃/CH₃OH/H₂O (10:10:3, v/v/v) for 3 hr at 50 °C. Organic extracts were combined with 1.75 ml CHCl₃ and 0.75 ml H₂O, mixed and centrifuged at 1,500 x g for 5 mins. The lower organic phase was recovered, back washed twice with 2 ml of CHCl₃/CH₃OH/H₂O (3:47:48, v/v/v), dried and resuspended with 200 µl of CHCl₃/CH₃OH/H₂O (10:10:3, v/v/v). An aliquot of each extraction was subjected to scintillation counting using 10 ml EcoScint and analysed by TLC using silica gel plates (5554 silica gel 60F₂₅₄, Merck) developed in CHCl₃/CH₃OH/H₂O (60:16:2, v/v/v). TLCs were exposed to X-ray film (Kodak X-Omat) for 2 days to visualise radiolabelled lipids by autoradiography.

6.3.3. Cell wall bound lipid extraction

Cells were grown as described, harvested, washed and freeze-dried. Cells (100 mg) were extracted by two consecutive extractions with 2 ml of CHCl₃/CH₃OH/H₂O (10:10:3, v/v/v) for 3 hr at 50°C. The bound lipids from the de-lipidated extracts were released by the addition of 2 ml of 5% aqueous solution of tetra-butyl ammonium hydroxide (TBAH),

followed by overnight incubation at 100 °C. After cooling, water (2 ml), CH₂Cl₂ (4 ml) and CH₃I (500 µl) were added and mixed thoroughly for 30 min. The lower organic phase was recovered following centrifugation and washed three times with water (4 ml), dried and resuspended in diethyl ether (4 ml). After centrifugation, the clear supernatant was again dried and resuspended in CH₂Cl₂ (100 µl). An aliquot (10 µl) from each strain was subjected to TLC, using silica gel plates (5554 silica gel 60F₂₅₄, Merck), developed in petroleum ether/acetone (95:5, v/v) and charred using 5% MPA in ethanol at 100 °C to reveal CMAMES/MAMES and compared to known standards (Gande *et al.*, 2004).

6.3.4. Analysis of AftB muteins

Recombinant *C. glutamicum* strains deleted of the chromosomal Cg-*aftB* copy, but carrying either pMSX, pMSX-Mt-*aftB*, pMSX-Mt-*aftB*-D29A or pMSX-Mt-*aftB*-D30A were each grown in LB up to an OD of 4. Cells were harvested by centrifugation, washed and resuspended in 30 ml of 50 mM TrisHCl pH 7.4 buffer, containing 200 mM NaCl and 50 mM imidazole, and disrupted by probe sonication. Centrifugation at 27,000 x g resulted in a clear supernatant, which was applied to a 1 ml HiTrap™ Chelating HP column (GE Healthcare) using an ÅTKA chromatography system. The column was initially washed with 10 ml of the aforementioned buffer and bound proteins subsequently eluted with 2 ml of the same buffer, but containing 500 mM imidazole. Eluted proteins were precipitated, dried, and resuspended in 10 µl loading buffer and SDS-PAGE carried out on a 10% polyacrylamide gel, which was subsequently stained using 0.05% Coomassie-G250 in 10% acetic acid and 25% isopropanol. Bands of interest were excised and subjected to in-gel digestion with trypsin before peptide mass fingerprinting. Peptides were extracted by sequential addition of water (12 µl) and 0.1% (v/v) trifluoroacetic acid (TFA) in 30% (v/v) acetonitrile (10 µl), and

analyzed manually, using an Applied Biosystems Voyager STR MALDI-TOF mass spectrometer.

6.4. Extraction and Purifications of lipoglycans

Lipoglycans were extracted from delipidated cells as described previously (Nigou *et al.*, 1997; Mishra *et al.*, 2008). Dried cells were resuspended in water, disrupted by sonication (MSE Soniprep 150, 12 micron amplitude, 60s ON, 90s OFF for 10 cycles, on ice) and an equal volume of ethanol was added and the mixture heated under reflux, followed by centrifugation and recovery of the supernatant. This extraction process was repeated five times and the combined supernatants, containing lipoglycans, neutral glycans and proteins were dried, followed by hot-phenol-H₂O treatment. The aqueous phase was dialysed against water, performed using a low molecular weight cut off dialysis tubing, (Spectra/Por membrane 6, MWCO 3,500 kDA from Spectrum Labs). The retentate was dried, resuspended in water and digested with α -amylase, DNase, RNase, chymotrypsin and trypsin, and dialysed once again to remove residual impurities and enzymes.

The crude lipoglycan extract was dried and resuspended in buffer A (50 mM ammonium acetate and 15% propan-1-ol) and subjected to Octyl Sepharose CL- 4B HIC (2.5 cm x 50 cm) (Leopold & Fischer, 1993). The column was washed initially with 4 column volumes of buffer A to ensure removal of neutral glycans followed by buffer B (50 mM ammonium acetate and 50% propan-1-ol). The eluent was collected and concentrated to approximately 1 ml and precipitated using 5 ml of ethanol. The sample was dried using a Savant Speedvac and then resuspended in buffer C (0.2 M NaCl, 0.25% sodium deoxycholate (w/v), 1 mM EDTA and 10 mM Tris-HCl, pH 8) to a final concentration of 200 mg/ml.

The sample was gently mixed and left to incubate for 48 h at room temperature. The sample was then loaded onto a 200 ml Sephacryl S-200 column previously equilibrated with buffer C. The sample was eluted with 400 ml of buffer C at a flow rate of 3 ml/h, collecting 1.5 ml fractions.

The fractions were monitored by SDS-PAGE using Pro-Q emerald glycoprotein stain and individual fractions pooled and dialyzed extensively against buffer D (10 mM Tris-HCl, pH 8, 0.2 M NaCl, 1 mM EDTA) for 72 h with frequent changes of buffer. The samples were further dialyzed against deionized water for 48 h with frequent changes of water, lyophilized and stored at - 20°C.

6.4.1. NMR spectroscopic analysis of WT-LAM and AftC-LAM.

NMR spectra of LAM samples were recorded on a Bruker DMX-500 equipped, with a double resonance (1H/X)-BBi z-gradient probe head. All samples were exchanged in D₂O (D, 99.97% from Euriso-top, Saint-Aubin, France), with intermediate lyophilization, and then dissolved in 0.5 ml D₂O and analyzed at 313K. The ¹H and ¹³C NMR chemical shifts were referenced relative to internal acetone at 2.225 and 34.00 ppm, respectively. All the details concerning NMR sequences used and experimental procedures were described previously (Gilleron *et al.*, 1999; Gilleron *et al.*, 2000).

6.4.2. SDS PAGE

The method used in this study was the discontinuous gel method using a Hoefer “mighty small” SE200 vertical slab gel system. Resolving gels of either 12 % or 15% acrylamide (w/v) and a stacking gel of 6 % (w/v) acrylamide were prepared and cast in the apparatus according to the manufacturer’s specifications and run at 300 mV and 20 mA/gel until completion. Lipoglycan samples (10 µg) were analysed on 15% polyacrylamide gels and

visualised using Pro-Q Emerald Glycoprotein stain (Invitrogen) according to the manufacturer's protocol. Protein samples (usually 10–20 µg) were run on 12% polyacrylamide gels and visualised by immersing gels in 20 ml Coomassie brilliant blue R-250 (CBB) stain (5 % glacial acetic acid, 0.0025 % CBB (w/v), 50 % methanol) and left for 3-4 hr on a rotating platform. Excess stain was removed by rinsing in destaining solution (10% glacial acetic acid in 40% methanol).

6.5. Cell free [14C]-labeling assays

6.5.1. Preparation of *C. glutamicum* and *M. smegmatis* membranes

Pelleted cells, wet weight 5 g were resuspended in 50 mM MOPS (pH 7.9), 5 mM β-mercaptoethanol and 10 mM MgCl₂. Resuspended cells were sonicated (MSE Soniprep 150, 12 micron amplitude, 60s ON, 90s OFF for 10 cycles, on ice), centrifuged at 23000 x g for 20 mins at 4°C, and the resulting supernatant re-centrifuged at 100,000 x g for 90 mins at 4°C to isolate cell membranes which were collected and concentrated to a protein concentration of 15-20 mg/ml in 50 mM MOPS (pH 7.9), 10 mM MgSO₄, 5 mM β-mercaptoethanol (Chapter 6.5.3).

6.5.2. Preparation of *C. glutamicum* and *M. smegmatis* cell wall material

Cells (10 g) were resuspended in 35 ml of 50 mM MOPS (pH 7.9), 10 mM MgSO₄, 5 mM β-mercaptoethanol and subject to probe sonication (MSE Soniprep 150, 12 micron amplitude, 60s ON, 90s OFF for 10 cycles, on ice). The cell slurry was centrifuged at 27, 000 x g for 20 min at 4 °C, the pellet was recovered and the resulting supernatant further centrifuged at 100,000 x g for 90 min at 4 °C. The pellet from the 27, 000 x g spin was resuspended in 24 ml 50 mM MOPS (pH 7.9), 10 mM MgSO₄, 5 mM β-mercaptoethanol and 32 ml of Percoll (Sigma-Aldrich), mixed thoroughly and centrifuged at 27, 000 x g for 60 min at 4 °C. The

upper band (corresponding to *C. glutamicum* cell wall “P60” material) was removed, washed with 50 mM MOPS (pH 7.9), 10 mM MgSO₄, 5 mM β-mercaptoethanol with further centrifugation to remove Percoll and the final cell wall fraction resuspended in 50 mM MOPS (pH 7.9), 10 mM MgSO₄, 5 mM β-mercaptoethanol to a final protein concentration of 8 – 10 mg/ml (Chapter 6.5.3).

6.5.3. Estimation of protein concentration

The concentration of total protein present in cell wall material and membranes were measured using the Bicinchoninic protein assay (BCA) kit (Pierce). The assay was performed according to the manufacturer’s protocol. The assay was calibrated over the range 2.5 – 5.0 µg/ml by using a range of standards derived from a 2 mg/ml stock solution of bovine serum albumin (BSA) (Pierce). Samples, standards and blanks were assayed in triplicate. Samples were also diluted 1 in 5 to ensure a reading was obtained within the limits of the standard curve. The assay was incubated at 37 °C for 30 min and the colorimetric change was measured at 562 nm.

6.5.4. Arabinofuranosyltransferase assays

6.5.4.1. Arabinofuranosyltransferase activity with membrane preparations of *C. glutamicum*, *C. glutamicum*Δ*aftB*, and *C. glutamicum*Δ*aftB* pMSX-Mt-*aftB*

Membranes were prepared as described previously (Alderwick *et al.*, 2006; Lee *et al.*, 1997) and resuspended in 50 mM MOPS (pH 7.9), containing 5 mM β-mercaptoethanol and 10 mM MgCl₂ (buffer A) to a final concentration of 15-10 mg/ml. The neoglycolipid acceptor α-**D**-Araf-(1→5)-α-**D**-Araf-O-C₈ (stored in C₂H₅OH) and DP[¹⁴C]A (Lee *et al.*, 1995; Lee *et al.*, 1998) (stored in CHCl₃/CH₃OH, 2:1, v/v) were aliquoted into a 1.5 ml Eppendorf tube to a final concentration of 2 mM and 200,000 cpm (90 µM), respectively, and dried under nitrogen. The basic arabinofuranosyltransferase assay was carried out as described previously

(Lee *et al.*, 1997) with modifications. IgePalTM (Sigma-Aldrich) was added (0.1%, v/v) with the appropriate amount of buffer A (final volume 80 μ l). Tubes were sonicated for 15 min to resuspend lipid linked substrates and then mixed with the remaining assay components, which included membrane protein (1 mg) from either *C. glutamicum*, *C. glutamicum* Δ *aftB* or *C. glutamicum* Δ *aftB* pMSX-Mt-*aftB*, 1 mM ATP, 1 mM NADP and in some cases EMB (0-1 mg/ml). Assays were incubated for 1 h at 37 °C and quenched by the addition of 533 μ l CHCl₃/CH₃OH (1:1, v/v). After mixing and centrifugation at 27,000 x g for 15 min at 4 °C, the supernatant was removed and dried under nitrogen. The residue was then resuspended in 700 μ l of CH₃CH₂OH/H₂O (1:1, v/v) and loaded onto a 1 ml SepPak strong anion exchange cartridge (Supelco), pre-equilibrated with CH₃CH₂OH/H₂O (1:1, v/v). The column was washed with 2 ml CH₃CH₂OH and the eluate collected, dried and partitioned between the two phases, arising from a mixture of *n*-butanol (3 ml) and water (3 ml). The resulting organic phase was recovered following centrifugation at 3,500 x g and the aqueous phase again extracted twice with 3 ml of water-saturated *n*-butanol. The pooled extracts were back-washed twice with *n*-butanol-saturated water (3 ml). The *n*-butanol fraction was dried and resuspended in 200 μ l *n*-butanol. The extracted radiolabeled material was quantified by liquid scintillation counting using 10 % of the labelled material and 5 ml of EcoScintA (National Diagnostics, Atlanta). The incorporation of [¹⁴C]Araf was determined by subtracting counts present in control assays (incubations in the absence of acceptor). The remaining labeled material was subjected to TLC using silica gel plates (5735 silica gel 60F₂₅₄, Merck) developed in CHCl₃:CH₂OH:H₂O:NH₄OH (65:25:3.6:0.5, v/v/v/v). TLC-autoradiograms were obtained by exposing TLCs to Kodak X-Omat film for 3 days.

6.5.4.2. Analysis of arabinofuranosyltransferase reaction products prepared from *C. glutamicum* and *C. glutamicum* Δ *aftB* membranes

Large-scale reaction mixtures containing cold DPA (200 μ g, 0.75 mM) (Lee *et al.*, 1997) and 50 mM of the acceptor α -**D**-Araf-(1 \rightarrow 5)- α -**D**-Araf-O-C₈ were mixed and given an initial incubation at 37 °C with membranes prepared from either *C. glutamicum* (EMB also added to reaction mixtures at a concentration of 100 μ g/ml) or *C. glutamicum* Δ *aftB* for 1 h. The assays were replenished with fresh membranes (1 mg) and re-incubated for 1 h at 37 °C with the entire process repeated thrice. Products were extracted from reaction mixtures by *n*-butanol/water phase separation as described earlier to extract products. Products were applied to preparative TLC plates, developed in CHCl₃:CH₃OH:H₂O:NH₄OH (65:25:3.6:0.5, v/v/v/v) and sprayed with 0.01% 1,6-diphenylhexatriene in petroleum-ether:acetone (9:1, v/v), and the products localized under long-wave (366 nm) UV light (Lee *et al.*, 1997). The plate was then re-developed in toluene to remove the reagent and the bands recovered from the plates by extraction with *n*-butanol. The butanol phases were washed with water saturated with *n*-butanol and the dried products subjected to ¹H-NMR, ES-MS and GC/MS as previously described (Lee *et al.*, 1997).

6.5.4.3. Arabinofuranosyltransferase activity with membrane preparations of *M. smegmatis*, *M. smegmatis* pMV261-Mt-*aftC*, *M. smegmatis* Δ *aftC* and *M. smegmatis* Δ *aftC* pMV261-Mt-*aftC*

Membranes were prepared as described previously (Lee *et al.*, 1997; Alderwick *et al.*, 2006a) and re-suspended in 50 mM MOPS (pH 7.9), containing 5 mM β -mercaptoethanol and 10mM MgCl₂ (buffer A) to a final concentration of 15–10 mg/ml. The neoglycolipid acceptors used in this study were α -**D**-Araf-(1 \rightarrow 5)- α -**D**-Araf-(1 \rightarrow 5)- α -**D**-Araf-(1 \rightarrow 5)- α -**D**-Araf-(1 \rightarrow 5)- α -**D**-Araf-O-(CH₂)₈NH₂ (Ara₅,) and α -**D**-Araf-(1 \rightarrow 5)- α -**D**-Araf-O-(CH₂)₇CH₃ (Ara₂) (Lee *et al.*, 1995; 1998). The acceptors (either Ara₂ or Ara₅) and DP[¹⁴C]A (Lee *et al.*, 1995; 1998) (stored in CHCl₃/CH₃OH, 2:1, v/v) were aliquoted into 1.5 ml Eppendorf tubes

to a final concentration of 2mM and 200 000 cpm (90 mM), respectively, and dried under nitrogen. The arabinofuranosyltransferase assay was carried out as described previously (Lee *et al.*, 1997) with modifications. IgePal™ (Sigma-Aldrich) was added (0.1%, v/v) with the appropriate amount of buffer A (final volume 80 ml). Tubes were sonicated for 15 min to re-suspend lipid linked substrates and then mixed with the remaining assay components, which included membrane protein from either *M. smegmatis*, *M. smegmatis*Δ*aftC*, *M. smegmatis* pMV261-Mt-*aftC* and *M. smegmatis*Δ*aftC* pMV261-Mt-*aftC*.

M. smegmatis pMV261-Mt-*aftC* *M. smegmatis*Δ*aftC* or *M. smegmatis*Δ*aftC* pMV261-Mt-*aftC* (1 mg), 1 mM ATP, 1 mM NADP and in some cases EMB (0–1 mg ml⁻¹). Assays were incubated for 1 h at 37°C and quenched by the addition of 533 ml CHCl₃/CH₃OH (1:1, v/v). After mixing and centrifugation at 27 000 g for 15 min at 4°C, the supernatant was removed and dried under nitrogen. The residue was then re-suspended in 700ml of CH₃CH₂OH/H₂O (1:1, v/v) and loaded onto a 1 ml SepPak strong anion exchange cartridge (Supelco), pre-equilibrated with CH₃CH₂OH/H₂O (1:1, v/v). The column was washed with 2 ml CH₃CH₂OH and the eluate collected, dried and partitioned between the two phases arising from a mixture of *n*-butanol (3 ml) and water (3 ml). The resulting organic phase was recovered, following centrifugation at 3500 g, and the aqueous phase again extracted twice with 3 ml of water- saturated *n*-butanol. The pooled extracts were back-washed twice with *n*-butanol-saturated water (3 ml). The *n*-butanol fraction was dried and re-suspended in 200 ml butanol. The extracted radiolabelled material was quantified by liquid scintillation counting, using 10% of the labelled material and 5 ml of EcoScintA (National Diagnostics, Atlanta). The incorporation of [¹⁴C]Araf was determined by subtracting counts present in control assays (incubations in the absence of acceptor). The remaining labelled material was subjected to thin-layer chromatography (TLC) using either isopropanol/ acetic acid/water (8:1:1, v/v/v) for the assays utilizing the Ara₅ acceptor or CHCl₃/CH₂OH/H₂O/NH₄OH

(65:25:3.6:0.5, v/v/v/v) in the case of the Ara₅ acceptor on aluminum- backed Silica Gel 60 F254 plates (Merck, Darmstadt, Germany). Autoradiograms were obtained by exposing TLCs to X-ray film (Kodak X-Omat) for 3 days.

6.5.4.4. Characterization of a(1→3)-arabinofuranosyltransferase activity with membranes prepared from *M. smegmatis*, *M. smegmatis*Δ*aftC* and *M. smegmatis*Δ*aftC* pMV261-Mt-*aftC*

Large-scale reaction mixtures containing cold DPA (200 mg, 0.75 mM) (Lee *et al.*, 1997) and 50 mM of the acceptor Ara₅ were mixed and given an initial incubation at 37°C with membranes prepared from either *M. smegmatis*, *M. smegmatis*Δ*aftC* or *M. smegmatis*Δ*aftC* pMV261-Mt-*aftC* for 1 h. The assays were replenished with fresh membranes (1 mg) and re-incubated for 1 h at 37°C with the entire process repeated thrice. Products were extracted from reaction mixtures by *n*-butanol/water phase separation as described earlier to extract products. Products were applied to preparative TLC plates, developed in isopropanol/acetic acid/water (8:1:1, v/v/v) and sprayed with 0.01% 1,6- diphenylhexatriene in petroleum-ether/acetone (9:1, v/v), and the products localised under long-wave (366 nm) UV light (Lee *et al.*, 1997). The plate was then re-developed in toluene to remove the reagent and the bands recovered from the plates by extraction with *n*-butanol. The *n*-butanol phases were washed with water saturated with *n*-butanol and the dried products subjected to GC (Sasaki *et al.*, 2005) and GC/MS as described (Lee *et al.*, 1997; Alderwick *et al.*, 2006a).

6.5.4.5. [¹⁴C]-carbohydrate labeling of *C. glutamicum* and *C. glutamicum*Δ*rptA* glycolipids.

Cells (10 g) from *C. glutamicum* and *C. glutamicum*Δ*rptA* were resuspended in 35 mL of 50 mM MOPS (pH 7.9), 10 mM MgSO₄, 5 mM β-mercaptoethanol (buffer A) and subjected to probe sonication for 60 s on and 90 s off (repeated for a total of 10 cycles). The cell slurry was centrifuged at 27,000 × *g* for 20 min at 4°C; the pellet was recovered and the resulting

supernatant further centrifuged at $100,000 \times g$ for 90 min at 4°C. Purified *C. glutamicum* membranes were recovered and resuspended in buffer A to a final concentration of 15–20 mg/mL. The pellet from the $27,000 \times g$ spin was resuspended in 24 mL of buffer A and 32 mL of Percoll, mixed thoroughly, and centrifuged at 27,000g for 60 min at 4°C. The upper band (corresponding to *C. glutamicum* cell wall “P60” material) was removed, washed with buffer A with further centrifugation to remove Percoll, and the final cell wall fraction resuspended in buffer A to a final concentration of 8–10 mg/mL.

The initial, standard reaction to measure incorporation of [^{14}C]GlcNAc from UDP-[^{14}C]GlcNAc, [^{14}C]Rha from dTDP-[^{14}C]Rha, [^{14}C]Gal from UDP-[^{14}C]Gal, and [^{14}C]Ara from p[^{14}C]Rpp were as follows. Decaprenol phosphate (50 μg , 5 mg/mL stored in ethanol, 10 μL) was dried under nitrogen and was resuspended by the addition of 50 μL of a 1% IgePal CA-630 (Sigma Aldrich) solution in buffer A and sonicated. The basic assay mix consisted of 2 mg of membranes and 0.5 mg cell wall “P60” from either *C. glutamicum* or *C. glutamicum* ΔrptA , 1 mM ATP, and 1 mM NADP in a final volume of 160 μL of buffer A and initiated by the addition of either 100,000 cpm UDP-[^{14}C]GlcNAc (ammonium salt; Amersham, Bucks, United Kingdom, specific activity 214 mCi/mmol), 200,000 cpm dTDP-[^{14}C]Rha (enzymatically synthesized as described in Mikusova *et al.* (1996) specific activity 300 $\mu\text{Ci}/\mu\text{mol}$ kindly donated by Prof Michael McNeil, Colorado State University), UDP-[^{14}C]Gal (ammonium salt; Amersham, Bucks, United Kingdom, specific activity 257 mCi/mmol) and 50,000cpm p[^{14}C]Rpp (enzymatically synthesized as described in section 6.6.2, specific activity 250 $\mu\text{Ci}/\mu\text{mol}$). Reactions were incubated at 37°C for 2 hr and quenched by the addition of $\text{CHCl}_3/\text{CH}_3\text{OH}$ (1066 μl , 1:1, v/v) and mixed at room temperature for 30 min. The samples were then centrifuged at $27,000 \times g$ at room temperature for 20 min and the supernatant was removed from the pelleted material and H_2O

(230 μ l) and CHCl_3 (537 μ l) added to the previously extracted supernatant, mixed at room temperature for 30 min and then centrifuged at $5,000 \times g$. The lower organic fraction was recovered and washed twice with $\text{CHCl}_3/\text{CH}_3\text{OH}/\text{H}_2\text{O}$ (613 μ l, 3:47:48, v/v/v). After centrifugation at $5,000 \times g$ for 10 min, the lower organic fraction was recovered and dried under compressed nitrogen. The resulting extract was resuspended in $\text{CHCl}_3/\text{CH}_3\text{OH}$ (100 μ l, 2:1, v/v). An aliquot (10 μ l) from each assay was subjected to scintillation counting and the remainder of the sample analyzed by TLC using silica gel plates (5735 silica gel 60F₂₅₄, Merck), developed in $\text{CHCl}_3/\text{CH}_3\text{OH}/\text{NH}_4\text{OH}/\text{H}_2\text{O}$ (65:25:0.5:3.6, v/v/v/v) and visualized by autoradiography by exposure of Kodak X-Omat AR film to the TLC plates to reveal incorporation of either [^{14}C]GlcNAc, [^{14}C]Rha, [^{14}C]Gal or [^{14}C]Ara into solvent extractable lipids.

6.5.4.5.1. Preparation of p[^{14}C]Rpp

Radiolabelled p[^{14}C]Rpp was prepared as described (Hove-Jensen, 1985), but with modifications. 200 μCi [^{14}C]-**D**-glucose (0.7 μmoles , Amersham) was dried under compressed N_2 and resuspended in 400 μ l of 50 mM HEPES (pH 7.6), 5 mM MgCl_2 and 0.5 mM MnCl_2 . ATP (1 mM) and β -NADP (4 mM) was added to the reaction mixture before the addition of 5 units of hexokinase powder (Sigma Aldrich, UK) and the reaction mixture was incubated at room temperature for 5 min. Glucose-6-phosphate dehydrogenase (5 units, Sigma Aldrich, UK) was added and incubated for 5 min at room temperature before the addition of 6-phosphogluconate dehydrogenase (5 units, Sigma Aldrich, UK) and further incubated at 37 $^\circ\text{C}$ for 5 min. Phosphoriboseisomerase (5 units, Sigma Aldrich, UK) was then added and the reaction mixture incubated at 30 $^\circ\text{C}$ for 5 min. PRPP synthetase was prepared as described in Huang *et al.* (2005).

6.5.4.6. Chemical identification of decaprenol-1-monophosphate-rhamnopyranose.

Membranes from *C. glutamicum* or *C. glutamicum* Δ rptA were assayed as described above, but with or without the addition of 50 μ g/mL tunicamycin. Decaprenylmonophosphate (50 μ g, 5 mg/ml stored in $\text{CHCl}_3/\text{CH}_3\text{OH}$ (2:1, v/v)), was dried under nitrogen and resuspended by the addition of 107 μ l of a 1% IgePal CA-630 (Sigma Aldrich) solution in buffer A and sonicated. The basic assay mix consisted of 2 mg of membranes, 0.5 mg cell wall “P60”, 1 mM ATP, 1 mM NADP in a final volume of 160 μ l and initiated by the addition of 5 mM of dTDP-Rha or 200,000 cpm of dTDP-[^{14}C]Rha chemically synthesized as previously described (enzymatically synthesized as described in Mikusova *et al.*, (1996) specific activity 300 $\mu\text{Ci}/\mu\text{mol}$ kindly donated by Prof Michael McNeil, Colorado State University) and incubated at 37 °C for 1 h. Assays performed using dTDP-[^{14}C]Rha were processed as described above, whereas assays performed using cold dTDP-Rha were replenished by the addition of a further 2 mg of membranes and 0.5 mg of cell wall “P60” with further incubation at 37°C for 1 h. This process was repeated for a total of three additions with a final assay volume of 250 μL . Assays were quenched by the addition of $\text{CHCl}_3/\text{CH}_3\text{OH}$ (3330 μl , 1:1, v/v), 1.6 M NaOH (250 μl) and mixed at room temperature for 30 min. The samples were then centrifuged at $27,000 \times g$ at room temperature for 30 min and the supernatant was removed from the pelleted material. H_2O (720 μl) and CHCl_3 (1678 μl) was added to the previously extracted supernatant, mixed at room temperature for 30 min and then centrifuged at $5,000 \times g$. The lower organic fraction was recovered and washed twice with 1.92 ml of $\text{CHCl}_3/\text{CH}_3\text{OH}/\text{H}_2\text{O}$ (1.92 ml, 3:47:48, v/v/v). After centrifugation at $5,000 \times g$ for 10 min, the lower organic fraction was recovered and dried under nitrogen. The resulting extract was resuspended in $\text{CHCl}_3/\text{CH}_3\text{OH}$ (100 μl , 2:1, v/v) and analyzed by electrospray mass spectrometry (ES-MS) in the negative mode on a Micromass LCT mass spectrometer.

6.5.5. Treatment of *M. smegmatis* and *M. smegmatis* Δ *aftC* with sub-inhibitory concentrations of EMB and subsequent lipoglycan analysis.

M. smegmatis and *M. smegmatis* Δ *aftC* were grown in 100 mL TSB as described above. Once an O.D₆₀₀ of 0.4 was reached, EMB was added to cultures of *M. smegmatis* Δ *aftC* at a concentration of 0 and 0.5 and 1.0 μ g ml⁻¹. After a further 2 h incubation, 66 μ Ci of [U-¹⁴C]-D-glucose (specific activity 300 mCi/mmol, ARC radiochemicals) was added to all cultures and incubated for a further 48 h. Cells were harvested by centrifugation and the lipoglycans were extracted and analysed by SDS-PAGE, as described above. Further analysis on the [¹⁴C]-incorporated sugars was performed as described. Equal counts of extracted [¹⁴C]-labelled lipoglycans (50,000 cpm) from each growing culture were then hydrolyzed by using 100 μ L of 2 M TFA for 1 h at 120°C, dried, resuspended in 2 mL of CHCl₃/H₂O (1:1, v/v), and the upper aqueous phase recovered and dried. The residual radiolabeled sugars were resuspended in 20 μ L of H₂O and subjected to TLC using cellulose-coated aluminum plates (HPTLC-Aluminum Cellulose, Merck) and developed three times in formic acid/H₂O/tert-butanol/methyl ethyl ketone (3:3:8:6, v/v/v/v). Sugars were visualized by TLC exposure to X-ray film (Kodak X-Omat) and quantified by densitometry.

6.5.6. Treatment of WT-LAM, AftC-LAM and Pam₃CSK₄ with H₂O₂

All immunomodulatory analyses were conducted by Jerome Nigou at the Department of Medical Microbiology and Infection Control, Amsterdam, Netherlands. WT-LAM, AftC-LAM and Pam₃CSK₄ (Invivogen) were treated with H₂O₂ as described (Morr *et al.*, 2002; Zahringer *et al.*, 2008). WT-LAM and AftC-LAM (0.2 mg ml⁻¹) and Pam₃CysK₄ (1 μ g ml⁻¹) were incubated in the dark at 4°C in the absence or presence of 1% H₂O₂. After incubation for various periods of time, the samples were snap-frozen, using liquid nitrogen, and lyophilized.

6.5.7. Cell culture

The human myeloid THP-1 monocyte/macrophage human cell line was maintained in continuous culture with RPMI 1640 medium (Invitrogen), 10% fetal calf serum (Lonza) in an atmosphere of 5% CO₂ at 37 °C, as non-adherent cells. Purified native or modified lipoglycans as well as the other stimuli were added in duplicate or triplicate to monocyte/macrophage cells and then incubated for 20 h at 37 °C. HEK293 cells transfected with TLR2 (Mambula *et al.*, 2002) were kept in DMEM (Invitrogen) containing 10% FCS, 100 units ml⁻¹ penicillin, 100 µg ml⁻¹ streptomycin, 0.5 mg ml⁻¹ GW418, 2 mM L-glutamine, and 110 mg L⁻¹ pyruvate.

6.5.8. Cell stimulation assays

Cells (HEK293 cells were first released by trypsinisation) were washed with and resuspended in culture medium at 1.25x10⁶ cells ml⁻¹. 80 µl (1x10⁵ cells) was transferred to a 96-well U-bottom plate (Greiner) and left for 2 h, followed by incubations in triplicate with H₂O₂-treated WT-LAM, AftC-LAM, Pam₃CSK₄ or with LPS (from *Salmonella enterica* serovar Abortusequi (Sigma-Aldrich L5886)) in a final stimulation volume of 100 µl. Unstimulated cells served as controls. Culture supernatants were harvested after 24 h by centrifugation and stored at -80°C for cytokine measurements using enzyme-linked immunosorbent assay (ELISA). Human IL-8 and TNF-α concentrations were determined in ELISA according to the manufacturer's instructions (Invitrogen and R&D systems, respectively).

6.5.9. DC-SIGN-Fc ELISA

WT-LAM and AftC-LAM (1 µg ml⁻¹ in saline (100 µL) were coated on NUNC Maxisorp plates (Roskilde) overnight at 4°C. Plates were blocked with 1% bovine serum albumine (BSA) and serially diluted DC-SIGN-Fc (van Die I *et al.*, 2003) was added for 2 h at room

temperature. Then the plates were washed four times with Tris-buffered saline with 1 mM MgCl_2 , 2 mM CaCl_2 , 0.05% Tween-80 (TSMT) and incubated with goat-anti-human IgG antibody conjugated with peroxidase (Jackson ImmunoResearch). Plates were washed eight times with TSMT and developed using *o*-phenylenediamine dihydrochloride and absorption measured at 490 nm.

Chapter 7

7. References

- Adam, A., Petit, J. F., Wietzerbin-Falszpan, J., Sinay, P., Thomas, D. W. & Lederer, E. (1969).** L'acide N-glycolylmuramique, constituant des parois de *Mycobacterium smegmatis*: Identification par spectrometrie de masse. *FEBS Lett* **4**, 87-92.
- Akira, S. & Takeda, K. (2004).** Toll-like receptor signaling. *Nat. Rev. Immunol.* **4**, 499-511.
- Alcaide, F., Pfyffer, G. E. & Telenti, A. (1997).** Role of embB in natural and acquired resistance to ethambutol in mycobacteria. *Antimicrobial agents and chemotherapy* **41**, 2270-2273.
- Alderwick, L. J., Radmacher, E., Seidel, M. & other authors (2005).** Deletion of Cg-emb in *corynebacterineae* leads to a novel truncated cell wall arabinogalactan, whereas inactivation of Cg-ubiA results in an arabinan-deficient mutant with a cell wall galactan core. *J Biol Chem* **280**, 32362-32371.
- Alderwick, L. J., Dover, L. G., Seidel, M., Gande, R., Sahm, H., Eggeling, L. & Besra, G. S. (2006a).** Arabinan-deficient mutants of *Corynebacterium glutamicum* and the consequent flux in decaprenylmonophosphoryl-D-arabinose metabolism. *Glycobiology* **16**, 1073-1081.
- Alderwick, L. J., Seidel, M., Sahm, H., Besra, G. S. & Eggeling, L. (2006b).** Identification of a novel Arabinofuranosyltransferase (AftA) involved in cell wall arabinan biosynthesis in *Mycobacterium tuberculosis*. *J Biol Chem* **281**, 15653-15661.
- Alderwick, L. J., Birch, H. L., Mishra, A. K., Eggeling, L. & Besra, G. S. (2007).** Structure, function and biosynthesis of the *Mycobacterium tuberculosis* cell wall: arabinogalactan and lipoarabinomannan assembly with a view to discovering new drug targets. *Biochem Soc Trans* **35**, 1325-1328.
- Alderwick L.J., Dover L.G., Veerapen N., Gurcha S.S., Kremer L., Roper D.L., Pathak A.K., Reynolds R.C., Besra G.S. (2008).** Expression, purification and characterization of soluble GlfT and the identification of a novel galactofuranosyl transferase Rv3782 involved in priming GlfT-mediated galactan polymerization in *Mycobacterium tuberculosis*. *Protein Expr Purif.* **58**, 332-41.
- Alderwick, L. J., Lloyd, G. S., Lloyd, A. J., Lovering, A. L., Eggeling, L. & Besra, G. S. (2010).** Biochemical characterization of the *Mycobacterium tuberculosis* phosphoribosyl-1-pyrophosphate synthetase. *Glycobiology* **21**, 410-425.
- Amar, C. & Vilkas, E. (1973).** (Isolation of arabinose phosphate from the walls of *Mycobacterium tuberculosis* H 37 Ra). *C R Acad Sci Hebd Seances Acad Sci D* **277**, 1949-1951.
- Amer, A. O. & Valvano, M. A. (2002).** Conserved aspartic acids are essential for the enzymic activity of the WecA protein initiating the biosynthesis of O-specific

lipopolysaccharide and enterobacterial common antigen in *Escherichia coli*. *Microbiology (Reading, England)* **148**, 571-582.

Amin, A. G., Goude, R., Shi, L., Zhang, J., Chatterjee, D., & Parish, T. (2008). EmbA is an essential arabinosyltransferase in *Mycobacterium tuberculosis*. *Microbiology* **154**, 240-248.

Appelmek, B. J., den Dunnen, J., Driessen, N. N. & other authors (2008). The mannose cap of mycobacterial lipoarabinomannan does not dominate the *Mycobacterium*-host interaction. *Cell Microbiol* **10**, 930-944.

Armstrong, J. A. & Hart, P. D. (1971). Response of cultured macrophages to *Mycobacterium tuberculosis*, with observations on fusion of lysosomes with phagosomes. *The Journal of experimental medicine* **134**, 713-740.

Asselineau, C., Asselineau, J., Lan  lle, G. & Lan  lle, M. A. (2002). The biosynthesis of mycolic acids by mycobacteria: current and alternative hypotheses. *Prog Lipid Res* **41**, 501-523.

Asselineau, J. & Lederer, E. (1950). Structure of the mycolic acids of mycobacteria. *Nature* **166**, 782-783.

Aziz M.A., Wright A., Laszlo A., De Muynck A., Portaels F., & Van Deun A., (2006). Epidemiology of antituberculosis drug resistance (the global project on anti-tuberculosis drug resistance surveillance): an updated analysis. *Lancet* **368**, 2142-54

Azuma, I., Yamamura, Y. & Fukushi, K. (1968). Fractionation of mycobacterial cell wall. Isolation of arabinose mycolate and arabinogalactan from cell wall fraction of *Mycobacterium tuberculosis* strain Aoyama B. *J Bacteriol* **96**, 1885-1887.

Babaoglu, K., Page, M. A., Jones, V. C., McNeil, M. R., Dong, C., Naismith, J. H. & Lee, R. E. (2003). Novel inhibitors of an emerging target in *Mycobacterium tuberculosis*; substituted thiazolidinones as inhibitors of dTDP-rhamnose synthesis. *Bioorg Med Chem Lett* **13**, 3227-3230.

Baddiley, J. 1972. Teichoic acids in cell walls and membranes of bacteria. *Essays Biochem.* **8**, 35-77.

Ballou, C. E., Vilkas, E. & Lederer, E. (1963). Structural studies on the myo-inositol phospholipids of *Mycobacterium tuberculosis* (var. bovis, strain BCG). *J Biol Chem* **238**, 69-76.

Ballou, C. E. & Lee, Y. C. (1964). The structure of a myo-inositol mannoside from *Mycobacterium tuberculosis* glycolipid. *Biochemistry* **3**, 682-685.

Banerjee, A., Dubnau, E., Qu  mard, A., Balasubramanian, V., Um, K. S., Wilson, T., Collins, D., de Lisle, G. & Jacobs, W. R., Jr. (1994). inhA, a gene encoding a target for isoniazid and ethionamide in *Mycobacterium tuberculosis*. *Science* **263**, 227-230.

- Banerjee, A., Sugantino, M., Sacchetti, J. C. & Jacobs, W. R., Jr. (1998).** The *mabA* gene from the *inhA* operon of *Mycobacterium tuberculosis* encodes a 3-ketoacyl reductase that fails to confer isoniazid resistance. *Microbiology* **144**, 2697-2704.
- Bardarov, S., Bardarov Jr, S., Jr., Pavelka Jr, M. S., Jr., Sambandamurthy, V., Larsen, M., Tufariello, J., Chan, J., Hatfull, G. & Jacobs Jr, W. R., Jr. (2002).** Specialized transduction: an efficient method for generating marked and unmarked targeted gene disruptions in *Mycobacterium tuberculosis*, *M. bovis* BCG and *M. smegmatis*. *Microbiology* **148**, 3007-3017.
- Belanger, A. E., Besra, G. S., Ford, M. E., Mikusova, K., Belisle, J. T., Brennan, P. J. & Inamine, J. M. (1996).** The *embAB* genes of *Mycobacterium avium* encode an arabinosyl transferase involved in cell wall arabinan biosynthesis that is the target for the antimycobacterial drug ethambutol. *Proc Natl Acad Sci U S A* **93**, 11919-11924.
- Belanger, A.E., & Inamine, J.M. (2000).** *Mycobacterium tuberculosis* lipoarabinomannan. Relationship to chemical structure. *J Immunol* **149**, 541-547.
- Belisle, J. T., Vissa, V. D., Sievert, T., Takayama, K., Brennan, P. J. & Besra, G. S. (1997).** Role of the major antigen of *Mycobacterium tuberculosis* in cell wall biogenesis. *Science* **276**, 1420-1422.
- Ben-Ali, M., Barreiro, L. B., Chabbou, A. & other authors (2007).** Promoter and neck region length variation of DC-SIGN is not associated with susceptibility to tuberculosis in Tunisian patients. *Hum. Immunol.* **68**, 908-912.
- Berg, S., Starbuck, J., Torrelles, J. B., Vissa, V. D., Crick, D. C., Chatterjee, D. & Brennan, P. J. (2005).** Roles of conserved proline and glycosyltransferase motifs of EmbC in biosynthesis of lipoarabinomannan. *J Biol Chem* **280**, 5651-5663.
- Berg, S., Kaur, D., Jackson, M. & Brennan, P. J. (2007).** The glycosyltransferases of *Mycobacterium tuberculosis* - roles in the synthesis of arabinogalactan, lipoarabinomannan, and other glycoconjugates. *Glycobiology* **17**, 35-56R.
- Besra, G. S., Khoo, K. H., McNeil, M. R., Dell, A., Morris, H. R. & Brennan, P. J. (1995).** A new interpretation of the structure of the mycolyl-arabinogalactan complex of *Mycobacterium tuberculosis* as revealed through characterization of oligoglycosylalditol fragments by fast-atom bombardment mass spectrometry and ¹H nuclear magnetic resonance spectroscopy. *Biochemistry* **34**, 4257-4266.
- Besra, G. S., Sievert, T., Lee, R. E., Slayden, R. A., Brennan, P. J. & Takayama, K. (1994).** Identification of the apparent carrier in mycolic acid synthesis. *Proc Natl Acad Sci U S A* **94**, 12735-12739.
- Besra, G. S. & Brennan, P. J. (1997).** The mycobacterial cell wall: biosynthesis of arabinogalactan and lipoarabinomannan. *Biochem Soc Trans* **25**, 845-850.
- Besra, G. S., Morehouse, C. B., Rittner, C. M., Waechter, C. J. & Brennan, P. J. (1997).** Biosynthesis of mycobacterial lipoarabinomannan. *J Biol Chem* **272**, 18460-18466.

- Bhakta, S. & Basu, J. (2002).** Overexpression, purification and biochemical characterization of a class A high-molecular-mass penicillin-binding protein (PBP), PBP1* and its soluble derivative from *Mycobacterium tuberculosis*. *The Biochemical journal* **361**, 635-639
- Bhamidi, S., Scherman, M.S., Rithner, C.D., Prenni, J.E., Chatterjee, D., Khoo, K.H., and McNeil, M.R. (2008).** The identification and location of succinyl residues and the characterization of the interior arabinan region allows for a model of the complete primary structure of *Mycobacterium tuberculosis* mycolyl arabinogalactan. *J Biol Chem* **283**, 12992–13000.
- Bhatt, A., Kremer, L., Dai, A. Z., Sacchettini, J. C. & Jacobs, W. R., Jr. (2005).** Conditional depletion of KasA, a key enzyme of mycolic acid biosynthesis, leads to mycobacterial cell lysis. *J Bacteriol* **187**, 7596-7606.
- Bhatt, A., Fujiwara, N., Bhatt, K. & other authors (2007a).** Deletion of *kasB* in *Mycobacterium tuberculosis* causes loss of acid-fastness and subclinical latent tuberculosis in immunocompetent mice. *Proc Natl Acad Sci U S A* **104**, 5157-5162.
- Bhatt, A., Molle, V., Besra, G. S., Jacobs, W. R., Jr. & Kremer, L. (2007b).** The *Mycobacterium tuberculosis* FAS-II condensing enzymes: their role in mycolic acid biosynthesis, acid-fastness, pathogenesis and in future drug development. *Mol Microbiol* **64**, 1442-1454.
- Bhatt, A., Brown, A. K., Singh, A., Minnikin, D. E. & Besra, G. S. (2008).** Loss of a mycobacterial gene encoding a reductase leads to an altered cell wall containing beta-oxo-mycolic acid analogs and accumulation of ketones. *Chem Biol* **15**, 930-939.
- Bhowruth, V., Dover, L. G. & Besra, G. S. (2007).** Tuberculosis chemotherapy: recent developments and future perspectives. *Prog Med Chem* **45**, 169-203.
- Bhowruth, V., Brown, A. K. & Besra, G. S. (2008).** Synthesis and biological evaluation of NAS-21 and NAS-91 analogues as potential inhibitors of the mycobacterial FAS-II dehydratase enzyme Rv0636. *Microbiology (Reading, England)* **154**, 1866-1875.
- Birch, H. L., Alderwick, L. J., Bhatt, A. & other authors (2008).** Biosynthesis of mycobacterial arabinogalactan: identification of a novel $\alpha(1\rightarrow3)$ arabinofuranosyltransferase. *Mol Microbiol* **69**, 1191-1206.
- Birch, H. L., Alderwick, L. J., Rittmann, D., Krumbach, K., Etterich, H., Grzegorzewicz, A., McNeil, M. R., Eggeling, L. & Besra, G. S. (2009).** Identification of a terminal rhamnopyranosyltransferase (RptA) involved in *Corynebacterium glutamicum* cell wall biosynthesis. *J Bacteriol* **191**, 4879-4887.
- Blanchard, J. S. (1996).** Molecular mechanisms of drug resistance in *Mycobacterium tuberculosis*. *Annu Rev Biochem* **65**, 215-239.
- Bloch, K. (1977).** Control mechanisms for fatty acid synthesis in *Mycobacterium smegmatis*. *Adv Enzymol Relat Areas Mol Biol* **45**, 1-84.
- Bloch, K. & Vance, D. (1977).** Control mechanisms in the synthesis of saturated fatty acids.

Annu Rev Biochem **46**, 263-298.

Boonyarattanakalin, S., Liu, X., Michieletti, M., Lepenies, B. & Seeberger, P. H. (2008). Chemical synthesis of all phosphatidylinositol mannoside (PIM) glycans from *Mycobacterium tuberculosis*. *J. Am. Chem. Soc.* **130**, 16791-16799.

Bozic, C. M., McNeil, M., Chatterjee, D., Jardine, I. & Brennan, P. J. (1988). Further novel amido sugars within the glycopeptidolipid antigens of *Mycobacterium avium*. *J Biol Chem* **263**, 14984-14991.

Brennan, P. & Ballou, C. E. (1967). Biosynthesis of mannophosphoinositides by *Mycobacterium phlei*. The family of dimannophosphoinositides. *J Biol Chem* **242**, 3046-3056.

Brennan, P. & Ballou, C. E. (1968a). Phosphatidylmyoinositol monomannoside in *Propionibacterium shermanii*. *Biochem Biophys Res Commun* **30**, 69-75.

Brennan, P. & Ballou, C. E. (1968b). Biosynthesis of mannophosphoinositides by *Mycobacterium phlei*. Enzymatic acylation of the dimannophosphoinositides. *J Biol Chem* **243**, 2975-2984.

Brennan, P. J. & Nikaido, H. (1995). The envelope of mycobacteria. *Annu Rev Biochem* **64**, 29-63.

Brennan, P. J. (2003). Structure, function, and biogenesis of the cell wall of *Mycobacterium tuberculosis*. *Tuberculosis (Edinb)* **83**, 91-97.

Brennan, P. J. & Crick, D. C. (2007). The cell-wall core of *Mycobacterium tuberculosis* in the context of drug discovery. *Curr Top Med Chem* **7**, 475-488.

Brewer, T. F. & Colditz, G. A. (1995). Relationship between bacille Calmette-Guerin (BCG) strains and the efficacy of BCG vaccine in the prevention of tuberculosis. *Clin Infect Dis* **20**, 126-135.

Briken, V., Porcelli, S. A., Besra, G. S. & Kremer, L. (2004). Mycobacterial lipoarabinomannan and related lipoglycans: from biogenesis to modulation of the immune response. *Mol Microbiol* **53**, 391-403.

Brosch, R., Gordon, S. V., Marmiesse, M. & other authors (2002). A new evolutionary scenario for the *Mycobacterium tuberculosis* complex. *Proc Natl Acad Sci U S A* **99**, 3684-3689.

Brown, A. K., Sridharan, S., Kremer, L., Lindenberg, S., Dover, L. G., Sacchettini, J. C. & Besra, G. S. (2005). Probing the mechanism of the *Mycobacterium tuberculosis* β -ketoacyl-acyl carrier protein synthase III mtFabH: factors influencing catalysis and substrate specificity. *J Biol Chem* **280**, 32539-32547.

Brown, A. K., Bhatt, A., Singh, A., Saparia, E., Evans, A. F. & Besra, G. S. (2007a). Identification of the dehydratase component of the mycobacterial mycolic acid-synthesizing fatty acid synthase-II complex. *Microbiology* **153**, 4166-4173.

- Brown, A. K., Papaemmanouil, A., Bhowruth, V., Bhatt, A., Dover, L. G. & Besra, G. S. (2007b).** Flavonoid inhibitors as novel antimycobacterial agents targeting Rv0636, a putative dehydratase enzyme involved in *Mycobacterium tuberculosis* fatty acid synthase II. *Microbiology* **153**, 3314-3322.
- Brown-Elliott B.A., Griffith D.E., Wallace R.J. Jr. (2002).** Newly described or emerging human species of nontuberculous mycobacteria. *Infect Dis Clin North Am.* **16**, 187-220.
- Calmette, A. (1928).** On preventative vaccination of the new-born against tuberculosis by B.C.G. *Br J Tuberc* **22**, 161-165.
- CDC (2006).** Emergence of *Mycobacterium tuberculosis* with extensive resistance to second-line drugs--worldwide, 2000-2004. *MMWR Morb Mortal Wkly Rep* **55**, 301-305.
- Cerdeno-Tarraga, A. M., Efstratiou, A., Dover, L. G. & other authors (2003).** The complete genome sequence and analysis of *Corynebacterium diphtheriae* NCTC13129. *Nucleic Acids Res* **31**, 6516-6523.
- Chatterjee, D., Bozic, C. M., McNeil, M. & Brennan, P. J. (1991).** Structural features of the arabinan component of the lipoarabinomannan of *Mycobacterium tuberculosis*. *J Biol Chem* **266**, 9652-9660.
- Chatterjee, D., Hunter, S. W., McNeil, M. & Brennan, P. J. (1992a).** Lipoarabinomannan. Multiglycosylated form of the mycobacterial mannosylphosphatidylinositols. *J Biol Chem* **267**, 6228-6233.
- Chatterjee, D., Lowell, K., Rivoire, B., McNeil, M. R. & Brennan, P. J. (1992b).** Lipoarabinomannan of *Mycobacterium tuberculosis*. Capping with mannosyl residues in some strains. *J Biol Chem* **267**, 6234-6239.
- Chatterjee, D., Roberts, A. D., Lowell, K., Brennan, P. J. & Orme, I. M. (1992c).** Structural basis of capacity of lipoarabinomannan to induce secretion of tumor necrosis factor. *Infect Immun* **60**, 1249-1253.
- Chatterjee, D., Khoo, K. H., McNeil, M. R., Dell, A., Morris, H. R. & Brennan, P. J. (1993).** Structural definition of the non-reducing termini of mannose-capped LAM from *Mycobacterium tuberculosis* through selective enzymatic degradation and fast atom bombardment-mass spectrometry. *Glycobiology* **3**, 497-506.
- Chatterjee, D. & Khoo, K. H. (1998).** Mycobacterial lipoarabinomannan: an extraordinary lipoheteroglycan with profound physiological effects. *Glycobiology* **8**, 113-120.
- Choi, K. H., Kremer, L., Besra, G. S. & Rock, C. O. (2000).** Identification and substrate specificity of β -ketoacyl (acyl carrier protein) synthase III (mtFabH) from *Mycobacterium tuberculosis*. *J Biol Chem* **275**, 28201-28207.
- Chua, J. & Deretic, V. (2004).** *Mycobacterium tuberculosis* reprograms waves of phosphatidylinositol-phosphate on phagosomal organelles. *J. Biol. Chem.* **279**, 36982-36992.

- Coar, T. (1982).** The aphorisms of Hippocrates with a Translation into Latin, and English. Edited by G. Editions. Birmingham, AB.
- Cohen-Gonsaud, M., Ducasse, S., Hoh, F., Zerbib, D., Labesse, G. & Quémard, A. (2002).** Crystal structure of MabA from *Mycobacterium tuberculosis*, a reductase involved in long-chain fatty acid biosynthesis. *J Mol Biol* **320**, 249-261.
- Colditz, G. A., Brewer, T. F., Berkey, C. S., Wilson, M. E., Burdick, E., Fineberg, H. V. & Mosteller, F. (1994).** Efficacy of BCG vaccine in the prevention of tuberculosis. Meta-analysis of the published literature. *Jama* **271**, 698-702.
- Cole, S. T. (1994).** *Mycobacterium tuberculosis*: drug-resistance mechanisms. *Trends Microbiol* **2**, 411-415.
- Cole, S. T. & Barrell, B. G. (1998).** Analysis of the genome of *Mycobacterium tuberculosis* H37Rv. *Novartis Foundation symposium* **217**, 160-172; discussion 172-167
- Cole, S. T., Brosch, R., Parkhill, J. & other authors (1998).** Deciphering the biology of *Mycobacterium tuberculosis* from the complete genome sequence. *Nature* **393**, 537-544.
- Coutinho, P. M. & Henrissat, B. (1999).** Carbohydrate-active enzymes: an integrated database approach. In *Recent Advances in Carbohydrate Bioengineering*, pp. 3-12. Edited by H. J. Gilbert, G. Davies, B. Henrissat & B. Svensson. Cambridge: The Royal Society of Chemistry.
- Cox, G. (1923).** Sanatorium treatment contrasted with home treatment. After-histories of 4,067 cases. *Br J Tuberc* **17**.
- Crellin, P. K., Kovacevic, S., Martin, K. L., Brammananth, R., Morita, Y. S., Billman-Jacobe, H., McConville, M. J. & Coppel, R. L. (2008).** Mutations in *pimE* restore lipoarabinomannan synthesis and growth in a *Mycobacterium smegmatis* *lpqW* mutant. *J Bacteriol* **190**, 3690-3699.
- Cserzo, M., Wallin, E., Simon, I., von Heijne, G. & Elofsson, A. (1997).** Prediction of transmembrane alpha-helices in prokaryotic membrane proteins: the dense alignment surface method. *Protein Eng* **10**, 673-676.
- Daffé, M., Brennan, P. J. & McNeil, M. (1990).** Predominant structural features of the cell wall arabinogalactan of *Mycobacterium tuberculosis* as revealed through characterization of oligoglycosyl alditol fragments by gas chromatography/mass spectrometry and by ¹H and ¹³C NMR analyses. *J Biol Chem* **265**, 6734-6743.
- Daffé, M. & Draper, P. (1998).** The envelope layers of mycobacteria with reference to their pathogenicity. *Adv Microb Physiol* **39**, 131-201
- Daffé, M., McNeil, M. & Brennan, P. J. (1993).** Major structural features of the cell wall arabinogalactans of *Mycobacterium*, *Rhodococcus*, and *Nocardia* spp. *Carbohydr Res* **249**, 383-398.

- Dal Nogare, A. R., Dan, N. & Lehrman, M. A. (1998).** Conserved sequences in enzymes of the UDP-GlcNAc/MurNAc family are essential in hamster UDP-GlcNAc:dolichol-P GlcNAc-1-P transferase. *Glycobiology* **8**, 625-632
- Daniel, T. M. (2005).** Robert Koch and the pathogenesis of tuberculosis. *Int J Tuberc Lung Dis* **9**, 1181-1182.
- Daniel, T. M. (2006).** The history of tuberculosis. *Respir Med* **100**, 1862-1870.
- Dannenberg, A. M., Jr and Rook, G. A. (1964).** Pathogenesis of pulmonary tuberculosis: an interplay between tissue-damaging and macrophage-activating immune responses: dual mechanisms that control bacilliary multiplication., pp. 459-484. Edited by B. R. Bloom. Washington, D. C.: ASM Press.
- Dannenberg A. M, Jr., Sugimoto M. (1976).** Liquefaction of caseous foci in tuberculosis. *Am Rev Respir Dis.* **113**, 257–259.
- Dao, D. N., Kremer, L., Guerardel, Y., Molano, A., Jacobs, W. R., Jr., Porcelli, S. A. & Briken, V. (2004).** Mycobacterium tuberculosis lipomannan induces apoptosis and interleukin-12 production in macrophages. *Infection and immunity* **72**, 2067-2074.
- De Smet, K. A., Kempell, K. E., Gallagher, A., Duncan, K., and Young, D. B. (1999).** Alteration of a single amino acid residue reverses fosfomycin resistance of recombinant MurA from Mycobacterium tuberculosis. *Microbiology*, **145**, 3177–3184.
- Dell, A., Khoo, K. H., Panico, M., McDowell, R. A., Etienne, A. T., Reason, A. J. & Morris, H. R. (1993).** FAB-MS and ES-MS of glycoproteins. In *Glycobiology: a practical approach*, pp. 187-222. Edited by M. Fukuda & A. Kobata. Oxford. Oxford University Press.
- Delmas, C., Gilleron, M., Brando, T., Vercellone, A., Gheorghui, M., Riviere, M. & Puze, G. (1997).** Comparative structural study of the mannosylated-lipoarabinomannans from *Mycobacterium bovis* BCG vaccine strains: characterization and localization of succinates. *Glycobiology* **7**, 811-817.
- Deng, L., Mikusova, K., Robuck, K. G., Scherman, M., Brennan, P. J. & McNeil, M. R. (1995).** Recognition of multiple effects of ethambutol on metabolism of mycobacterial cell envelope. *Antimicrob Agents Chemother* **39**, 694-701.
- Dinadayala, P., Kaur, D., Berg, S., Amin, A. G., Vissa, V. D., Chatterjee, D., Brennan, P. J. & Crick, D. C. (2006).** Genetic basis for the synthesis of the immunomodulatory mannose caps of lipoarabinomannan in *Mycobacterium tuberculosis*. *J Biol Chem* **281**, 20027-20035.
- Dittmer, J. C. & Lester, R. L. (1964).** A simple, specific spray for the detection of phospholipids on thin-layer chromatograms. *J Lipid Res* **15**, 126-127.
- Dmitriev, B. A., Ehlers, S., Rietschel, E. T. & Brennan, P. J. (2000).** Molecular mechanics of the mycobacterial cell wall: from horizontal layers to vertical scaffolds. *Int J Med Microbiol* **290**, 251-258.

- Dmitriev, B. A., Toukach, F. V., Schaper, K. J., Holst, O., Rietschel, E. T. & Ehlers, S. (2003).** Tertiary structure of bacterial murein: the scaffold model. *J Bacteriol* **185**, 3458-3468.
- Donoghue, H. D., Spigelman, M., Greenblatt, C. L., Lev-Maor, G., Bar-Gal, G. K., Matheson, C., Vernon, K., Nerlich, A. G. & Zink, A. R. (2004).** Tuberculosis: from prehistory to Robert Koch, as revealed by ancient DNA. *The Lancet infectious diseases* **4**, 584-592.
- Doetsch, R. N. (1978).** Benjamin Marten and his "New Theory of Consumptions". *Microbiol Rev* **42**, 521-528.
- Dover, L. G., Cerdeno-Tarraga, A. M., Pallen, M. J., Parkhill, J. & Besra, G. S. (2004).** Comparative cell wall core biosynthesis in the mycolated pathogens, *Mycobacterium tuberculosis* and *Corynebacterium diphtheriae*. *FEMS Microbiol Rev* **28**, 225-250.
- Doz, E., Rose, S., Nigou, J., Gilleron, M., Puzo, G., Erard, F., Ryffel, B. & Quesniaux, V. F. (2007).** Acylation determines the toll-like receptor (TLR)-dependent positive versus TLR2-mannose receptor-, and SIGNR1-independent negative regulation of pro-inflammatory cytokines by mycobacterial lipomannan. *J. Biol. Chem.* **282**, 26014-26025.
- Driessen, N. N., Ummels, R., Maaskant, J. J. & other authors (2009).** Role of phosphatidylinositol mannosides in the interaction between mycobacteria and DC-SIGN. *Infect. Immun.* **77**, 4538-4547.
- Dubnau, E., Chan, J., Raynaud, C., Mohan, V. P., Laneelle, M. A., Yu, K., Quemard, A., Smith, I. & Daffe, M. (2000).** Oxygenated mycolic acids are necessary for virulence of *Mycobacterium tuberculosis* in mice. *Molecular microbiology* **36**, 630-637.
- Durocher, D., Taylor, I. A., Sarbassova, D., Haire, L. F., Westcott, S. L., Jackson, S. P., Smerdon, S. J. & Yaffe, M. B. (2000).** The molecular basis of FHA domain:phosphopeptide binding specificity and implications for phospho-dependent signaling mechanisms. *Mol Cell* **6**, 1169-1182.
- Dye, C., Watt, C. J., Bleed, D. M., Hosseini, S. M. & Raviglione, M. C. (2005).** Evolution of tuberculosis control and prospects for reducing tuberculosis incidence, prevalence, and deaths globally. *Jama* **293**, 2767-2775.
- Dye, C. (2006).** Global epidemiology of tuberculosis. *Lancet* **367**, 938-940.
- Eggeling, L. & Bott, M. (2005).** *Handbook of Corynebacterium glutamicum*.: CRC Press, Taylor Francis Group.
- Ehlers, S. (2009).** DC-SIGN and mannosylated surface structures of *Mycobacterium tuberculosis*: a deceptive liaison. *Eur. J. Cell. Biol.* **89**, 95-101.
- Eikmanns, B. J., Kleinertz, E., Liebl, W. & Sahm, H. (1991).** A family of *Corynebacterium glutamicum*/*Escherichia coli* shuttle vectors for cloning, controlled gene expression, and promoter probing. *Gene* **102**, 93-98.

- Elass, E., Aubry, L., Masson, M., Denys, A., Guerardel, Y., Maes, E., Legrand, D., Mazurier, J. & Kremer, L. (2005). Mycobacterial lipomannan induces matrix metalloproteinase-expression in human macrophagic cells through a Toll-like receptor 1 (TLR1). *Infect. Immun.* **73**, 7064-7068.
- Ernst, W. A., Maher, J., Cho, S. & other authors (1998). Molecular interaction of CD1b with lipoglycan antigens. *Immunity* **8**, 331-340.
- Escuyer, V. E., Lety, M. A., Torrelles, J. B. & other authors (2001). The role of the *emba* and *embB* gene products in the biosynthesis of the terminal hexaarabinofuranosyl motif of *Mycobacterium smegmatis* arabinogalactan. *J Biol Chem* **276**, 48854-48862.
- Fang, Z., Doig, C., Rayner, A., Kenna, D. T., Watt, B. & Forbes, K. J. (1999). Molecular evidence for heterogeneity of the multiple-drug-resistant *Mycobacterium tuberculosis* population in Scotland (1990 to 1997). *J Clin Microbiol* **37**, 998-1003.
- Farmer, P. & Kim, J. Y. (1998). Community based approaches to the control of multidrug resistant tuberculosis: introducing "DOTS-plus". *BMJ* **317**, 671-674.
- Ferguson, J. S., Martin, J. L., Azad, A. K., McCarthy, T. R., Kang, P. B., Voelker, D. R., Crouch, E. C. & Schlesinger, L. S. (2006). Surfactant protein D increases fusion of *Mycobacterium tuberculosis*-containing phagosomes with lysosomes in human macrophages. *Infection and immunity* **74**, 7005-7009.
- Fratti, R. A., Backer, J. M., Gruenberg, J., Corvera, S. & Deretic, V. (2001). Role of phosphatidylinositol 3-kinase and Rab5 effectors in phagosomal biogenesis and mycobacterial phagosome maturation arrest. *J Cell Biol.* **154**, 631-644.
- Fratti, R. A., Chua, J., Vergne, I. & Deretic, V. (2003). *Mycobacterium tuberculosis* glycosylated phosphatidylinositol causes phagosome maturation arrest. *Proc. Natl. Acad. Sci. USA* **100**, 5437-5442.
- Gande, R., Gibson, K. J., Brown, A. K. & other authors (2004). Acyl-CoA carboxylases (accD2 and accD3), together with a unique polyketide synthase (Cg-pks), are key to mycolic acid biosynthesis in *Corynebacterianae* such as *Corynebacterium glutamicum* and *Mycobacterium tuberculosis*. *J Biol Chem* **279**, 44847-44857.
- Gande, R., Dover, L. G., Krumbach, K., Besra, G. S., Sahm, H., Oikawa, T. & Eggeling, L. (2007). The two carboxylases of *Corynebacterium glutamicum* essential for fatty acid and mycolic acid synthesis. *J Bacteriol* **189**, 5257-5264.
- Gao, L. Y., Laval, F., Lawson, E. H., Groger, R. K., Woodruff, A., Morisaki, J. H., Cox, J. S., Daffé, M. & Brown, E. J. (2003). Requirement for kasB in *Mycobacterium* mycolic acid biosynthesis, cell wall impermeability and intracellular survival: implications for therapy. *Mol Microbiol* **49**, 1547-1563.
- Garton, N. J., Gilleron, M., Brando, T., Dan, H. H., Giguere, S., Puzo, G., Prescott, J. F. & Sutcliffe, I. C. (2002). A novel lipoarabinomannan from the equine pathogen *Rhodococcus equi*. Structure and effect on macrophage cytokine production. *The Journal of biological chemistry* **277**, 31722-31733.

- Geijtenbeek, T. B., Van Vliet, S. J., Koppel, E. A., Sanchez-Hernandez, M., Vandenbroucke-Grauls, C. M., Appelmelk, B. & Van Kooyk, Y. (2003).** Mycobacteria target DC-SIGN to suppress dendritic cell function. *The Journal of experimental medicine* **197**, 7-17.
- George, K.M., Yuan, Y., Sherman, D.R. & Barry, C.E (1995).** The Biosynthesis of cyclopropanated mycolic acids in *Mycobacterium tuberculosis*. *J Biol Chem* **270**, 27292-27298.
- Ghuysen, J. M., Bricas, E., Lache, M. & Leyh-Bouille, M. (1968).** Structure of the cell walls of *Micrococcus lysodeikticus*. 3. Isolation of a new peptide dimer, N-alpha-[L-alanyl-gamma-(alpha-D-glutamylglycine)]-L-lysyl-D-alanyl-N-alpha-[L-alanyl-gamma-(alpha-D-glutamylglycine)]-L-lysyl-D-alanine. *Biochemistry* **7**, 1450-1460.
- Gibson, K. J., Eggeling, L., Maughan, W. N., Krumbach, K., Gurcha, S. S., Nigou, J., Puzo, G., Sahm, H. & Besra, G. S. (2003).** Disruption of Cg-Ppm1, a polyprenyl monophosphomannose synthase, and the generation of lipoglycan-less mutants in *Corynebacterium glutamicum*. *J Biol Chem* **278**, 40842-40850.
- Gibson, K. J., Gilleron, M., Constant, P., Brando, T., Puzo, G., Besra, G. S. & Nigou, J. (2004).** Tsukamurella paurometabola lipoglycan, a new lipoarabinomannan variant with pro-inflammatory activity. *The Journal of biological chemistry* **279**, 22973-22982.
- Gibson, K. J., Gilleron, M., Constant, P., Sichi, B., Puzo, G., Besra, G. S. & Nigou, J. (2005).** A lipomannan variant with strong TLR-2-dependent pro-inflammatory activity in *Saccharothrix aerocolonigenes*. *The Journal of biological chemistry* **280**, 28347-28356.
- Gilleron, M., Himoudi, N., Adam, O., Constant, P., Venisse, A., Riviere, M. & Puzo, G. (1997).** *Mycobacterium smegmatis* phosphoinositols-glyceroarabinomannans. Structure and localization of alkali-labile and alkali-stable phosphoinositides. *The Journal of biological chemistry* **272**, 117-124.
- Gilleron, M., Nigou, J., Cahuzac, B. & Puzo, G. (1999).** Structural study of the lipomannans from *Mycobacterium bovis* BCG: characterisation of multiacylated forms of the phosphatidyl-myo-inositol anchor. *J Mol Biol* **285**, 2147-2160.
- Gilleron, M., Bala, L., Brando, T., Vercellone, A. & Puzo, G. (2000).** *Mycobacterium tuberculosis* H37Rv parietal and cellular lipoarabinomannans. Characterization of the acyl- and glyco-forms. *J Biol Chem* **275**, 677-684.
- Gilleron, M., Nigou, J., Nicolle, D., Quesniaux, V. & Puzo, G. (2006).** The acylation state of mycobacterial lipomannans modulates innate immunity response through toll-like receptor 2. *Chem Biol* **13**, 39-47.
- Glickman, M. S., Cox, J. S. & Jacobs, W. R., Jr. (2000).** A novel mycolic acid cyclopropane synthetase is required for cording, persistence, and virulence of *Mycobacterium tuberculosis*. *Molecular cell* **5**, 717-727.
- Glickman, M. S., Cahill, S. M. & Jacobs, W. R., Jr. (2001).** The *Mycobacterium tuberculosis* *cmaA2* gene encodes a mycolic acid trans-cyclopropane synthetase. *J Biol Chem*

276, 2228-2233.

Goffin, C. & Ghuysen, J. M. (2002). Biochemistry and comparative genomics of SxxK superfamily acyltransferases offer a clue to the mycobacterial paradox: presence of penicillin-susceptible target proteins versus lack of efficiency of penicillin as therapeutic agent. *Microbiol Mol Biol Rev* **66**, 702-738, table of contents.

Goodfellow, M. & Minnikin, D. E. (1981). Classification of Nocardioform Actinomycetes. *Zentralbl Bakteriol Mikrobiol Hyg Suppl* **11**, 7-16.

Gringhuis, S. I., den, D. J., Litjens, M., van het, H. B., van, K. Y. & Geijtenbeek, T. B. (2007). C-type lectin DC-SIGN modulates Toll-like receptor signaling via Raf-1 kinase-dependent acetylation of transcription factor NF-kappaB. *Immunity* **26**, 605-616.

Gringhuis, S. I., den, D. J., Litjens, M., van, d. V. & Geijtenbeek, T. B. (2009). Carbohydrate-specific signaling through the DC-SIGN signalosome tailors immunity to *Mycobacterium tuberculosis*, HIV-1 and *Helicobacter pylori*. *Nat Immunol* **10**, 1081-1088.

Gupta, R., Kim, J. Y., Espinal, M. A., Caudron, J. M., Pecoul, B., Farmer, P. E. & Raviglione, M. C. (2001). Public health. Responding to market failures in tuberculosis control. *Science* **293**, 1049-1051.

Guerardel Y, et al. (2002). Structural study of lipomannan and lipoarabinomannan from *Mycobacterium chelonae*. Presence of unusual components with α -1,3-mannopyranose side chains. . *J Biol Chem* **277**, 30635-30648.

Gurcha, S. S., Baulard, A. R., Kremer, L. & other authors (2002). Ppm1, a novel polyprenol monophosphomannose synthase from *Mycobacterium tuberculosis*. *Biochem J* **365**, 441-450.

Gurvitz, A., Hiltunen, J. K. & Kastaniotis, A. J. (2008). Function of heterologous *Mycobacterium tuberculosis* InhA, a type 2 fatty acid synthase enzyme involved in extending C20 fatty acids to C60-to-C90 mycolic acids, during de novo lipoic acid synthesis in *Saccharomyces cerevisiae*. *Appl Environ Microbiol* **74**, 5078-5085.

Gurvitz, A. (2009). The essential mycobacterial genes, fabG1 and fabG4, encode 3-oxoacyl-thioester reductases that are functional in yeast mitochondrial fatty acid synthase type 2. *Mol Genet Genomics* **282**, 407-416.

Gutierrez, M. C., Brisse, S., Brosch, R., Fabre, M., Omais, B., Marmiesse, M., Supply, P. & Vincent, V. (2005). Ancient origin and gene mosaicism of the progenitor of *Mycobacterium tuberculosis*. *PLoS Pathog* **1**, e5.

Guvener, Z.T., & McCarter, L.L. (2003). Multiple regulators control capsular polysaccharide production in *Vibrio parahaemolyticus*. *J Bacteriol* **185**, 5431-5441.

Haite, R. E., Morita, Y. S., McConville, M. J. & Billman-Jacobe, H. (2005). Function of phosphatidylinositol in mycobacteria. *J Biol Chem* **280**, 10981-10987.

- Hancock, I. C., Carman, S., Besra, G. S., Brennan, P. J. & Waite, E. (2002).** Ligation of arabinogalactan to peptidoglycan in the cell wall of *Mycobacterium smegmatis* requires concomitant synthesis of the two wall polymers. *Microbiology* **148**, 3059-3067.
- Hayman, J. (1984).** *Mycobacterium ulcerans*: an infection from Jurassic time? *Lancet* **2**, 1015-1016.
- Heath, R. J. & Rock, C. O. (2002).** The Claisen condensation in biology. *Nat Prod Rep* **19**, 581-596.
- Heymann, S. J., Brewer, T. F., Wilson, M. E. & Fineberg, H. V. (1999).** The need for global action against multidrug-resistant tuberculosis. *Jama* **281**, 2138-2140.
- Hill, D. L. & Ballou, C. E. (1966).** Biosynthesis of mannophospholipids by *Mycobacterium phlei*. *J Biol Chem* **241**, 895-902.
- Hinshaw, H. & Feldman, W. (1945).** Streptomycin in the treatment of clinical tuberculosis: a preliminary report. *Proc Staff Meetings Mayo Clinic* **20**, 313-318.
- Hoang, T. T., Ma, Y., Stern, R. J., McNeil, M. R. & Schweizer, H. P. (1999).** Construction and use of low-copy number T7 expression vectors for purification of problem proteins: purification of *Mycobacterium tuberculosis* RmlD and *Pseudomonas aeruginosa* LasI and RhlI proteins, and functional analysis of purified RhlI. *Gene* **237**, 361-371.
- Holm, L. & Sander, C. (1998).** Touring protein fold space with Dali/FSSP. *Nucleic Acids Res* **26**, 316-319.
- Hove-Jensen, B. (1985).** Cloning and characterization of the *prs* gene encoding phosphoribosylpyrophosphate synthetase of *Escherichia coli*. *Mol Gen Genet* **201**, 269-276.
- Howard, C. F., Jr. (1968).** De novo synthesis and elongation of fatty acids by subcellular fractions of monkey aorta. *J Lipid Res* **9**, 254-261.
- Hsieh, P. C., Shenoy, B. C., Samols, D. & Phillips, N. F. (1996).** Cloning, expression, and characterization of polyphosphate glucokinase from *Mycobacterium tuberculosis*. *J Biol Chem* **271**, 4909-4915.
- Huang, H., Scherman, M. S., D'Haeze, W., Vereecke, D., Holsters, M., Crick, D. C. & McNeil, M. R. (2005).** Identification and active expression of the *Mycobacterium tuberculosis* gene encoding 5-phospho- α -D-ribose-1-diphosphate: decaprenyl-phosphate 5-phosphoribosyltransferase, the first enzyme committed to decaprenylphosphoryl-D-arabinose synthesis. *J Biol Chem* **280**, 24539-24543.
- Hunter, S. W. & Brennan, P. J. (1990).** Evidence for the presence of a phosphatidylinositol anchor on the lipoarabinomannan and lipomannan of *Mycobacterium tuberculosis*. *J Biol Chem* **265**, 9272-9279.
- Ikeda, M., Wachi, M., Jung, H. K., Ishino, F. & Matsuhashi, M. (1991).** The *Escherichia coli* *mraY* gene encoding UDP-N-acetylmuramoyl-pentapeptide: undecaprenyl-phosphate phospho-N-acetylmuramoyl-pentapeptide transferase. *Journal of bacteriology* **173**, 1021-1026.

- Jackson, M., Crick, D. C. & Brennan, P. J. (2000).** Phosphatidylinositol is an essential phospholipid of mycobacteria. *J Biol Chem* **275**, 30092-30099.
- Jo, E. K. (2008).** Mycobacterial interaction with innate receptors: TLRs, C-type lectins, and NLRs. *Curr Opin Infect Dis* **21**, 279-286.
- Jones, T. A., Thirup, S. (1986).** Using known substructures in protein model building and crystallography. *EMBO J* **5**, 819-822.
- Jozefowski S, Sobota A, & Kwiatkowska K (2008).** How *Mycobacterium tuberculosis* subverts host immune responses. *Bioessays* **30**, 943-954 .
- Kalinowski, J., Bathe, B., Bartels, D. & other authors (2003).** The complete *Corynebacterium glutamicum* ATCC 13032 genome sequence and its impact on the production of L-aspartate-derived amino acids and vitamins. *J Biotechnol* **104**, 5-25.
- Kanetsuna, F. (1968).** Chemical analyses of mycobacterial cell walls. *Biochim Biophys Acta* **158**, 130-143.
- Kanetsuna, F., Imaeda, T. & Cunto, G. (1969).** On the linkage between mycolic acid and arabinogalactan in phenol-treated mycobacterial cell walls. *Biochim Biophys Acta* **173**, 341-344.
- Kang, P. B., Azad, A. K., Torrelles, J. B., Kaufman, T. M., Beharka, A., Tibesar, E., DesJardin, L. E. & Schlesinger, L. S. (2005).** The human macrophage mannose receptor directs *Mycobacterium tuberculosis* lipoarabinomannan-mediated phagosome biogenesis. *J. Exp. Med.* **202**, 987-999.
- Kantardjieff, K. A., Kim, C. Y., Naranjo, C. & other authors (2004).** *Mycobacterium tuberculosis* RmlC epimerase (Rv3465): a promising drug-target structure in the rhamnose pathway. *Acta Crystallogr D Biol Crystallogr* **60**, 895-902.
- Kapur, V., Whittam, T. S. & Musser, J. M. (1994).** Is *Mycobacterium tuberculosis* 15,000 years old? *J Infect Dis* **170**, 1348-1349.
- Kaufmann, S. H. (2001).** How can immunology contribute to the control of tuberculosis? *Nat Rev Immunol* **1**, 20-30.
- Kaur, D., Berg, S., Dinadayala, P. & other authors (2006).** Biosynthesis of mycobacterial lipoarabinomannan: role of a branching mannosyltransferase. *Proc Natl Acad Sci U S A* **103**, 13664-13669.
- Kaur, D., McNeil, M. R., Khoo, K. H., Chatterjee, D., Crick, D. C., Jackson, M. & Brennan, P. J. (2007).** New insights into the biosynthesis of mycobacterial lipomannan arising from deletion of a conserved gene. *The Journal of biological chemistry* **282**, 27133-27140.
- Kaur, D., Obregon-Henao, A., Pham, H., Chatterjee, D., Brennan, P. J. & Jackson, M. (2008).** Lipoarabinomannan of *Mycobacterium*: mannose capping by a multifunctional terminal mannosyltransferase. *Proc Natl Acad Sci U S A* **105**, 17973-17977.

- Kaye, K. & Frieden, T.R. (1996).** Tuberculosis control: the relevance of classic principles in an era of acquired immunodeficiency syndrome and multidrug resistance. *Epidemiol Rev* **18**, 52-63.
- Kelley, V. A. & Schorey, J. S. (2003).** Mycobacterium's arrest of phagosome maturation in macrophages requires Rab5 activity and accessibility to iron. *Molecular biology of the cell* **14**, 3366-3377.
- Khasnobis, S., Zhang, J., Angala, S. K., Amin, A. G., McNeil, M. R., Crick, D. C. & Chatterjee, D. (2006).** Characterization of a specific arabinosyltransferase activity involved in mycobacterial arabinan biosynthesis. *Chemistry & biology* **13**, 787-795
- Khoo, K. H., Dell, A., Morris, H. R., Brennan, P. J. & Chatterjee, D. (1995).** Inositol phosphate capping of the nonreducing termini of lipoarabinomannan from rapidly growing strains of *Mycobacterium*. *J Biol Chem* **270**, 12380-12389.
- Khoo, K. H., Douglas, E., Azadi, P., Inamine, J. M., Besra, G. S., Mikusova, K., Brennan, P. J. & Chatterjee, D. (1996).** Truncated structural variants of lipoarabinomannan in ethambutol drug-resistant strains of *Mycobacterium smegmatis*. Inhibition of arabinan biosynthesis by ethambutol. *J Biol Chem* **271**, 28682-28690.
- Khoo, K. H., Tang, J. B. & Chatterjee, D. (2001).** Variation in mannose-capped terminal arabinan motifs of lipoarabinomannans from clinical isolates of *Mycobacterium tuberculosis* and *Mycobacterium avium* complex. *J Biol Chem* **276**, 3863-3871.
- Kiehn T.E., Edwards F.F., Brannon P., Tsang A.Y., Maio M., Gold J.W., Whimbey E., Wong B., McClatchy J.K., & Armstrong D. (1985).** Infections caused by *Mycobacterium avium* complex in immunocompromised patients: diagnosis by blood culture and fecal examination, antimicrobial susceptibility tests, and morphological and seroagglutination characteristics. *J Clin Microbiol.* **21**, 168–173
- Kilburn J. O., & Greenberg J. (1977).** Effect of ethambutol on the viable cell count in *Mycobacterium smegmatis*. *Antimicrob Agents Chemother.* **11**, 534–540
- Kilburn, J. O., & Takayama, K. (1981).** Effects of ethambutol on accumulation and secretion of trehalose mycolates and free mycolic acid in *Mycobacterium smegmatis*. *Antimicrob Agents Chemother* **20**, 401-404.
- Koch, R. (1931).** Die aetiologie der tuberculose, a translation by Berna Pinnr and Max Pinner with an introduction by Allen K. Krause. *Am Rev Tuberc* **25**, 285-323.
- Koppel, E. A., Ludwig, I. S., Hernandez, M. S. & other authors (2004).** Identification of the mycobacterial carbohydrate structure that binds the C-type lectins DC-SIGN, L-SIGN and SIGNR1. *Immunobiology* **209**, 117-127.
- Kordulakova, J., Gilleron, M., Mikusova, K., Puzo, G., Brennan, P. J., Gicquel, B. & Jackson, M. (2002).** Definition of the first mannosylation step in phosphatidylinositol mannoside synthesis. PimA is essential for growth of mycobacteria. *J Biol Chem* **277**, 31335-31344.

- Kordulakova, J., Gilleron, M., Puzo, G., Brennan, P. J., Gicquel, B., Mikusova, K. & Jackson, M. (2003).** Identification of the required acyltransferase step in the biosynthesis of the phosphatidylinositol mannosides of *Mycobacterium* species. *J Biol Chem* **278**, 36285-36295.
- Kovacevic, S., Anderson, D., Morita, Y. S., Patterson, J., Haites, R., McMillan, B. N., Coppel, R., McConville, M. J. & Billman-Jacobe, H. (2006).** Identification of a novel protein with a role in lipoarabinomannan biosynthesis in mycobacteria. *J Biol Chem* **281**, 9011-9017.
- Kremer, L., Dover, L. G., Morehouse, C. & other authors (2001a).** Galactan biosynthesis in *Mycobacterium tuberculosis*. Identification of a bifunctional UDP-galactofuranosyltransferase. *J Biol Chem* **276**, 26430-26440.
- Kremer, L., Nampoothiri, K. M., Lesjean, S. & other authors (2001b).** Biochemical characterization of acyl carrier protein (AcpM) and malonyl-CoA:AcpM transacylase (mtFabD), two major components of *Mycobacterium tuberculosis* fatty acid synthase II. *J Biol Chem* **276**, 27967-27974.
- Kremer, L., and Besra, G.S. (2002)** Re-emergence of tuberculosis: strategies and treatment. *Expert Opin Investig Drugs* **11**, 153-157.
- Kremer, L., Dover, L. G., Carrere, S. & other authors (2002a).** Mycolic acid biosynthesis and enzymic characterization of the beta-ketoacyl-ACP synthase A-condensing enzyme from *Mycobacterium tuberculosis*. *Biochem J* **364**, 423-430.
- Kremer, L., Gurcha, S. S., Bifani, P., Hitchen, P. G., Baulard, A., Morris, H. R., Dell, A., Brennan, P. J. & Besra, G. S. (2002b).** Characterization of a putative alpha-mannosyltransferase involved in phosphatidylinositol trimannoside biosynthesis in *Mycobacterium tuberculosis*. *Biochem J* **363**, 437-447.
- Kremer, L., Dover, L. G., Morbidoni, H. R. & other authors (2003).** Inhibition of InhA activity, but not KasA activity, induces formation of a KasA-containing complex in mycobacteria. *J Biol Chem* **278**, 20547-20554.
- Landt, O., Grunert, H. P. & Hahn, U. (1990).** A general method for rapid site-directed mutagenesis using the polymerase chain reaction. *Gene* **96**, 125-128.
- Lea-Smith, D. J., Pyke, J. S., Tull, D., McConville, M. J., Coppel, R. L. & Crellin, P. K. (2007).** The reductase that catalyzes mycolic motif synthesis is required for efficient attachment of mycolic acids to arabinogalactan. *J Biol Chem* **282**, 11000-11008.
- Lea-Smith, D. J., Martin, K. L., Pyke, J. S., Tull, D., McConville, M. J., Coppel, R. L. & Crellin, P. K. (2008).** Analysis of a new mannosyltransferase required for the synthesis of phosphatidylinositol mannosides and lipoarabinomannan reveals two lipomannan pools in *Corynebacterineae*. *J Biol Chem* **283**, 6773-6782.

- Lechevalier, M. P., Prauser, H., Labeda, D. P. & Ruan, J. S. (1986).** Two new genera of Nocardioform Actinomycetes: *Amycolata* gen. nov and *Amycolatopsis* gen. nov. *Int J Syst Bacteriol* **36**, 29-37.
- Lederer, E., Adam, A., Ciorbaru, R., Petit, J. F. & Wietzerbin, J. (1975).** Cell walls of mycobacteria and related organisms; chemistry and immunostimulant properties. *Mol Cell Biochem* **7**, 87-104.
- Lee, A. S., Teo, A. S. & Wong, S. Y. (2001).** Novel mutations in *ndh* in isoniazid-resistant *Mycobacterium tuberculosis* isolates. *Antimicrob Agents Chemother* **45**, 2157-2159.
- Lee, R. E., Mikusova, K., Brennan, P. J. & Besra, G. S. (1995).** Synthesis of the arabinose aonor β -D-arabinofuranosyl-1-monophosphoryldecaprenol, development of a basic arabinosyl-transferase assay, and identification of ethambutol as an arabinosyltransferase inhibitor. *J Am Chem Soc* **117**, 11829-11832.
- Lee, R. E., Brennan, P. J. & Besra, G. S. (1997).** Mycobacterial arabinan biosynthesis: the use of synthetic arabinoside acceptors in the development of an arabinosyl transfer assay. *Glycobiology* **7**, 1121-1128.
- Lee, R. E., Brennan, P. J. & Besra, G. S. (1998).** Synthesis of β -D-arabinofuranosyl-1-monophosphoryl polyprenols: examination of their function as mycobacterial arabinosyl transferase donors. *Bioorg Med Chem Lett* **8**, 951-954.
- Lee, R. E., Li, W., Chatterjee, D. & Lee, R. E. (2005).** Rapid structural characterization of the arabinogalactan and lipoarabinomannan in live mycobacterial cells using 2D and 3D HR-MAS NMR: structural changes in the arabinan due to ethambutol treatment and gene mutation are observed. *Glycobiology* **15**, 139-151.
- Lee, R., Monsey, D., Weston, A., Duncan, K., Rithner, C. & McNeil, M. (1996).** Enzymatic synthesis of UDP-galactofuranose and an assay for UDP-galactopyranose mutase based on high-performance liquid chromatography. *Anal Biochem* **242**, 1-7.
- Lee, Y. C. & Ballou, C. E. (1964).** Structural studies on the *myo*-inositol mannosides from the glycolipids of *Mycobacterium tuberculosis* and *Mycobacterium phlei*. *J Biol Chem* **239**, 1316-1327.
- Lee, Y. C. & Ballou, C. E. (1965).** Complete structures of the glycopospholipids of mycobacteria. *Biochemistry* **4**, 1395-1404.
- Lemaire, H. G. & Muller-Hill, B. (1986).** Nucleotide sequences of the gal E gene and the gal T gene of E. coli. *Nucleic acids research* **14**, 7705-7711.
- Leopold, K. & Fischer, W. (1993).** Molecular analysis of the lipoglycans of *Mycobacterium tuberculosis*. *Anal Biochem* **208**, 57-64.
- Letek, M., Ordóñez, E. Fernández-Natal, I. Gil, J. A. & L. M. Mateos. (2006).** Identification of the emerging skin pathogen *Corynebacterium amycolatum* using PCR-amplification of the essential *divIVA* gene as a target. *FEMS Microbiol Lett* **265**, 256-63.

- Lety, M. A., Nair, S., Berche, P. & Escuyer, V. (1997).** A single point mutation in the embB gene is responsible for resistance to ethambutol in *Mycobacterium smegmatis*. *Antimicrob Agents Chemother* **41**, 2629-2633.
- Lewin, N. & Aronovitch, M. (1953).** Changing indications for collapse therapy in pulmonary tuberculosis. *Canadian Medical Association Journal* **69**, 481-486.
- Lewin, A. & Sharbati-Tehrani, S. (2005).** Slow growth rate of mycobacteria. Possible reasons and significance for their pathogenicity *Bundesgesundheitsblatt Gesundheitsforschung Gesundheitsschutz*. **48**, 1390–1399
- Li, W., Xin, Y., McNeil, M. R. & Ma, Y. (2006).** rmlB and rmlC genes are essential for growth of mycobacteria. *Biochem Biophys Res Commun* **342**, 170-178.
- Liu, J. & Mushegian, A. (2003).** Three monophyletic superfamilies account for the majority of the known glycosyltransferases. *Protein Sci* **12**, 1418-1431.
- Liu, T. Y. & Gotschlich, E. C. (1967).** Muramic acid phosphate as a component of the mucopeptide of Gram-positive bacteria. *J Biol Chem* **242**, 471-476.
- Ludwiczak, P., Brando, T., Monsarrat, B. & Puzo, G. (2001).** Structural characterization of *Mycobacterium tuberculosis* lipoarabinomannans by the combination of capillary electrophoresis and matrix-assisted laser desorption/ionization time-of-flight mass spectrometry. *Anal Chem* **73**, 2323-2330.
- Lurie M.B. (1950).** Native and acquired resistance to tuberculosis. *Am J Med.* **9**, 591-610
- Ma, Y., Mills, J. A., Belisle, J. T., Vissa, V., Howell, M., Bowlin, K., Scherman, M. S. & McNeil, M. (1997).** Determination of the pathway for rhamnose biosynthesis in mycobacteria: cloning, sequencing and expression of the *Mycobacterium tuberculosis* gene encoding α -D-glucose-1-phosphate thymidyltransferase. *Microbiology* **143**, 937-945.
- Ma, Y., Stern, R. J., Scherman, M. S. & other authors (2001).** Drug targeting *Mycobacterium tuberculosis* cell wall synthesis: genetics of dTDP-rhamnose synthetic enzymes and development of a microtiter plate-based screen for inhibitors of conversion of dTDP-glucose to dTDP-rhamnose. *Antimicrob Agents Chemother* **45**, 1407-1416.
- Ma, Y., Pan, F. & McNeil, M. (2002).** Formation of dTDP-rhamnose is essential for growth of mycobacteria. *J Bacteriol* **184**, 3392-3395.
- Maeda, N., Nigou, J., Herrmann, J. L., Jackson, M., Amara, A., Lagrange, P. H., Puzo, G., Gicquel, B. & Neyrolles, O. (2003).** The cell surface receptor DC-SIGN discriminates between *Mycobacterium* species through selective recognition of the mannose caps on lipoarabinomannan. *J Biol Chem* **278**, 5513-5516.
- Mahapatra, S., Crick, D. C. & Brennan, P. J. (2000).** Comparison of the UDP-N-acetylmuramate:L-alanine ligase enzymes from *Mycobacterium tuberculosis* and *Mycobacterium leprae*. *Journal of bacteriology* **182**, 6827-6830.

- Mahapatra, S., Scherman, H., Brennan, P. J. & Crick, D. C. (2005a).** N-Glycolylation of the nucleotide precursors of peptidoglycan biosynthesis of *Mycobacterium sp.* is altered by drug treatment. *J Bacteriol* **187**, 2341-2347.
- Mahapatra, S., Yagi, T., Belisle, J. T., Espinosa, B. J., Hill, P. J., McNeil, M. R., Brennan, P. J. & Crick, D. C. (2005b).** Mycobacterial lipid II is composed of a complex mixture of modified muramyl and peptide moieties linked to decaprenyl phosphate. *J Bacteriol* **187**, 2747-2757.
- Mambula S. S, Sau K., Henneke P., Golenbock D. T., Levitz S. M. (2002)** Toll-like receptor (TLR) signaling in response to *Aspergillus fumigatus* . *J Biol Chem.* **277**, 39320–39326
- Marrakchi, H., Ducasse, S., Labesse, G., Montrozier, H., Margeat, E., Emorine, L., Charpentier, X., Daffé, M. & Quémard, A. (2002).** MabA (FabG1), a *Mycobacterium tuberculosis* protein involved in the long-chain fatty acid elongation system FAS-II. *Microbiology* **148**, 951-960.
- McCarthy, T. R., Torrelles, J. B., MacFarLane, A. S., Katawczik, M., Kutzbach, B., Desjardin, L. E., Clegg, S., Goldberg, J. B. & Schlesinger, L. S. (2005).** Overexpression of *Mycobacterium tuberculosis manB*, a phosphomannomutase that increases phosphatidylinositol mannoside biosynthesis in *Mycobacterium smegmatis* and mycobacterial association with human macrophages. *Mol Microbiol* **58**, 774-790.
- McNeil, M., Wallner, S. J., Hunter, S. W. & Brennan, P. J. (1987).** Demonstration that the galactosyl and arabinosyl residues in the cell-wall arabinogalactan of *Mycobacterium leprae* and *Mycobacterium tuberculosis* are furanoid. *Carbohydr Res* **166**, 299-308.
- McNeil, M., Daffé, M. & Brennan, P. J. (1990).** Evidence for the nature of the link between the arabinogalactan and peptidoglycan of mycobacterial cell walls. *J Biol Chem* **265**, 18200-18206.
- McNeil, M., Daffé, M. & Brennan, P. J. (1991).** Location of the mycolyl ester substituents in the cell walls of mycobacteria. *J Biol Chem* **266**, 13217-13223.
- McNeil, M. R. & Brennan, P. J. (1991).** Structure, function and biogenesis of the cell envelope of mycobacteria in relation to bacterial physiology, pathogenesis and drug resistance; some thoughts and possibilities arising from recent structural information. *Res Microbiol* **142**, 451-463.
- McNeil, M. R., Robuck, K. G., Harter, M. & Brennan, P. J. (1994).** Enzymatic evidence for the presence of a critical terminal hexa-arabinoside in the cell walls of *Mycobacterium tuberculosis*. *Glycobiology* **4**, 165-173.
- Malik, Z. A., Iyer, S. S. & Kusner, D. J. (2001).** *Mycobacterium tuberculosis* phagosomes exhibit altered calmodulin-dependent signal transduction: contribution to inhibition of phagosome-lysosome fusion and intracellular survival in human macrophages. *J Immunol* **166**, 3392-3401.

- Mdluli, K., Slayden, R. A., Zhu, Y., Ramaswamy, S., Pan, X., Mead, D., Crane, D. D., Musser, J. M. & Barry, C. E., 3rd (1998).** Inhibition of a *Mycobacterium tuberculosis* β -ketoacyl ACP synthase by isoniazid. *Science* **280**, 1607-1610.
- Meroueh, S. O., Bencze, K. Z., Heseck, D., Lee, M., Fisher, J. F., Stemmler, T. L. & Mobashery, S. (2006).** Three-dimensional structure of the bacterial cell wall peptidoglycan. *Proc Natl Acad Sci U S A* **103**, 4404-4409.
- Mikusova, K., Slayden, R. A., Besra, G. S. & Brennan, P. J. (1995).** Biogenesis of the mycobacterial cell wall and the site of action of ethambutol. *Antimicrob Agents Chemother* **39**, 2484-2489.
- Mikusova, K., Mikus, M., Besra, G. S., Hancock, I. & Brennan, P. J. (1996).** Biosynthesis of the linkage region of the mycobacterial cell wall. *J Biol Chem* **271**, 7820-7828.
- Mikusova, K., Yagi, T., Stern, R., McNeil, M. R., Besra, G. S., Crick, D. C. & Brennan, P. J. (2000).** Biosynthesis of the galactan component of the mycobacterial cell wall. *J Biol Chem* **275**, 33890-33897.
- Mikusova, K., Huang, H., Yagi, T. & other authors (2005).** Decaprenylphosphoryl arabinofuranose, the donor of the D-arabinofuranosyl residues of mycobacterial arabinan, is formed via a two-step epimerization of decaprenylphosphoryl ribose. *J Bacteriol* **187**, 8020-8025.
- Mikusova, K., Belanova, M., Kordulakova, J., Honda, K., McNeil, M. R., Mahapatra, S., Crick, D. C. & Brennan, P. J. (2006).** Identification of a novel galactosyl transferase involved in biosynthesis of the mycobacterial cell wall. *J Bacteriol* **188**, 6592-6598.
- Mills, J. A., Motichka, K., Jucker, M. & other authors (2004).** Inactivation of the mycobacterial rhamnosyltransferase, which is needed for the formation of the arabinogalactan-peptidoglycan linker, leads to irreversible loss of viability. *J Biol Chem* **279**, 43540-43546.
- Minnikin, D. E. & Goodfellow, M. (1980).** Lipid composition in the classification and identification of acid-fast bacteria. *Soc Appl Bacteriol Symp Ser* **8**, 189-256.
- Minnikin, D. E. (1982).** Lipids: complex lipids, their chemistry, biosynthesis and roles. In *The Biology of the Mycobacteria* pp. 95-184. Edited by C. Ratledge & J. Stanford. London: Academic Press Inc. Ltd.
- Minnikin, D. E., Minnikin, S. M., Goodfellow, M. & Stanford, J. L. (1982).** The mycolic acids of *Mycobacterium chelonae*. *Journal of general microbiology* **128**, 817-822.
- Minnikin, D. E. (1991).** Chemical principles in the organization of lipid components in the mycobacterial cell envelope. *Research in microbiology* **142**, 423-427.
- Minnikin, D. E., Kremer, L., Dover, L. G. & Besra, G. S. (2002).** The methyl-branched fortifications of *Mycobacterium tuberculosis*. *Chem Biol* **9**, 545-553.

- Misaki, A. & Yukawa, S. (1966).** Studies on cell walls of Mycobacteria. II. Constitution of polysaccharides from BCG cell walls. *J Biochem (Tokyo)* **59**, 511-520.
- Misaki A, Seto N, Azuma I. (1974).** Structure and immunological properties of D-arabino-D-galactans isolated from cell walls of Mycobacterium species. *J. Biochem* **76**, 15-27.
- Mishra, A. K., Alderwick, L. J., Rittmann, D., Tatituri, R. V., Nigou, J., Gilleron, M., Eggeling, L. & Besra, G. S. (2007).** Identification of an $\alpha(1\rightarrow6)$ mannopyranosyltransferase (MptA), involved in *Corynebacterium glutamicum* lipomannan biosynthesis, and identification of its orthologue in *Mycobacterium tuberculosis*. *Mol Microbiol* **65**, 1503-1517.
- Mishra, A. K., Alderwick, L. J., Rittmann, D., Wang, C., Bhatt, A., Jacobs, W. R., Jr., Takayama, K., Eggeling, L. & Besra, G. S. (2008a).** Identification of a novel $\alpha(1\rightarrow6)$ mannopyranosyltransferase MptB from *Corynebacterium glutamicum* by deletion of a conserved gene, NCgl1505, affords a lipomannan- and lipoarabinomannan-deficient mutant. *Mol Microbiol* **68**, 1595-1613.
- Mishra, A. K., Klein, C., Gurcha, S. S. & other authors (2008b).** Structural characterization and functional properties of a novel lipomannan variant isolated from a *Corynebacterium glutamicum* Δ pimB' mutant. *Antonie Van Leeuwenhoek* **94**, 277-287.
- Mishra, A. K., Batt, S., Krumbach, K., Eggeling, L. & Besra, G. S. (2009).** Characterization of the *Corynebacterium glutamicum* Δ pimB' Δ mgtA double deletion mutant and the role of *Mycobacterium tuberculosis* orthologues Rv2188c and Rv0557 in glycolipid biosynthesis. *J Bacteriol* **191**, 4465-4472.
- Morita, Y. S., Patterson, J. H., Billman-Jacobe, H. & McConville, M. J. (2004).** Biosynthesis of mycobacterial phosphatidylinositol mannosides. *Biochem J* **378**, 589-597.
- Morita, Y. S., Sena, C. B., Waller, R. F. & other authors (2006).** PimE Is a polyprenol-phosphate-mannose-dependent mannosyltransferase that transfers the fifth mannose of phosphatidylinositol mannoside in Mycobacteria. *J Biol Chem* **281**, 25143-25155..
- Morr, M., Takeuchi, O., Akira, S., Simon, M. M. & Muhlradt P. F. (2002).** Differential recognition of structural details of bacterial lipopeptides by toll-like receptors. *Eur J Immunol* **32**, 3337-3347.
- Munro, S. A., Lewin, S. A., Smith, H. J., Engel, M. E., Fretheim, A. & Volmink, J. (2007).** Patient adherence to tuberculosis treatment: a systematic review of qualitative research. *PLoS Med* **4**, e238.
- Murray, C. J. & Salomon, J. A. (1998).** Modeling the impact of global tuberculosis control strategies. *Proc Natl Acad Sci U S A* **95**, 13881-13886.
- Nachega, J. B., & Chaisson, R. E. (2003)** Tuberculosis drug resistance: a global threat. *Clin Infect Dis* **36**, S24-30.

- Nassau, P. M., Martin, S. L., Brown, R. E., Weston, A., Monsey, D., McNeil, M. R., and Duncan, K. (1996)** Galactofuranose biosynthesis in *Escherichia coli* K-12: identification and cloning of UDP-galactopyranose mutase. *J Bacteriol* **178**, 1047-1052.
- Nations, J. A., Lazarus, A. A. & Walsh, T. E. (2006).** Drug-resistant tuberculosis. *Dis Mon* **52**, 435-440.
- Nerlich, A. G., Haas, C. J., Zink, A., Szeimies, U. & Hagedorn, H. G. (1997).** Molecular evidence for tuberculosis in an ancient Egyptian mummy. *Lancet* **350**, 1404.
- Neyrolles, O., Gicquel, B. & Quintana-Murci, L. (2006).** Towards a crucial role for DC-SIGN in tuberculosis and beyond. *Trends Microbiol.* **14**, 383-387.
- Nguyen, L. & Pieters, J. (2005).** The Trojan horse: survival tactics of pathogenic mycobacteria in macrophages. *Trends in cell biology* **15**, 269-276
- Nguyen, L., Thompson, C.J. (2006).** Foundations of antibiotic resistance in bacterial physiology: the mycobacterial paradigm. *Trends Microbiol* **14**, 304-312
- Nigou, J., Gilleron, M., Cahuzac, B., Bounery, J. D., Herold, M., Thurnher, M. & Puzo, G. (1997).** The phosphatidyl-myo-inositol anchor of the lipoarabinomannans from *Mycobacterium bovis* BCG. Heterogeneity, structure, and role in the regulation of cytokine secretion. *J Biol Chem* **272**, 23094-23103.
- Nigou, J., Gilleron, M., Cahuzac, B., Bounery, J. D., Herold, M., Thurnher, M. & Puzo, G. (1997).** The phosphatidyl-myo-inositol anchor of the lipoarabinomannans from *Mycobacterium bovis* bacillus Calmette Guerin. Heterogeneity, structure, and role in the regulation of cytokine secretion. *J Biol Chem* **272**, 23094-23103.
- Nigou, J. & Besra, G. S. (2002a).** Characterization and regulation of inositol monophosphatase activity in *Mycobacterium smegmatis*. *Biochem J* **361**, 385-390.
- Nigou, J. & Besra, G. S. (2002b).** Cytidine diphosphate-diacylglycerol synthesis in *Mycobacterium smegmatis*. *Biochem J* **367**, 157-162.
- Nigou, J., Gilleron, M., Rojas, M., Garcia, L. F., Thurnher, M. & Puzo, G. (2002).** Mycobacterial lipoarabinomannans: modulators of dendritic cell function and the apoptotic response. *Microbes Infect* **4**, 945-953.
- Nigou, J., Gilleron, M. & Puzo, G. (2003).** Lipoarabinomannans: from structure to biosynthesis. *Biochimie* **85**, 153-166.
- Nigou, J., Vasselon, T., Ray, A., Constant, P., Gilleron, M., Besra, G. S., Sutcliffe, I., Tiraby, G. & Puzo, G. (2008).** Mannan chain length controls lipoglycans signaling via and binding to TLR2. *J. Immunol.* **180**, 6696-6702.
- Nikaido, H. (1993).** Transport across the bacterial outer membrane. *Journal of bioenergetics and biomembranes* **25**, 581-589.

- Ning, B. & Elbein, A. D. (1999).** Purification and properties of mycobacterial GDP-mannose pyrophosphorylase. *Arch Biochem Biophys* **362**, 339-345.
- Ormerod, L. P. (2005).** Multidrug-resistant tuberculosis (MDR-TB): epidemiology, prevention and treatment. *Br Med Bull* **73-74**, 17-24.
- Owens, R. M., Hsu, F. F., VanderVen, B. C. & other authors (2006).** *M. tuberculosis* Rv2252 encodes a diacylglycerol kinase involved in the biosynthesis of phosphatidylinositol mannosides (PIMs). *Mol Microbiol* **60**, 1152-1163.
- Pablos-Mendez, A., Raviglione, M. C., Laszlo, A. & other authors (1998).** Global surveillance for antituberculosis-drug resistance, 1994-1997. World Health Organization-International Union against Tuberculosis and Lung Disease Working Group on Anti-Tuberculosis Drug Resistance Surveillance. *N Engl J Med* **338**, 1641-1649.
- Pan, F., Jackson, M., Ma, Y. & McNeil, M. (2001).** Cell wall core galactofuran synthesis is essential for growth of mycobacteria. *J Bacteriol* **183**, 3991-3998.
- Patterson, J. H., Waller, R. F., Jeevarajah, D., Billman-Jacobe, H. & McConville, M. J. (2003).** Mannose metabolism is required for mycobacterial growth. *Biochem J* **372**, 77-86.
- Petit, J. F., Adam, A., Wietzerbin-Falszpan, J., Lederer, E. & Ghuysen, J. M. (1969).** Chemical structure of the cell wall of *Mycobacterium smegmatis*. I. Isolation and partial characterization of the peptidoglycan. *Biochem Biophys Res Commun* **35**, 478-485.
- Petit, J., Adam, A. & Wietzerbin-Falszpan, J. (1970).** Isolation of UDP-N-glycolylmuramyl-(Ala, Glu, DAP) from *Mycobacterium phlei*. *FEBS Lett* **6**, 55-57.
- Petzold C.J., Stanton L.H., & Leary J.A., (2005).** Structural characterization of Lipoarabinomannans from *Mycobacterium tuberculosis* and *Mycobacterium smegmatis* by ESI mass spectrometry. *J Am Soc Mass Spectrom* **16**, 1109-1116
- Pitarque, S., Larrouy-Maumus, G., Payre, B., Jackson, M., Puzo, G. & Nigou, J. (2008).** The immune-modulatory lipoglycans, lipoarabinomannan and lipomannan, are exposed at the mycobacterial cell surface. *Tuberculosis (Edinb)* **88**, 560-565.
- Pohlschroder, M., Hartmann, E., Hand, N. J., Dilks, K. & Haddad, A. (2005).** Diversity and evolution of protein translocation. *Annu Rev Microbiol* **59**, 91-111.
- Portevin, D., De Sousa-D'Auria, C., Houssin, C., Grimaldi, C., Chami, M., Daffé, M. & Guilhot, C. (2004).** A polyketide synthase catalyzes the last condensation step of mycolic acid biosynthesis in mycobacteria and related organisms. *Proc Natl Acad Sci U S A* **101**, 314-319.
- Prigozy, T. I., Sieling, P. A., Clemens, D., Stewart, P. L., Behar, S. M., Porcelli, S. A., Brenner, M. B., Modlin, R. L. & Kronenberg, M. (1997).** The mannose receptor delivers lipoglycan antigens to endosomes for presentation to T cells by CD1b molecules. *Immunity* **6**, 187-197.

- Puech, V., Chami, M., Lemassu, A., Lan  elle, M. A., Schiffler, B., Gounon, P., Bayan, N., Benz, R. & Daff  , M. (2001).** Structure of the cell envelope of corynebacteria: importance of the non-covalently bound lipids in the formation of the cell wall permeability barrier and fracture plane. *Microbiology* **147**, 1365-1382.
- Puech, V., Guilhot, C., Perez, E., Tropis, M., Armitige, L. Y., Gicquel, B. & Daff  , M. (2002).** Evidence for a partial redundancy of the fibronectin-binding proteins for the transfer of mycoloyl residues onto the cell wall arabinogalactan termini of *Mycobacterium tuberculosis*. *Mol Microbiol* **44**, 1109-1122.
- Pugin, J., Heumann, I. D., Tomasz, A., Kravchenko, V. V., Akamatsu, Y., Nishijima, M., Glauser, M. P., Tobias, P. S. & Ulevitch, R. J. (1994).** CD14 is a pattern recognition receptor. *Immunity* **1**, 509-516.
- Puissegur, M. P., Lay, G., Gilleron, M. & other authors (2007).** Mycobacterial lipomannan induces granuloma macrophage fusion via a TLR2-dependent, ADAM9- and beta1 integrin- mediated pathway. *J Immunol* **178**, 3161-3169.
- Quesniaux, V., Fremond, C., Jacobs, M. & other authors (2004a).** Toll-like receptor pathways in the immune responses to mycobacteria. *Microbes Infect* **6**, 946-959.
- Quesniaux, V. J., Nicolle, D. M., Torres, D., Kremer, L., Guerardel, Y., Nigou, J., Puzo, G., Erard, F. & Ryffel, B. (2004b).** Toll-like receptor 2 (TLR2)-dependent-positive and TLR2-independent-negative regulation of proinflammatory cytokines by mycobacterial lipomannans. *J.Immunol.* **172**, 4425-4434.
- Qureshi, N., Takayama, K., Jordi, H. C. & Schnoes, H. K. (1978).** Characterization of the purified components of a new homologous series of alpha-mycolic acids from *Mycobacterium tuberculosis* H37Ra. *J Biol Chem* **253**, 5411-5417.
- Radmacher, E., Stansen, K. C., Besra, G. S., Alderwick, L. J., Maughan, W. N., Hollweg, G., Sahm, H., Wendisch, V. F. & Eggeling, L. (2005).** Ethambutol, a cell wall inhibitor of *Mycobacterium tuberculosis*, elicits L-glutamate efflux of *Corynebacterium glutamicum*. *Microbiology* **151**, 1359-1368.
- Ramaswamy, S. V., Amin, A. G., Goksel, S., Stager, C. E., Dou, S. J., El Sahly, H., Moghazeh, S. L., Kreiswirth, B. N. & Musser, J. M. (2000).** Molecular genetic analysis of nucleotide polymorphisms associated with ethambutol resistance in human isolates of *Mycobacterium tuberculosis*. *Antimicrob Agents Chemother* **44**, 326-336.
- Ramaswamy, S. V., Dou, S. J., Rendon, A., Yang, Z., Cave, M. D. & Graviss, E. A. (2004).** Genotypic analysis of multidrug-resistant *Mycobacterium tuberculosis* isolates from Monterrey, Mexico. *J Med Microbiol* **53**, 107-113.
- Raupach, B. & Kaufmann, S. H. (2001).** Immune responses to intracellular bacteria. *Current opinion in immunology* **13**, 417-428.
- Raymond, J. B., Mahapatra, S., Crick, D. C. & Pavelka, M. S., Jr. (2005).** Identification of the namH gene, encoding the hydroxylase responsible for the N-glycolylation of the mycobacterial peptidoglycan. *The Journal of biological chemistry* **280**, 326-333.

- Rojas, M., Garcia, L. F., Nigou, J., Puzo, G. & Olivier, M. (2000).** Mannosylated lipoarabinomannan antagonizes *Mycobacterium tuberculosis*-induced macrophage apoptosis by altering Ca²⁺-dependent cell signaling. *The Journal of infectious diseases* **182**, 240-251.
- Rose, N. L., Completo, G. C., Lin, S. J., McNeil, M., Palcic, M. M. & Lowary, T. L. (2006).** Expression, purification, and characterization of a galactofuranosyltransferase involved in *Mycobacterium tuberculosis* arabinogalactan biosynthesis. *J Am Chem Soc* **128**, 6721-6729.
- Rozwarski, D. A., Grant, G. A., Barton, D. H., Jacobs, W. R., Jr. & Sacchettini, J. C. (1998).** Modification of the NADH of the isoniazid target (InhA) from *Mycobacterium tuberculosis*. *Science* **279**, 98-102.
- Russell, D. G. (2001).** *Mycobacterium tuberculosis*: here today, and here tomorrow. *Nature reviews* **2**, 569-577.
- Sacco, E., Covarrubias, A. S., O'Hare, H. M., Carroll, P., Eynard, N., Jones, T.A., Parish, T, Daffé, M., Bäckbro, K., Quémard, A. (2007).** The missing piece of the type II fatty acid synthase system from *Mycobacterium tuberculosis*. *Proc Natl Acad Sci U S A*. **104**, 14628-33.
- Sahm, H., Eggeling, L. & de Graaf, A. A. (2000).** Pathway analysis and metabolic engineering in *Corynebacterium glutamicum*. *Biol Chem* **381**, 899-910.
- Salman, M., Lonsdale, J. T., Besra, G. S. & Brennan, P. J. (1999).** Phosphatidylinositol synthesis in mycobacteria. *Biochim Biophys Acta* **1436**, 437-450.
- Salo, W. L., Aufderheide, A. C., Buikstra, J. & Holcomb, T. A. (1994).** Identification of *Mycobacterium tuberculosis* DNA in a pre-Columbian Peruvian mummy. *Proc Natl Acad Sci U S A* **91**, 2091-2094.
- Sassaki, G.L., Iacaomini, M., and Gorin, P.A.J. (2005).** Methylation-GC-MS analysis of arabinofuranose-and galactofuranose-containing structures; rapid synthesis of partially *O*-methylated alditol acetates. *An Acad Bras Cienc* **77**, 223–234.
- Sasseti, C. M., Boyd, D. H. & Rubin, E. J. (2003).** Genes required for mycobacterial growth defined by high density mutagenesis. *Mol Microbiol* **48**, 77-84.
- Schaeffer, M. L., Khoo, K. H., Besra, G. S., Chatterjee, D., Brennan, P. J., Belisle, J. T. & Inamine, J. M. (1999).** The *pimB* gene of *Mycobacterium tuberculosis* encodes a mannosyltransferase involved in lipoarabinomannan biosynthesis. *J Biol Chem* **274**, 31625-31631.
- Schaeffer, M. L., Agnihotri, G., Volker, C., Kallender, H., Brennan, P. J. & Lonsdale, J. T. (2001).** Purification and biochemical characterization of the *Mycobacterium tuberculosis* β -ketoacyl-acyl carrier protein synthases KasA and KasB. *J Biol Chem* **276**, 47029-47037.
- Schafer, A., Tauch, A., Jager, W., Kalinowski, J., Thierbach, G. & Puhler, A. (1994).** Small mobilizable multi-purpose cloning vectors derived from the *Escherichia coli* plasmids

pK18 and pK19: selection of defined deletions in the chromosome of *Corynebacterium glutamicum*. *Gene* **145**, 69-73.

Scherman, M., Weston, A., Duncan, K., Whittington, A., Upton, R., Deng, L., Comber, R., Friedrich, J. D. & McNeil, M. (1995). Biosynthetic origin of mycobacterial cell wall arabinosyl residues. *J Bacteriol* **177**, 7125-7130.

Scherman, M. S., Kalbe-Bournonville, L., Bush, D., Xin, Y., Deng, L. & McNeil, M. (1996). Polyprenylphosphate-pentoses in mycobacteria are synthesized from 5-phosphoribose pyrophosphate. *J Biol Chem* **271**, 29652-29658.

Scherman, H., Kaur, D., Pham, H., Skovierova, H., Jackson, M. & Brennan, P. J. (2009). Identification of a polyprenylphosphomannosyl synthase involved in the synthesis of mycobacterial mannosides. *Journal of bacteriology* **191**, 6769-6772.

Schleifer, K. H. & Kandler, O. (1972). Peptidoglycan types of bacterial cell walls and their taxonomic implications. *Bacteriol Rev* **36**, 407-477.

Schlesinger, L. S., Hull, S. R. & Kaufman, T. M. (1994). Binding of the terminal mannosyl units of lipoarabinomannan from a virulent strain of *Mycobacterium tuberculosis* to human macrophages. *J Immunol* **152**, 4070-4079.

Schultz, J., and A. D. Elbein. 1974. Biosynthesis of mannosyl--and glucosyl-phosphoryl polyprenols in *Mycobacterium smegmatis*. Evidence for oligosaccharide-phosphoryl-polyprenols. *Arch Biochem Biophys* **160**, 311-322.

Scorpio, A. & Zhang, Y. (1996). Mutations in *pncA*, a gene encoding pyrazinamidase/nicotinamidase, cause resistance to the antituberculous drug pyrazinamide in tubercle bacillus. *Nat Med* **2**, 662-667.

Scorpio, A., Lindholm-Levy, P., Heifets, L., Gilman, R., Siddiqi, S., Cynamon, M. & Zhang, Y. (1997). Characterization of *pncA* mutations in pyrazinamide-resistant *Mycobacterium tuberculosis*. *Antimicrob Agents Chemother* **41**, 540-543.

Seidel, M., Alderwick, L. J., Birch, H. L., Sahm, H., Eggeling, L. & Besra, G. S. (2007a). Identification of a Novel Arabinofuranosyltransferase AftB Involved in a Terminal Step of Cell Wall Arabinan Biosynthesis in Corynebacteriaceae, such as *Corynebacterium glutamicum* and *Mycobacterium tuberculosis*. *J Biol Chem* **282**, 14729-14740.

Seidel, M., Alderwick, L. J., Sahm, H., Besra, G. S. & Eggeling, L. (2007b). Topology and mutational analysis of the single Emb arabinofuranosyltransferase of *Corynebacterium glutamicum* as a model of Emb proteins of *Mycobacterium tuberculosis*. *Glycobiology* **17**, 210-219.

Shah, N.S., Wright, A., Bai, G.H., Barrera, L., Boulahbal, F., Martin-Casabona, N., et al. (2007). Worldwide emergence of extensively drug-resistant tuberculosis. *Emerg Infect Dis* **13**, 380-387.

Sharma, S. K. & Mohan, A. (2006). Multidrug-resistant tuberculosis: a menace that threatens to destabilize tuberculosis control. *Chest* **130**, 261-272.

- Shi, L., Berg, S., Lee, A., Spencer, J. S., Zhang, J., Vissa, V., McNeil, M. R., Khoo, K. H. & Chatterjee, D. (2006).** The carboxy terminus of EmbC from *Mycobacterium smegmatis* mediates chain length extension of the arabinan in lipoarabinomannan. *J Biol Chem* **281**, 19512-19526.
- Sidobre, S., Nigou, J., Puze, G. & Riviere, M. (2000).** Lipoglycans are putative ligands for the human pulmonary surfactant protein A attachment to mycobacteria. Critical role of the lipids for lectin-carbohydrate recognition. *J. Biol. Chem.* **275**, 2415-2422.
- Singh, J. A., Upshur, R., & Padayatchi, N. (2007).** XDR-TB in South Africa: No time for denial or complacency. *PLoS Med* **4**, e50
- Simonsen, A., Gaullier, J. M., D'Arrigo, A. & Stenmark, H. (1999).** The Rab5 effector EEA1 interacts directly with syntaxin-6. *J. Biol. Chem.* **274**, 28857-28860.
- Skovierova, H., Larrouy-Maumus, G., Zhang, J. & other authors (2009).** AftD, a novel essential arabinofuranosyltransferase from mycobacteria. *Glycobiology*.
- Skovierova, H., Larrouy-Maumus, G., Pham, H. & other authors (2010).** Biosynthetic origin of the galactosamine substituent of Arabinogalactan in *Mycobacterium tuberculosis*. *The Journal of biological chemistry* **285**, 41348-41355.
- Slayden, R. A. & Barry, C. E., 3rd (2002).** The role of KasA and KasB in the biosynthesis of meromycolic acids and isoniazid resistance in *Mycobacterium tuberculosis*. *Tuberculosis (Edinburgh)* **82**, 149-160.
- Smith, S., Witkowski, A. & Joshi, A. K. (2003).** Structural and functional organization of the animal fatty acid synthase. *Prog Lipid Res* **42**, 289-317.
- Snider, D. E., Jr. & La Montagne, J. R. (1994).** The neglected global tuberculosis problem: a report of the 1992 World Congress on Tuberculosis. *J Infect Dis* **169**, 1189-1196.
- Sreevatsan, S., Pan, X., Stockbauer, K. E., Connell, N. D., Kreiswirth, B. N., Whittam, T. S. & Musser, J. M. (1997a).** Restricted structural gene polymorphism in the *Mycobacterium tuberculosis* complex indicates evolutionarily recent global dissemination. *Proc Natl Acad Sci U S A* **94**, 9869-9874.
- Sreevatsan, S., Stockbauer, K. E., Pan, X., Kreiswirth, B. N., Moghazeh, S. L., Jacobs, W. R., Jr., Telenti, A. & Musser, J. M. (1997b).** Ethambutol resistance in *Mycobacterium tuberculosis*: critical role of embB mutations. *Antimicrob Agents Chemother* **41**, 1677-1681.
- Stern, R. J., Lee, T. Y., Lee, T. J., Yan, W., Scherman, M. S., Vissa, V. D., Kim, S. K., Wanner, B. L. & McNeil, M. R. (1999).** Conversion of dTDP-4-keto-6-deoxyglucose to free dTDP-4-keto-rhamnose by the rmlC gene products of *Escherichia coli* and *Mycobacterium tuberculosis*. *Microbiology* **145**, 663-671.
- Stevenson, G., Neal, B., Liu, D., Hobbs, M., Packer, N. H., Batley, M., Redmond, J. W., Lindquist, L. & Reeves, P. (1994).** Structure of the O antigen of *Escherichia coli* K-12 and the sequence of its rfb gene cluster. *Journal of bacteriology* **176**, 4144-4156.

- Stover, C. K., de la Cruz, V. F., Fuerst, T. R. & other authors (1991).** New use of BCG for recombinant vaccines. *Nature* **351**, 456-460.
- Subramanian, A. R., Weyer-Menkhoff, J., Kaufmann, M. & Morgenstern, B. (2005).** DIALIGN-T: an improved algorithm for segment-based multiple sequence alignment. *BMC Bioinformatics* **6**, 66.
- Sweet, L., Singh, P. P., Azad, A. K., Rajaram, M. V., Schlesinger, L. S. & Schorey, J. S. (2009).** Mannose receptor-dependent delay in phagosome maturation by *Mycobacterium avium* glycopeptidolipids. *Infect Immun* **78**, 518-526.
- Tailleux, L., Pham-Thi, N., Bergeron-Lafaurie, A. & other authors (2005).** DC-SIGN induction in alveolar macrophages defines privileged target host cells for mycobacteria in patients with tuberculosis. *PLoS Med.* **2**, e381.
- Takayama, K., David, H. L., Wang, L. & Goldman, D. S. (1970).** Isolation and characterization of uridine diphosphate-N-glycolylmuramyl-L-alanyl-gamma-D-glutamyl-meso-alpha,alpha'-diaminopimelic acid from *Mycobacterium tuberculosis*. *Biochem Biophys Res Commun* **39**, 7-12.
- Takayama, K. & Goldman, D. S. (1970).** Enzymatic synthesis of mannosyl-1-phosphoryl-decaprenol by a cell-free system of *Mycobacterium tuberculosis*. *J Biol Chem* **245**, 7.
- Takayama, K., Armstrong, E. L., Kunugi, K. A. & Kilburn, J. O. (1979).** Inhibition by ethambutol of mycolic acid transfer into the cell wall of *Mycobacterium smegmatis*. *Antimicrob Agents Chemother* **16**, 240-242.
- Takayama, K. & Kilburn, J. O. (1989).** Inhibition of synthesis of arabinogalactan by ethambutol in *Mycobacterium smegmatis*. *Antimicrob Agents Chemother* **33**, 1493-1499.
- Takayama, K., Wang, C. & Besra, G. S. (2005).** Pathway to synthesis and processing of mycolic acids in *Mycobacterium tuberculosis*. *Clin Microbiol Rev* **18**, 81-101.
- Takeuchi, O., Sato, S., Horiuchi, T., Hoshino, K., Takeda, K., Dong, Z., Modlin, R. L. & Akira, S. (2002).** Cutting edge: role of Toll-like receptor 1 in mediating immune response to microbial lipoproteins. *J Immunol* **169**, 10-14.
- Taniguchi, H., Aramaki, H., Nikaido, Y., Mizuguchi, Y., Nakamura, M., Koga, T. & Yoshida, S. (1996).** Rifampicin resistance and mutation of the *rpoB* gene in *Mycobacterium tuberculosis*. *FEMS Microbiol Lett* **144**, 103-108.
- Tapping, R. I. & Tobias, P. S. (2003).** Mycobacterial lipoarabinomannan mediates physical interactions between TLR1 and TLR2 to induce signaling. *Journal of endotoxin research* **9**, 264-268.
- Tatituri, R. V., Alderwick, L. J., Mishra, A. K. & other authors (2007a).** Structural characterization of a partially arabinosylated lipoarabinomannan variant isolated from a *Corynebacterium glutamicum* *ubiA* mutant. *Microbiology* **153**, 2621-2629.
- Tatituri, R. V., Illarionov, P. A., Dover, L. G. & other authors (2007b).** Inactivation of

Corynebacterium glutamicum NCgl0452 and the role of MgtA in the biosynthesis of a novel mannosylated glycolipid involved in lipomannan biosynthesis. *J Biol Chem* **282**, 4561-4572.

Taylor, G. M., Young, D. B. & Mays, S. A. (2005). Genotypic analysis of the earliest known prehistoric case of tuberculosis in Britain. *Clin Microbiol* **43**, 2236-2240.

Tauch, A., Kaiser, O., Hain, T., Goesmann, A., Weisshaar, B., Albersmeier, A., Bekel, T., Bischoff, N. Brune, I. Chakraborty, T. Kalinowski, J., Meyer, F., Rupp, O., Schneiker, S., Viehoveer, P., & Pühler, A., (2005). Complete genome sequence and analysis of the multiresistant nosocomial pathogen *Corynebacterium jeikeium* K411, a lipid-requiring bacterium of the human skin flora. *J Bacteriol* **187**, 4671-82.

Telenti, A., Philipp, W. J., Sreevatsan, S., Bernasconi, C., Stockbauer, K. E., Wieles, B., Musser, J. M. & Jacobs, W. R., Jr. (1997). The *emb* operon, a gene cluster of *Mycobacterium tuberculosis* involved in resistance to ethambutol. *Nat Med* **3**, 567-570.

Thomas, J. P., Baughn, C. O., Wilkinson, R. G. & Shepherd, R. G. (1961). A new synthetic compound with antituberculous activity in mice: ethambutol (dextro-2,2'-(ethylenediimino)-di-l-butanol). *Am Rev Respir Dis* **83**, 891-893.

Torrelles, J. B., Azad, A. K. & Schlesinger, L. S. (2006). Fine discrimination in the recognition of individual species of phosphatidyl-myo-inositol mannosides from *Mycobacterium tuberculosis* by C-type lectin pattern recognition receptors. *J Immunol* **177**, 1805-1816.

Torrelles, J. B., DesJardin, L. E., MacNeil, J. & other authors (2009). Inactivation of *Mycobacterium tuberculosis* mannosyltransferase *pimB* reduces the cell wall lipoarabinomannan and lipomannan content and increases the rate of bacterial-induced human macrophage cell death. *Glycobiology* **19**, 743-755.

Torrelles, J. B. & Schlesinger, L. S. (2010). Diversity in *Mycobacterium tuberculosis* mannosylated cell wall determinants impacts adaptation to the host. *Tuberculosis (Edinburgh, Scotland)* **90**, 84-93.

Treumann, A., Xidong, F., McDonnell, L., Derrick, P. J., Ashcroft, A. E., Chatterjee, D. & Homans, S. W. (2002). 5-Methylthiopentose: a new substituent on lipoarabinomannan in *Mycobacterium tuberculosis*. *J Mol Biol* **316**, 89-100.

Trivedi, O. A., Arora, P., Sridharan, V., Tickoo, R., Mohanty, D. & Gokhale, R. S. (2004). Enzymic activation and transfer of fatty acids as acyl-adenylates in mycobacteria. *Nature* **428**, 441-445.

Underhill, D. M., Ozinsky, A., Hajjar, A. M., Stevens, A., Wilson, C. B., Bassetti, M. & Aderem, A. (1999). The Toll-like receptor 2 is recruited to macrophage phagosomes and discriminates between pathogens. *Nature* **401**, 811-815.

Unligil, U. M. & Rini, J. M. (2000). Glycosyltransferase structure and mechanism. *Current opinion in structural biology* **10**, 510-517.

- Van Delden, C., and Iglewski B. H., (1998)** Cell-to-cell signaling and *Pseudomonas aeruginosa* infections. *Emerging Infect Dis* **4**, 551-60.
- van Die, I., van Vliet, S. J., Nyame, A. K., Cummings, R. D., Bank, C. M., Appelmelk, B., Geijtenbeek, T. B. & van Kooyk, Y. (2003).** The dendritic cell-specific C-type lectin DC-SIGN is a receptor for *Schistosoma mansoni* egg antigens and recognizes the glycan antigen Lewis X. *Glycobiology* **13**, 471–478.
- van Heijenoort, J. (2001a).** Formation of the glycan chains in the synthesis of bacterial peptidoglycan. *Glycobiology* **11**, 25R-36R.
- van Heijenoort, J. (2001b).** Recent advances in the formation of the bacterial peptidoglycan monomer unit. *Nat Prod Rep* **18**, 503-519.
- van Heijenoort, J. (2007).** Lipid intermediates in the biosynthesis of bacterial peptidoglycan. *Microbiol Mol Biol Rev* **71**, 620-635
- Venisse, A., Berjeaud, J. M., Chaurand, P., Gilleron, M. & Puzo, G. (1993).** Structural features of lipoarabinomannan from *Mycobacterium bovis* BCG. Determination of molecular mass by laser desorption mass spectrometry. *J Biol Chem* **268**, 12401-12411.
- Vercellone, A., Nigou, J., & Puzo, G. (1998).** Relationships between the structure and the roles of lipoarabinomannans and related glycoconjugates in tuberculosis pathogenesis. *Frontiers in Bioscience* **3**, 149-163.
- Vergne, I., Chua, J. & Deretic, V. (2003a).** *Mycobacterium tuberculosis* phagosome maturation arrest: selective targeting of PI3P-dependent membrane trafficking. *Traffic* **4**, 600-606.
- Vergne, I., Chua, J. & Deretic, V. (2003b).** Tuberculosis toxin blocking phagosome maturation inhibits a novel Ca²⁺/calmodulin-PI3K hVPS34 cascade. *J Exp Med* **198**, 653-659.
- Vergne, I., Chua, J., Singh, S. B. & Deretic, V. (2004a).** Cell biology of *Mycobacterium tuberculosis* phagosome. *Annu Rev Cell Dev Biol.* **20**, 367-394.
- Vergne, I., Fratti, R. A., Hill, P. J., Chua, J., Belisle, J. & Deretic, V. (2004b).** *Mycobacterium tuberculosis* phagosome maturation arrest: mycobacterial phosphatidylinositol analog phosphatidylinositol mannoside stimulates early endosomal fusion. *Mol Biol Cell* **15**, 751-760.
- Vergne, I., Chua, J., Lee, H. H., Lucas, M., Belisle, J. & Deretic, V. (2005).** Mechanism of phagolysosome biogenesis block by viable *Mycobacterium tuberculosis*. *Proc. Natl. Acad. Sci. USA* **102**, 4033-4038.
- Vignal, C., Guerardel, Y., Kremer, L., Masson, M., Legrand, D., Mazurier, J. & Ellass, E. (2003).** Lipomannans, but not lipoarabinomannans, purified from *Mycobacterium chelonae* and *Mycobacterium kansasii* induce TNF- α and IL-8 secretion by a CD14-toll-like receptor 2-dependent mechanism. *J. Immunol.* **171**, 2014-2023.

- Vilcheze, C., Morbidoni, H. R., Weisbrod, T. R., Iwamoto, H., Kuo, M., Sacchettini, J. C. & Jacobs, W. R., Jr. (2000).** Inactivation of the inhA-encoded fatty acid synthase II (FASII) enoyl-acyl carrier protein reductase induces accumulation of the FASII end products and cell lysis of *Mycobacterium smegmatis*. *J Bacteriol* **182**, 4059-4067.
- Vilkas, E. & Lederer, E. (1956).** (Isolation of a phosphatidyl-inositol-di-D-mannoside from a mycobacterial phosphatide.). *Bull Soc Chim Biol (Paris)* **38**, 111-121.
- Vilkas, E., Amar, C., Markovits, J., Vliegthart, J. F. & Kamerling, J. P. (1973).** Occurrence of a galactofuranose disaccharide in immunoadjuvant fractions of *Mycobacterium tuberculosis* (Cell walls and wax D). *Biochimica et Biophysica Acta (BBA)* **297**, 423-435.
- Walker, R. W., Prome, J. C. & Lacave, C. S. (1973).** Biosynthesis of mycolic acids. Formation of a C32 beta-keto ester from palmitic acid in a cell-free system of *Corynebacterium diphtheriae*. *Biochimica et biophysica acta* **326**, 52-62.
- Weidenmaier, C. & Peschel, A. (2008).** Teichoic acids and related cell-wall glycopolymers in Gram-positive physiology and host interactions. *Nat Rev Microbiol* **6**, 276-287.
- Weitzman, D., de Wend Cayley, F. & Wingfield, A. (1950).** Streptomycin in the treatment of pulmonary tuberculosis. *Brit J Tuberc Dis Chest* **44**, 98-104.
- Welin, A., Winberg, M. E., Abdalla, H., Sarndahl, E., Rasmusson, B., Stendahl, O. & Lerm, M. (2008).** Incorporation of *Mycobacterium tuberculosis* lipoarabinomannan into macrophage membrane rafts is a prerequisite for the phagosomal maturation block. *Infect Immun* **76**, 2882-2887.
- Weston, A., Stern, R. J., Lee, R. E. & other authors (1997).** Biosynthetic origin of mycobacterial cell wall galactofuranosyl residues. *Tuber Lung Dis* **78**, 123-131.
- Wietzerbin, J., Das, B. C., Petit, J. F., Lederer, E., Leyh-Bouille, M. & Ghuysen, J. M. (1974).** Occurrence of D-alanyl-(D)-meso-diaminopimelic acid and meso-diaminopimelyl-meso-diaminopimelic acid interpeptide linkages in the peptidoglycan of *Mycobacteria*. *Biochemistry* **13**, 3471-3476.
- WHO (2009).** The World Health Organisation Global Tuberculosis Programm,: World Health Organisation.
- Winder, F. G. & Collins, P. B. (1970).** Inhibition by isoniazid of synthesis of mycolic acids in *Mycobacterium tuberculosis*. *J Gen Microbiol* **63**, 41-48.
- Wolucka, B. A., McNeil, M. R., de Hoffmann, E., Chojnacki, T. & Brennan, P. J. (1994).** Recognition of the lipid intermediate for arabinogalactan/arabinomannan biosynthesis and its relation to the mode of action of ethambutol on mycobacteria. *J Biol Chem* **269**, 23328-23335.
- Wolucka, B. A. & de Hoffmann, E. (1995).** The presence of β -D-ribosyl-1-monophosphodecaprenol in mycobacteria. *J Biol Chem* **270**, 20151-20155.

- Wolucka, B. A. (2008).** Biosynthesis of D-arabinose in mycobacteria - a novel bacterial pathway with implications for antimycobacterial therapy. *FEBS J* **275**, 2691-2711.
- Xin, Y., Y. Huang, and M.R. McNeil. 1999.** The presence of an endogenous endo-D-arabinase in *Mycobacterium smegmatis* and characterization of its oligoarabinoside product. *Biochim Biophys Acta* **1473** 267-271.
- Yagi, T., Mahapatra, S., Mikusova, K., Crick, D. C. & Brennan, P. J. (2003).** Polymerization of mycobacterial arabinogalactan and ligation to peptidoglycan. *J Biol Chem* **278**, 26497-26504.
- Yokoyama, K. & Ballou, C. E. (1989).** Synthesis of alpha 1----6-mannooligosaccharides in *Mycobacterium smegmatis*. Function of beta-mannosylphosphoryldecaprenol as the mannosyl donor. *The Journal of biological chemistry* **264**, 21621-21628.
- Zahringer U, Lindner B, Inamura S, Heine H, & Alexander C (2008).** TLR2-promiscuous or specific? A critical re-evaluation of a receptor expressing apparent broad specificity. *Immunobiology* **213**, 205-224.
- Zhang, N., Torrelles, J. B., McNeil, M. R., Escuyer, V. E., Khoo, K. H., Brennan, P. J. & Chatterjee, D. (2003a).** The Emb proteins of mycobacteria direct arabinosylation of lipoarabinomannan and arabinogalactan via an N-terminal recognition region and a C-terminal synthetic region. *Mol Microbiol* **50**, 69-76.
- Zhang, Y., Heym, B., Allen, B., Young, D. & Cole, S. (1992).** The catalase-peroxidase gene and isoniazid resistance of *Mycobacterium tuberculosis*. *Nature* **358**, 591-593.
- Zhang, Y. & Young, D. (1994).** Molecular genetics of drug resistance in *Mycobacterium tuberculosis*. *J Antimicrob Chemother* **34**, 313-319.
- Zhang, Y. (2003).** Isoniazid. In *Tuberculosis*, pp. 739-758. Edited by W. Rom & S. Garay. New York: Lippincott.
- Zhang, Y., Wade, M. M., Scorpio, A., Zhang, H. & Sun, Z. (2003b).** Mode of action of pyrazinamide: disruption of *Mycobacterium tuberculosis* membrane transport and energetics by pyrazinoic acid. *J Antimicrob Chemother* **52**, 790-795.
- Zhang, Y. (2004).** Persistent and dormant tubercle bacilli and latent tuberculosis. *Front Biosci* **9**, 1136-1156.
- Zhang, Y. (2005).** The magic bullets and tuberculosis drug targets. *Annu Rev Pharmacol Toxicol* **45**, 529-564.
- Zignol, M., Hosseini, M. S., Wright, A., Weezenbeek, C. L., Nunn, P., Watt, C. J., Williams, B. G., and Dye, C. (2006).** Global incidence of multidrug-resistant tuberculosis. *J Infect Dis* **194**, 479-485
- Zink, A., Haas, C. J., Reischl, U., Szeimies, U. & Nerlich, A. G. (2001).** Molecular analysis of skeletal tuberculosis in an ancient Egyptian population. *J Med Microbiol* **50**, 355-

366.